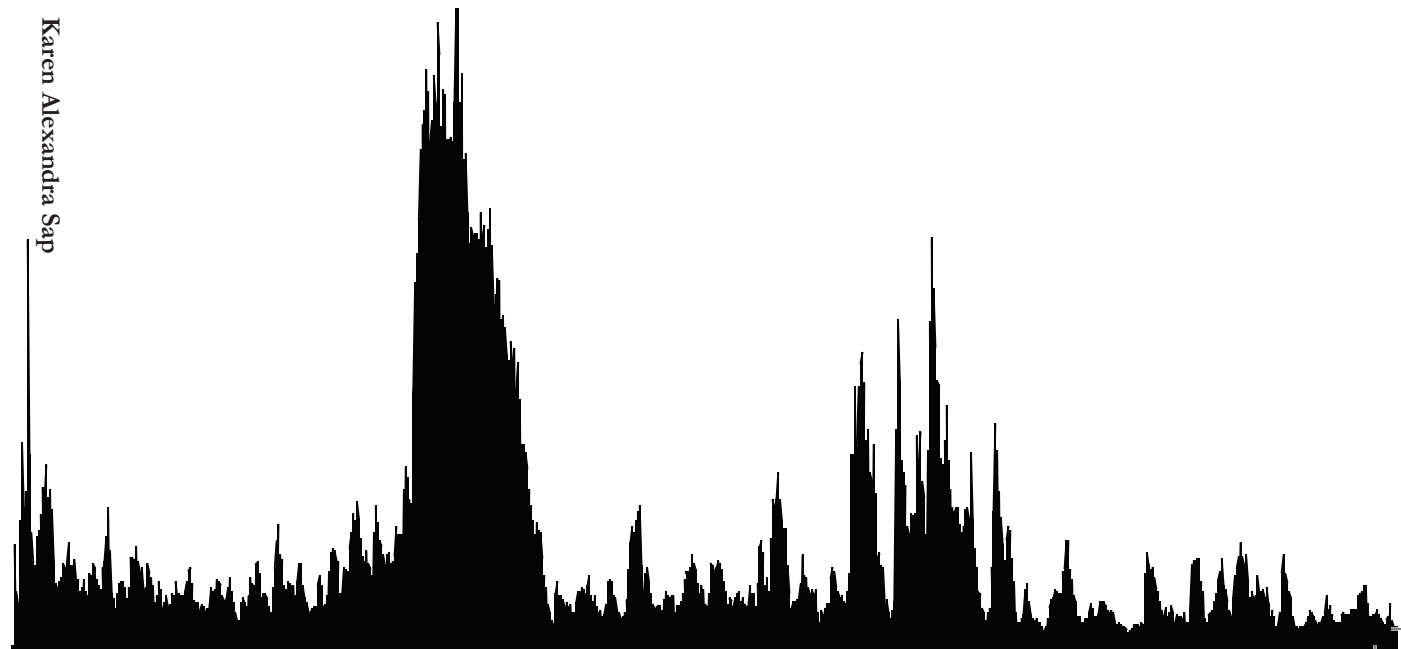


Dynamics of Protein Ubiquitination Upon Proteasome Modulation

A Quantitative Mass Spectrometry Approach

Karen Alexandra Sap



Dynamics of Protein Ubiquitination upon Proteasome Modulation

A Quantitative Mass Spectrometry Approach

Karen Alexandra Sap

© 2018 Karen Sap

Cover design: Karen Sap & Frank Sap

ISBN: 978-94-93019-55-3

Printed by: ProefschriftMaken.nl | | www.proefschriftmaken.nl

Published by: ProefschriftMaken.nl | | www.proefschriftmaken.nl

The studies described in this thesis were performed in the Proteomics Center which is embedded in the Department of Biochemistry of the Erasmus University Medical Center in Rotterdam, The Netherlands

The research described in this thesis was financially supported by the Netherlands Proteomics Center (project number 184.032.201)

Dynamics of Protein Ubiquitination upon Proteasome Modulation

A Quantitative Mass Spectrometry Approach

Dynamiek van eiwit ubiquitinatie als gevolg van proteasoom modulatie

Onderzocht door middel van kwantitatieve massaspectrometrie

Proefschrift

ter verkrijging van de graad van doctor aan de

Erasmus Universiteit Rotterdam

op gezag van de

rector magnificus

Prof.dr. R.C.M.E. Engels

en volgens besluit van het College voor Promoties.

De openbare verdediging zal plaatsvinden op

donderdag 20 september 2018 om 11.30 uur

door

Karen Alexandra Sap

geboren te Rotterdam

Promotiecommissie

Promotor: Prof.dr. C.P. Verrijzer

Overige leden: Prof.dr. J.H. Gribnau

Dr. J.A.F. Marteiijn

Dr. A.C.O. Vertegaal

Copromotor: Dr. J.A.A. Demmers

Table of Contents

Chapter 1	General Introduction	7
	Scope of the Thesis	30
Chapter 2	Labeling Methods in Mass Spectrometry Based Quantitative Proteomics	31
Chapter 3	Quantitative Proteomics Reveals Extensive Changes in the Ubiquitinome After Perturbation of the Proteasome by Targeted dsRNA Mediated Subunit Knockdown in <i>Drosophila</i>	55
Chapter 4	Depletion of the Proteasome-Associated Deubiquitinase RPN11, but not UCHL5 and USP14, Results in an Extensive Remodeling of the Ubiquitinome	81
Chapter 5	The <i>Drosophila</i> 26S Proteasome Interactome is Modulated Under Stress Conditions as Revealed by LFQ Mass Spectrometry	119
Chapter 6	Global Quantitative Proteomics Reveals Novel Factors in the Ecdysone Signaling Pathway in <i>Drosophila melanogaster</i>	155
Chapter 7	General Discussion	183
Appendix	Summary	198
	Nederlandse Samenvatting	200
	Curriculum Vitae	203
	List of Publications	204
	Portfolio	205
	Dankwoord	206

Chapter 1

General Introduction

Ubiquitin Proteasome System

Through targeted degradation of both cytoplasmic and nuclear short-lived proteins the 26S proteasome complex regulates the concentration of the large majority of the proteins in the cell (Rock *et al.*, 1994; Collins and Goldberg, 2017). Furthermore, the proteasome functions as a quality control system by degrading potentially harmful damaged or misfolded proteins (Goldberg, 2003; Kostova and Wolf, 2003). Proteins are targeted for proteasome-mediated degradation by degrons or polyubiquitin chains. Ubiquitin is an 8.5kDa modular protein which can be attached with its C-terminus to the epsilon-amino group of lysine residues on target proteins, or more rarely, to the protein N-terminus, or to the side chain of a cysteine residue in the target protein (Komander and Rape, 2012). Conjugation of ubiquitin to target proteins is regulated by the sequential action three enzymes: ubiquitin is first activated by an E1 ubiquitin-activating enzyme through thioester bond formation between the E1's active cysteine residue and ubiquitin's C-terminal carboxyl group in an ATP-dependent manner. The ubiquitin protein is then transferred to a cysteine residue of an E2 ubiquitin-conjugating enzyme. An E3 ubiquitin ligase catalyzes the transfer of ubiquitin from the E2 enzyme to specific target proteins. Ubiquitin conjugates on proteins can in turn also become targets for ubiquitination, which can result in the formation of polyubiquitin chains on target proteins (Figure 1).

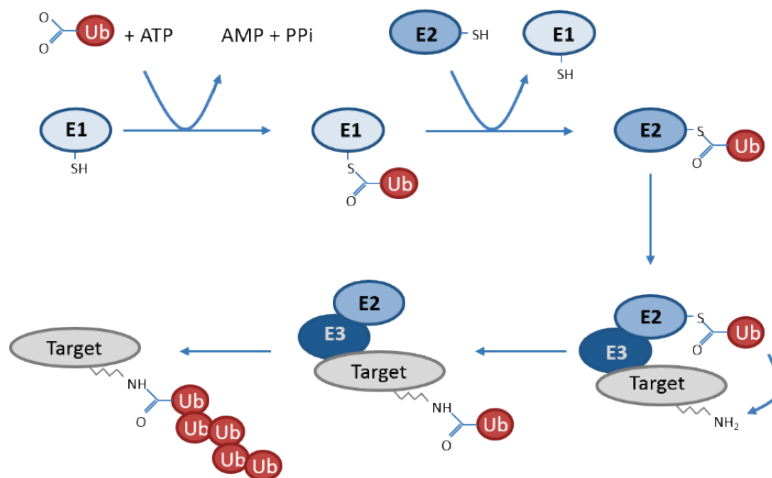


Figure 1. Schematic representation of the ubiquitination pathway. Ubiquitin is activated by an E1 ubiquitin activating enzyme in an ATP dependent manner. Then ubiquitin is transferred from the E1 enzyme to an E2 ubiquitin conjugating enzyme. The ubiquitin-conjugated E2 enzyme interacts with an E3 ubiquitin ligase which can bind specific target proteins. Ubiquitin can be transferred either to substrate proteins or to other ubiquitin molecules to form a polyubiquitin chain.

The concerted action of ubiquitin targeting via E1, E2 and E3 enzymes and proteasome-dependent degradation is also referred to as the ubiquitin-proteasome system, or UPS. As such

the UPS plays a central role in the cell by regulating processes such as cell cycle progression, DNA repair, protein quality control, transcription, signal transduction, antigen processing and the maintenance of protein and cellular homeostasis (Kloetzel, 2004; Geng, Wenzel and Tansey, 2012; Tu *et al.*, 2012). Malfunctioning of the Ubiquitin Proteasome System has been implicated in a wide variety of diseases such as cancer and neurodegenerative disorders (Schwartz and Ciechanover, 2009).

Proteasome structure

The 26S proteasome is functionally and structurally divided into two parts *i.e.*, the 20S catalytic core particle (CP) and the 19S regulatory particles (RP) (Hough, Pratt and Rechsteiner, 1986; Chu-Ping *et al.*, 1994; Walz *et al.*, 1998) (Figure 2). The 20S proteolytic core particles can also function independently and have been identified in eukaryotes, archaea, and in bacteria of the Actinomycetes phylum (Gille *et al.*, 2003), whereas the 19S RPs were found only in eukaryotes and archaea. The 19S RP was already identified in the last eukaryotic common ancestor, LECA, and evolved independently through duplications and loss events in specific lineages (Fort *et al.*, 2015). Table 1 gives a collection of different names and abbreviations of 26S proteasome subunits in different eukaryotes. The 20S CP has the shape of a barrel made up of two identical outer α -rings and two identical inner β -rings. Both types of rings consist of 7 subunits (Prosalpha1 – Prosalpha7 and Prosbeta1 – Prosbeta7) (Groll *et al.*, 1997; Unno *et al.*, 2002). The alpha rings are responsible for the regulation of substrate entrance to the inner proteolytic chamber by forming a gate at the center of the ring with their subunits' N-termini. Prosbeta1, Prosbeta2 and Prosbeta5 exhibit respectively caspase-like (cleaving after acidic amino acids), trypsin-like (cleaving after basic amino acids) and chymotrypsin-like (cleaving after neutral amino acids) proteolytic activity which is buried within the barrel (Marques *et al.*, 2009). Typical products of proteasomal degradation are oligopeptides with lengths between 3 and 30 amino acids with an average length of 8 residues (Kisselev, Akopian and Goldberg, 1998). Mutations in genes coding for catalytic subunits of the proteasome, such as prosbeta5i of the immunoproteasome may trigger abnormal inflammation which damages tissues and organs, as observed in several related but different syndromes: CANDLE syndrome, Nakajo-Nishimura syndrome and JMP syndrome. Usually, the 20S proteasome is found in the cell in its inactive state. The 20S core can be activated by docking of regulators (19S, 11S, PA200), unfolded proteins, or proteasomal substrates to the α -ring (Liu *et al.*, 2003; Stadtmueller and Hill, 2011). Damaged proteins can activate the proteasome by binding directly to the α -subunits with their exposed hydrophobic patches, while native and correctly folded proteins have to be targeted (via polyubiquitin) for proteasomal degradation. The most important regulator for the recognition of ubiquitin-conjugated proteins is the 19S regulatory particle (19S RP).

Table 1. Proteasome subunit names across species

Proteasome subunits	<i>D. melanogaster</i>	<i>S. cerevisiae</i>	Mammals
20S CP			
Prosalpha1	Prosalpha1/CG30382	Sc11/Prc2/Prs2/C7	PSMA6/Pros27/Iota
Prosalpha2	Prosalpha2/Pros25/PROS25/CG5266	Pre8/Prs4/Y7	PSMA2/C3/Lmpc3
Prosalpha3	Prosalpha3/Pros29/PROS-29/CG9327	Pre9/Prs5/Y13	PSMA4/C9
Prosalpha4	Prosalpha4/Pros28.1/PROS28.1/CG3422	Pre6	PSMA7/C7/XAPC7
Prosalpha5	Prosalpha5/ProsMA5/CG10938	Pup2/Doa5	PSMA5/Zeta
Prosalpha6	Prosalpha6/Pros35/PROS35/CG4904	Pre5	PSMA1/C2/Pros30
Prosalpha7	Prosalpha7/CG1519	Pre10/Prc1/Prs1/C1	PSMA3/C8
Prosbeta1	Prosbeta1/I(2)05070/CG8392	Pre3	PSMB6/Y/delta/LMPY/LMP19
Prosbeta2	Prosbeta2	Pup1	PSMB7/Z/Mmc14
Prosbeta3	Prosbeta3/CG11980	Pup3	PSMB3/C10
Prosbeta4	CG17331	Pre1/C11	PSMB2/C7
Prosbeta5	Prosbeta5/Pros-beta-5/CG12323	Pre2/Doa3/Prg1	PSMB5/X/MB1
Prosbeta6	Prosbeta6/Pros26/PROS26/I(3)37Ai/CG4097	Pre7/Prs3/Pts1/C5	PSMB1/C5
Prosbeta7	Prosbeta7/Prosb4/Prosbeta4/CG12000	Pre4	PSMB4/N3/beta/LMP3
19S RP ATPases			
Rpt1/S7	Rpt1/p48B/CG1341	Rpt1/Cim5/Yta3	PSMC2/Mss1
Rpt2/S4	Rpt2/Pros26.4/p56/p26s4/CG5289	Rpt2/Yhs4/Yta5	PSMC1
Rpt3/S6b	Rpt3/p48A/CG16916	Rpt3/Tnt1/Yta2/Ynt1	PSMC4/Mip224/Tbp7
Rpt4/S10b	Rpt4/p42D	Rpt4/Crl13/Pcs1/Sug2	PSMC6/Sug2/P42
Rpt5/S6a	Tbp-1/p50	Rpt5/Yta1	PSMC3/Tbp1
Rpt6/S8	Rpt6/Pros45/p42C/DUG/Ug/CG1489	Rpt6/Cim3/Crl3/Sug/TbpY/Tby1	PSMC5/p45/Sug1/Trip1
19S RP non-ATPases			
Rpn1/S2	Rpn1/p97	Rpn1/Hrd2/Nas1/Rpd1	PSMD2/p97/Trap2
Rpn2/S1	Rpn2/p110/CG11888	Rpn2/Sen3	PSMD1/p112
Rpn3/S3	Rpn3/p58/Dox-A2/CG42641	Rpn3/Sun2	PSMD3/p58
Rpn4/P27	CG9588/p27	Nas2/Rpn4/Son1/Ufd5	PSMD9/p27/Rpn4
Rpn5/p55	Rpn5/p55/CG1100	Rpn5/Nas5	PSMD12/p55
Rpn6/S9	Rpn6/p42B/CG10149	Rpn6/Nas4	PSMD11/p44.5
Rpn7/S10a/S10	Rpn7/p42A/CG5378	Rpn7	PSMD6/p42a
Rpn8/S12	Mov34/p39B/CG3416	Rpn8/Nas3	PSMD7/p40/Mov34

Proteasome subunits	<i>D. melanogaster</i>	<i>S. cerevisiae</i>	Mammals
19S RP non-ATPases			
Rpn9/S11	Rpn9/p39A	Rpn9/Nas7	PSMD13/p40.5
Rpn10/S5a	Rpn10/Pros54/p54/PROS-54/CG7619	Rpn10/Sun1/Mcb1	PSMD4/S5a/Mcb1
S5b	CG12096	-	PSMD5/KIAA0072
Rpn11/S13	Rpn11/p37B/yip5/CG18174	Rpn11/Mpr1	PSMD14/Pad1/Poh1
Rpn12/S14	Rpn12/p30	Rpn12/Nin1	PSMD8/p31
Rpn13	Rpn13/p42E/CG13349	Rpn13/Daq1	ADRM1/-
p28	-	Nas6	PSMD10/p28/Gankyrin
P27	CG9588	Nas2	PSMD9/p27
Rpn15/Sem1	-	Rpn15/Sem1/Dsh1/DSS1/HOD1	SHFM1/DSS1/SHFDG1
UCHL5	UCHL5/Uch-L3/p37A/CG31639/CG3431	-	UCHL5/UCH37
Sub-stoichiometric proteasome protein			
USP14	USP14/CG5384	UBP6	USP14

The subunits of the 19S RP recognize, deubiquitinate and unfold ubiquitinated proteasome substrate and subsequently translocate it into the 20S CP. Elucidation of the structure of the 19S RP was challenging, partly due to the different conformational states of the 19S RP as well as due to the number of substoichiometric binding partners. Over the last years, advances in the determination of the structure of the 19S RP at high resolution were made with the aid of cryo-electronmicroscopy, crystallography, biochemistry and computer modeling (Bohn *et al.*, 2010; Beck *et al.*, 2012; Lander *et al.*, 2012; Lasker *et al.*, 2012; Sledz *et al.*, 2013). The 19S RP, also called the 19S cap, is composed of two distinct subcomplexes, the base and the lid (Glickman *et al.*, 1998). The base contains four non-ATPase subunits (RPN1, RPN2, RPN10 and RPN13) and six AAA-ATPase subunits *i.e.*, RPT1-RPT6. The Rpt proteins form a heterohexameric ring and dock with the C-termini of their AAA+ domains into the α -ring of the 20S CP. Their N-termini contain an OB-fold domain which assemble into a distinct N-ring above the AAA+ domain ring. The ATPase ring subunits form a channel which runs through approximately two-thirds of the 19S RP, basically extending the channel of the 20S RP. The ATPase ring engages an unstructured initiation region of the substrate and triggers unfolding, pore opening and active translocation of the substrate to the proteolytic sites of the 20S CP. Two large subunits, which serve as interaction platforms, bind with the ATPase channel: RPN1 binds to the outside of the channel and provides binding sites for non-stoichiometric proteasome interactors such as UBL-UBA proteins, but also for deubiquitinating enzyme USP14/Ubp6. RPN2 binds to the top of the ATPase ring and provides a binding site for ubiquitin receptor RPN13. The other intrinsic ubiquitin receptor of the proteasome, RPN10, interacts with RPN1 although this association is stabilized by RPN2. The proteasome lid contains eight subunits (RPN3, RPN5-RPN9, RPN11

and RPN12). RPN8 and RPN11 form dimers near the entrance of the ATPase ring. Both belong to the JAMM or MPN domain metallo-protease family of deubiquitinating (DUB) enzymes, however only RPN11 is an active DUB. RPN11 can cleave entire polyubiquitin chains off the substrates concomitant with translocation into the proteolytic core (Yao and Robert E. Cohen, 2002; M. J. Lee *et al.*, 2011). The other subunits of the lid might function as scaffolding proteins that bind to the outside of the cap, running from the entrance of the ATPase ring where they interact with RPN2 and ubiquitin receptor RPN10 all the way down via the ATPase ring to the α -ring of the 20S CP (Figure 2). They are suggested to stabilize the proteasome particle and to facilitate conformational changes upon substrate binding.

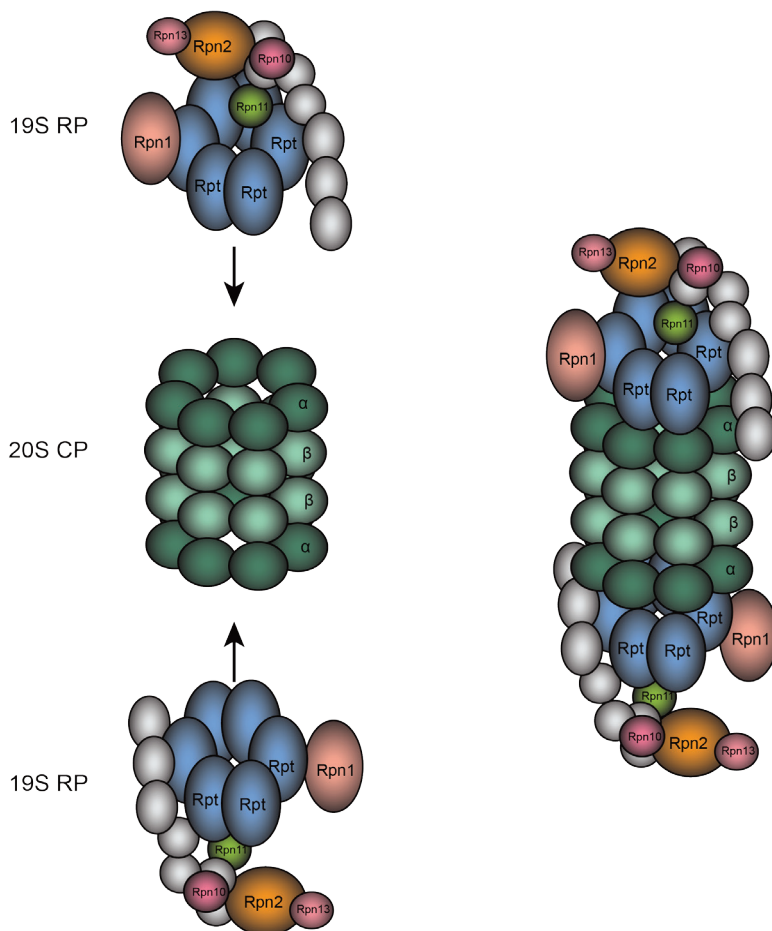


Figure 2. Illustration of the structure of the 26S proteasome consisting of two 19S regulatory particles and one 20S core particle.

Conformational changes of the 26S proteasome are mostly driven by ATP binding and hydrolysis. All RPT subunits of the proteasome are able to bind and hydrolyze ATP (Beckwith *et al.*, 2013; Peth, Nathan and Goldberg, 2013), which may theoretically give rise to a large number of different conformational states. To date three major 26S conformational states are identified: s1 (substrate-free state), s2 (intermediate state) and s3 (substrate engaged state). The s1 and s2 states are observed in the presence of both ATP and the slowly hydrolysable ATP analog ATP- γ S. As the relative abundance of s1:s2 was observed to be ~4:1 for both conditions, it might be reasonable to assume that s1, or the substrate-free state, corresponds to the ground state because it is more abundant (Unverdorben *et al.*, 2014). Also in intact neurons it was observed that ~80% of the proteasomes were present in the substrate-accepting ground state (Asano *et al.*, 2015). In the substrate-free state, the AAA+ domains of the RPTs adopt a steep spiral-staircase arrangement that restricts access to the proteolytic core, but may facilitate substrate engagement (Beckwith *et al.*, 2013). Substrate engagement in turn induces conformational changes. The s3 state is only observed with the use of ATP- γ S, suggesting that this is a high-energy pre-hydrolysis state. The RPTs adopt a more planar spiral-staircase arrangement in this state and both the N-ring and AAA+ ring of these proteins are coaxially aligned with the 20S pore, thereby creating a continuous central channel for substrate translocation into the proteolytic core (Matyskiela, Lander and Martin, 2013; Sledz *et al.*, 2013). Another characteristic of the s3 state is the placement of RPN11 above the entrance of the 20S pore, which is an ideal location for the removal of ubiquitin chains during polypeptide translocation. The s2 state is considered an intermediate state as the ATPase module remains in essentially the same conformation as in the s1 state, whereas the lid together with RPN2 is in a position and conformation similar to s3 (Unverdorben *et al.*, 2014).

Proteasome targeting

Proteins are targeted for proteolysis by the 26S proteasome via the attachment of ubiquitin residues. The amino acid sequence of ubiquitin is shown in Figure 3A. Proteins can undergo conjugation with a single ubiquitin moiety on one or multiple sites, which is referred to as respectively monoubiquitination or multi-monoubiquitination (Figure 3B). Additionally, proteins can become polyubiquitinated when other ubiquitin molecules bind to the conjugated ubiquitin moiety, leading to the formation of a polyubiquitin chain on target proteins (Figure 3C). Ubiquitin harbors 7 internal lysine residues and one N-terminal methionine residue which can function as a target for polyubiquitination: M1, K6, K11, K27, K29, K33, K48 and K63 (Figure 3A). Ubiquitin chains can be either homeotypic, that is when they harbor a single ubiquitin linkage type, or chains can be heterotypic when they contain mixed linkages. Mixed chains can furthermore be non-branched or branched/forked, of which the latter is the result of multi-ubiquitination of one or more ubiquitin moieties in the chain. Branched chains are frequently found on short-lived proteins *in vivo* (Liu *et al.*, 2017). Chains can furthermore consist of both ubiquitin and ubiquitin-like proteins, such as SUMO. Finally, ubiquitin can also be

modified by other post translational modifications, such as acetylation and phosphorylation (reviewed in (Swatek and Komander, 2016)). The tertiary structures of ubiquitin chains differ depending on which linkage types are present. K48 linkages result in rather compact structures (Tenno *et al.*, 2004; Ryabov and Fushman, 2006), however it was also shown to exhibit a predominantly open conformation (Hirano *et al.*, 2011), Met1-linked diubiquitin has been observed both as a compact (Rohaim *et al.*, 2012) and open structure (Komander *et al.*, 2009), while K63-linked chains exhibit a more open conformation (Tenno *et al.*, 2004; Varadan *et al.*, 2004; Komander *et al.*, 2009). Conjugation of different ubiquitin chain types has been shown to regulate the fate and/or function of target proteins in different ways (Kulathu and Komander, 2012) (Figure 3C).

Many aspects of substrate targeting to the proteasome remain unclear. Conventionally, K48-linked polyubiquitin chains of at least 4 ubiquitin moieties and anchored to a ϵ -NH₂ group of a lysine residue in the target substrate have been established as the canonical signal for targeted 26S proteasome-mediated proteolysis (Thrower *et al.*, 2000). However, a much broader set of ubiquitin-based signals for proteasomal targeting has been identified. For instance, multiple short heterotypic ubiquitin chains were shown to be a more effective signal for Cyclin B degradation compared to a single long chain (Kirkpatrick *et al.*, 2006). Furthermore, homotypic ubiquitin chains of all linkage types, except K63, are able to behave as proteasome targeting signals *in vivo* (Xu *et al.*, 2009; Bedford *et al.*, 2011; Nathan *et al.*, 2013). K11-linked polyubiquitin chains, for example, can target cell cycle proteins for proteasomal degradation (Jin *et al.*, 2008). To date, K63-linked ubiquitin chains were found in complex with the proteasome in cell free systems (Nathan *et al.*, 2013), however the involvement of K63 chains in the cellular UPS is not yet defined. Mixed chains made of both ubiquitin and ubiquitin-like proteins, such as SUMO, can target substrate for proteolysis (Tatham *et al.*, 2008). Ubiquitin chains can also be anchored to residues other than internal lysines in substrates, such as cysteine, serine and threonine residues and become a target for degradation (Tait *et al.*, 2007). However, ubiquitination on non-lysine residues is not common and it might just be a method by which the cell can target abnormal proteins, whose lysine residues are not exposed, masked or not present, for degradation (Wang, Herr and Hansen, 2012). Furthermore, several monoubiquitinated and multi-monoubiquitinated proteins were found to be targeted to the proteasome (Dimova *et al.*, 2012; Braten *et al.*, 2016; Livneh *et al.*, 2017). It is hypothesized that mono-ubiquitination or multi-monoubiquitination is especially a relevant proteasome targeting signal for relatively small proteins and that larger proteins require polyubiquitination in order to be properly docked at the 19S cap. Finally, some proteins can be degraded by the proteasome without prior ubiquitination. All non-canonical ubiquitin signals for proteasomal degradation are elegantly reviewed in (Kravtsova-Ivantsiv and Ciechanover, 2012; Swatek and Komander, 2016). The wide variety of ubiquitination signals suggests that there is a high level of specificity and selectivity in targeting proteins for degradation and/or recognition of ubiquitinated substrate by the proteasome. It is currently not clear what

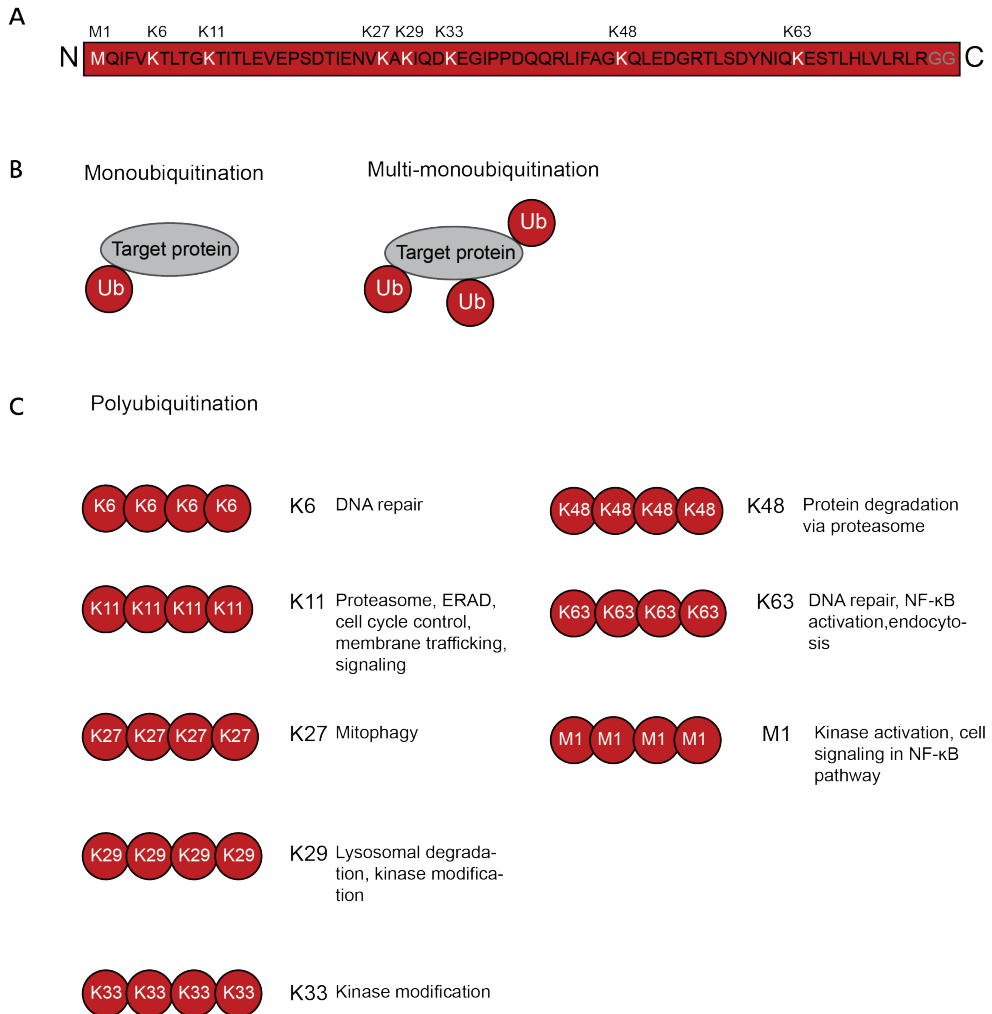


Figure 3. Illustration of multiple forms of ubiquitination. A) Ubiquitin amino acid sequence with methionine and lysine residues highlighted, as these may function as ubiquitination targets in polyubiquitin chains. The glycine residues are highlighted in grey. Gly76 is used for substrate binding, which may be either target substrate proteins as well as other ubiquitin molecules. Gly75 and Gly76 are both important for the recognition and purification of diGly-peptides by α -K- ϵ -GG antibodies, which greatly propelled the discovery of novel ubiquitination sites by mass spectrometry. B) Variations in mono ubiquitination. C) Selection of variations of polyubiquitination and their effects on the cellular level.

characteristics of the substrate drives these diverse ubiquitination patterns. It is also not clear which ubiquitin receptors or shuttle proteins recognize specific atypical ubiquitin linkage types. On the contrary, an ‘ubiquitination threshold’ model is proposed, where the amount of polyubiquitin is important as a degradation signal rather than the linkage type (Swatek and Komander, 2016). In another model, a minimal number of short (di)ubiquitin chains is required for tight interaction with the proteasome while a longer chain would promote translocation into the 20S core (Ying *et al.*, 2015). More research is required to better understand the characteristics of effective degradation signals as well as the biological significance of the wide variety of ubiquitin linkages.

Proteasome substrate recruitment

Proper regulation of the interaction between polyubiquitinated substrate and the 26S proteasome is essential for a functional UPS. Malfunctioning of this regulation may result in proteasome dysfunction and protein accumulation, features which are observed in a variety of malignancies (Ciechanover and Brundin, 2003). The central dogma is that 26S proteasome substrate is recognized by their polyubiquitin tags. The two intrinsic ubiquitin receptors of the proteasome are RPN10 (S5a in human) (Deveraux *et al.*, 1994) and RPN13 (Husnjak *et al.*, 2008). Proteasome subunits RPN1 (Archer *et al.*, 2008), RPT5 (Lam *et al.*, 2002) and RPT1 (Archer *et al.*, 2008) may provide additional ubiquitin docking sites near the 20S CP. Recently DSS1/SEM1/RPN15 was identified as additional ubiquitin receptor of the proteasome in *Saccharomyces pombe* (Paraskevopoulos *et al.*, 2014). Furthermore, RPN1 was identified as a receptor for both ubiquitin and UBL proteins (Shi *et al.*, 2016). The recognition pathways for ubiquitinated substrates appear to have diverged in different species. For instance, RPN10 and RPN13 are non-essential for the yeast 26S proteasome complex (Fu *et al.*, 1998; Husnjak *et al.*, 2008), while RPN10 is essential in mice and *Drosophila melanogaster* (Szlanke *et al.*, 2003; Hamazaki *et al.*, 2007). RPN10-null mice die at embryonic day 6.5 (Hamazaki *et al.*, 2007), while RPN13-null mice die soon after birth (Hamazaki, Hirayama and Murata, 2015). RPN10 recognizes ubiquitin via a C-terminal ubiquitin interacting motif (UIM). *S. cerevisiae* RPN10 has a single UIM that preferentially interacts with K48-linked ubiquitin chains (Fatimababy *et al.*, 2010), whereas human RPN10 harbors two UIMs (UIM1 and UIM2) which are located towards its C-terminus and joined by a flexible linker region (Wang, Young and Walters, 2005; Kang *et al.*, 2007). UIM1 of human RPN10 is comparable with the yeast UIM. The human UIM2 has about a 5-fold higher affinity for ubiquitin than the UIM1 of RPN10 (Wang, Young and Walters, 2005). RPN13 has an N-terminal pleckstrin-like receptor of ubiquitin (PRU) domain, which shows a preference for the proximal ubiquitin of K48-linked chains (Schreiner *et al.*, 2008). An NMR study showed the concurrent interaction of RPN10 and RPN13 with a diubiquitin molecule whereby RPN13 and RPN10 preferably associated with respectively the proximal and distal ubiquitin moiety (Zhang *et al.*, 2009). It is however unclear whether this also occurs *in vivo*. In addition, proteasome structures obtained by electron microscopy revealed that RPN10 and RPN13 are located in the proteasome in such a way that

they could both interact simultaneously with the same ubiquitin chain, thereby positioning it to facilitate deubiquitination (Lasker *et al.*, 2012; Sakata *et al.*, 2012). Ubiquitination of RPN13 through 26S proteasome-bound Ub ligase Ube3c inhibits association with ubiquitinated substrates and inactivates proteasomes in response to proteotoxic stress (Besche *et al.*, 2014).

Instead of direct interaction with the intrinsic ubiquitin receptors of the proteasome, ubiquitinated substrates can also be shuttled to the proteasome by UBL-UBA proteins, such as RAD23 (hHR23a/b in human) (Chen and Madura, 2002; Elsasser *et al.*, 2004), Dsk2 (hPLIC-1/2 in humans) (Kleijnen *et al.*, 2000), or Ddi1 (Saeki *et al.*, 2002; Kaplun *et al.*, 2005). UBL-UBA proteins bind ubiquitin via their ubiquitin-associating (UBA) domain (Bertolaet *et al.*, 2001; Wilkinson *et al.*, 2001; Wang *et al.*, 2003) and the proteasome via their ubiquitin-like (UBL) domain (Hiyama *et al.*, 1999; Elsasser *et al.*, 2002; Walters *et al.*, 2002). The UBL/UBA proteins are called “shuttle” proteins because they may bind substrates remotely from the proteasome, and subsequently bring them to this complex. The UBL-UBA proteins interact only weakly with proteasomes and are usually substoichiometric components of purified proteasomes. They dock generally at proteasome subunit RPN1 (Elsasser *et al.*, 2002). Additionally, yeast Dsk2 and human RAD23 can interact with RPN10 and RPN13 (Hiyama *et al.*, 1999; Walters *et al.*, 2002; Husnjak *et al.*, 2008), and yeast Rad23 may also bind to Rpt1 and Rpt6 (Schauber *et al.*, 1998). *Drosophila* DSK2 interacts only with proteasomes which harbor the RPN10 ubiquitin receptor, as the interaction is lost in $\Delta p54/RPN10$ proteasomes, whereas yeast Dsk2 interacts only with $\Delta RPN10$ proteasomes (Lipinszki *et al.*, 2011). RPN10 and RPN13 are also major acceptors of mHR23B and ubiquilin-1/DSK2 and ubiquilin-4/ataxin-1 in mice (Hamazaki, Hirayama and Murata, 2015). Human RAD23 preferably recruits substrate with K48-linked ubiquitin chains to the proteasome (Raasi and Pickart, 2003; Nathan *et al.*, 2013), whereas the UBA domains of Dsk2- and Ddi1 do not show linkage specificity. The UBA domain of DSK2 has a significantly higher affinity to monoubiquitin as compared to the UBA domain of human Rad23 (Zhang, Raasi and Fushman, 2008). UBL-UBA proteins share redundant functions (Medicherla *et al.*, 2004; Díaz-Martínez *et al.*, 2006; Kang *et al.*, 2006), but they also have distinct roles, such as Rad23 in DNA repair (Schauber *et al.*, 1998) and Dsk2 in neuropathology (Mah *et al.*, 2000).

While it is clear that substrates can use two different pathways to bind to the proteasome, we still do not understand how substrates are assigned to one targeting pathway or the other. Additionally, the extent of crosstalk between both pathways is also yet unclear. Data obtained by electron microscopy and quantitative mass spectrometry suggest that there is a pool of proteasome complexes which do not contain the intrinsic receptors (Nickell *et al.*, 2009; Sakata *et al.*, 2012), which may suggest that the intrinsic ubiquitin receptors are not essential for all proteasomal substrates. Another factor which increases the complexity of this targeting system is the fact that RPN10 also exists as an extra-proteasomal protein (Matiuhin *et al.*, 2008; Piterman *et al.*, 2014). The function of the free pool of RPN10 is not yet clear. Matiuhin and colleagues showed that the pool of free RPN10 can inhibit the interaction of ubiquitin shuttle protein Dsk

with the proteasome complex in yeast (Matiuhin *et al.*, 2008). In contrast, Piterman and colleagues showed that mammalian RPN10 is only able to interact with ubiquitin and ubiquitin-like harboring proteins such as hPLIC-2 (the mammalian homologue of yeast Dsk2) when it is incorporated in the proteasome complex (Piterman *et al.*, 2014). Also, ubiquitin shuttling proteins can, instead of facilitating, oppose substrate degradation by the UPS (Ortolan *et al.*, 2000; Raasi and Pickart, 2003). Thus, further research is required to reveal the complex mechanisms of substrate recruitment to the 26S proteasome, which would provide useful information for elucidating physiological functions and specificities of each ubiquitin receptor.

Substrate processing

Ubiquitinated substrate proteins are bound to the proteasome via interactions with the intrinsic receptors RPN10 and RPN13 or with transiently bound shuttle receptors. The ATPase ring of the proteasome base then engages an unstructured initiation region in the substrate protein which tightens the interaction with the proteasome and uses ATP hydrolysis to unfold and translocate the polypeptide into the proteolytic chamber (Peth, Uchiki and Goldberg, 2010). Ubiquitin is concurrently removed from the substrate by deubiquitinating enzymes. Substrate degradation requires several consecutive conformational changes of the proteasome regulatory particle (Lander *et al.*, 2012). For every substrate turnover, the proteasome transitions from a substrate-free to a substrate-engaged state in which the latter facilitates translocation, unfolding and deubiquitination. The engaged state facilitates translocation of the substrate since the channel axis of the 20S core particle is better aligned with the ATPase ring, as compared with the substrate-free state. Finally, the proteasome must switch back to the substrate-free conformation for the engagement of a new substrate.

Three proteins are known to be involved in the deubiquitination of substrate of the mammalian proteasome: RPN11 (POH1 or PSMD14 in human), UCHL5 (also UCH37) and USP14 (Ubp6 in yeast). This set of DUBs is well conserved evolutionary with the exception of the lack of a recognizable UCHL5 ortholog in *S. cerevisiae*. Consequently, the most intensively studied proteasomal DUBs are RPN11 and USP14. Each of the proteasomal DUBs belongs to a different DUB family and are thus anciently diverged in evolution: RPN11, UCHL5 and USP14 belong to the JAMM, UCH and USP families, respectively. There are evident differences between these DUBs. RPN11, a constituent stoichiometric subunit of the proteasome, is the only essential DUB of the proteasome (Gallery *et al.*, 2007; Finley, 2009) and is critical for both the stability of the 26S proteasome complex and for the promotion of substrate degradation (Verma *et al.*, 2002; Yao & Cohen, 2002, chapter 4 of this thesis). Cross-linking studies on *Schizosaccharomyces pombe* co-localize the RPN11 C-terminal domain with the N-terminal end of RPT3 (Bohn *et al.*, 2010), potentially linking its activity to this ATPase. Insertion sequence insert-2 of RPN11 contributes to proteasome binding (Pathare *et al.*, 2014; Worden, Padovani and Martin, 2014), whereas insertion sequence insert-1 is involved in ubiquitin binding (Worden, Padovani and Martin, 2014). It was found that insert-1 exhibits a closed conformation stabilized

by RPN5 in the 19S cap prior to incorporation in a 26S complex, which inhibits the access of ubiquitin to free 19S caps (Dambacher *et al.*, 2016). In contrast, the insert-1 closed conformation is only weakly stabilized in the 26S proteasome substrate-free s1 ground state (Worden, Dong and Martin, 2017). Substrate engagement induces a conformational change of the entire 19S particle from the s1 state via s2 to finally the s3 substrate engaged state (Unverdorben *et al.*, 2014), in which RPN11 is repositioned directly above the translocation channel of the 20S complex (Matyskiela, Lander and Martin, 2013). Ubiquitin binding then induces a conformational change of the RPN11 insert-1 loop from an inactive closed state to an active open state, which is further accelerated by mechanical translocation of ubiquitinated substrate into the proteolytic core (Worden, Dong and Martin, 2017). Due to this acceleration, RPN11-dependent deubiquitination of engaged substrates was found to be about ~40 times faster as compared to pre-engaged substrates (Worden, Dong and Martin, 2017). RPN11 cleaves entire polyubiquitin chains at the proximal ubiquitin (Yao and Robert E. Cohen, 2002; M. J. Lee *et al.*, 2011) and does not confer ubiquitin linkage type specificity. Furthermore, deubiquitination by RPN11 is dependent on ATP hydrolysis by the proteasome base (Verma *et al.*, 2002; Yao and Robert E. Cohen, 2002). The timing of RPN11 deubiquitination activity is relatively late in the degradation process, *i.e.*, during substrate translocation, thereby probably avoiding premature substrate deubiquitination and release. On the other hand, UCHL5 and USP14 act already before the commitment step. UCHL5 is not essential for the structure and the activity of the proteasome (Elena Koulich, Xiaohua Li, 2008, chapter 4 of this thesis). UCHL5 is activated and recruited to the proteasome by ubiquitin receptor RPN13 (Hamazaki *et al.*, 2006; Qiu *et al.*, 2006; Yao *et al.*, 2006). Isolated UCHL5 displays an 8-fold increased catalytic activity when complexed with RPN13 compared to UCHL5 alone (VanderLinden *et al.*, 2015). The N-terminal catalytic UCH domain of UCHL5 contains active-site residues which can interact with ubiquitin (Burgie *et al.*, 2012). UCHL5 can only deubiquitinate proteins when it is in complex with the proteasome, in its free form it can only remove small peptides from the C-terminus of ubiquitin (Yao *et al.*, 2006). The role of UCHL5 in the proteasome has not yet been clearly defined. One suggestion is that UCHL5 performs an editing function by removing single ubiquitin moieties from the distal end of polyubiquitin chains which results in the release of substrate from the proteasome prior to degradation (Lam *et al.*, 1997). Another suggestion is that UCHL5 regulates proteasome activity via deubiquitination of proteasome subunits that can undergo regulatory ubiquitination (Jacobson *et al.*, 2014). Yet another suggestion is that UCHL5 clears unanchored polyubiquitin chains from proteasome-associated ubiquitin receptors (Zhang *et al.*, 2011). Lastly, deubiquitinating enzyme USP14 is a substoichiometric interactor of the proteasome and RNAi of USP14 does not affect proteasome stability (Elena Koulich, Xiaohua Li, 2008, chapter 4 of this thesis). USP14 interacts reversibly with the proteasome and is the most abundant proteasome interacting protein (PIP). Dependent on the study, Ubp6/USP14 interacts with about 10-40% of the proteasome 19S caps (Aufderheide *et al.*, 2015; Kim and Goldberg, 2017; Kuo and Goldberg, 2017). The DUB interacts via its N-terminal UBL domain with proteasome

subunit RPN1 (David S Leggett *et al.*, 2002; Rosenzweig *et al.*, 2012) whereby its catalytic USP domain is rather mobile (Aufderheide *et al.*, 2015). A substantial fraction of USP14 is not in complex with proteasomes (Elena Koulich, Xiaohua Li, 2008). Free USP14 is relatively inactive whereas its activity is enormously enhanced upon interaction with the purified proteasome base complex or the entire proteasome complex (David S Leggett *et al.*, 2002; Lee *et al.*, 2010). Hu *et al.*, found that the active site of free USP14 is present in a productive conformation, but the interaction of the active site with ubiquitin is inhibited by two loops, BL1 and BL2 (Hu *et al.*, 2005). Activation of USP14 can also (or further) be mediated via phosphorylation by the Akt protein kinase (Xu *et al.*, 2015). USP14 shows a preference for K11, K33 and K48 ubiquitin linkages (Flierman *et al.*, 2016). Recently it was found that the deubiquitinating activity of USP14 is enhanced when the proteasome switches from the substrate-free state towards the substrate engagement conformation (Bashore *et al.*, 2015). Ubiquitin-bound Ubp6/USP14 stabilizes this conformation to prevent a return to the substrate-free conformation while substrate is engaged for degradation. Polyubiquitin-bound USP14 also stimulates the ATPase rate of the proteasome and regulates channel opening of the 20S CP (Peth, Besche and Goldberg, 2009). Ubp6 is furthermore involved in RP assembly (Sakata *et al.*, 2011).

The current model couples the activity of RPN11 with the promotion of substrate degradation whereas the activity of UCHL5 and USP14 could counteract this process by trimming ubiquitin moieties from the distal end of the chains thereby detaching substrate from the proteasome prior to degradation (Lam *et al.*, 1997; Hu *et al.*, 2005; Lee *et al.*, 2010). However, recent findings of the lab of Andreas Martin reveal that Ubp6/USP14 is involved in the regulation of the 19S RP conformational changes and inhibition of RPN11 DUB activity. Their results suggest a degradation-facilitating role for Ubp6, rather than an inhibitory role, as USP14 is mainly active on already engaged substrate (Bashore *et al.*, 2015). For instance, they show with Ub-AMC substrates that Ubp6 is activated when its USP domain interacts with the proteasome ATPase base, probably as the result of conformational changes of two surface loops, BL1 and BL2, in the USP domain. The deubiquitinating activity of Ubp6 was then further increased when the proteasome switched to the ATP- γ S-induced substrate-engaged conformation, even in combination with RPN11 catalytic mutants, which suggests that Ubp6 is responsible for the enhanced deubiquitinating activity of the proteasome in the engaged state. Furthermore, by EM they showed that ubiquitin binding of Ubp6 stabilized the engaged state via interactions with both the N-ring and the AAA+ ring of the RPT subunits in the proteasome base, thereby preserving the coaxial alignment of both rings with the 20S core channel. In the engaged state ubiquitin-bound Ubp6 is placed in close proximity with RPN11. Biochemical assays showed that ubiquitin-bound Ubp6 inhibits the degradation-coupled DUB activity of RPN11 (Bashore *et al.*, 2015). Lastly, stabilization of the engaged state by ubiquitin-bound Ubp6 also prevented the engagement of subsequent substrates prior to ubiquitin dissociation. These results suggest a model in which substrate engagement induces conformational changes in the 19S RP which in

turn facilitate substrate unfolding, deubiquitination, translocation and degradation. Ubp6 plays two important roles in this process: Ubp6 can inhibit the deubiquitination activity of RPN11 and it can prevent the return to the substrate-free conformation. Inhibition of RPN11 might be a way to extend the time window in which Ubp6 can deubiquitinate the engaged substrate. This may be important to process complex substrates with multiple long and/or branched polyubiquitin chains that need to be co-translocationally trimmed (Bashore *et al.*, 2015). There are more studies which show contrasting USP14 functionalities compared to the ubiquitin editing model. It was for instance found that instead of removing single ubiquitin moieties, USP14 removes polyubiquitin chains en bloc until a single polyubiquitin chain remains on the substrate. Substrates might be spared from degradation when the remaining polyubiquitin chain is relatively short whereas a relatively long chain would be a target for RPN11-dependent deubiquitination followed by proteasomal degradation. After en bloc removal of polyubiquitin chains by RPN11 and subsequent translocation and degradation of the substrate, USP14/Ubp6 may trap the substrate-engaged state until it trimmed all remaining polyubiquitin chains of the just processed substrate, thereby maintaining the high levels of free ubiquitin. When all ubiquitin is removed, the proteasome can switch back to the substrate-free state. In this model Ubp6 thus facilitates protein degradation and confers clearance of proteasome-bound polyubiquitin chains during translocation (Lee *et al.*, 2016).

Ubiquitin proteasome system and disease

Cancer

Proteasome inhibitors have effective anti-tumor activity in cell culture, inducing apoptosis by disrupting the regulated degradation of pro-growth cell cycle proteins (Adams *et al.*, 1999). This approach of selectively inducing apoptosis in tumor cells has proven effective in animal models and human trials, although the development of drug resistance in relapsed patients is a problem (Tew, 2016). Lactacystin, a natural product synthesized by *Streptomyces* bacteria, was the first non-peptidic proteasome inhibitor discovered (Omura *et al.*, 1991) and is widely used as a research tool in biochemistry and cell biology. Lactacystin covalently modifies the amino-terminal threonine of catalytic β -subunits of the proteasome, particularly the $\beta 5$ subunit of the proteasome's chymotrypsin-like activity (Fenteany *et al.*, 1995). The discovery helped to establish the proteasome as a mechanistically novel class of protease: an amino-terminal threonine protease. Another commonly used proteasome inhibitor in laboratories is the peptide aldehyde MG132. MG132 binds to all beta subunits of the proteasome, thereby effectively blocking its proteolytic activity. MG132 inhibits the growth of tumor cells by inducing the cell cycle arrest as well as triggering apoptosis (Han and Park, 2010). Different mechanisms of apoptosis induction by MG132 are nicely reviewed (Guo and Peng, 2013). Bortezomib is the first proteasome inhibitor to reach clinical use as a chemotherapy agent and was brought to the market for the treatment of multiple myeloma (Adams and Kauffman, 2004; Richardson *et al.*, 2005). It reversibly inhibits the chymotrypsin-like activity of Prosbeta5 (Crawford *et al.*, 2006). This results

in a dysregulation of the ER-associated degradation (ERAD) pathway and induces the terminal Unfolded Protein Response (UPR), leading to apoptosis (Obeng *et al.*, 2006). Initially, Bortezomib may improve the outcome for myeloma patients, however relapses are frequent and patients often develop resistance against the therapy. Advances and challenges of the application of proteasome inhibitors in the clinic are nicely reviewed (Manasanch and Orlowski, 2017).

Neurodegenerative diseases

A characteristic of many neurodegenerative disorders, including Huntington's disease (HD), Alzheimer's disease (AD), Parkinson's disease (PD), and amyotrophic lateral sclerosis (ALS), is the accumulation of toxic protein species which results in the formation of protein inclusions and/or plaques in degenerating brains. This implies that protein homeostasis is poorly regulated in this type of diseases. Therefore, both autophagy and the UPS are topics of intense research in this field. There is currently no effective treatment that could cure or considerably delay the onset or progression of the neurodegenerative diseases described above. Drug development strategies aim to increase the proteolytic activity in the cell. For instance, the upregulation of proteasomal gene expression, upregulation of proteasome activators such as PA28 or PA200 or the identification of small molecules that can activate the CP. Another strategy is to enhance the targeting of disease-associated proteins to the proteasome by altering activities of relevant ubiquitin ligases or deubiquitinating enzymes.

References

- Adams, J. *et al.* (1999) 'Proteasome Inhibitors : A Novel Class of Potent and Effective Antitumor Agents', *Cancer Research*, 59, pp. 2615–2622.
- Adams, J. and Kauffman, M. (2004) 'Development of the Proteasome Inhibitor Velcade™ (Bortezomib)', *Cancer Investigation*, 22(2), pp. 304–311.
- Archer, C. T. *et al.* (2008) 'Physical and functional interactions of monoubiquitylated transactivators with the proteasome', *Journal of Biological Chemistry*. 283(31), pp. 21789–21798.
- Asano, S. *et al.* (2015) 'Proteasomes. A molecular census of 26S proteasomes in intact neurons', *Science*, 347(6220), pp. 439–443
- Aufderheide, A. *et al.* (2015) 'Structural characterization of the interaction of Ubp6 with the 26S proteasome.', *Proceedings of the National Academy of Sciences of the United States of America*, 112(28), pp. 8626–31.
- Bashore, C. *et al.* (2015) 'Ubp6 deubiquitinase controls conformational dynamics and substrate degradation of the 26S proteasome', *Nature Structural & Molecular Biology*. Nature Publishing Group, 22(9), pp. 712–719.
- Beck, F. *et al.* (2012) 'Near-atomic resolution structural model of the yeast 26S proteasome.', *Proceedings of the National Academy of Sciences of the United States of America*, 109(37), pp. 14870–5.
- Beckwith, R. *et al.* (2013) 'Reconstitution of the 26S proteasome reveals functional asymmetries in its AAA+ unfoldase.', *Nature structural molecular biology*, 20(10), pp. 1164–1172.

- Bedford, L. *et al.* (2011) 'Ubiquitin-like protein conjugation and the ubiquitin-proteasome system as drug targets', *Drug Discovery*, 10, pp. 29–46.
- Bertolaet, B. L. *et al.* (2001) 'UBA domains of DNA damage-inducible proteins interact with ubiquitin.', *Nature structural biology*, 8(5), pp. 417–422.
- Besche, H. C. *et al.* (2014) 'Autoubiquitination of the 26S Proteasome on Rpn13 Regulates Breakdown of Ubiquitin Conjugates', *The EMBO Journal*, 33, pp. 1159–1176.
- Bohn, S. *et al.* (2010) 'Structure of the 26S proteasome from *Schizosaccharomyces pombe* at subnanometer resolution', *Proceedings of the National Academy of Sciences of the United States of America*, 107(49), pp. 20992–20997.
- Braten, O. *et al.* (2016) 'Numerous proteins with unique characteristics are degraded by the 26S proteasome following monoubiquitination.', *Proceedings of the National Academy of Sciences of the United States of America*, 113(32), pp. E4639–47.
- Burgie, S. E. *et al.* (2012) 'Structural characterization of human Uch37', *Proteins: Structure, Function and Bioinformatics*, 80(2), pp. 649–654.
- Chen, L. and Madura, K. (2002) 'Rad23 Promotes the Targeting of Proteolytic Substrates to the Proteasome', *molecular and cellular biology*, 22(13), pp. 4902–4913.
- Chu-Ping, M. *et al.* (1994) 'Identification, purification, and characterization of a high molecular weight, ATP-dependent activator (PA700) of the 20 S proteasome.', *The Journal of biological chemistry*, 269(5), pp. 3539–3547.
- Ciechanover, A. and Brundin, P. (2003) 'Review The Ubiquitin Proteasome System in Neurodegenerative Diseases: Sometimes the Chicken, Sometimes the Egg', *Neuron*, 40, pp. 427–446.
- Collins, G. A. and Goldberg, A. L. (2017) 'The Logic of the 26S Proteasome', *Cell*, 169(5), pp. 792–806.
- Crawford, L. J. A. *et al.* (2006) 'Comparative Selectivity and Specificity of the Proteasome Inhibitors BzLLCOCOCHO, PS-341, and MG-132', *Cancer Res*, 66(12), pp. 6379–86.
- Dambacher, C. M. *et al.* (2016) 'Atomic structure of the 26S proteasome lid reveals the mechanism of deubiquitinase inhibition', *eLife*, 5(January), pp. 1–17.
- Deverauxf, Q. *et al.* (1994) 'A 26 S Protease Subunit That Binds Ubiquitin Conjugates*', *Journal of Biological Chemistry* 269(10), pp. 7059–7061.
- Díaz-Martínez, L. A. *et al.* (2006) 'Yeast UBL-UBA proteins have partially redundant functions in cell cycle control.', *Cell division*, 1(28), pp. 1–11.
- Dimova, N. V. *et al.* (2012) 'APC/C-mediated multiple monoubiquitylation provides an alternative degradation signal for cyclin B1', *Nature Cell Biology*, 14(2), pp. 168–176.
- Elena Koulich, Xiaohua Li, and G. N. D. (2008) 'Relative Structural and Functional Roles of Multiple Deubiquitylating Proteins Associated with Mammalian 26S Proteasome', *Molecular biology of the cell*, 19, pp. 1072–1082.
- Elsasser, S. *et al.* (2002) 'Proteasome subunit Rpn1 binds ubiquitin-like protein domains', *Nature Cell Biology*, 4(9), pp. 725–730.
- Elsasser, S. *et al.* (2004) 'Rad23 and Rpn10 serve as alternate ubiquitin receptors for the proteasome', *Journal of Biological Chemistry*, 279(26), pp. 26817–26822.
- Fatimababy, A. S. *et al.* (2010) 'Cross-species divergence of the major recognition pathways of ubiquitylated substrates for ubiquitin/26S proteasome-mediated proteolysis', *FEBS Journal*. Blackwell Publishing Ltd, 277(3), pp. 796–816.
- Fenteany, G. *et al.* (1995) 'Inhibition of proteasome activities and subunit-specific amino-terminal threonine modification by lactacystin', *Science*, 268(5211), pp. 726–731.
- Finley, D. (2009) 'Recognition and Processing of Ubiquitin-Protein Conjugates by the Proteasome', *Annual review of biochemistry*, pp. 477–513.
- Flierman, D. *et al.* (2016) 'Non-hydrolyzable Diubiquitin Probes Reveal Linkage-Specific

Reactivity of Deubiquitylating Enzymes Mediated by S2 Pockets', *Cell Chemical Biology*, 23(4), pp. 472–482.

Fort, P. *et al.* (2015) 'Evolution of proteasome regulators in Eukaryotes', *Genome Biology and Evolution*, 7(5), pp. 1363–1379.

Fu, H. *et al.* (1998) 'Multiubiquitin chain binding and protein degradation are mediated by distinct domains within the 26 S proteasome subunit Mcb1', *Journal of Biological Chemistry*, 273(4), pp. 1970–1981.

Gallery, M. *et al.* (2007) 'The JAMM motif of human deubiquitinase Poh1 is essential for cell viability', *Molecular Cancer Therapeutics*, 6(1), pp. 262–268.

Geng, F., Wenzel, S. and Tansey, W. P. (2012) 'Ubiquitin and Proteasomes in Transcription.', *Annual review of biochemistry*, 81, pp. 177–201.

Gille, C. *et al.* (2003) 'A comprehensive view on proteasomal sequences: Implications for the evolution of the proteasome', *Journal of Molecular Biology*, 326(5), pp. 1437–1448.

Glickman, M. H. *et al.* (1998) 'A subcomplex of the proteasome regulatory particle required for ubiquitin-conjugate degradation and related to the COP9-signalosome and eIF3', *Cell*, 94(5), pp. 615–623.

Goldberg, A. L. (2003) 'Protein degradation and protection against misfolded or damaged proteins', *Nature*, 426, pp. 895–899.

Groll, M. *et al.* (1997) 'Structure of 20S proteasome from yeast at 2.4 Å resolution.', *Nature*, pp. 463–471.

Guo, N. and Peng, Z. (2013) 'MG132, a proteasome inhibitor, induces apoptosis in tumor cells', *Asia-Pacific Journal of Clinical Oncology*, 9(1), pp. 6–11.

Hamazaki, J. *et al.* (2006) 'A novel proteasome interacting protein recruits the deubiquitinating enzyme UCH37 to 26S proteasomes', *The EMBO Journal*, 25(19), pp. 4524–4536.

Hamazaki, J. *et al.* (2007) 'Rpn10-Mediated Degradation of Ubiquitinated Proteins Is

Essential for Mouse Development', *molecular and cellular biology*, 27(19), pp. 6629–6638.

Hamazaki, J., Hirayama, S. and Murata, S. (2015) 'Redundant Roles of Rpn10 and Rpn13 in Recognition of Ubiquitinated Proteins and Cellular Homeostasis', *PLoS Genetics*, 11(7), pp. 1–20.

Han, Y. H. and Park, W. H. (2010) 'MG132, a proteasome inhibitor decreased the growth of Calu-6 lung cancer cells via apoptosis and GSH depletion', *Toxicology in Vitro*, 24(4), pp. 1237–1242.

Hirano, T. *et al.* (2011) 'Conformational Dynamics of Wild-type Lys-48-linked Diubiquitin in Solution'. *Journal of Biological Chemistry*, 286(43), pp. 37496–37502

Hiyama, H. *et al.* (1999) 'Interaction of hHR23 with S5a - the ubiquitin-like domain of hhr23 mediates interaction with s5a subunit of 26 s proteasome*', *The Journal of biological chemistry*, 274(39), pp. 28019–28025.

Hough, R., Pratt, G. and Rechsteiner, M. (1986) 'Ubiquitin-lysozyme conjugates. Identification and characterization of an ATP-dependent protease from rabbit reticulocyte lysates', *Journal of Biological Chemistry*, 261(5), pp. 2400–2408.

Hu, M. *et al.* (2005) 'Structure and mechanisms of the proteasome-associated deubiquitinating enzyme USP14', *The EMBO Journal*, 24(21), pp. 3747–3756.

Husnjak, K. *et al.* (2008) 'Proteasome subunit Rpn13 is a novel ubiquitin receptor', *Nature*, 453(7194), pp. 481–488.

Jacobson, A. D. *et al.* (2014) 'Autoregulation of the 26S proteasome by in situ ubiquitination.', *Molecular biology of the cell*, 25(12), pp. 1824–35.

Jin, L. *et al.* (2008) 'Mechanism of Ubiquitin-Chain Formation by the Human Anaphase-Promoting Complex', *Cell*, 133(4), pp. 653–665.

Kang, Y. *et al.* (2006) 'UBL/UBA ubiquitin receptor proteins bind a common tetraubiquitin chain', *Journal of Molecular Biology*, 356(4), pp. 1027–1035.

- Kang, Y. *et al.* (2007) 'Defining how Ubiquitin Receptors hHR23a and S5a Bind Polyubiquitin', *Journal of Molecular Biology*, 369(1), pp. 168–176.
- Kaplun, L. *et al.* (2005) 'The DNA Damage-Inducible UbL-UbA Protein Ddi1 Participates in Mec1-Mediated Degradation of Ho Endonuclease', *molecular and cellular biology*, 25(13), pp. 5355–5362.
- Kim, H. T. and Goldberg, A. L. (2017) 'The Deubiquitinating Enzyme Usp14 Allosterically Inhibits Multiple Proteasomal Activities and Ubiquitin-Independent Proteolysis.', *The Journal of biological chemistry*, (3), p. jbc.M116.763128.
- Kirkpatrick, D. S. *et al.* (2006) 'Quantitative analysis of in vitro ubiquitinated cyclin B1 reveals complex chain topology', *Nature Cell Biology*, 8(7), pp. 700–710.
- Kisselev, A. F., Akopian, T. N. and Goldberg, A. L. (1998) 'Range of Sizes of Peptide Products Generated during Degradation of Different Proteins by Archaeal Proteasomes*', *The Journal of biological chemistry*, 273(4), pp. 1982–1989.
- Kleijnen, M. F. *et al.* (2000) 'The hPLIC proteins may provide a link between the ubiquitination machinery and the proteasome.', *Molecular cell*, 6(2), pp. 409–419.
- Kloetzel, P.-M. (2004) 'The proteasome and MHC class I antigen processing', *Biochimica et Biophysica Acta*, 1695 pp.225-233
- Komander, D. *et al.* (2009) 'Molecular discrimination of structurally equivalent Lys 63-linked and linear polyubiquitin chains', *EMBO reports*, 10, pp. 466–473.
- Komander, D. and Rape, M. (2012) 'The Ubiquitin Code', *Annual Review of Biochemistry*, 81(1), pp. 203–229.
- Kostova, Z. and Wolf, D. H. (2003) 'For whom the bell tolls: Protein quality control of the endoplasmic reticulum and the ubiquitin-proteasome connection', *EMBO Journal*, pp. 2309–2317.
- Kravtsova-Ivantsiv, Y. and Ciechanover, a. (2012) 'Non-canonical ubiquitin-based signals for proteasomal degradation', *Journal of Cell Science*, 125(3), pp. 539–548.
- Kulathu, Y. and Komander, D. (2012) 'Atypical ubiquitylation — the unexplored world of polyubiquitin beyond Lys48 and Lys63 linkages', *Nature Reviews Molecular Cell Biology*, 13, pp. 508–523.
- Kuo, C.-L. and Goldberg, A. L. (2017) 'Ubiquitinated proteins promote the association of proteasomes with the deubiquitinating enzyme Usp14 and the ubiquitin ligase Ubc3c', *Proceedings of the National Academy of Sciences*, 114(17), pp. E3404–E3413.
- Lam, Y. A. *et al.* (1997) 'Editing of ubiquitin conjugates by an isopeptidase in the 26S proteasome.', *Nature*, pp. 737–740.
- Lam, Y. A. *et al.* (2002) 'A proteasomal ATPase subunit recognizes the polyubiquitin degradation signal', *Nature*, 416(6882), pp. 763–767.
- Lander, G. C. *et al.* (2012) 'Complete subunit architecture of the proteasome regulatory particle', *Nature*, 482(7384), pp. 186–191.
- Lasker, K. *et al.* (2012) 'Molecular architecture of the 26S proteasome holocomplex determined by an integrative approach.', *Proceedings of the National Academy of Sciences of the United States of America*, 109(5), pp. 1380–1387.
- Lee, B.-H. *et al.* (2010) 'Enhancement of proteasome activity by a small-molecule inhibitor of USP14', *Nature*. Nature Publishing Group, 467(7312), pp. 179–184.
- Lee, B.-H. *et al.* (2016) 'USP14 deubiquitinates proteasome-bound substrates that are ubiquitinated at multiple sites', *Nature*. Nature Publishing Group, pp. 1–16.
- Lee, M. J. *et al.* (2011) 'Trimming of ubiquitin chains by proteasome-associated deubiquitinating enzymes.', *Molecular & cellular proteomics: MCP*, 10(5), p. R110.003871.
- Leggett, D. S. *et al.* (2002) 'Multiple associated proteins regulate proteasome structure and function', *Molecular Cell*, 10(3), pp. 495–507.

- Lipinski, Z. *et al.* (2011) 'Overexpression of Dsk2/dUbqln results in severe developmental defects and lethality in *Drosophila melanogaster* that can be rescued by overexpression of the p54/Rpn10/S5a proteasomal subunit', *FEBS Journal*. Blackwell Publishing Ltd, 278(24), pp. 4833–4844.
- Liu, C.-W. *et al.* (2003) 'Endoproteolytic activity of the proteasome.', *Science*, 299(5605), pp. 408–11.
- Liu, C. *et al.* (2017) 'Ufd2p synthesizes branched ubiquitin chains to promote the degradation of substrates modified with atypical chains', *Nature Communications*, 8.
- Livneh, I. *et al.* (2017) 'Monoubiquitination joins polyubiquitination as an esteemed proteasomal targeting signal', *BioEssays*, 39(6), p. 1700027.
- Mah, A. L. *et al.* (2000) 'Identification of Ubiquilin, a Novel Presenilin Interactor That Increases Presenilin Protein Accumulation', *The Journal of Cell Biology*, 151(4), pp. 847–862.
- Manasanch, E. E. and Orlowski, R. Z. (2017) 'Proteasome inhibitors in cancer therapy', *Nature Reviews Clinical Oncology*, 14(7), pp. 417–433.
- Marques, A. J. *et al.* (2009) 'Catalytic mechanism and assembly of the proteasome', *Chemical Reviews*, 109(4), pp. 1509–1536.
- Matiuhin, Y. *et al.* (2008) 'Extrapolysomal Rpn10 Restricts Access of the Polyubiquitin-Binding Protein Dsk2 to Proteasome', *Molecular Cell*. Elsevier Inc., 32(3), pp. 415–425.
- Matyskiela, M. E., Lander, G. C. and Martin, A. (2013) 'Conformational switching of the 26S proteasome enables substrate degradation.', *Nature structural & molecular biology*. Nature Publishing Group, 20(7), pp. 781–8.
- Medicherla, B. *et al.* (2004) 'A genomic screen identifies Dsk2p and Rad23p as essential components of ER-associated degradation', *EMBO reports*, 5(7), pp. 692–697.
- Nathan, J. A. *et al.* (2013) 'Why do cellular proteins linked to K63-polyubiquitin chains not associate with proteasomes?' *The EMBO Journal*, 32, pp. 552–565.
- Nickell, S. *et al.* (2009) 'Insights into the molecular architecture of the 26S proteasome.', *Proceedings of the National Academy of Sciences of the United States of America*. National Academy of Sciences, 106(29), pp. 11943–7.
- Obeng, E. A. *et al.* (2006) 'Proteasome inhibitors induce a terminal unfolded protein response in multiple myeloma cells.', *Blood*, 107(12), pp. 4907–4916.
- Omura, S. *et al.* (1991) 'Lactacystin, a novel microbial metabolite, induces neuritogenesis of neuroblastoma cells.', *The Journal of antibiotics*, 44(1), pp. 113–6.
- Ortolan, T. G. *et al.* (2000) 'The DNA repair protein rad23 is a negative regulator of multi-ubiquitin chain assembly.', *Nature cell biology*, 2(9), pp. 601–8.
- Paraskevopoulos, K. *et al.* (2014) 'Dss1 is a 26S proteasome ubiquitin receptor', *Molecular Cell*, 56(3), pp. 453–461.
- Pathare, G. R. *et al.* (2014) 'Crystal structure of the proteasomal deubiquitylation module Rpn8-Rpn11', *Proceedings of the National Academy of Sciences*, 111(8), pp. 2984–2989.
- Peth, A., Besche, H. C. and Goldberg, A. L. (2009) 'Ubiquitinated Proteins Activate the Proteasome by Binding to Usp14/Ubp6, which Causes 20S Gate Opening', *Molecular Cell*, 36(5), pp. 794–804.
- Peth, A., Nathan, J. A. and Goldberg, A. L. (2013) 'The ATP Costs and Time Required to Degrade Ubiquitinated Proteins by the 26 S Proteasome *', *Journal of Biological Chemistry*, 288(40), pp. 29215–29222.
- Peth, A., Uchiki, T. and Goldberg, A. L. (2010) 'ATP-Dependent Steps in the Binding of Ubiquitin Conjugates to the 26S Proteasome that Commit to Degradation', *Molecular Cell*, 40, pp. 671–681.
- Piterman, R. *et al.* (2014) 'VWA domain of S5a restricts the ability to bind ubiquitin and Ubl to the 26S proteasome.', *Molecular biology of the cell*, 25(25), pp. 3988–98.
- Qiu, X. *et al.* (2006) 'hRpn13/ADRM1/GP110 is a novel proteasome subunit that binds the

deubiquitinating enzyme, UCH37', *The EMBO Journal*, 25(24), pp. 5742–5753.

Raasi, S. and Pickart, C. M. (2003) 'Rad23 ubiquitin-associated domains (UBA) inhibit 26 S proteasome-catalyzed proteolysis by sequestering lysine 48-linked polyubiquitin chains', *Journal of Biological Chemistry*, 278(11), pp. 8951–8959.

Richardson, P. G. *et al.* (2005) 'Bortezomib or High-Dose Dexamethasone for Relapsed Multiple Myeloma', *New England Journal of Medicine*, 352(24), pp. 2487–2498.

Rock, K. L. *et al.* (1994) 'Inhibitors of the Proteasome Block the Degradation of Most Cell Proteins and the Generation of Peptides Presented on MHC Class I Molecules', *Cell*, 78, pp. 761–771.

Rohaim, A. *et al.* (2012) 'Structure of a compact conformation of linear diubiquitin', *Acta Cryst*, 68, pp. 102–108.

Rosenzweig, R. *et al.* (2012) 'Rpn1 and Rpn2 coordinate ubiquitin processing factors at proteasome', *Journal of Biological Chemistry*, 287(18), pp. 14659–14671.

Ryabov, Y. and Fushman, D. (2006) 'Interdomain mobility in di-ubiquitin revealed by NMR', *Proteins: Structure, Function, and Bioinformatics*. Wiley Subscription Services, Inc., A Wiley Company, 63(4), pp. 787–796.

Saeki, Y. *et al.* (2002) 'Ubiquitin-like proteins and Rpn10 play cooperative roles in ubiquitin-dependent proteolysis', *Biochemical and Biophysical Research Communications*, 293(3), pp. 986–992.

Sakata, E. *et al.* (2011) 'The Catalytic Activity of Ubp6 Enhances Maturation of the Proteasomal Regulatory Particle', *Molecular Cell*, 42(5), pp. 637–649.

Sakata, E. *et al.* (2012) 'Localization of the proteasomal ubiquitin receptors Rpn10 and Rpn13 by electron cryomicroscopy', *Proceedings of the National Academy of Sciences of the United States of America*. National Academy of Sciences, 109(5), pp. 1479–84.

Schauber, C. *et al.* (1998) 'Rad23 links DNA repair to the ubiquitin/proteasome pathway.', *Nature*, 391(6668), pp. 715–718.

Schreiner, P. *et al.* (2008) 'Ubiquitin docking at the proteasome through a novel pleckstrin-homology domain interaction', *Nature*, 453(7194), pp. 548–552.

Schwartz, A. L. and Ciechanover, A. (2009) 'Targeting Proteins for Destruction by the Ubiquitin System: Implications for Human Pathobiology', *Annu. Rev. Pharmacol. Toxicol.*, 49, pp. 73–96.

Shi, Y. *et al.* (2016) 'Rpn1 provides adjacent receptor sites for substrate binding and deubiquitination by the proteasome.', *Science*, 351(6275), p. aad9421.

Sledz, P. *et al.* (2013) 'Structure of the 26S proteasome with ATP-gammaS bound provides insights into the mechanism of nucleotide-dependent substrate translocation', *Proceedings of the National Academy of Sciences of the United States of America*, 110(18), pp. 7264–7269.

Stadtmueller, B. and Hill, C. (2011) 'Proteasome Activators', *Mol Cell*, 41(1), pp. 8–19.

Swatek, K. N. and Komander, D. (2016) 'Ubiquitin modifications.', *Cell research*. Nature Publishing Group, 26(4), pp. 399–422.

Szlanka, T. *et al.* (2003) 'Deletion of proteasomal subunit S5a/Rpn10/p54 causes lethality, multiple mitotic defects and overexpression of proteasomal genes in *Drosophila melanogaster*', *Journal of Cell Science*, 116(6), pp. 1023–1033.

Tait, S. W. G. *et al.* (2007) 'Apoptosis induction by Bid requires unconventional ubiquitination and degradation of its N-terminal fragment', *Journal of Cell Biology*, 179, pp. 1453–1466.

Tatham, M. H. *et al.* (2008) 'RNF4 is a poly-SUMO-specific E3 ubiquitin ligase required for arsenic-induced PML degradation', *Nature Cell Biology*. Nature Publishing Group, 10(5), pp. 538–546.

Tenno, T. *et al.* (2004) 'Structural basis for distinct roles of Lys63- and Lys48-linked polyubiquitin

chains', *Genes to Cells*. Blackwell Science Ltd, 9(10), pp. 865–875.

Tew, K. D. (2016) 'Commentary on Proteasome Inhibitors: A Novel Class of Potent and Effective Antitumor Agents', *Cancer research*, 76(17), pp. 4916–7.

Thrower, J. S. *et al.* (2000) 'Recognition of the polyubiquitin proteolytic signal', *The EMBO Journal*, 19(1), pp. 94–102.

Tu, Y. *et al.* (2012) 'The Ubiquitin Proteasome Pathway (UPP) in the regulation of cell cycle control and DNA damage repair and its implication in tumorigenesis.', *International journal of clinical and experimental pathology*, 5(8), pp. 726–38.

Unno, M. *et al.* (2002) 'The structure of the mammalian 20S proteasome at 2.75 Å resolution', *Structure*, 10(5), pp. 609–618.

Unverdorben, P. *et al.* (2014) 'Deep classification of a large cryo-EM dataset defines the conformational landscape of the 26S proteasome.', *Proceedings of the National Academy of Sciences of the United States of America*, 111(15), pp. 5544–9.

VanderLinden, R. T. *et al.* (2015) 'Structural Basis for the Activation and Inhibition of the UCH37 Deubiquitylase', *Molecular Cell*. Elsevier, 57(5), pp. 901–911.

Varadan, R. *et al.* (2004) 'Solution Conformation of Lys63-linked Di-ubiquitin Chain Provides Clues to Functional Diversity of Polyubiquitin Signaling', *Journal of Biological Chemistry*, 279(8), pp. 7055–7063.

Verma, R. *et al.* (2002) 'Role of Rpn11 Metalloprotease in Deubiquitination and Degradation by the 26S Proteasome', *Science*, 298(5593), pp. 611–615.

Walters, K. J. *et al.* (2002) 'Structural studies of the interaction between ubiquitin family proteins and proteasome subunit S5a', *Biochemistry*, 41(6), pp. 1767–1777.

Walz, J. *et al.* (1998) '26S proteasome structure revealed by three-dimensional electron microscopy.', *Journal of structural biology*, 121(1), pp. 19–29.

Wang, Q. *et al.* (2003) 'Ubiquitin Recognition by the DNA Repair Protein hHR23a', *Biochemistry*, 42(46), pp. 13529–13535.

Wang, Q., Young, P. and Walters, K. J. (2005) 'Structure of S5a bound to monoubiquitin provides a model for polyubiquitin recognition', *Journal of Molecular Biology*, 348(3), pp. 727–739.

Wang, X., Herr, R. A. and Hansen, T. H. (2012) 'Ubiquitination of substrates by esterification', *Traffic*, pp. 19–24.

Wilkinson, C. R. *et al.* (2001) 'Proteins containing the UBA domain are able to bind to multi-ubiquitin chains.', *Nature Cell Biology*, 3(10), pp. 939–943.

Worden, E. J., Dong, K. C. and Martin, A. (2017) 'An AAA Motor-Driven Mechanical Switch in Rpn11 Controls Deubiquitination at the 26S Proteasome', *Molecular Cell*. Elsevier Inc., pp. 1–13.

Worden, E. J., Padovani, C. and Martin, A. (2014) 'Structure of the Rpn11-Rpn8 dimer reveals mechanisms of substrate deubiquitination during proteasomal degradation.', *Nature structural & molecular biology*. Nature Publishing Group, 21(3), pp. 220–7.

Xu, D. *et al.* (2015) 'Phosphorylation and activation of ubiquitin-specific protease-14 by Akt regulates the ubiquitin-proteasome system.', *eLife*, 4, p. e10510.

Xu, P. *et al.* (2009) 'Quantitative Proteomics Reveals the Function of Unconventional Ubiquitin Chains in Proteasomal Degradation', *Cell*, 137(1), pp. 133–145.

Yao, T. *et al.* (2006) 'Proteasome recruitment and activation of the Uch37 deubiquitinating enzyme by Adrm1', *Nature Cell Biology*, 8(9), pp. 994–1002.

Yao, T. and Cohen, R. E. (2002) 'A cryptic protease couples deubiquitination and degradation by the proteasome.', *Nature*, 419(6905), pp. 403–407.

Ying Lu, Byung-hoon Lee, Randall W King, Daniel Finley, and M. W. K. (2015) 'Substrate degradation by the proteasome: a single-molecule kinetic analysis', *Science*, 348(6231), pp. 1–20.

Zhang, D., Raasi, S. and Fushman, D. (2008) 'Affinity Makes the Difference: Nonselective Interaction of the UBA Domain of Ubiquilin-1 with Monomeric Ubiquitin and Polyubiquitin Chains', *Journal of Molecular Biology*, 377(1), pp. 162–180.

Zhang, N. *et al.* (2009) 'Structure of the S5a:K48-Linked Diubiquitin Complex and Its Interactions with Rpn13', *Molecular Cell*, 35(3), pp. 280–290.

Zhang, N. Y. *et al.* (2011) 'Ubiquitin chain trimming recycles the substrate binding sites of the 26 S proteasome and promotes degradation of lysine 48-linked polyubiquitin conjugates', *Journal of Biological Chemistry*, 286(29), pp. 25540–25546.

Scope of the Thesis

The proteasome is a protein complex mostly known for its role in the degradation of unneeded, damaged or misfolded proteins. The proteasome plays a central role in all cells and hence a widely studied protein assembly. Malfunctioning of this protein complex has major effects on cellular processes and is known to lead to the development of a variety of diseases such as cancer and neurodegenerative disorders. The proteasome is also an important target for drug discovery; for instance, proteasome inhibitors are used for the treatment of multiple myeloma. However, not much is known about the biological mechanisms behind these treatments. In this project we monitored the cellular responses in terms of protein abundance and protein ubiquitination dynamics upon proteasome malfunctioning (**Chapter 3**). In order to gain more insight into the specificity and function of individual proteasome complex components, we also manipulated single proteasome subunits, *i.e.*, the proteasome-bound deubiquitinating enzymes (DUBs) and monitored the effects on the cellular (modified) proteome (**Chapter 4**). The proteasome is a key player in maintaining a balance in proteostasis under both normal and abnormal cellular conditions. In order to gain further knowledge about the functioning of the proteasome under such conditions we characterized the proteasome interactome under different stress conditions, such as oxidative stress, endoplasmic reticulum stress and proteasome inhibition (**Chapter 5**). Large scale quantitative mass spectrometry is the central methodology applied in all studies described in this thesis. These types of global and unbiased approaches make it possible to study the relation of a protein complex with its direct cellular protein environment. In **Chapter 6** we have monitored changes in the cellular environment upon activation of ecdysone-responsive genes, in terms of global transcriptome and global proteome dynamics, as well as in terms of ecdysone-receptor interactome dynamics. As such, this work provides several clues to address the relationship between mRNA and protein abundances in *Drosophila*.

Chapter 1 gives a general introduction into the structure and function of the proteasome, while **Chapter 2** gives an introduction into quantitative mass spectrometry-based proteomics. In **Chapter 7** the results presented in this thesis are summarized and placed into context with the current literature. The research described in this thesis primarily contributes to the fundamental knowledge about proteasome functioning and the application of quantitative mass spectrometry-based proteomic approaches in biomedical research.

For several chapters supplementary information is provided online at the following location: www.proteomicscenter.nl/thesisSap

Chapter 2

Labeling Methods in Mass Spectrometry Based Quantitative Proteomics

Karen A. Sap and Jeroen A.A. Demmers

Published in Integrative Proteomics (2012), ISBN 978-953-51-0070-6

Introduction

Proteomics is loosely defined as the description of sets of proteins from any biological source, which have in most cases been identified by using mass spectrometry. However, only the mere identity of proteins present in a certain sample does not give any information about the dynamics of the proteome, involving relevant cellular events such as protein synthesis and degradation, or the formation of protein assemblies. In order to retrieve information on proteome dynamics, relative protein abundances between different protein samples should be assessed. Comparative or differential proteomics aims to identify *and* quantify proteins in different samples, to study *e.g.* differences between healthy and diseased states, mutant and wildtype cell lines, undifferentiated and differentiated cells, etc. Since mass spectrometry is in itself only a qualitative technique, various methods to obtain quantitative information of the proteome have been developed over the past decade and will be described in this Chapter.

We will focus on post-digestion labeling methods in the field of functional proteomics. Functional proteomics focuses on characterizing the composition of protein complexes, and generally involves the affinity purification of a protein of interest followed by the identification of co-purifying proteins by mass spectrometry (AP-MS). Generally, proteins in a negative control sample and those identified in the sample containing the protein of interest and its interacting partners are directly compared to determine which of the proteins interact in a specific manner. However, the mere presence or absence of a certain protein in protein data sets as a measure for either overlap or specificity is generally not sufficient, as this gives no information about the relative abundances of the present proteins. A generally recognized problem is the presence of contaminating proteins that are identified in the mass spectrometric screen, but do not really make part of the protein complex. Often, these background proteins are highly abundant proteins that stick to the complex or to beads to which the antibody is conjugated in a non-specific manner. A more accurate and correct approach would therefore involve a strategy in which protein abundance differences between sample and control can be assessed in a quantitative manner and which helps in discriminating *bona fide* interaction partners from such background proteins. Ideally, a differential mass spectrometric method would allow for an unbiased, sensitive, and high-throughput screening for protein-protein interaction networks.

SDS-PAGE based methods for protein quantitation

Two-dimensional sodium dodecylsulfate polyacrylamide gel electrophoresis (2D-SDS-PAGE) has traditionally been a popular method for differential-display proteomics on a global scale, although recently the popularity and applicability of stable isotope LC-MS based methods has exceeded those presented by gel based methods. 2D-SDS-PAGE based methods enable the separation of complex protein mixtures on a single gel. Proteins are separated in two dimensions: in the first dimension, they are fractionated according to their isoelectric point using a pH gradient gel, which is subsequently placed on a polyacrylamide gel slab for further separation

based on their molecular weight using SDS-PAGE. Proteins are then visualized by staining the gel with a dye such as Coomassie, silver or Sypro Ruby. In principle, for comparative issues, samples are loaded on separate gels and protein spot patterns are compared visually. Proteins that differ in abundance can then be punched out of the gel, digested with a suitable protease and analyzed by mass spectrometry. In a variation of this technique, difference gel electrophoresis (DIGE), proteins from two samples are first labeled with different fluorescent dyes and then mixed, making it possible to compare two different samples on a single gel. Two fluorescence images are recorded and overlayed, and differentially expressed proteins appear in only one of the images (Unlu et al., 1997). Limitations of this method include the manual selection of proteins to be analyzed, making it a time-consuming technique, as well as the limited sensitivity, as a consequence of which that proteins with a low concentration may be failed to be selected. Nowadays, in many laboratories there is a tendency to replace 2D-SDS-PAGE based methods by more powerful, LC-MS based methods for relative protein quantitation.

Protein and peptide quantitation using LC-MS based methods

Rather than by comparing protein spot intensities on a gel, quantification of proteins in LC/MS based methods is based on the peak height or area of the proteolytic peptide peaks in the mass spectrum and/or chromatogram. As mentioned before, mass spectrometry is not an inherently quantitative analytical technique, meaning that the peak height or area in a mass spectrum in itself does not accurately reflect the abundance of a peptide in the sample. The main reasons for this are the differences in ionization efficiency and detectability of peptides because of their different physicochemical characteristics, as well as the limited reproducibility of an LC-MS experiment. Altogether, this makes it difficult to compare peptide peak intensities between different mass spec runs. In principle however, peak intensity differences of the same analyte within one LC-MS run do accurately reflect the abundance difference. One way to distinguish the same analyte from different sample sources within one LC-MS experiment is by using stable heavy isotope labeling. When different stable isotope labels are used for proteins or peptides which are derived from different samples, the same analyte can in principle be quantified in one experiment. Such heavy stable isotope labels should in principle not affect the biophysical and chemical properties of peptides and proteins, but solely the mass, designating one of the samples as 'light' and the other sample 'heavy' according to the mass introduced by the label. The heavy and light peptides co-elute from the LC column at the same retention time and the heavy stable isotope leads to a mass shift in the mass spectrum, resulting in the observation of peak pairs. The peak heights or areas of such pairs can be compared and give an accurate reflection of the difference in abundance of this peptide between both samples. Heavy stable isotope labels can be introduced at different stages in the sample treatment protocol. Below, we will give an overview of the most widely used labeling techniques.

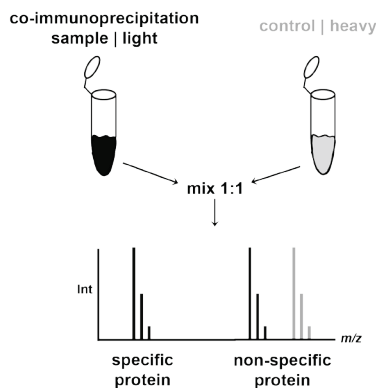


Figure 1. In a differential labeling AP-MS experiment, proteins in a control sample are labeled with a heavy stable isotope label, whereas proteins in the experimental sample are labeled with a light label. Incorporation of the heavy label results in a shift of the m/z value and allows one to differentiate between the sources of the protein of interest.

LC-MS-based quantitation methods

Incorporation of stable isotopes by metabolic labeling

Heavy stable isotope labels can be introduced *in vivo* by growing cells or even whole organisms in the presence of amino acids or nutrients carrying such stable isotopes. Metabolic labeling is often the preferred labeling technique, since incorporation occurs at the earliest possible moment in the sample preparation process, thereby minimizing the error in quantification (see Figure 2). Several methods based on metabolic labeling have been developed and here we will give a brief overview. The first metabolic labeling studies were performed utilizing ^{15}N -enriched media to grow *S. cerevisiae* (Oda et al., 1999) and *E. coli* (Conrads et al., 2001). Next, the method was extended towards multicellular organisms which were ^{15}N labeled, such as *D. melanogaster* and *C. elegans* by feeding them on labeled yeast or bacteria, respectively (Krijgsveld et al., 2003). Even a higher eukaryote like a rat has been labeled with ^{15}N (McClatchy et al., 2007). Plants, as they are autotrophic organisms, can easily be labeled metabolically through feeding of labeled inorganic compounds in the form of ^{15}N -nitrogen-containing salts, as first demonstrated in NMR studies (Ippel et al., 2004), and later in MS-based proteomics (Engelsberger et al., 2006; Lanquar et al., 2007). ^{15}N atoms are incorporated into the sample during cell growth, eventually replacing all natural isotopic (*i.e.*, ^{14}N) nitrogen atoms. The corresponding mass shift depends on the number of nitrogen atoms present in each of the resulting proteolytic peptides. However, this variable mass shift complicates data analysis to a large extent and requires high resolution mass spectrometry for the analysis (Conrads et al., 2001). Specific software for the analysis of ^{15}N labeled samples has been developed (Mortensen et al., 2010).

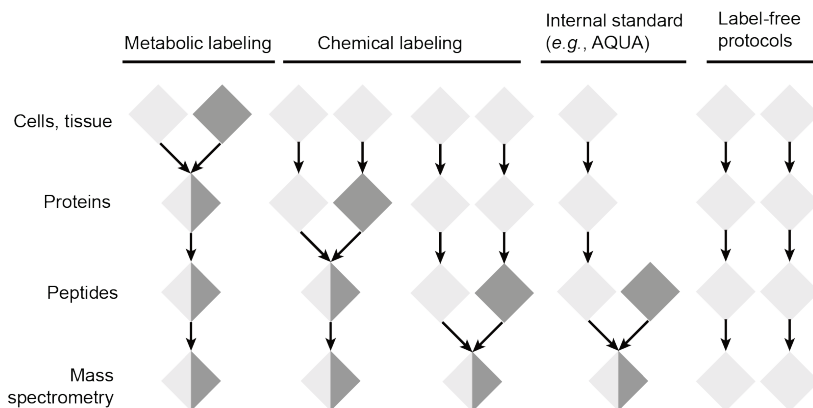


Figure 2. Stages of incorporation of stable isotope labels in typical labeling workflows in quantitative proteomics. The light and dark grey diamonds represent the two protein samples to be differentially labeled and compared. Figure adapted from (Ong & Mann, 2005).

Stable isotope labeling in cell culture (SILAC) is a metabolic labeling approach first published in 2002 by the lab of Matthias Mann (Ong et al., 2002). During cell growth, essential amino acids that carry heavy stable isotopes and which have been added to the culturing medium are introduced in all newly synthesized proteins. After several cell doublings, the complete cellular proteome will have incorporated the supplied labeled amino acid(s). This results in a shift of the proteolytic peptide mass after protein digestion and subsequent MS analysis. When labeled and non-labeled cell cultures are now mixed and analyzed in the same experiment, peptides will be represented by peak pairs in the mass spectrum, where the mass difference will depend on the number and nature of the labeled amino acid(s). Usually, labeled lysine and arginine are used, with the result that every peptide will carry a label except for the carboxyl-terminal peptide of the protein, when digested with trypsin, as does labeling with lysine when digested with Lys-C (Ibarrola et al., 2003). In contrast to ^{15}N labeling, the number of incorporated labels in SILAC is defined and not dependent on the peptide sequence, thus facilitating data analysis. SILAC has been successfully applied in global proteome studies (de Godoy et al., 2006), for functional proteomics assays, as well as for the study of post-translational modifications (Blagoev et al., 2003; Blagoev & Mann, 2006).

Because of the label incorporation at early stages in the sample preparation protocol, SILAC is generally the preferred choice of labeling method. However, SILAC is limited in sample applicability, for example, not every cell line can grow in an efficient manner in media optimized for SILAC, often due to the requirement of dialyzed serum in the medium to prevent contamination with natural amino acids. Besides, the method may be hampered by *in vitro* conversion of labeled arginine to proline (Van Hoof et al., 2007). SILAC has been used to label

higher organisms, for instance flies (Sury et al., 2010) and mice (Kruger et al., 2008), by feeding them with labeled food. In general though, this is a time consuming and expensive process. In the plant, SILAC has only yielded label incorporation of approximately 70% (Gruhler et al., 2005), which is not satisfying for many proteomics applications. Moreover, there are practical and moral limitations to SILAC labeling of human tissue. For these cases, methods for stable isotope label incorporation at a later stage in the sample preparation protocol are required. Chemical and enzymatic labeling techniques have been developed that can introduce the heavy stable isotope label only after sample collection and proteolytic digestion at the peptide level.

Incorporation of stable heavy isotope labels by chemical or enzymatic labeling

In general, the advantage of chemical labeling over metabolic labeling is the possibility to label a wide range of different sample types, since incorporation of the label is performed only after harvesting cells and subsequent purification of proteins. Chemical labeling is essentially based on similar mechanisms as metabolic labeling, except that the label is introduced into proteins or peptides by a chemical reaction, *e.g.*, with sulfhydryl groups or amine groups, or through acetylation or esterification of amino acid residues. Alternatively, the heavy stable isotope label can be introduced into the peptide during an enzymatic reaction with heavy water (H_2^{18}O). Below, several of the most widely applied chemical and enzymatic labeling approaches are described.

Isotope-Coded Affinity Tags (ICAT)

Isotope-Coded Affinity Tagging (ICAT) is a chemical labeling method that was first described by the Aebersold lab in 1999 (Gygi et al., 1999). In chemical modification-based approaches, stable isotope-bearing chemical reagents are targeted towards reactive sites on a protein or peptide. The ICAT reagent consists of a reactive group that is cysteine-directed, a polyether linker region with eight deuteriums, and a biotin group that allows purification of labeled peptides. In an ICAT experiment, two pools of proteins are denatured and reduced, and the cysteine residues of the proteins are subsequently derivatized with either the 'heavy' or 'light' ICAT reagent. The labeled pools are then combined, cleaned up to remove excess reagent, and digested with an appropriate protease. The cysteine-containing peptides, carrying 'heavy' and 'light' isotope tags, are then captured on an avidin column via the biotin moiety present at the incorporated label. Peptides are then eluted from the column and analyzed by mass spectrometry. Since only cysteine-containing peptides are isolated, the peptide mixture complexity is in general limited, which in principle would enable identification of lower abundant proteins. On the other hand, some proteins contain no cysteines, while others would have to be quantified on the basis of just a single peptide. Additionally, the large biotin tag significantly increases the complexity of fragmentation spectra, complicating peptide identification, and, besides that, it has been demonstrated that deuterium atoms that are associated with the tag can cause a shift in retention time between the light and heavy peptides in reverse phase chromatography (Zhang et al., 2001). Subsequent iterations of the ICAT approach by

substituting a cleavable and co-eluting tag have improved the method (Hansen et al., 2003; Li et al., 2003).

Dimethyl labeling

An alternative method based on chemical labeling is dimethylation of peptides. In this workflow, samples are first digested with proteases such as trypsin and the derived peptides of the different samples are then labeled with isotopomeric dimethyl labels. The labeled samples are mixed and simultaneously analyzed by LC-MS whereby the mass difference of the dimethyl labels is used to compare the peptide abundance in the different samples. Stable isotope labeling by dimethylation is based on the reaction of peptide primary amines (peptide N-termini and the epsilon amino group of lysine residues) with formaldehyde to generate a Schiff base that is rapidly reduced by the addition of cyanoborohydride to the mixture. These reactions occur optimally between pH 5 and 8.5. Dimethyl labeling can be used as a triplex reagent, making it possible to quantitatively analyze three different samples in a single MS run. Labeling with the light reagent generates a mass increase of 28 Da per primary amine on a peptide and is obtained by using regular formaldehyde and cyanoborohydride. Using deuterated formaldehyde in combination with regular cyanoborohydride generates a mass increase of 32 Da per primary amine; this is referred to as the intermediate label (Hsu et al., 2003). Incorporation of the heavy label can be achieved through combining deuterated and ^{13}C -labeled formaldehyde with cyanoborodeuteride, resulting in a mass increase of 36 Da (Boersema et al., 2008). These reactions are visualized in Figure 3.

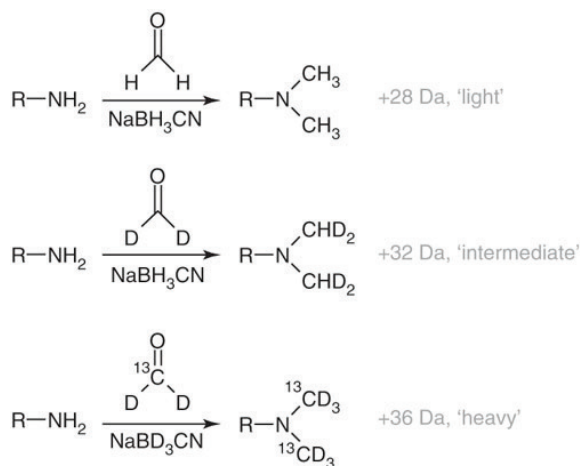


Figure 3. Labeling schemes of triplex stable isotope dimethyl labeling. R: remainder of the peptide. Figure adapted from (Boersema et al., 2008).

One drawback of the incorporation of deuterium is that deuterated peptides show a small but significant retention time difference in reversed phase chromatography compared to their non-deuterated counterparts (Zhang et al., 2001). This complicates data analysis because the relative quantities of the two peptide species cannot be determined accurately from one spectrum but requires integration across the chromatographic time scale. As the stable isotope dimethyl labeling is performed at the peptide level, the method is not subjected to restrictions on the origin of the biological sample. Stable isotope dimethyl labeling can be performed in up to 8M urea, as well as after in-gel digestion protocols. It should be noted that during the sample preparation workflow, no buffers and solutions containing primary amines (such as ammonium bicarbonate and Tris) ought to be used, as formaldehyde would react with these, which would affect the labeling efficiency. This can be circumvented by desalting the peptide sample before the labeling reaction or by performing the digestion in buffers without primary amines (*e.g.*, triethyl ammonium bicarbonate (TEAB)). Since both the peptide N-termini and lysine side chain amino groups are labeled in this protocol, it is compatible with the peptide products of virtually any protease, such as trypsin, Lys-C, Lys-N, Arg-C, and V8 (Boersema et al., 2008). Typically, for proteomics experiments trypsin is used, which cleaves C-terminal of lysine and arginine residues. Labeling of tryptic peptides using the method described here results in a mass shift of either 4 Da (when cleaved after an arginine residue) or 8 Da (when cleaved after a lysine residue) between the light and intermediate and between the intermediate and heavy label. Differential labeling of peptides resulting from digestion with Lys-C or Lys-N (cleaving respectively C- and N-terminal of lysine residues) will result in a mass difference of mainly 8 Da (both the N-terminus and the lysine residues are labeled), whereas peptide products from Arg-C and V8 will result in varying mass differences as the number of lysine residues per peptide will typically vary. After proteolytic digestion, the samples are labeled separately by incubation with CH_2O and NaBH_3CN (light), CD_2O and NaBH_3CN (intermediate) or $^{13}\text{CD}_2\text{O}$ and NaBD_3CN (heavy).

Boersema and co-workers have described three different experimental protocols for dimethyl labeling, *i.e.* in-solution, online, and on-column (Boersema et al., 2009). In-solution labeling (Boersema et al., 2008; Hsu et al., 2003) can be used for sample amounts from 1 μg to several milligrams of sample and is most suitable for experiments in which large sample numbers have to be labeled since labeling can be performed in parallel here. Online stable isotope labeling is the optimal method for the labeling of small quantities ($< 1 \mu\text{g}$) of sample, because the sample loss is diminished by combining sample clean-up and labeling and by performing LC-MS directly after labeling. Finally, the on-column stable isotope labeling method is most suited for larger (up to milligrams) sample amounts, as sample clean-up and labeling steps are combined and the quenching step is avoided. After labeling, the samples are mixed and analyzed by mass spectrometry. Finally, quantification is performed by comparing the signal intensities of the differentially labeled peptides (see section on Data Analysis).

Protein quantitation by dimethyl labeling has been applied in a variety of studies, *e.g.* for the investigation of tyrosine phosphorylation sites in HeLa cells upon EGF stimulation (Boersema et al., 2010). Proteins in a HeLa cell extract were dimethyl labeled and subsequently enriched for phosphorylated-tyrosine-containing peptides using immunoaffinity assays. Several tens of unique phosphotyrosine peptides were found to be regulated by EGF, illustrating that such a targeted quantitative phosphoproteomics approach has the potential to study signaling events in detail. Furthermore, the method has been applied to unravel differences in composition between highly related protein complexes, such as tissue-specific bovine proteasomes (Raijmakers et al., 2008) and the yeast nuclear and cytoplasmic exosome protein complex (Synowsky et al., 2009).

In conclusion, dimethyl labeling is a reliable, cost-effective and undemanding procedure that can be easily automated and applied in high-throughput proteomics experiments. It is applicable to virtually any sample, including tissue samples derived from animals or humans and up to three samples can be analyzed simultaneously. Like other chemical labeling methods though, stable isotope dimethyl labeling is performed in one of the final steps of a typical proteomics workflow and is therefore more prone to errors in the quantitative analysis as compared to workflows in which the label is added at an earlier stage.

¹⁸O labeling

¹⁸O labeling relies on class-2 proteases, such as trypsin, to catalyze the exchange of two ¹⁶O atoms for two ¹⁸O atoms at the C-terminal carboxyl group of proteolytic peptides, resulting in a mass shift of 4 Da between differently labeled peptides, as illustrated in Figure 4.

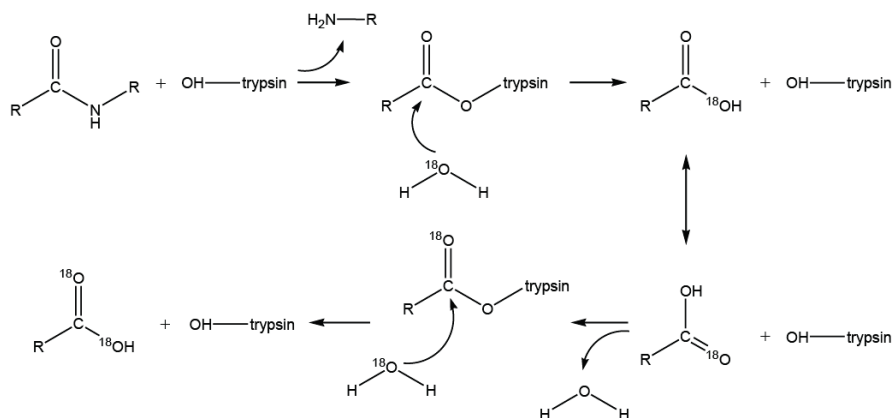


Figure 4. Principle of trypsin catalyzed ¹⁸O labeling. Incorporation of two ¹⁸O labels at the C-terminus of a tryptic peptide takes place in a two-step reaction.

Hydrolysis of a protein in H_2^{18}O by a protease results in the incorporation of one ^{18}O atom into the carboxyl terminus of each proteolytically generated peptide. This mechanism involves a nucleophilic attack by a solvent water molecule on the carbonyl carbon of the scissile peptide bond (reaction 1). Following this hydrolysis reaction, the protease incorporates one more ^{18}O atom into the carboxyl terminus of the proteolytically generated peptide. This second incorporation results in two ^{18}O atoms being incorporated into the carboxyl terminus of the peptides (reaction 2). The second ^{18}O atom-incorporation is essentially the reverse reaction of peptide-bond hydrolysis or the peptide-bond formation reaction (Miyagi & Rao, 2007).

Proteolytic ^{18}O labeling has shown to be a useful tool in the field of comparative proteomics. A number of studies have been published, involving among others relative protein quantitation of the virus proteome (Yao et al., 2001), proteomes of cultured cells (Blonder et al., 2005; Brown & Fenselau, 2004; Rao et al., 2005) and proteins in serum (Hood, Lucas et al., 2005; Qian et al., 2005) and tissues (Hood, Darfler et al., 2005; Zang et al., 2004). In addition, ^{18}O labeling has been used for the relative quantitation of post-translational modification, *e.g.* changes of protein phosphorylation in response to a stimulus (Bonenfant et al., 2003). In the latter study, pools of differentially labeled phosphorylated proteins were enriched by using immobilized metal-affinity chromatography. Peptides were then dephosphorylated by alkaline phosphatase in order to quantify the changes in phosphorylation by mass spectrometry. A similar approach has been used for the global phosphoproteome analysis of human HepG2 cells (Gevaert et al., 2005).

Despite its relatively simple mechanism and low costs, ^{18}O labeling has not become the preferred method for differential proteomics based on heavy stable isotope labeling. The practical difficulties involved, most importantly the occurrence of incomplete incorporation of two ^{18}O atoms into the proteolytic peptide, and, as a consequence, the difficulties in data analysis and interpretation are the most likely reasons for this. Several factors are responsible for the variable degree of ^{18}O incorporation, including variable enzyme substrate specificity, oxygen back exchange, pH dependency and peptide physicochemical properties. To overcome inefficient labeling, algorithms for the correction of ^{18}O labeling efficiency have been developed (Ramos-Fernandez et al., 2007), while other studies have focused on minimizing back exchange of ^{18}O to ^{16}O . It was found that the latter can be achieved by either decreasing the pH value for trypsin catalyzed incorporation reactions (Hajkova et al., 2006; Staes et al., 2004; Zang et al., 2004), or by using immobilized trypsin for the exchange reaction (Chen et al., 2005; Fenselau & Yao, 2007; Sevinsky et al., 2007). Trypsin immobilization allows the investigator to significantly increase the molar ratio of protease-to-substrate ratio, which subsequently increases the labeling efficiency. Another advantage of using immobilized proteases is that no protease-catalyzed oxygen back exchange reaction occurs, because the immobilized proteases are completely removed from the peptides after the labeling reaction.

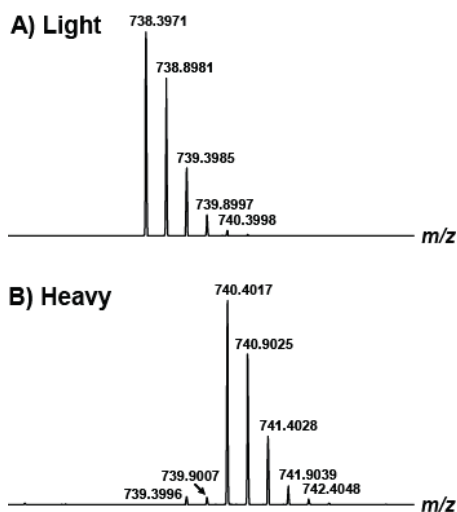


Figure 5. Doubly charged tryptic peptide FLEQQNQVLQTK A) in the absence of ^{18}O label and B) after incorporation of the label. The two-step labeling reaction in the presence of immobilized trypsin as described here ultimately results in the complete incorporation of two ^{18}O labels, with no intermediary products present. The peptide isotope peaks in B) at m/z 739.39 and 739.90 are due to impurities of commercial H_2^{18}O , containing only 97% ^{18}O .

Our lab has developed a two-step approach in order to completely label all proteolytic peptides (Bezstarosti et al., 2010). In this method, proteins are first digested with soluble trypsin. Subsequently, proteolytic peptides are incubated with H_2^{18}O at pH 4.5 in the presence of immobilized trypsin. Clearly, no singly ^{18}O labeled variants were observed in any of the peptide mass spectra (see Figure 5), indicating that no partial labeling whatsoever occurred, nor did any back exchange from ^{18}O to ^{16}O take place during sample treatment or analysis. Thus, complete incorporation of two ^{18}O labels into each of the tryptic peptides in a mixture can be achieved routinely.

It was shown in this study that ^{18}O labeling can be applied in a functional proteomics assay to discriminate background proteins from specific interactors of a protein of interest. Generally, controls are heavy labeled and the coimmunoprecipitation (co-IP) sample is labeled light. Specific interactors are expected not to be present in the control and would thus have a ratio of (close to) zero, whereas background proteins would show heavy-to-light (H:L) ratios of (close to) 1 (Figure 1). ^{18}O labeling was used in order to differentiate between non-specific background proteins and specific, *bona fide* interactors of the Cyclin dependent kinase 9 (Cdk9) purified from nuclear extracts of murine erythroleukemia (MEL) cells. Biotinylated Cdk9 was expressed in MEL cells and purified using streptavidin beads under relatively mild conditions (de Boer et al.,

2003). The proteins that co-purified with Cdk9 were washed and digested with trypsin while still bound to the beads and subsequently identified by tandem mass spectrometry. A control sample was taken following the same procedure from an equal number of cells, but using non-transfected MEL cells. Proteolytic peptides from the control sample were then labeled using H_2^{18}O in the two-step approach mentioned earlier, while proteolytic peptides from the Cdk9 pulldown sample underwent the same procedure with unlabeled H_2O . The peptide mixtures were dissolved in equal volumes of buffer, mixed in a 1:1 volume ratio and identified by LC-MS/MS. H:L ratios were calculated for all proteins identified from the mixed sample. As expected, H:L ratios of close to 1 were observed for typical background proteins, such as ribosomal, housekeeping, and structural proteins, which were present as non-specific background proteins (see Figure 6). In contrast, among the proteins that were quantified with H:L ratios close to 0, indicating specificity for the Cdk9 co-immunopurification sample, the far majority of interacting proteins that have been described in different studies in the literature were identified in a single experiment, as well as several novel interaction partners of diverse functionalities, suggesting putative additional roles for Cdk9 in various nuclear events such as transcription and cell cycle control (Bezstarosti et al., 2010). It was shown in this study that complete ^{18}O labeling of peptides in complex mixtures can be routinely achieved. This greatly simplifies the analysis of peak intensity ratios, since only two components (*i.e.*, 'light' and 'heavy') need to be considered and no correction algorithms have to be applied to convert peak intensities of intermediately labeled peptide species.

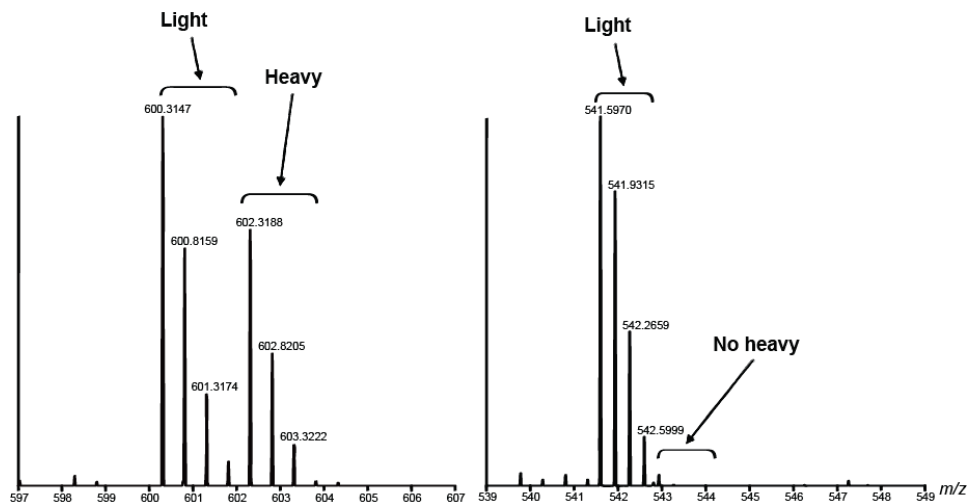


Figure 6. MS spectra of two tryptic peptides from a 1:1 mixture of a digest of a Cdk9 co-IP experiment (H_2^{16}O) and a control sample (in H_2^{18}O). (A) Doubly charged peptide LGTPELSPTER of the contaminant acetyl-CoA carboxylase shows both the “light” and “heavy” forms and is therefore marked as a nonspecific protein. (B) Triply charged peptide GPPEETGAAVFDHPAK of cyclin T1 is only present in the “light” form and is therefore specific for the Cdk9 sample (see (Bezstarosti et al., 2010)).

Labeling with isobaric tags

Metabolic labeling, ICAT, enzymatic labeling and most other chemical labeling approaches for relative quantification are based on the mass difference between differentially labeled peptides. There are, however, some limitations imposed by mass difference labeling. The mass difference concept of many practical purposes is limited to a binary (2-plex) or ternary (3-plex) set of reagents; higher order multiplexing would increase the complexity of MS¹ spectra too much. This limitation makes comparison of multiple states difficult to undertake. Therefore, multiplexed sets of reagents for quantitative protein analysis have been developed. The isobaric tag for relative and absolute quantitation (iTRAQ) (Ross et al., 2004) and tandem mass tag (TMT) (Thompson et al., 2003) technologies are commercially available isobaric mass tagging reagents and protocols (Figure 7).

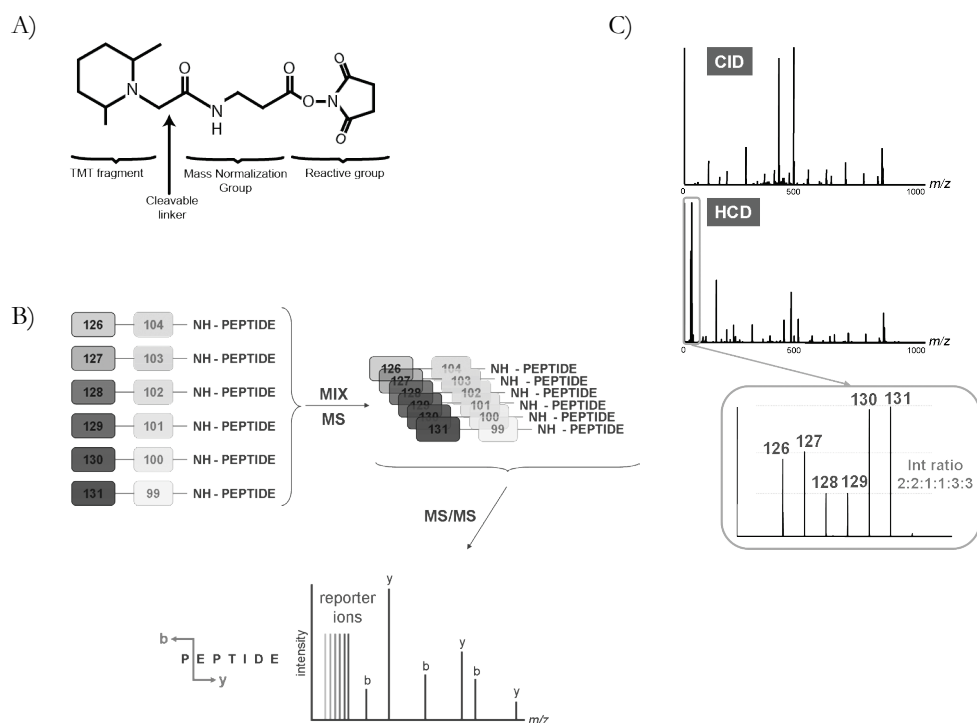


Figure 7. A) Chemical structure of the TMT tag. The 6-plex tags have different distributions of the stable heavy isotopes of carbon and nitrogen in the molecule, resulting in different fragmentation spectra. B) A peptide that is present in 6 different samples is differentially labeled with a 6-plex TMT tag, containing reporter-balancer combinations, resulting in all conjugated peptides having the same m/z value. Upon high energy collision dissociation (HCD), the differentially labeled peptides show identical b and y fragment ions, but the reporter ion masses in the low m/z region are different. C) As an example, a protein was

labeled in a 6-plex (TMT-126 through TMT-131) protocol and mixed in a 2:2:1:1:3:3 ratio. The resulting reporter ion intensity ratios show an excellent correlation with the mixing ratios. Panels A and C were adapted from (Thompson et al., 2003).

In these procedures, both N-termini and lysine side chains of peptides in a digest mixture are labeled with different isobaric mass reagents in such a way that all derivatized peptides are isobaric and chromatographically indistinguishable. Only upon peptide fragmentation can the different mass tags be distinguished. As each tag adds the same total mass to a given peptide, each peptide species produces only a single peak during liquid chromatography, even when two or more samples are mixed. Thus, there will be only one peak in the MS¹ scan, and, therefore, only a single m/z will be isolated for fragmentation. The different mass tags only separate upon fragmentation, when reporter ions that are typical for each of the different labels are generated. These reporter ions are in the low mass range, which usually is not covered by typical peptide fragment ions. The intensity ratio of the different reporter ions is used as a quantitative readout. Thus, quantitation in combination with isobaric mass tagging is based on peptide fragmentation (MS²) spectra rather than on the survey scans and quantitative accuracy will depend on the isolation width of precursor ions for fragmentation, since all ions isolated in that window will contribute to fragments in the reporter ion mass ranges. One drawback of such a method is that often only a single fragmentation spectrum per peptide is available, while in quantitation based MS¹ scans, usually several data points across the eluting peptide peak are sampled, which may result in a lower overall sensitivity.

Label free quantitation

Over the past few years, mainly as a result of constantly improving LC-MS equipment, there has been growing interest in the use of label-free approaches for quantitative proteomic analysis (see (Neilson et al., 2011) for a recent review). In a label free quantitative proteomic analysis, protein mixtures are analyzed directly and samples are compared to each other after independent analyses. As a result, there is no mixing of samples, so that higher proteome coverage can be achieved and there is no limit to the number of experiments that can be compared (Bantscheff et al., 2007). The disadvantage of this approach is a lack of a formal internal standard, which can lead to greater error in individual datasets but is minimized through the analysis of several biological replicates.

Label-free approaches may be divided into two main groups by the way that the abundance of a peptide is measured. The first group comprises methods that are based on the ion count and compare either maximum abundance or volume of ion count for peptide peaks at specific retention times between different samples (Chelius & Bondarenko, 2002; Listgarten & Emili, 2005; Silva et al., 2005; Wiener et al., 2004). As ionized peptides elute from a reversed-phase column into the mass spectrometer, their ion intensities can be measured within the given detection limits of the experimental setup. Although this method is relatively straightforward

conceptually, several considerations must be taken into account to ensure reproducible and accurate detection and quantitation between individual sample runs. Concerns with LC signal resolution can arise when peptide signals are spread over a large retention time range causing overlap with co-eluting peptides. Similar concerns include biological variations resulting in multiple signals for the same peptide as well as technical variations in retention time, MS intensity, and sample background noise from chemical interference. These aspects of quantitation based on 'area under the curve' necessitate a computational 'clean up' of the raw LC-MS data (Neilson et al., 2011).

The second group is based on the identification of peptides by MS/MS and uses sampling statistics such as peptide count, spectral counts (Lundgren et al., 2010), or sequence coverage to quantify the differences between samples (Choi et al., 2008; Liu et al., 2004; Old et al., 2005; Rappsilber et al., 2002). For protein quantification based on spectrum counting, the data processing steps are basically identical to the general protein identification workflow in proteomics, which is one of the reasons why this approach has become so popular. The rationale behind this quantitation method is that more abundant proteins are sampled more often in fragment ion scans than are low abundance peptides or proteins. Obviously, the outcome of spectrum counting depends on the settings of data-dependent acquisition on the mass spectrometer. In particular the linear range for quantitation and the number of proteins to be quantified are influenced by different settings for dynamic exclusion (Wang & Li, 2008); the optimal settings will depend on sample complexity. The most significant disadvantage of spectrum counting is that it behaves very poorly with proteins of low abundance and few spectra. The accuracy of the spectrum count method, especially for low abundance proteins, suffers from the fact that each spectrum is scored independently of its ion intensities.

Comparison of different methods for quantitation

With the existence of a wide variety of LC-MS based quantitation methods, it may be hard to decide which approach to utilize for a certain application. As described earlier, each approach has its own strengths and limitations, and, additionally, other factors may play a role, such as available equipment, level of experience and budget. In the following section we summarize the pros and cons of earlier described quantitation methods which might serve as a guidance to decide which approach is most suitable in a specific situation.

Metabolic labeling

If it is possible to label samples metabolically, this would be the most advantageous option to quantitate proteins. The most important reason for this is that different samples can be combined at the level of intact cells, which, as a result, excludes all sources of quantitation error introduced by biochemical and mass spectrometric procedures, as these will affect both protein populations in the same way. Metabolic labeling is therefore the most sensitive MS based labeling technique to date, making it possible to study small protein abundance differences as small as 1.5-fold changes or even smaller. Despite a number of cases that demonstrate the feasibility of metabolic labeling of higher organisms using ^{15}N sources *in vivo*, such as *C. elegans*, *D. Melanogaster* (Krijgsveld et al., 2003) and the rat (Wu et al., 2004), it is not practical to apply this strategy routinely. The most important reason for this is that labeling with ^{15}N complicates data analysis to a large extent, as discussed in section 2.1. Nowadays, the most widely applied method to metabolically label material of eukaryotic origin is SILAC in immortalized cell lines. SILAC based MS has been extensively applied for the study of global proteomes, in the field of functional proteomics, and for the analysis of post-translational modifications. Additionally, SILAC can be applied to whole organisms, such as *E. coli*, *S. cerevisiae*, and *D. melanogaster*. Even metabolic labeling of higher eukaryotes like the mouse (Kruger et al., 2008) has shown to be possible.

Although SILAC is the most accurate MS based quantitation approach, it might not always be possible or preferable to use SILAC. As mentioned earlier, not every cell type might grow well in the SILAC medium. Some cell lines readily convert arginine to proline, which complicates data analysis, and require adaptation of the protocol such as titration of arginine in the medium (Ong et al., 2003). Otherwise, computational approaches to correct arginine-to-proline conversion may be applied (Park et al., 2009). Finally, cell lines that are sensitive to changes in media composition or are otherwise difficult to grow or maintain in culture may not be amenable to metabolic labeling at all. When it is not possible to label a cell culture in SILAC medium, post-digestion incorporation methods may serve as an alternative. Moreover, post-digestion labeling might be the preferred method for affinity purification mass spectrometry (AP-MS) applications, as the starting material for co-IP assays is typically several milligrams of proteins. The use of stable isotope labeling by SILAC can be cost-prohibitive, whereas post-digestion labeling approaches such as stable isotope dimethyl labeling and ^{18}O labeling are performed with

inexpensive generic reagents and do not pose severe financial restrictions to the amount of sample to be labeled.

In conclusion, SILAC can be applied in almost all sorts of proteomic applications since it is very sensitive, and limitations are mainly biological applicability or involve practical issues such as time, cost, or available equipment.

Chemical and enzymatic post-digestion labeling

One of the advantages of a chemical modification approach over metabolic labeling is the ability to label proteins after cell lysis and in a post-digestion manner. This makes the approach generically applicable, since it allows the quantitative analysis of biological samples that cannot be grown in culture, such as human body fluids or human tissue. ICAT was one of the first chemical labeling methods introduced for quantitative mass spectrometry. Although often and successfully applied, its main drawbacks are adverse side reactions and its inability to label peptides that do not contain cysteine residues. As a result, in many laboratories, ICAT has been substituted by other approaches, such as chemical dimethyl labeling or enzymatic ^{18}O labeling. Compared to ICAT, both ^{18}O labeling and dimethyl labeling are simple, free of extensive sample manipulations, virtually free of side reactions, and amenable to all protein species (*i.e.*, proteins that contain no cysteine residues). In contrast to ICAT, there is no lower limit of the protein amount that can be labeled for ^{18}O and dimethyl. Another advantage of the latter two labeling approaches is that they are cost-effective. This, together with the fact that proteins for any species can be labeled and the ease of sample preparation, makes chemical labeling the preferred method for the quantitative analysis of for instance size-limited human tissue specimens. Also, post-digestion labeling is practical for tissue samples of higher organisms such as mice, or cell lines that cannot be metabolically labeled.

One drawback of dimethyl labeling is that deuterated peptides show a small but significant retention time difference in reversed-phase HPLC compared to their non-deuterated counterparts (Zhang et al., 2001). This complicates data analysis because the relative quantities of the two peptide species cannot be determined accurately from one spectrum but requires integration across the chromatographic time scale. Retention time shifts are far less pronounced for labels such as ^{13}C , ^{15}N , or ^{18}O isotopes (Zhang & Regnier, 2002), so that the additional signal integration step over retention time can generally be omitted in approaches based on incorporation of these labels. However, compared to iTRAQ and TMT, dimethyl labeling is performed with inexpensive generic reagents and do not pose severe financial restrictions to the amount of sample to be labeled.

Multiplex labeling using TMT or iTRAQ has turned out to be particularly useful for following biological systems over multiple time points or, more generally, for comparing multiple treatments in the same experiment. With dimethylation labeling, iTRAQ and TMT labeling, multiplexing can be achieved, which is not possible for ^{18}O labeling. iTRAQ is capable of

simultaneously analyzing eight samples (Pierce et al., 2008), whereas with TMT labeling, six samples can be measured together (Thompson et al., 2003). It should be noted that the use of commercial isobaric iTRAQ or TMT labels can be cost-prohibitive. In terms of equipment, TMT and iTRAQ labeling approaches are limited to mass spectrometers which are capable of efficiently detecting ions that are present at a relatively low m/z and peptide quantification is based on a single fragmentation mass spectrum. An advantage of isobaric tags is that the labeled peptides co-elute from the chromatographic column which means that the MS signal is not split into different peaks, as in conventional isotope labeling, improving sensitivity in the MS mode.

In conclusion, chemical and enzymatic labeling can be applied to virtually any biological sample since incorporation is performed after cell lysis and generally also after digestion. Therefore, post-digestion labeling is specifically useful for the study of mammalian and human tissue or body fluids. Importantly, compared to metabolic labeling, label incorporation in chemical and enzymatic labeling approaches takes place at a later stage in the sample treatment protocol and are therefore in general less accurate. For absolute protein quantitation, peptides have to be labeled with stable heavy isotopes, which is usually done by synthesizing them with labeled amino acids, in order to serve as an internal standard.

Label free approaches

Since no labels are used whatsoever in label free quantitative proteomics, these approaches are inexpensive, they can be applied to any kind of biological material and the proteome coverage of quantified proteins is high because basically every protein that is identified by at least one peptide spectrum can in principle be quantified. In addition, the complexity of the sample is not increased by mixing different samples. Label free methods therefore usually have a high analytical depth and dynamic range, giving this method an advantage when large, global protein changes between treatments are expected. Also, since the samples are not mixed and quantification is done after MS analysis, the obtained data is not fixed and can be used in other contexts as well. These advantages make label free quantification an attractive approach for *e.g.* clinicians who have large patient material-derived datasets and want to compare multiple datasets, and have no wet lab available.

Despite the many advantages of label free quantitation, it is probably the least accurate among the mass spectrometric quantification methods when considering the overall experimental process because all the systematic and non-systematic variations between experiments are reflected in the obtained data. Consequently, the number of experimental steps should be kept to a minimum and every effort should be made to control reproducibility at each step.

There has been growing interest in the use of label-free approaches for quantitative proteomic analyses over the recent years, particularly because of ever increasing accuracy and reproducibility of high-resolution LC-MS equipment. Most MS analysis is performed with data dependent analysis (DDA) where the mass spectrometer runs a parent ion scan and selects the

most abundant ions on which to conduct fragmentation scans, typically 4-10 scans, before returning to a parent ion scan. There may be a bias in this type of data for co-eluting peptides towards omitting the lower abundant peptides from MS/MS (Venable et al., 2004). This bias creates a subset of proteins effectively unseen due to the resultant level of detection limit. An experimental setup has been developed in which the mass spectrometer no longer cycles between MS and MS/MS mode but aims to detect and fragment all peptides in a chromatographic window simultaneously by rapidly alternating between high- and low-energy conditions in the mass spectrometer (Silva et al., 2006). Obviously, there are challenges with analyzing such data from complex samples as many fragmentation spectra will be populated with sequence ions from multiple peptides each contributing differently to the overall spectral content.

Also, there is evidence that label-free methods provide higher dynamic range of quantification than any stable isotope labeling approach (*i.e.*, 2-3 orders of magnitude) and therefore may be advantageous when large and global protein changes between experiments are observed (Old et al., 2005).

Data analysis

No matter the choice of quantitative method, quantitative proteomic data are typically very complex and often of variable quality. The main challenge stems from incomplete data, since even today's most advanced mass spectrometers cannot sample and fragment every peptide ion present in complex samples. As a consequence, only a subset of peptides and proteins present in a sample can be identified. Over the past years, a series of experimental strategies for mass spectrometry based quantitative proteomics and corresponding computational methodology for the processing of quantitative data have been generated (reviewed in (Matthiesen et al., 2011; Mueller et al., 2008)). Conceptually different methods to perform quantitative LC-MS experiments demand different quantification principles and available software solutions for data analysis. Quantification can be achieved by comparing peak intensities in differential stable isotopic labeling, via spectral counting, or by using the ion current in label-free LC-MS measurements. Numerous software solutions have been presented, with specific instrument compatibility and processing functionality and which can cope with these basically different quantitation methods. It is important for researchers to choose an appropriate software solution for quantitative proteomic experiments based on their experimental and analytical requirements. However, it goes beyond the scope of this Chapter to discuss all of the available software tools separately. For an extensive and up-to-date overview of software solutions including links to websites for downloads, the reader is referred to <http://www.ms-utils.org>.

Concluding remarks

As we have discussed in this Chapter, all of the mass spectrometry-based quantification methods have their particular strengths and weaknesses. The researcher has to choose the best method from the multitude of methods that have emerged for the analysis of simple and complex (sub-)proteomes using quantitative mass spectrometry for his or her specific research; a choice that depends on the financial aspects involved, the availability of high-resolution mass spectrometer and LC equipment and the available expertise present in the lab. Quantitative proteomics methods are now starting to mature to an extent that they can be meaningfully applied to the study of proteomes and their dynamics. Using the labeling methods described in this Chapter, it is now possible to identify and quantitate several thousands of proteins in a single experiment. However, there is still room for significant improvements to the experimental strategies that are required for the quantitative analysis of very complex mixtures and of post-translational modifications, with the ultimate aim to generate quantitative proteomic data at a scale which would allow the comprehensive investigation of a biological phenomenon. At the same time, the recent exponential increase in data volume and complexity demands the development of appropriate bioinformatic and statistical approaches in order to arrive at meaningful interpretations of the results. This can only be achieved if the influence of the employed technologies on the results obtained is well understood.

References

- Bantscheff, M., Schirle, M., Sweetman, G., Rick, J. & Kuster, B. (2007). Quantitative Mass Spectrometry in Proteomics: A Critical Review. *Anal Bioanal Chem*, 389(4), 1017-1031.
- Bezstarosti, K., Ghamari, A., Grosveld, F. G. & Demmers, J. A. (2010). Differential Proteomics Based on ¹⁸O Labeling to Determine the Cyclin Dependent Kinase 9 Interactome. *J Proteome Res*, 9(9), 4464-4475.
- Blagoev, B., Kratchmarova, I., Ong, S. E., Nielsen, M., Foster, L. J. & Mann, M. (2003). A Proteomics Strategy to Elucidate Functional Protein-Protein Interactions Applied to Egf Signaling. *Nat Biotechnol*, 21(3), 315-318.
- Blagoev, B. & Mann, M. (2006). Quantitative Proteomics to Study Mitogen-Activated Protein Kinases. *Methods*, 40(3), 243-250.
- Blonder, J., Hale, M. L., Chan, K. C., Yu, L. R., Lucas, D. A., Conrads, T. P., Zhou, M., Popoff, M. R., Issaq, H. J., Stiles, B. G. & Veenstra, T. D. (2005). Quantitative Profiling of the Detergent-Resistant Membrane Proteome of Iota-B Toxin Induced Vero Cells. *J Proteome Res*, 4(2), 523-531.
- Boersema, P. J., Aye, T. T., van Veen, T. A., Heck, A. J. & Mohammed, S. (2008). Triplex Protein Quantification Based on Stable Isotope Labeling by Peptide Dimethylation Applied to Cell and Tissue Lysates. *Proteomics*, 8(22), 4624-4632.
- Boersema, P. J., Foong, L. Y., Ding, V. M., Lemeer, S., van Breukelen, B., Philp, R., Boekhorst, J., Snel, B., den Hertog, J., Choo, A. B. & Heck, A. J. (2010). In-Depth Qualitative and Quantitative Profiling of Tyrosine Phosphorylation Using a Combination of

Phosphopeptide Immunoaffinity Purification and Stable Isotope Dimethyl Labeling. *Mol Cell Proteomics*, 9(1), 84-99.

Boersema, P. J., Raijmakers, R., Lemeer, S., Mohammed, S. & Heck, A. J. (2009). Multiplex Peptide Stable Isotope Dimethyl Labeling for Quantitative Proteomics. *Nat Protoc*, 4(4), 484-494.

Bonenfant, D., Schmelzle, T., Jacinto, E., Crespo, J. L., Mini, T., Hall, M. N. & Jenoe, P. (2003). Quantitation of Changes in Protein Phosphorylation: A Simple Method Based on Stable Isotope Labeling and Mass Spectrometry. *Proc Natl Acad Sci U S A*, 100(3), 880-885.

Brown, K. J. & Fenselau, C. (2004). Investigation of Doxorubicin Resistance in MCF-7 Breast Cancer Cells Using Shot-Gun Comparative Proteomics with Proteolytic 18O Labeling. *J Proteome Res*, 3(3), 455-462.

Chelius, D. & Bondarenko, P. V. (2002). Quantitative Profiling of Proteins in Complex Mixtures Using Liquid Chromatography and Mass Spectrometry. *J Proteome Res*, 1(4), 317-323.

Chen, X., Cushman, S. W., Pannell, L. K. & Hess, S. (2005). Quantitative Proteomic Analysis of the Secretory Proteins from Rat Adipose Cells Using a 2D Liquid Chromatography-Ms/Ms Approach. *J Proteome Res*, 4(2), 570-577.

Choi, H., Fermin, D. & Nesvizhskii, A. I. (2008). Significance Analysis of Spectral Count Data in Label-Free Shotgun Proteomics. *Mol Cell Proteomics*, 7(12), 2373-2385.

Conrads, T. P., Alving, K., Veenstra, T. D., Belov, M. E., Anderson, G. A., Anderson, D. J., Lipton, M. S., Pasa-Tolic, L., Udseth, H. R., Chrisler, W. B., Thrall, B. D. & Smith, R. D. (2001). Quantitative Analysis of Bacterial and Mammalian Proteomes Using a Combination of Cysteine Affinity Tags and 15N-Metabolic Labeling. *Anal Chem*, 73(9), 2132-2139.

de Boer, E., Rodriguez, P., Bonte, E., Krijgsveld, J., Katsantoni, E., Heck, A., Grossveld, F. & Strouboulis, J. (2003). Efficient Biotinylation and

Single-Step Purification of Tagged Transcription Factors in Mammalian Cells and Transgenic Mice. *Proc Natl Acad Sci U S A*, 100(13), 7480-7485.

de Godoy, L. M., Olsen, J. V., de Souza, G. A., Li, G., Mortensen, P. & Mann, M. (2006). Status of Complete Proteome Analysis by Mass Spectrometry: Silac Labeled Yeast as a Model System. *Genome Biol*, 7(6), R50.

Engelsberger, W. R., Erban, A., Kopka, J. & Schulze, W. X. (2006). Metabolic Labeling of Plant Cell Cultures with K(15)NO₃ as a Tool for Quantitative Analysis of Proteins and Metabolites. *Plant Methods*, 2, 14.

Fenselau, C. & Yao, X. (2007). Proteolytic Labeling with 18O for Comparative Proteomics Studies: Preparation of 18O-Labeled Peptides and the 18O/16O Peptide Mixture. *Methods Mol Biol*, 359, 135-142.

Gevaert, K., Staes, A., Van Damme, J., De Groot, S., Hugelier, K., Demol, H., Martens, L., Goethals, M. & Vandekerckhove, J. (2005). Global Phosphoproteome Analysis on Human HepG2 Hepatocytes Using Reversed-Phase Diagonal LC. *Proteomics*, 5(14), 3589-3599.

Gruhler, A., Schulze, W. X., Matthiesen, R., Mann, M. & Jensen, O. N. (2005). Stable Isotope Labeling of Arabidopsis Thaliana Cells and Quantitative Proteomics by Mass Spectrometry. *Mol Cell Proteomics*, 4(11), 1697-1709.

Gygi, S. P., Rist, B., Gerber, S. A., Turecek, F., Gelb, M. H. & Aebersold, R. (1999). Quantitative Analysis of Complex Protein Mixtures Using Isotope-Coded Affinity Tags. *Nat Biotechnol*, 17(10), 994-999.

Hajkova, D., Rao, K. C. & Miyagi, M. (2006). Ph Dependency of the Carboxyl Oxygen Exchange Reaction Catalyzed by Lysyl Endopeptidase and Trypsin. *J Proteome Res*, 5(7), 1667-1673.

Hansen, K. C., Schmitt-Ulms, G., Chalkley, R. J., Hirsch, J., Baldwin, M. A. & Burlingame, A. L. (2003). Mass Spectrometric Analysis of Protein Mixtures at Low Levels Using Cleavable

- 13c-Isotope-Coded Affinity Tag and Multidimensional Chromatography. *Mol Cell Proteomics*, 2(5), 299-314.
- Hood, B. L., Darfler, M. M., Guiel, T. G., Furusato, B., Lucas, D. A., Ringeisen, B. R., Sesterhenn, I. A., Conrads, T. P., Veenstra, T. D. & Krizman, D. B. (2005). Proteomic Analysis of Formalin-Fixed Prostate Cancer Tissue. *Mol Cell Proteomics*, 4(11), 1741-1753.
- Hood, B. L., Lucas, D. A., Kim, G., Chan, K. C., Blonder, J., Issaq, H. J., Veenstra, T. D., Conrads, T. P., Pollet, I. & Karsan, A. (2005). Quantitative Analysis of the Low Molecular Weight Serum Proteome Using 18o Stable Isotope Labeling in a Lung Tumor Xenograft Mouse Model. *J Am Soc Mass Spectrom*, 16(8), 1221-1230.
- Hsu, J. L., Huang, S. Y., Chow, N. H. & Chen, S. H. (2003). Stable-Isotope Dimethyl Labeling for Quantitative Proteomics. *Anal Chem*, 75(24), 6843-6852.
- Ibarrola, N., Kalume, D. E., Gronborg, M., Iwahori, A. & Pandey, A. (2003). A Proteomic Approach for Quantitation of Phosphorylation Using Stable Isotope Labeling in Cell Culture. *Anal Chem*, 75(22), 6043-6049.
- Ippel, J. H., Pouvreau, L., Kroef, T., Gruppen, H., Versteeg, G., van den Putten, P., Struik, P. C. & van Mierlo, C. P. (2004). In Vivo Uniform (15)N-Isotope Labelling of Plants: Using the Greenhouse for Structural Proteomics. *Proteomics*, 4(1), 226-234.
- Krijgsveld, J., Ketting, R. F., Mahmoudi, T., Johansen, J., Artal-Sanz, M., Vrijz, C. P., Plasterk, R. H. & Heck, A. J. (2003). Metabolic Labeling of C. Elegans and D. Melanogaster for Quantitative Proteomics. *Nat Biotechnol*, 21(8), 927-931.
- Kruger, M., Moser, M., Ussar, S., Thievensen, I., Lub, C. A., Forner, F., Schmidt, S., Zanivan, S., Fassler, R. & Mann, M. (2008). Silac Mouse for Quantitative Proteomics Uncovers Kindlin-3 as an Essential Factor for Red Blood Cell Function. *Cell*, 134(2), 353-364.
- Lanquar, V., Kuhn, L., Lelievre, F., Khafif, M., Espagne, C., Bruley, C., Barbier-Brygoo, H., Garin, J. & Thomine, S. (2007). 15n-Metabolic Labeling for Comparative Plasma Membrane Proteomics in Arabidopsis Cells. *Proteomics*, 7(5), 750-754.
- Li, J., Steen, H. & Gygi, S. P. (2003). Protein Profiling with Cleavable Isotope-Coded Affinity Tag (Cicat) Reagents: The Yeast Salinity Stress Response. *Mol Cell Proteomics*, 2(11), 1198-1204.
- Listgarten, J. & Emili, A. (2005). Statistical and Computational Methods for Comparative Proteomic Profiling Using Liquid Chromatography-Tandem Mass Spectrometry. *Mol Cell Proteomics*, 4(4), 419-434.
- Liu, H., Sadygov, R. G. & Yates, J. R., 3rd. (2004). A Model for Random Sampling and Estimation of Relative Protein Abundance in Shotgun Proteomics. *Anal Chem*, 76(14), 4193-4201.
- Lundgren, D. H., Hwang, S. I., Wu, L. & Han, D. K. (2010). Role of Spectral Counting in Quantitative Proteomics. *Expert Rev Proteomics*, 7(1), 39-53.
- Matthiesen, R., Azevedo, L., Amorim, A. & Carvalho, A. S. (2011). Discussion on Common Data Analysis Strategies Used in Ms-Based Proteomics. *Proteomics*, 11(4), 604-619.
- McClatchy, D. B., Dong, M. Q., Wu, C. C., Venable, J. D. & Yates, J. R., 3rd. (2007). 15n Metabolic Labeling of Mammalian Tissue with Slow Protein Turnover. *J Proteome Res*, 6(5), 2005-2010.
- Miyagi, M. & Rao, K. C. (2007). Proteolytic 18o-Labeling Strategies for Quantitative Proteomics. *Mass Spectrom Rev*, 26(1), 121-136.
- Mortensen, P., Gouw, J. W., Olsen, J. V., Ong, S. E., Rigbolt, K. T., Bunkenborg, J., Cox, J., Foster, L. J., Heck, A. J., Blagoev, B., Andersen, J. S. & Mann, M. (2010). Msquant, an Open Source Platform for Mass Spectrometry-Based Quantitative Proteomics. *J Proteome Res*, 9(1), 393-403.
- Mueller, L. N., Brusniak, M. Y., Mani, D. R. & Aebersold, R. (2008). An Assessment of Software Solutions for the Analysis of Mass Spectrometry Based Quantitative Proteomics Data. *J Proteome Res*, 7(1), 51-61.

- Neilson, K. A., Ali, N. A., Muralidharan, S., Mirzaei, M., Mariani, M., Assadourian, G., Lee, A., van Sluyter, S. C. & Haynes, P. A. (2011). Less Label, More Free: Approaches in Label-Free Quantitative Mass Spectrometry. *Proteomics*, 11(4), 535-553.
- Oda, Y., Huang, K., Cross, F. R., Cowburn, D. & Chait, B. T. (1999). Accurate Quantitation of Protein Expression and Site-Specific Phosphorylation. *Proc Natl Acad Sci U S A*, 96(12), 6591-6596.
- Old, W. M., Meyer-Arendt, K., Aveline-Wolf, L., Pierce, K. G., Mendoza, A., Sevinisky, J. R., Resing, K. A. & Ahn, N. G. (2005). Comparison of Label-Free Methods for Quantifying Human Proteins by Shotgun Proteomics. *Mol Cell Proteomics*, 4(10), 1487-1502.
- Ong, S. E., Blagoev, B., Kratchmarova, I., Kristensen, D. B., Steen, H., Pandey, A. & Mann, M. (2002). Stable Isotope Labeling by Amino Acids in Cell Culture, Silac, as a Simple and Accurate Approach to Expression Proteomics. *Mol Cell Proteomics*, 1(5), 376-386.
- Ong, S. E., Kratchmarova, I. & Mann, M. (2003). Properties of ^{13}C -Substituted Arginine in Stable Isotope Labeling by Amino Acids in Cell Culture (Silac). *J Proteome Res*, 2(2), 173-181.
- Ong, S. E. & Mann, M. (2005). Mass Spectrometry-Based Proteomics Turns Quantitative. *Nat Chem Biol*, 1(5), 252-262.
- Park, S. K., Liao, L., Kim, J. Y. & Yates, J. R., 3rd. (2009). A Computational Approach to Correct Arginine-to-Proline Conversion in Quantitative Proteomics. *Nat Methods*, 6(3), 184-185.
- Pierce, A., Unwin, R. D., Evans, C. A., Griffiths, S., Carney, L., Zhang, L., Jaworska, E., Lee, C. F., Blinco, D., Okoniewski, M. J., Miller, C. J., Bitton, D. A., Spooncer, E. & Whetton, A. D. (2008). Eight-Channel Itraq Enables Comparison of the Activity of Six Leukemogenic Tyrosine Kinases. *Mol Cell Proteomics*, 7(5), 853-863.
- Qian, W. J., Monroe, M. E., Liu, T., Jacobs, J. M., Anderson, G. A., Shen, Y., Moore, R. J., Anderson, D. J., Zhang, R., Calvano, S. E., Lowry, S. F., Xiao, W., Moldawer, L. L., Davis, R. W., Tompkins, R. G., Camp, D. G., 2nd & Smith, R. D. (2005). Quantitative Proteome Analysis of Human Plasma Following in Vivo Lipopolysaccharide Administration Using $^{16}\text{O}/^{18}\text{O}$ Labeling and the Accurate Mass and Time Tag Approach. *Mol Cell Proteomics*, 4(5), 700-709.
- Raijmakers, R., Berkers, C. R., de Jong, A., Ovaa, H., Heck, A. J. & Mohammed, S. (2008). Automated Online Sequential Isotope Labeling for Protein Quantitation Applied to Proteasome Tissue-Specific Diversity. *Mol Cell Proteomics*, 7(9), 1755-1762.
- Ramos-Fernandez, A., Lopez-Ferrer, D. & Vazquez, J. (2007). Improved Method for Differential Expression Proteomics Using Trypsin-Catalyzed ^{18}O Labeling with a Correction for Labeling Efficiency. *Mol Cell Proteomics*, 6(7), 1274-1286.
- Rao, K. C., Palamalai, V., Dunlevy, J. R. & Miyagi, M. (2005). Peptidyl-Lys Metalloendopeptidase-Catalyzed ^{18}O Labeling for Comparative Proteomics: Application to Cytokine/Lipopolysaccharide-Treated Human Retinal Pigment Epithelium Cell Line. *Mol Cell Proteomics*, 4(10), 1550-1557.
- Rappsilber, J., Ryder, U., Lamond, A. I. & Mann, M. (2002). Large-Scale Proteomic Analysis of the Human Spliceosome. *Genome Res*, 12(8), 1231-1245.
- Ross, P. L., Huang, Y. N., Marchese, J. N., Williamson, B., Parker, K., Hattan, S., Khainovski, N., Pillai, S., Dey, S., Daniels, S., Purkayastha, S., Juhasz, P., Martin, S., Bartlett-Jones, M., He, F., Jacobson, A. & Pappin, D. J. (2004). Multiplexed Protein Quantitation in *Saccharomyces Cerevisiae* Using Amine-Reactive Isobaric Tagging Reagents. *Mol Cell Proteomics*, 3(12), 1154-1169.
- Sevinisky, J. R., Brown, K. J., Cargile, B. J., Bundy, J. L. & Stephenson, J. L., Jr. (2007). Minimizing Back Exchange in $^{18}\text{O}/^{16}\text{O}$ Quantitative Proteomics Experiments by Incorporation of Immobilized Trypsin into the Initial Digestion Step. *Anal Chem*, 79(5), 2158-2162.
- Silva, J. C., Denny, R., Dorschel, C., Gorenstein, M. V., Li, G. Z., Richardson, K., Wall, D. &

- Geromanos, S. J. (2006). Simultaneous Qualitative and Quantitative Analysis of the Escherichia Coli Proteome: A Sweet Tale. *Mol Cell Proteomics*, 5(4), 589-607.
- Silva, J. C., Denny, R., Dorschel, C. A., Gorenstein, M., Kass, I. J., Li, G. Z., McKenna, T., Nold, M. J., Richardson, K., Young, P. & Geromanos, S. (2005). Quantitative Proteomic Analysis by Accurate Mass Retention Time Pairs. *Anal Chem*, 77(7), 2187-2200.
- Staes, A., Demol, H., Van Damme, J., Martens, L., Vandekerckhove, J. & Gevaert, K. (2004). Global Differential Non-Gel Proteomics by Quantitative and Stable Labeling of Tryptic Peptides with Oxygen-18. *J Proteome Res*, 3(4), 786-791.
- Sury, M. D., Chen, J. X. & Selbach, M. (2010). The Silac Fly Allows for Accurate Protein Quantification in Vivo. *Mol Cell Proteomics*, 9(10), 2173-2183.
- Synowsky, S. A., van Wijk, M., Raijmakers, R. & Heck, A. J. (2009). Comparative Multiplexed Mass Spectrometric Analyses of Endogenously Expressed Yeast Nuclear and Cytoplasmic Exosomes. *J Mol Biol*, 385(4), 1300-1313.
- Thompson, A., Schafer, J., Kuhn, K., Kienle, S., Schwarz, J., Schmidt, G., Neumann, T., Johnstone, R., Mohammed, A. K. & Hamon, C. (2003). Tandem Mass Tags: A Novel Quantification Strategy for Comparative Analysis of Complex Protein Mixtures by Ms/Ms. *Anal Chem*, 75(8), 1895-1904.
- Unlu, M., Morgan, M. E. & Minden, J. S. (1997). Difference Gel Electrophoresis: A Single Gel Method for Detecting Changes in Protein Extracts. *Electrophoresis*, 18(11), 2071-2077.
- Van Hoof, D., Pinkse, M. W., Oostwaard, D. W., Mummery, C. L., Heck, A. J. & Krijgsveld, J. (2007). An Experimental Correction for Arginine-to-Proline Conversion Artifacts in Silac-Based Quantitative Proteomics. *Nat Methods*, 4(9), 677-678.
- Venable, J. D., Dong, M. Q., Wohlschlegel, J., Dillin, A. & Yates, J. R. (2004). Automated Approach for Quantitative Analysis of Complex Peptide Mixtures from Tandem Mass Spectra. *Nat Methods*, 1(1), 39-45.
- Wang, N. & Li, L. (2008). Exploring the Precursor Ion Exclusion Feature of Liquid Chromatography-Electrospray Ionization Quadrupole Time-of-Flight Mass Spectrometry for Improving Protein Identification in Shotgun Proteome Analysis. *Anal Chem*, 80(12), 4696-4710.
- Wiener, M. C., Sachs, J. R., Deyanova, E. G. & Yates, N. A. (2004). Differential Mass Spectrometry: A Label-Free Lc-Ms Method for Finding Significant Differences in Complex Peptide and Protein Mixtures. *Anal Chem*, 76(20), 6085-6096.
- Wu, C. C., MacCoss, M. J., Howell, K. E., Matthews, D. E. & Yates, J. R., 3rd. (2004). Metabolic Labeling of Mammalian Organisms with Stable Isotopes for Quantitative Proteomic Analysis. *Anal Chem*, 76(17), 4951-4959.
- Yao, X., Freas, A., Ramirez, J., Demirev, P. A. & Fenselau, C. (2001). Proteolytic 18O Labeling for Comparative Proteomics: Model Studies with Two Serotypes of Adenovirus. *Anal Chem*, 73(13), 2836-2842.
- Zang, L., Palmer Toy, D., Hancock, W. S., Sgroi, D. C. & Karger, B. L. (2004). Proteomic Analysis of Ductal Carcinoma of the Breast Using Laser Capture Microdissection, Lc-Ms, and 16o/18o Isotopic Labeling. *J Proteome Res*, 3(3), 604-612.
- Zhang, R. & Regnier, F. E. (2002). Minimizing Resolution of Isotopically Coded Peptides in Comparative Proteomics. *J Proteome Res*, 1(2), 139-147.
- Zhang, R., Sioma, C. S., Wang, S. & Regnier, F. E. (2001). Fractionation of Isotopically Labeled Peptides in Quantitative Proteomics. *Anal Chem*, 73(21), 5142-5149.

Chapter 3

Quantitative proteomics reveals extensive changes in the ubiquitinome after perturbation of the proteasome by targeted dsRNA mediated subunit knockdown in *Drosophila*.

Karen A. Sap, Karel Bezstarosti, Dick H. W. Dekkers, Olaf Voets,

Jeroen A. A. Demmers

Published in Journal of Proteome Research (2017)

Abstract

The ubiquitin–proteasome system (UPS), a highly regulated mechanism including the active marking of proteins by ubiquitin in order to be degraded, is critical in regulating proteostasis. Dysfunctioning of the UPS has been implicated in diseases such as cancer and neurodegenerative disorders. Here, we investigate the effects of proteasome malfunctioning on global proteome and ubiquitinome dynamics using SILAC proteomics in *Drosophila* S2 cells. dsRNA mediated knockdown of specific proteasome target subunits is used to inactivate the proteasome. Upon this perturbation, both the global proteome and the ubiquitinome become modified to a great extent, the overall impact on the ubiquitinome being most dramatic. The abundances of approx. 10% of all proteins are increased, while the abundances of the far majority of over 14 thousand detected diGly peptides are increased, suggesting that the pool of ubiquitinated proteins is highly dynamic. Remarkably, several proteins show heterogeneous ubiquitination dynamics, with different lysine residues on the same protein showing either increased or decreased ubiquitination. This suggests the occurrence of simultaneous and functionally different ubiquitination events. This strategy offers a powerful tool to study the response of the ubiquitinome upon interruption of normal UPS activity by targeted interference and opens up new avenues for the dissection of the mode of action of individual components of the proteasome. Since this is to our knowledge the first comprehensive ubiquitinome screen upon proteasome malfunctioning in a fruit fly cell system, this data set will serve as a valuable repository for the *Drosophila* community.

Introduction

In eukaryotic cells, short-lived, regulatory, misfolded and denatured proteins are degraded by the ubiquitin–proteasome system (UPS), a highly regulated mechanism involving the active marking of proteins for proteasomal degradation by ubiquitin. The 26S proteasome is the central protease in nonlysosomal ubiquitin-dependent degradation. It is involved in diverse processes such as protein quality control, antigen processing, signal transduction, cell cycle control, cell differentiation and apoptosis (Hershko and Ciechanover, 1998) and, as such, is critical in regulating proteostasis. Aberrations in the UPS have been implicated in cancers and in the pathogenesis of neurodegenerative diseases, such as Parkinson's (PD), Alzheimer's (AD), Huntington's (HD), prion diseases, as well as amyotrophic lateral sclerosis (ALS) (Keller, Gee and Ding, 2002; Ciechanover and Brundin, 2003; Giasson and Lee, 2003). The critical roles played by ubiquitin-mediated protein turnover in cell cycle regulation makes this process a target for oncogenic mutations. The proteasome serves as a target for cancer chemotherapy, as exemplified by bortezomib (Velcade), a proteasome inhibitor that binds proteolytic pockets in

the 20S core (Groll *et al.*, 2006; San Miguel *et al.*, 2008). Proteasome inhibitors exert anti-tumor activity *in vivo* and potently induce apoptosis in tumor cells *in vitro* (Almond and Cohen, 2002).

Ubiquitylation, the covalent attachment of ubiquitin to the ϵ -amino group of substrate lysine (Lys) residues, is a versatile posttranslational modification (PTM). A key feature of ubiquitin is its ability to form polymeric chains, in which individual moieties are linked via one of seven Lys residues or the N-terminal methionine (Komander, 2009). Only a few of these distinct linkage types have been studied extensively: K48-linked polyubiquitin serves as a targeting signal for proteasomal degradation (Chau *et al.*, 1989), whereas K63-linked polyubiquitin is thought to be involved in cell signaling, membrane trafficking, and the DNA damage response (Chen and Sun, 2009). K11-linked polyubiquitin has been suggested to have both degradative and non-degradative roles (Xu *et al.*, 2009), while the M1-linkage has a crucial role in the canonical NF- κ B activation pathway (Iwai and Tokunaga, 2009). The biological significance of ubiquitin chains linked through K6, K27, K29, or K33 is still poorly understood (Komander and Rape, 2012).

Over the past years, proteomic tools have been developed to identify and quantify ubiquitin-dependent signaling systems and to elucidate details of UPS functioning (Kim, Eric J. Bennett, *et al.*, 2011; Wagner *et al.*, 2011; Udeshi *et al.*, 2013; Ordureau, M?nch and Harper, 2015). These novel technologies to study global protein ubiquitination (the ‘ubiquitinome’) are based on highly specific antibody enrichment of peptides carrying the diGly remnant motif as a result of tryptic cleavage of ubiquitinated proteins and have taken over low- to medium-throughput approaches (*e.g.*, (Mayor *et al.*, 2007)). The diGly peptide enrichment technology has been applied *e.g.* to study ubiquitylation site specificity and topology of PARKIN-dependent target modification in response to mitochondrial depolarization (Sarraf *et al.*, 2013), to find novel substrates of HUWE1 using an inducible loss of function approach (Thompson *et al.*, 2014), and, recently, to identify specific substrates of a novel class of proteasome inhibitors (capzimin) (Li *et al.*, 2017).

Here, we investigate the effect of proteasome inhibition on the global cellular proteome and the ubiquitinome-by means of SILAC based proteomics. Two different approaches to inactivate the proteasome are compared: first, by the addition of the chemical agents MG132 (Lee and Goldberg, 1998a) and Lactacystin (Fenteany *et al.*, 1995), which target the proteolytic activity of the proteasome; second, by double-stranded RNA (dsRNA)-mediated interference (RNAi) of proteasome subunit gene expression. The latter approach presents several advantages in investigating the molecular mechanisms of the UPS, since individual functional subunits can be inactivated by RNAi in a highly selective manner in *Drosophila* cells, as has been shown before by various groups (Wójcik and DeMartino, 2002; Lundgren *et al.*, 2003; Elena Koulich, Xiaohua Li, 2008). *Drosophila* cell systems in general provide an excellent tool to study basic cellular processes and subsequent translation to the whole organism is relatively straightforward. The fruit fly has an established role as a model system for the study of the nervous system in general and the role of proteasome impairment and neurodegeneration in particular (Yeh, Jansen and

Schmidt-Glenewinkel, 2011). There is a public collection of transgenic flies available, accommodating over 22,000 different transgenic fly lines that provide knockdowns for over 88 % of *Drosophila* genes (Dietzl *et al.*, 2007). Expression of these transgenic RNAi constructs can even be driven in a tissue specific manner (Brand and Perrimon, 1993), providing a simple yet powerful strategy to study the role of individual genes in diverse biological processes.

Our results reveal that a substantial part of the detectable global proteome is affected in cells that have (partially) inactivated proteasomes. The ubiquitinome analysis based on > 14,000 identified diGly peptides (of which > 11,000 could be quantified), revealed that the far majority of all ubiquitination sites are upregulated after inactivation of the proteasome, indicating that the pool of ubiquitinated proteins and the extent of ubiquitination are highly dynamic. We highlight several interesting examples of proteins with different target Lys residues showing either increased or decreased ubiquitination, which suggests the occurrence of simultaneous and functionally different ubiquitination events on a single protein or protein population.

In conclusion, we show that manipulation of proteasome functioning by targeted dsRNA mediated perturbation in *Drosophila* has major effects on the global cellular proteome and ubiquitinome. The novelty of this work lies in 1) the combination of ubiquitinome profiling with dsRNA mediated knockdown of proteasome subunits, 2) mimicking complete proteasome inactivation by dsRNA mediated knockdown of a dedicated selection of multiple subunits, and, 3) the use of *Drosophila* as the model organism for ubiquitinome profiling. The strategy applied here opens up avenues for the dissection of the mode of action of this intriguing cellular machinery by knocking down every single protein building block, both under proteostasis as well as abnormal conditions. As this study is the first large-scale investigation of protein ubiquitination in a *Drosophila* model system, it provides a valuable source of information for the community at large.

Material and Methods

Cell culture and sample preparation: *Drosophila melanogaster* Schneider's line 2 cells (S2 cells, R690-07, Invitrogen) were cultured in Schneider's medium (Invitrogen) supplemented with 10% fetal calf serum (Thermo) and 1% penicillin-streptomycin.

Antigen production: Full length cDNA of RPN11, Prosalpha5, Prosbeta6, RPN8, RPN10, RPT4 and C-terminal (aa 220–405) RPT6, were cloned into pGEX-2TKN vectors (Pharmacia). GST fusion protein expression, purification, and subsequent immunization were performed as described previously (Chalkley and Verrijzer, 2004). Other antibodies used were α -FK2 and α -polyubiquitin SPA-200 (both Enzo Life Sciences), 20S- α (sc- 65755) (Santa Cruz Biotechnology), and α -H2B (described in (Chalkley and Verrijzer, 2004)), dGMPS (described in

(Reddy *et al.*, 2014)) and dISWI (described in (Kal *et al.*, 2000)). Immunoblotting assays were performed using standard procedures.

FACS analysis: FACS analysis was performed essentially as described in (Moshkin *et al.*, 2007).

Glycerol gradients: Glycerol gradients were prepared essentially as described previously (Mohrmann *et al.*, 2004). Briefly, 5-30% gradients were generated in Beckman polyallomer tubes (331374). Whole cell lysates were prepared under non-denaturing conditions in 50 mM HEPES-KOH pH 7.6 / 100 mM KCl / 0.1% NP40, including protease inhibitors and loaded on top of the gradient and ultracentrifuged at 32 krpm for 17 h at 4°C (Beckman L-80 SW40 rotor). Thirteen 500 µl fractions were taken starting from the top of the gradient and fractions were analyzed by immunoblotting.

SILAC labeling: S2 cells were grown in custom made Schneider's medium (Athena Enzyme Systems, Baltimore, MD). This medium is based on Schneider's *Drosophila* medium from Invitrogen (#21720024) but is deficient for both lysine and arginine and contains dialyzed yeastolate (3,500 kDa MWCO). Before use, the medium is supplemented with 10% dialyzed fetal bovine serum (F0392, Sigma-Aldrich), 1% penicillin-streptomycin and 2 mg/ml light ($^{12}\text{C}_6$) lysine (A6969, Sigma-Aldrich) and 0.5 mg/ml light ($^{12}\text{C}_6$, $^{14}\text{N}_4$) arginine (L5751, Sigma-Aldrich), or heavy ($^{13}\text{C}_6$) lysine (CLM-2247, Cambridge Isotope laboratories) and heavy ($^{13}\text{C}_6$, $^{15}\text{N}_4$) arginine (CNLM-539, Cambridge Isotope Laboratories). Cells were cultured at 27°C for at least 7 cell doublings to reach complete labelling. Duplicate experiments were carried out by 'label swapping', *i.e.* switching the isotopically labeled state of the control *c.q.* treated cells and *vice versa* (termed 'forward' and 'reverse' here).

Proteasome inhibition: Cells were treated with 50 µM MG132 (Calbiochem) and 5 µM Lactacystin (Cayman Chemical) simultaneously, both dissolved in a 2000x DMSO stock solution. Mock samples were treated with equal volumes of DMSO. Cells were incubated for 4h or 16h at 27 °C.

dsRNA constructs: Constructs were synthesized using the Ambion Megascript T7 kit according to the manufacturer's protocol. Knockdown experiments were further performed as described previously (Worby, Simonson-Leff and Dixon, 2001). For dsRNA mediated targeted proteasome subunit knockdown, S2 cells were treated with dsRNA constructs directed against Prosalpha5 (Uniprot identifier Q95083), Probeta6 (P40304) and RPN11 (Q9V3H2). Mock samples were treated with dsRNA directed against GFP, which is absent in the cell lines used for these experiments. The final concentration of total dsRNA was 6 µg/ml. S2 cells were incubated with dsRNA for either 48h or 96h at 27°C.

SILAC sample preparation: Cells grown in SILAC light or heavy medium were harvested and used for immunoblotting or proteome and ubiquitinome analyses. For immunoblotting, cells

were washed three times with ice-cold PBS and spun down for 5 min at 1,100 rpm at 4°C. Cell pellets were lysed in SDS-PAGE sample buffer and sonicated as described earlier. BCA assays (Pierce) were used to estimate protein concentrations. After proteasome perturbation with either inhibitors or dsRNA mediated knockdown, cells were mixed in a 1:1 ratio based on cell count. Cells were washed three times with ice-cold PBS and lysed in 200 µl of an 8 M urea / 50 mM Tris-HCl pH 8.0 / 50 mM NaCl lysis buffer (7 ml of this buffer was used for lysates for diGly enrichment IP assays). Lysates were then incubated on ice for 10 min, sonicated, and debris was removed by centrifugation. BCA assays were used to estimate protein concentrations. 20 mg total protein was used for diGly peptide enrichment for ubiquitinome analyses; for global proteome analyses 0.5 mg lysate was used. All SILAC experiments were performed in duplicate, *i.e.* in a ‘forward’ and ‘reverse’ manner.

Cycloheximide treatment: Cells were treated with either 50 µM cycloheximide (CHX, Sigma), with 50 µM cycloheximide plus MG132/Lactacystin or with MG132/Lactacystin alone, or mock treated with DMSO. Cell cultures were treated with CHX 1 h before MG132/Lactacystin was added for 4 h. Treated and control cell cultures were then mixed in a 1:1 ratio based on cell count and prepared for further analysis.

Protein digestion and fractionation: Protein lysates were reduced with 10 mM dithiotreitol (DTT) for 1 h at room temperature followed by alkylation with 55 mM chloroacetamide (CAM) for 1 h in the dark. The mixture was diluted four times with 50 mM ammonium bicarbonate buffer before the addition of CaCl₂ (1 mM final concentration). Proteins were digested with sequencing grade trypsin (1:100 (w:w), Roche) overnight at room temperature. Alternatively, proteins were digested with LysC (1:100 (w:w), Wako Chemicals) for 1 h at room temperature before trypsinization. Protein digests were desalted using a Sep-Pak tC18 Vac cartridge (Waters) and eluted with 80% acetonitrile (AcN). Tryptic peptides were fractionated by HILIC on an Agilent 1100 HPLC system using a 5 µm particle size 4.6 x 250 mm TSKgel amide-80 column (Tosoh Biosciences). 200 µg of tryptic digest in 80% AcN was loaded onto the column. Peptides were eluted using a non-linear gradient from 80% B (100% AcN) to 100% A (20 mM ammonium formate in water) with a flow of 1 ml/min. Sixteen 6 ml fractions were collected, lyophilized and pooled into 8 final fractions. Each fraction was then analyzed by nanoflow LC-MS/MS as described below.

DiGly peptide enrichment: DiGly-modified peptides were enriched by immunoprecipitation using PTMScan® ubiquitin remnant motif (K-ε-GG) antibody bead conjugate (Cell Signaling Technology) starting from 20 mg total protein, essentially according to the manufacturer’s protocol. Unbound peptides were removed by washing and the captured peptides were eluted with a low pH buffer. Eluted peptides were analyzed by nanoflow LC-MS/MS as described below.

Nanoflow LC-MS/MS: was performed on an EASY-nLC system (Thermo) coupled to a Q Exactive mass spectrometer (Thermo), operating in positive mode and equipped with a nanospray source. Peptide mixtures were trapped on a ReproSil C18 reversed phase column (Dr Maisch GmbH; column dimensions 1.5 cm × 100 µm, packed in-house) at a flow rate of 8 µl/min. Peptide separation was performed on ReproSil C18 reversed phase column (Dr Maisch GmbH; column dimensions 15 cm × 50 µm, packed in-house) using a linear gradient from 0 to 80% B (A = 0.1% FA; B = 80% (v/v) AcN, 0.1 % FA) in 70 or 120 min and at a constant flow rate of 250 nl/min. The column eluent was directly sprayed into the ESI source of the mass spectrometer. All mass spectra were acquired in profile mode. The resolution in MS1 mode was set to 70,000 (AGC: 3E6), the m/z range 350-1700. Fragmentation of precursors was performed in data-dependent mode by HCD (Top15) with a precursor window of 3.0 m/z and a normalized collision energy between 26.0 and 28.0. MS2 spectra were recorded with a resolution of 17,500 (AGC: 5E4). Singly charged precursors were excluded from fragmentation. Dynamic exclusion was set to 20 seconds and the intensity threshold was set to 8E3. For the ubiquitinome analysis, a single LC-MS/MS run was performed for all immunoprecipitated peptide material from one sample.

Data analysis: Mass spectrometric raw data were analyzed using the MaxQuant software suite (version 1.5.2.8 (Tyanova, Temu and Cox, 2016)) for identification and relative quantification of proteins. A false discovery rate (FDR) of 0.01 for proteins and peptides and a minimum peptide length of 6 amino acids were required. The Andromeda search engine was used to search the MS/MS spectra against the *Drosophila melanogaster* Uniprot database (release DROME_2014_10.fasta, containing 23,336 entries) concatenated with the reversed versions of all sequences and a contaminant database listing typical background proteins and supplemented with several known *Drosophila* viral proteins. A maximum of two missed cleavages were allowed. Q Exactive spectra were analyzed using MaxQuant's default settings for Orbitrap spectra, including a main search peptide and MS/MS match tolerance of 4.5 and 20 ppm, respectively. The maximum precursor ion charge state used for searching was 7 and the enzyme specificity was set to trypsin. Further modifications were cysteine carbamidomethylation (fixed) as well as protein methionine oxidation, Lys ubiquitination and STY phosphorylation (variable). The minimum number of razor and unique peptides was set to 1. Heavy-to-light (H:L) ratios were calculated using MaxQuant's default settings, including a minimum ratio count of 2 for label based protein quantification and of 1 for diGly peptide quantification. Only unique and razor non-modified, methionine oxidized and protein N-terminal acetylated peptides were used for protein quantitation. The 'requantify' option was selected in all cases. The minimum score for modified peptides was set to 40 (default value). Only proteins that were identified and quantified both in the forward and reverse assays and with consistent ratios were taken into account for further analysis. Protein sets were further analyzed with Perseus (Tyanova *et al.*, 2016) (version 1.5.0.15), the gene ontology (GO) software DAVID (version 6.7, available from

<http://david.abcc.ncifcrf.gov/>, (Huang *et al.*, 2007)) and in-house developed software (Sap *et al.*, 2015). For the statistical testing of quantitative data, we used either two-sided two-sample t-test were performed in Perseus using 250 randomizations and settings FDR=0.05 and S0=0.5 or ‘significance B’ with p-value=0.05. For these statistical tests, additional control experiments were considered in which light and heavy labeled non-treated cells were mixed in a forward and reverse fashion. Hierarchical clustering was performed using the following settings: row tree: distance Euclidian; linkage: average; number of clusters: 300; column tree: distance Euclidian; linkage: average; number of clusters: 300.

MS raw data and data for protein identification and quantification were submitted as supplementary tables to the ProteomeXchange Consortium via the PRIDE partner repository with the data identifier PXD002552.

Results and Discussion

In order to investigate proteasome dysfunction by either chemical drugs or dsRNA mediated knockdown of specific subunits, we took a quantitative proteomics approach in *Drosophila*. We set off by selecting a combination of catalytic, structural and regulatory subunits that, when simultaneously depleted, resulted in abolishment of all proteasomal activity. Single dsRNA mediated knockdown for several subunits was performed but did not result in sufficient knockdown in all cases (results not shown). The most efficient knockdowns for individual subunits were obtained with Prosalpha5, Prosbeta6 and RPN11 (Figure S1A). Protein levels after four days of dsRNA treatment were as low as after two days, suggesting that protein depletion is already at a maximum after two days. We observed that many cells did not survive four days of dsRNA treatment and decided to use incubation times of two days for all further experiments. To test the efficiency of proteasome inactivation by simultaneous dsRNA mediated knockdown of Prosalpha5, Prosbeta6 and RPN11 (referred to as “3xKD”) treatment, cell lysates were analyzed for the presence of ubiquitinated proteins. The immunostaining patterns are comparable to those observed upon MG132/Lactacystin treatment for 16 h (Figure 1A, B), suggesting that the effect of proteasome activity intervention in terms of accumulation of ubiquitinated proteins and/or induction of protein ubiquitination was similar. dsRNA mediated knockdown, in contrast, results in subunit depletion and may therefore also affect proteasome structure and assembly. Indeed, 3xKD resulted in an at least partial disruption of the proteasome structure as suggested by glycerol density gradient centrifugation assays (Figure S1B). In contrast, MG132/Lactacystin treated proteasome samples showed a pattern that is indicative of intact proteasomes (fractions #7-9), but, in addition, suggested an increased presence of alpha subunits in the lower density fractions. The overall staining intensities increased in both cases, even though the total protein input amounts were kept constant. This suggests an abundance increase

of proteasome constituents as a result of these treatments, which was confirmed by the quantitative proteomics experiments described below while similar effects have been observed by others (Lundgren *et al.*, 2003, 2005; Szlanka *et al.*, 2003). In general, proteins with high turnover rates, such as cyclins, are expected to become deregulated upon proteasome malfunctioning. Cell cycle regulation is a process that particularly relies on the proper regulation of such proteins. We observed a disturbance of the cell cycle upon both perturbations by FACS analysis. The higher G2/M phase peak and the lower G1 phase peak compared to the control situation indicate a G2/M arrest in the affected cells (Figure S1C). One possible explanation is that cells go into apoptosis, which is also suggested by the upregulation of typical apoptosis markers (shown hereafter). In conclusion, both dsRNA mediated knockdown and treatment with chemical inhibitors interfere with proteasome functioning, result in elevated levels of ubiquitinated proteins and affect cell cycle regulation.

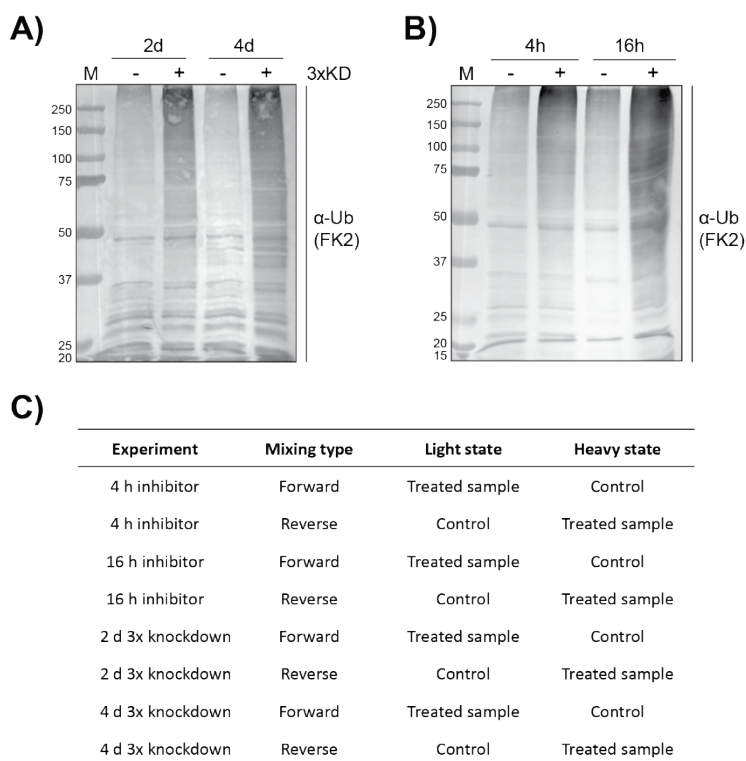


Figure 1. Immunoblots of proteasome samples treated with 3xKD (A) or MG132/Lactacystin (B) stained with FK2 antibody that recognizes conjugated ubiquitin branches, showed that global ubiquitination increases as a result of proteasome inactivation. C) Experimental design: SILAC samples were prepared in a forward and reverse manner to generate independent duplicates.

Next, we set out to investigate the effect of proteasome dysfunction on the global cellular proteome using a SILAC based mass spectrometry approach (Figure 1C). All experiments were performed in duplicate in a forward and reverse fashion, meaning that the SILAC labels were swapped for the duplicate experiment to correct for irregularities as a result of the stable isotope labeling procedure. Typically, over 5,000 proteins were identified and quantified per SILAC assay, with a total number of 5,899 proteins over all analyses (Table 1). Proteins with >1.5-fold abundance differences were defined as upregulated/accumulated or downregulated and were only selected for further analysis if consistent ratios in the forward and reverse experiments were observed.

Table 1. Numbers of identified up- and downregulated proteins.

Experiment	Exp #1	Exp #2	Total Exp #1 or Exp #2	Up in Exp #1	Up in Exp #2	Up in Exp #1 and Exp #2	Down in Exp #1	Down in Exp #2	Down in Exp #1 and Exp #2
4 h inhibitors	4862	4801	5056	223	212	78	45	66	1
16 h inhibitors	5025	5035	5282	749	723	466	90	74	11
2 d 3xKD	5166	5225	5367	851	769	545	139	162	50
4 d 3xKD	5128	5068	5331	922	939	598	287	355	109

Upon 16 h treatment with MG132/Lactacystin and upon 3xKD, more than 10% of the total measurable proteome was affected (Table 1, Figure S3). The dynamics of protein abundance and extent of upregulation are visualized in Figure 2 (see Table S1 for a complete list of proteins). After 4 h of treatment with chemical inhibitors a small set of stress responsive proteins were already extensively upregulated. These included the heat shock proteins Hsp22, Hsp23, Hsp26, Hsp70 and Hsp27, which have been shown to physically interact with the proteasome (Parcellier *et al.*, 2003) and to be induced upon proteasome inactivation (Lee and Goldberg, 1998b). Heat shock proteins remained present at highly elevated levels during prolonged exposure to inhibitors, as well as in 3xKD, suggesting that the cell maintains its stress responsive state as long as the proteasome's activity is reduced. Heat shock factor 1 (Hsf1), a master regulator of the heat shock genes that plays a significant role in suppressing protein misfolding in cells by

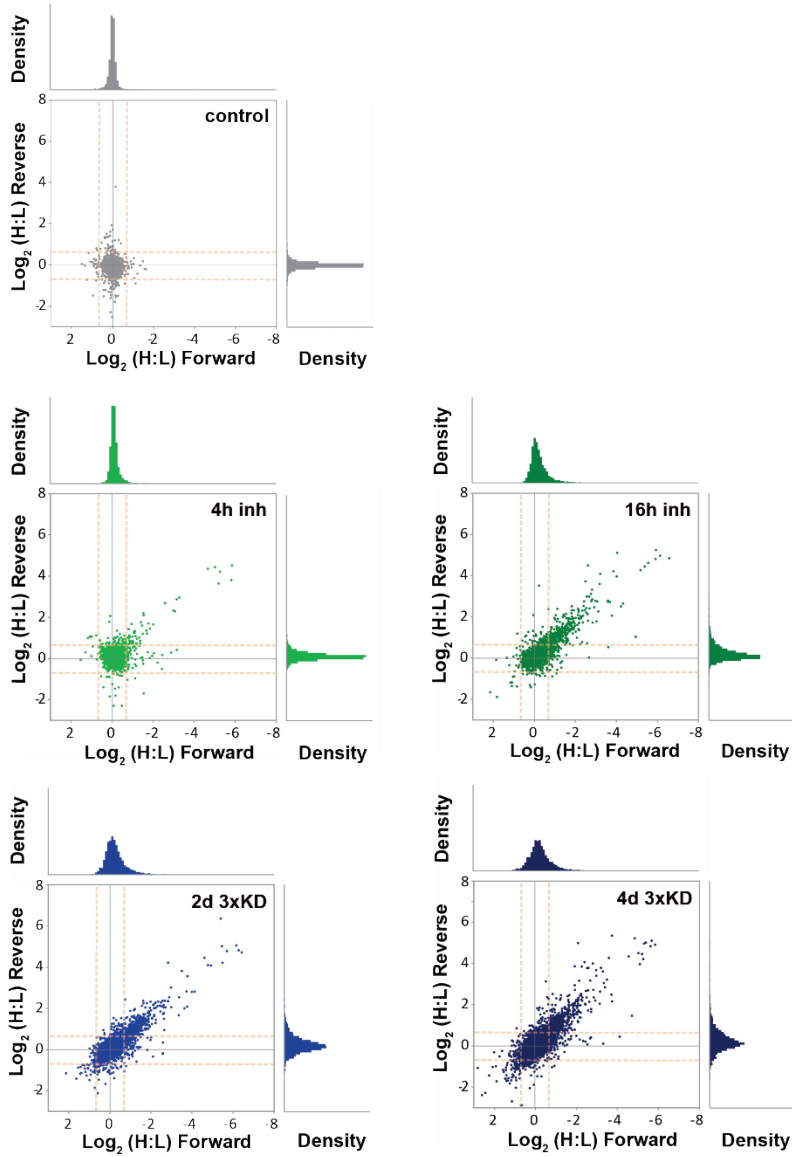


Figure 2. H:L ratios from forward and reverse SILAC experiments for the complete protein population and their distribution around the axis centers showed that a substantial part of the global proteome was remodeled. The H:L threshold ratio of 1.5-fold (corresponding to 0.59 at the Log2 scale) is indicated by the orange dashed line. The distribution of data points becomes less narrow as a result of proteasome perturbation, either with drugs or by dsRNA mediated knockdown of subunits.

inducing the expression of heat shock genes (Schubert *et al.*, 2000), is also present at elevated concentrations under all conditions tested. Ref(2)p, which has a ubiquitin binding domain and has been shown to localize to ubiquitin-positive protein aggregates (Nezis *et al.*, 2008), was increased to a similar extent as the heat shock proteins. Other ‘early responders’ included Pomp, the *Drosophila* homolog of human Ump1, a short-lived chaperone present in the precursor form of 20S that is required for the correct assembly and enzymatic activation of the proteasome (Ramos *et al.*, 1998; Burri *et al.*, 2000).

In general, the overlap between 16h drug treatment and 3xKD was quite extensive in spite of the slightly different time scales at which the perturbation mechanisms act (Figure 3). Gene Ontology (GO) analysis revealed that shared proteins include stress response proteins and proteins involved in the UPS, apoptosis, transcription and cell signaling (Figure S4). In addition, while upregulated proteins in the chemical inhibition experiments were enriched for in functional categories such as metabolic processes and development, increased proteins in 3xKD were also related to cytoskeleton organization and cell proliferation. Approximately 50 proteins were increased in all conditions, including additional stress response proteins such as DnaJ protein homolog, Methuselah and Thor. Proteins involved in the JNK cascade, Kayak (Fos), Jra (AP-1) and the phosphatase Puckered, as well as the transcription factors Apterous, Helix loop helix protein 106 and the transcriptional repressor Hairy were increased. Upregulated proteins involved in apoptosis included the Bcl-2 family member protein Debcl (dBorg or BG1), a key regulator of apoptosis (Quinn *et al.*, 2003), as well as Dcp-1, Diap (Thread/th), Dredd (Caspase-8), Drice (Caspase), Strica/Dream, UbcD1 (effete/eff) and Morgue. Ago, the substrate recognition component of a SKP1-CUL1-F-box protein E3 ubiquitin-protein ligase complex mediating the ubiquitination and subsequent proteasomal degradation of target proteins, also showed increased abundance in all cases. Cell cycle regulators (CycA, CycB, CycK CycH, CycE and Cks85A), mitotic spindle related proteins and c-Myc (dm) were also affected.

Interestingly, the relatively small pool of downregulated proteins in 3xKD consisted almost exclusively of mitochondrial ribosomal proteins (Figure 3A, Table S1). The perturbation of mitochondria has been described as a cellular event that follows the initial accumulation of short-lived proteins and concomitant induction of apoptosis by proteasome inhibition (Almond and Cohen, 2002). Also, a similar decline of ribosomal proteins and concomitant increase in proteasome complex constituents was recently observed in aging experiments in *C. elegans* (Walther *et al.*, 2015).

The global abundance levels of ubiquitin increased two- to five-fold upon proteasome inactivation (Figure S7). A bottom-up proteomics assay does not allow the differentiation between conjugated, polymeric, monomeric, free and activated ubiquitin and so the detected proteolytic fragments merely reflect all ubiquitin present in the cell. Using ‘tryptic’ proteomics it is however possible to identify and quantify the various linkage types of polyubiquitin in detail.

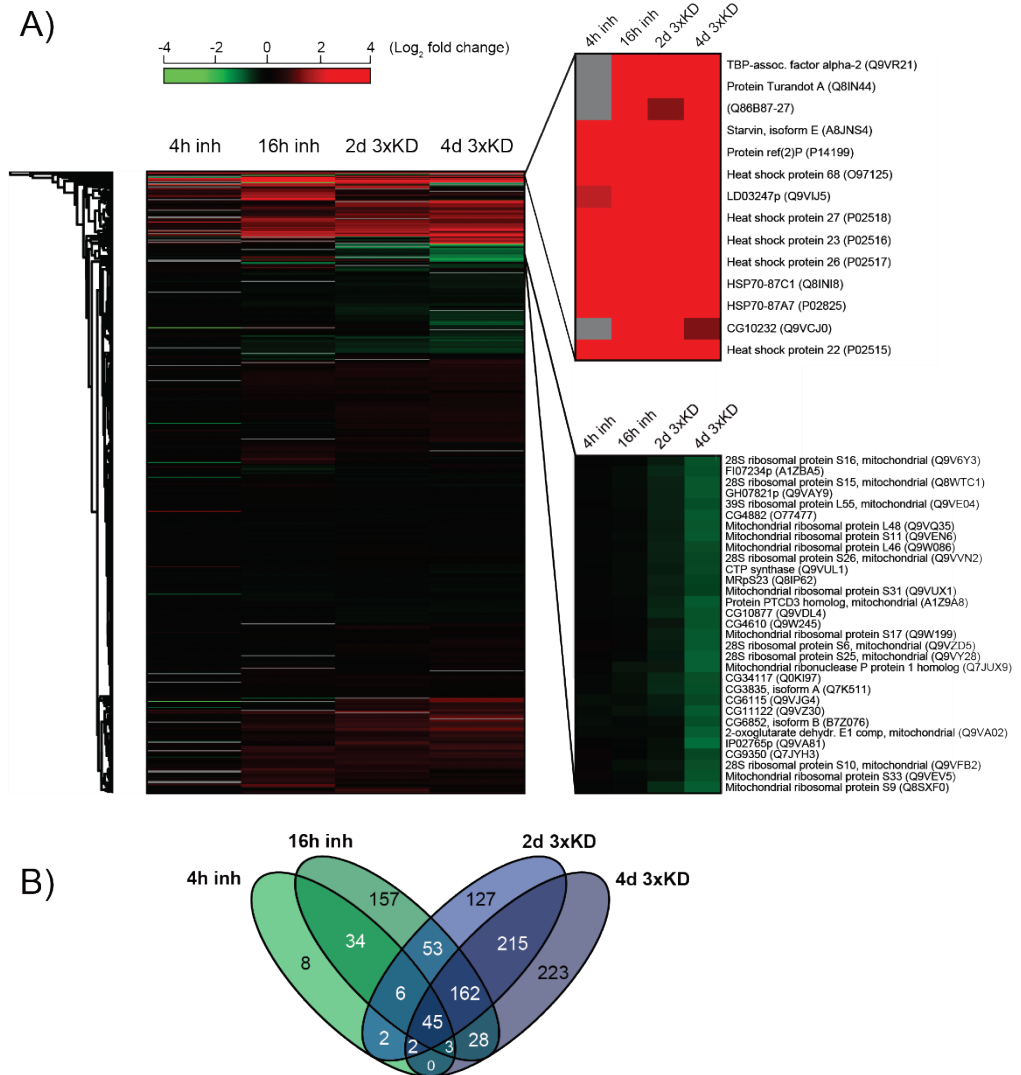


Figure 3. Clustering analysis revealed that many affected proteins in the 3xKD and chemical inhibitors experiments overlap (A, B). The magnification shows a subset of typical proteins that are upregulated in all conditions (red). Notably, many of the proteins that decreased in abundance in 4d 3xKD were related to the mitochondrial ribosome (magnified area, green). A complete list of proteins can be found in Supplementary Table 1.

An extensive analysis of the polyubiquitin dynamics is described in the ‘ubiquitinome’ section below. In addition, all proteasome subunits, except for Prosbeta7 in 3xKD, were increased upon inactivation by inhibition and subunit knockdown (Figure S7). This phenomenon, also observed by others (Wójcik and DeMartino, 2002; Lundgren *et al.*, 2005), may either be a consequence of the high turnover of proteasome subunits or may be an effect of elevated expression to compensate for loss of proteasomal activity sensed by the cell.

Next, we sought to determine whether the observed increased abundances are the result of protein accumulation or rather of *de novo* protein synthesis. For this, we combined proteasome inhibition with cycloheximide (CHX) treatment, which blocks the translational elongation thus inhibiting protein biosynthesis, in a SILAC based assay. Cells were either treated with CHX and MG132/Lactacystin for 4 hours or with MG132/Lactacystin alone, while CHX was added to the cell culture one hour prior to MG132/Lactacystin. Proteins with abundance dynamics effects upon CHX treatment, but non-responsive upon inhibitor treatment, were excluded from downstream analysis. The majority of proteins were indeed increased as a result of *de novo* synthesis (Figure 4, Table S2). Interestingly, ubiquitin was also *de novo* synthesized. While ubiquitin is recycled by specific proteasome modules and not degraded along with proteasome targeted proteins, the total ubiquitin pool in the cell is expected to be rather stable in proteostasis conditions. We hypothesize that the existing pool of ubiquitin is apparently not sufficient to accommodate for the need of ubiquitin under the here imposed stress conditions. This idea is supported by data from Kopito and coworkers on mouse embryonic fibroblasts (MEFs), who showed that proteasome inhibition leads to a robust increase in total ubiquitin because of transcriptional activation of ubiquitin gene expression, although this effect is cell type dependent (Kaiser *et al.*, 2011).

In conclusion, a substantial part of the proteome that was upregulated after proteasome inactivation consists of *de novo* synthesized proteins. Unfortunately, CHX treatment could not be prolonged for more than 4 hours, because longer incubation turned out to be lethal to S2 cells. It is expected that after prolonged inactivation the accumulation of polyubiquitinated proteins destined for degradation becomes an increasingly important factor to explain observed elevated protein abundances.

In order to understand how proteasome inactivation disturbs UPS regulation, we then focused on the analysis of protein ubiquitination. Since proteins destined for degradation by the proteasome carry a polyubiquitin tag, disruptions of the UPS are expected to result in substantial changes at the ubiquitin-modified proteome (‘ubiquitinome’) level. Ubiquitinome analysis revealed over 14,000 unique diGly peptides that were identified over all SILAC experiments (Table 2, Table S3), the majority of which could also be quantified.

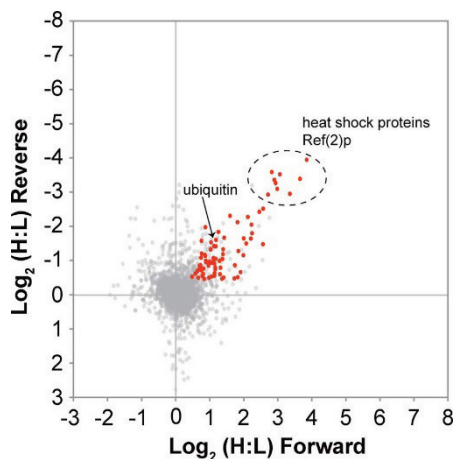


Figure 4. A comparison of cells that were treated with a combination of the translational inhibitor cycloheximide (CHX) and MG132/Lactacystin, and control cells treated with MG132/Lactacystin alone, revealed that the majority of the increased proteins upon proteasome inhibition were indeed synthesized but not accumulated. Red data points represent proteins that were also present with increased abundances in the MG132/Lactacystin *vs* untreated cells screen. For a complete list of synthesized proteins, see Supplementary Table 2.

Since, to our knowledge, this is the first large-scale ubiquitinome screen in *Drosophila*, we set out by searching for potential ubiquitination target consensus sites. A sequence context (motif) analysis carried out to determine how Lys ubiquitination may be regulated at the primary structure level did not reveal any consensus ubiquitination site whatsoever (Figure S5A). This is in agreement with a study in mammalian cells in which no enrichment for any particular motif was observed either (Kim, Eric J. Bennett, *et al.*, 2011). While for non-modified peptides there was a clear correlation between the number of identified peptides per protein corrected for the corresponding protein molecular mass on the one hand and the total protein intensity on the other hand, no such correlation was observed for diGly peptides (Figure S5B). This indicates that diGly peptides were not detected because they originate from abundant proteins *per se*. Instead, it suggests that the extent of ubiquitination is highly variable per protein and independent of absolute protein abundance levels. The overlap of diGly peptides that were identified in the various data sets was reasonable, but not extensive (Figure S5C). There may be both experimental and biological explanations for this. Different strategies to inactivate the proteasome may result in partially different ubiquitinome transformation effects, or degradation directed protein ubiquitination may not occur in a site-specific fashion. Also, we cannot exclude the possibility that only a fraction of the total ubiquitinome is captured in these diGly IP's. After 4 h proteasome inhibition ubiquitinome transformation may still be in its infancy and many of the target sites may not yet be modified, or their stoichiometry is too low so that they will simply

escape detection. The absolute intensities of diGly peptides of ubiquitin were roughly two orders of magnitude lower than those for its non-modified peptides (Figure S5D), which indeed indicates a low stoichiometry of ubiquitination modification.

Table 2. Numbers of identified and quantified diGly peptides over all experiments.

	# of diGly peptides
Total identified (heavy or light)	22,614
Total identified (heavy and light counterparts collapsed)	14,018
with 1 diGly site	13,641
with 2 diGly sites	344
with 3 diGly sites	28
with 4 diGly sites	5
Total identified and quantified	11,091
no reported H:L ratio in forward and reverse experiment	1,268
intensity value reported in only light channel or heavy channel	1,097

Next, we interrogated the dynamics of protein ubiquitination as a result of proteasome inactivation in a diGly peptide SILAC assay. Over 70% of all identified diGly peptides showed increased abundances as a result of proteasome inactivation (Figure 5A). For ubiquitination sites detected in multiple perturbation types, there was a substantial overlap in upregulation (Figure 5B). Proteins with increased ubiquitin modification were involved in diverse processes such as cell cycle regulation, (ubiquitin-dependent) protein catabolism, cytoskeleton and mitotic spindle organization, apoptosis, proteolysis and metabolism and have ubiquitin ligase, nucleotide binding and ATPase activities (Figure S6). There were no obvious differences in GO enrichment profiles between the different treatments.

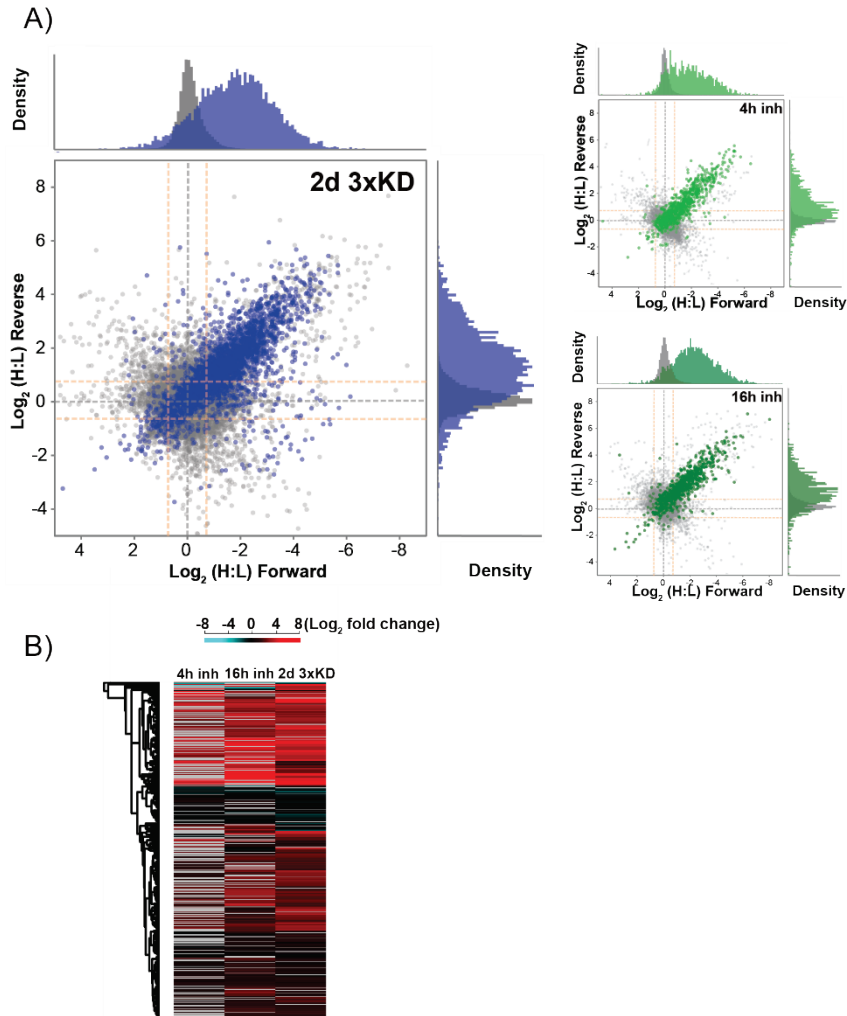


Figure 5. A) H:L ratios of non-modified (grey) and diGly (blue) peptides from the 2d 3xKD proteasome inactivation duplicate experiment. The deviation of the virtually complete diGly peptide population from the axis center indicates an enormous remodeling of the total ubiquitinome, while the remodeling of the non-modified peptidome was relatively limited (see also Figure 2 for global proteome profiles). B) Clustering analysis of diGly peptide dynamics revealed that there is a substantial overlap between the inhibition and knockdown experiments. Obviously, after relatively short incubation times, many of the diGly peptides were not upregulated yet.

We then integrated the protein abundance dynamics data with the associated dynamic ubiquitination profiles, which resulted in the formation of different categories of proteins with specific associations of ubiquitination profile and abundance dynamics (Figure 6, Table S4). Representative examples of each of these categories are discussed in more detail. The first - and largest - category consisted of proteins combining overall increased ubiquitination at all identified target sites with increased global abundance. As an example Proasalpha1 is shown, although all proteasome subunits display a similar behavior. Proteins with abundance changes accompanied by larger fold changes of diGly peptides are exemplified by Q7KN62. A third class is represented by Sgt, whose global abundance remained largely unchanged, although its site ubiquitination occupancy increased several fold. Besides these major categories, proteins were identified with opposite ubiquitination and abundance regulation behavior. One example is sta: while the overall protein abundance decreased, ubiquitination occupancies at several target sites increased.

For several other proteins different ubiquitination sites were identified with opposite dynamic behavior. For instance, CG5174 displayed a relatively stable global abundance level, but simultaneous heterogeneous ubiquitination. Similarly, the overall level of BTF3 remained constant, whereas at least one diGly peptide decreased three-fold. While the decrease of global RpL5 and RpS10b levels may be a result of decreased biosynthesis rates, it is more difficult to explain their dynamic ubiquitination profile. For RpL5, most ubiquitination sites were upregulated, but one site was downregulated. In contrast, for RpS10b most, but not all, ubiquitination sites were downregulated.

An intriguing example is RpS3, a constituent of the ribosome that is known to also have extra-ribosomal roles such as involvement in the repair of UV-induced DNA damage (Wilson 3rd, Deutsch and Kelley, 1993) and as an inducer of apoptosis (Jang, Lee and Kim, 2004). Its overall abundance decreased slightly, while the diGly peptide dynamics displayed an extremely heterogeneous profile. Remarkably, all downregulated ubiquitination sites are exclusively localized in the unstructured C-terminal domain, while all upregulated target sites are restricted to the structured domain (Figure 6B). One possibility is that the reported diGly peptides originate from different populations of RpS3, *e.g.* in isolated subcellular compartments. Alternatively, if the identified ubiquitination sites indeed coexist on the same individual RpS3 molecule and represent degradation signals, it would suggest opposing degradation signaling dynamics in different protein domains. Interestingly, it was shown recently that the proteasome prefers substrates that have disordered regions with complex amino acid composition to initiate degradation (Fishbain *et al.*, 2015; Humbard and Maurizi, 2015). Another possibility is that the structured and unstructured domains may be physically separated entities. Partial proteasomal degradation, ranging from complete degradation to complete protection of one particular domain, has been observed in *e.g.* signaling pathways (Kraut and Matouschek, 2011). However, perhaps the most likely explanation is that, while some of the ubiquitination sites may represent proteasomal degradation marks, others are involved in regulatory events.

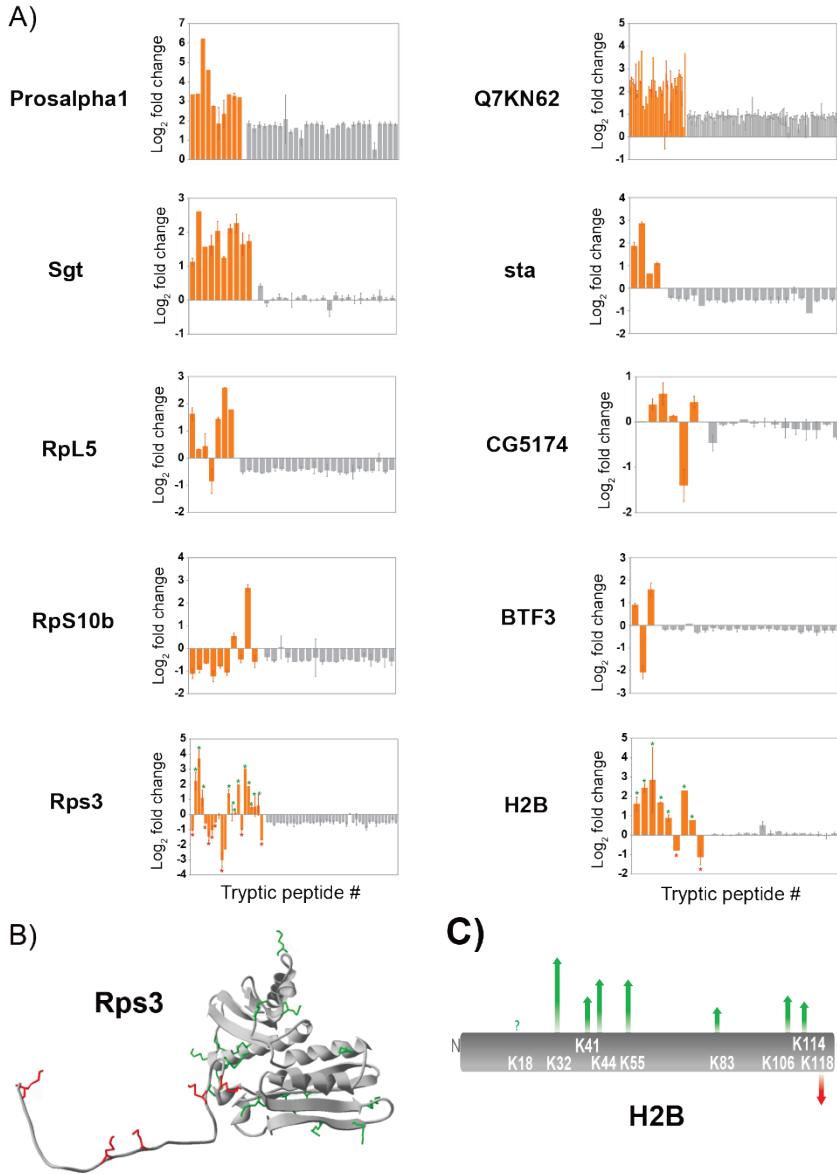


Figure 6. A) Dynamics of diGly (orange) and non-modified (grey) peptides upon proteasome inactivation for a selection of proteins. Fold change values are an average of at least two independent measurements, unless no error bar is indicated; the ranking of peptides on the x-axis is at random and does not reflect the position in the protein sequence. Multiple different diGly peptides may contain the same modified Lys residue. A question mark indicates that although diGly site was identified, the quantitative information data

quality was insufficient. B) Three-dimensional structure of the *Drosophila melanogaster* 40S ribosomal protein S3 based on PDB accession 4v6w (RpS3 / CG6779; chain AD; protein length 246) (Anger *et al.*, 2013). Lys residues with decreasing ubiquitination are indicated in red, Lys residues with increasing ubiquitination in green; the same color coding applies to RpS3 in Panel A. Two additional C-terminal Lys residues that were quantified with decreasing ubiquitination in the SILAC assay were not present in the 3D-structure (*i.e.*, K235 and K244). C) Schematic representation of the primary structure of histone H2B. The Lys residues that showed increased (green) or decreased (red) ubiquitination are indicated; color coding corresponds to the bar graph for H2B in Panel A. Multiple diGly peptides may represent the same ubiquitination site.

This hypothesis is supported by recent work from Higgins *et al.* (Higgins *et al.*, 2015), who identified similar RpS3 ubiquitination patterns suggesting that a subset of 40S ubiquitylation events must be regulatory in nature. This idea is consolidated by reports that ~65% of ubiquitin is present as monoubiquitinated substrates in mammalian cell lines (Kaiser *et al.*, 2011) and, thus, has regulatory functions. Another interesting case was presented by histone H2B (Figure 6C). All ubiquitination sites were upregulated, except for K118. It is known that monoubiquitination of this particular residue is a regulatory modification that plays a key role in transcriptional activation (Zhang, 2003), while other ubiquitination sites in (human) H2B have been identified although these are not well studied or understood yet (Molden *et al.*, 2015). One possibility is that the observed decreased ubiquitination at K118 indeed represents monoubiquitination and is the result of the stress imposed by proteasome inactivation that leads to a global decrease of transcription and protein synthesis such as has been observed for example in the case of ER stress that activates the unfolded protein response (Walter and Ron, 2011).

Our findings are in partial contrast to those of Kim *et al.* (Kim, Eric J. Bennett, *et al.*, 2011), who observed a similar decrease of diGly peptide representing this particular Lys (corresponding to K121 in human H2B), but a decrease instead of an increase of two other diGly sites. It should be noted that the coverage of diGly sites in our screen is higher (7 versus 3), that the timescale between chemical and dsRNA mediated proteasome inactivation may be different and that other cell types were used. In conclusion, the heterogeneous ubiquitination dynamics within proteins forms an intriguing observation. Further investigation should be focused on the identification of the linkage type of the (poly)ubiquitin modifications to differentiate between degradation marks and regulatory ubiquitination.

The analysis of diGly peptides from polyubiquitin allowed us to investigate whether there is a preference for specific linkage types at a global scale under the conditions tested. All chain types increased in all conditions, with no clear preference for K48-linked chains or any other chain type (Figure 7, Table S5). Surprisingly, only K27-linked chains stand out in the 16h MG132/Lactacystin and 3xKD experiments and show a slightly higher fold upregulation than the other linkage types. K27-linked polyubiquitin was recently shown to be required for promoting chromatin ubiquitination following DNA damage, which seemed strictly dependent on the activity of the ubiquitin ligase RNF168 (Gatti *et al.*, 2015). Whether or not K27-linked

Conclusions

We have shown here that the global proteome and, to a greater extent, the ubiquitinome are severely modified upon proteasome inactivation both by chemical inhibitors and by dsRNA mediated knockdown of specific subunits in *Drosophila* S2 cells. Affected ubiquitin-mediated protein degradation by decreased proteasome activity would lead to accumulation of polyubiquitin modified proteins. Therefore, the extent of protein accumulation would develop in parallel to the increase of ubiquitination stoichiometry. Based on mass spectral intensity analysis we have shown that the absolute ubiquitination stoichiometries are relatively low, which is in agreement with earlier observations of Kim *et al.* (Kim, Eric J. Bennett, *et al.*, 2011). Many proteins exhibit irregular ubiquitination profiles, with simultaneous increasing and decreasing site-specific ubiquitination within the same protein, with no apparent relationship to their overall protein abundance levels. Most likely, part of these ubiquitination events has non-degradative regulatory functions.

In our assay, 3,077 proteins with at least one diGly peptide were identified. With 5,899 proteins identified in total, this means that at least 52% of all proteins carry a ubiquitin modification, at least under proteotoxic conditions. We argue that proteins that do not represent conventional proteasome substrates, such as proteins that are part of ubiquitin signaling networks and that carry regulatory (poly)ubiquitin marks different from the canonical K48-linked polyubiquitin degradation signal mark, may represent a wide cross-section of the diGly-containing proteome, which has also been suggested by others (Kim, Eric J. Bennett, *et al.*, 2011; Komander and Rape, 2012). The fact that ~65% of ubiquitin is present as monoubiquitinated substrates in mammalian cell lines, as was reported by Kaiser *et al.* (Kaiser *et al.*, 2011), supports this hypothesis. As a result of tryptic cleavage in bottom-up proteomics approaches, it is not possible to differentiate between mono-, di- and polyubiquitination using the diGly enrichment protocol described here. It would be extremely interesting to be able to differentiate between structurally different ubiquitination modifications in this high-throughput assay, since this would shed more light on the various cellular functions and the relationship between these functions and the exact structure of polyubiquitin moieties.

In conclusion, we have shown that combining quantitative proteomics with dsRNA mediated knockdown of individual subunits of the 26S proteasome complex in *Drosophila* offers a powerful and easy to implement tool to study the dynamics of the (modified) proteome upon perturbation of the UPS. This strategy may pave the path for the dissection of the mode of action of this intriguing cellular machinery by screening individual subunit knockdowns in a systematic way, both under proteostasis as well as proteotoxic conditions. For instance, it is unclear why the 26S proteasome contains three different DUBs and the details of the interplay between them and the ubiquitin receptor proteins are not known. Targeted depletion of each of these proteins could present a far more subtle interference with proteasome functioning than using possibly

unspecific chemical inhibitors. Understanding the details of proteasome functioning is essential for the development of next generation proteasome inhibitors for clinical purposes. Finally, since this is to our knowledge the first comprehensive ubiquitinome screen in a fruit fly cell system, so this data set will serve as a valuable repository for the *Drosophila* community at large.

Supporting information available online

TABLE S1 - List of identified and quantified proteins in the global proteome assay.

TABLE S2 - List of *de novo* synthesized proteins.

TABLE S3 - List of identified and quantified diGly peptides.

TABLE S4 - List of all quantified non-modified and diGly peptides.

TABLE S5 - List of all quantified peptides of ubiquitin.

FIGURE S1 – Proteasome integrity and cell cycle regulation upon inhibition and 3xKD.

FIGURE S2 – Volcano plots showing significantly up- and downregulated proteins upon inhibition and 3xKD.

FIGURE S3 - Percentages of up- and downregulated proteins upon inhibition and 3xKD.

FIGURE S4 - Gene Ontology (GO) analysis of affected proteins upon inhibition and 3xKD.

FIGURE S5 - Consensus site analysis, mass spectral intensities and overlap of identified diGly peptides.

FIGURE S6 - GO analysis of upregulated diGly peptides upon inhibition and 3xKD.

FIGURE S7 - Upregulation of ubiquitin and proteasome subunits upon proteasome inactivation.

References

- Almond, J. B. and Cohen, G. M. (2002) 'The proteasome: a novel target for cancer chemotherapy', *Leukemia*. 2002/04/18, 16(4), pp. 433–443.
- Anger, A. M. *et al.* (2013) 'Structures of the human and *Drosophila* 80S ribosome', *Nature*. 2013/05/03, 497(7447), pp. 80–85.
- Brand, A. H. and Perrimon, N. (1993) 'Targeted gene expression as a means of altering cell fates and generating dominant phenotypes', *Development*, 118(2).
- Burri, L. *et al.* (2000) 'Identification and characterization of a mammalian protein interacting with 20S proteasome precursors', *Proc Natl Acad Sci U S A*. 2000/09/06, 97(19), pp. 10348–10353.
- Chalkley, G. E. and Verrijzer, C. P. (2004) 'Immuno-Depletion and Purification Strategies to Study Chromatin-Remodeling Factors In Vitro', *Methods in Enzymology*, 377(2001), pp. 421–442.
- Chau, V. *et al.* (1989) 'A multiubiquitin chain is confined to specific lysine in a targeted short-lived protein', *Science*. 1989/03/24, 243(4898), pp. 1576–1583.
- Chen, Z. J. and Sun, L. J. (2009) 'Nonproteolytic functions of ubiquitin in cell signaling', *Mol Cell*. 2009/02/17, 33(3), pp. 275–286.
- Ciechanover, A. and Brundin, P. (2003) 'Review The Ubiquitin Proteasome System in Neurodegenerative Diseases: Sometimes the Chicken, Sometimes the Egg', *Neuron*, 40, pp. 427–446.
- Dietzl, G. *et al.* (2007) 'A genome-wide transgenic RNAi library for conditional gene inactivation in *Drosophila*', *Nature*, 448(7150).
- Elena Koulich, Xiaohua Li, and G. N. D. (2008) 'Relative Structural and Functional Roles of Multiple Deubiquitylating Proteins Associated with Mammalian 26S Proteasome', *Molecular biology of the cell*, 19, pp. 1072–1082.
- Fenteany, G. *et al.* (1995) 'Inhibition of proteasome activities and subunit-specific amino-terminal threonine modification by lactacystin', *Science*, 268(5211), pp. 726–731.
- Fishbain, S. *et al.* (2015) 'Sequence composition of disordered regions fine-tunes protein half-life', *Nat Struct Mol Biol*. 2015/02/03, 22(3), pp. 214–221.
- Gatti, M. *et al.* (2015) 'RNF168 promotes noncanonical K27 ubiquitination to signal DNA damage', *Cell Rep*. 2015/01/13, 10(2), pp. 226–238.
- Giasson, B. I. and Lee, V. M. (2003) 'Are ubiquitination pathways central to Parkinson's disease?', *Cell*. 2003/07/16, 114(1), pp. 1–8.
- Groll, M. *et al.* (2006) 'Crystal structure of the boronic acid-based proteasome inhibitor bortezomib in complex with the yeast 20S proteasome.', *Structure (London, England: 1993)*, 14(3), pp. 451–6.
- Hershko, A. and Ciechanover, A. (1998) 'The ubiquitin system.', *Annual review of biochemistry*, 67, pp. 425–79.
- Higgins, R. *et al.* (2015) 'The Unfolded Protein Response Triggers Site-Specific Regulatory Ubiquitylation of 40S Ribosomal Proteins', *Molecular Cell*, pp. 1–15.
- Huang, D. W. *et al.* (2007) 'DAVID Bioinformatics Resources: expanded annotation database and novel algorithms to better extract biology from large gene lists', *Nucleic Acids Res*. 2007/06/20, 35(suppl_2), pp. W169–75.
- Humbard, M. A. and Maurizi, M. R. (2015) 'The proteasome gets a grip on protein complexity', *Nat Struct Mol Biol*. 2015/03/05, 22(3), pp. 181–183.
- Iwai, K. and Tokunaga, F. (2009) 'Linear polyubiquitination: a new regulator of NF-kappaB activation', *EMBO Rep*. 2009/06/23, 10(7), pp. 706–713.

- Jang, C.-Y., Lee, J. Y. and Kim, J. (2004) 'RpS3, a DNA repair endonuclease and ribosomal protein, is involved in apoptosis', *FEBS Letters*, 560(1-3), pp. 81-85.
- Kaiser, S. E. *et al.* (2011) 'Protein standard absolute quantification (PSAQ) method for the measurement of cellular ubiquitin pools.', *Nature methods*, 8(8), pp. 691-6.
- Kal, A. J. *et al.* (2000) 'The Drosophila brahma complex is an essential coactivator for the trithorax group protein zeste', *Genes Dev.* 2000/05/16, 14(9), pp. 1058-1071.
- Keller, J. N., Gee, J. and Ding, Q. (2002) 'The proteasome in brain aging', *Ageing Res. Rev.* 2002/06/01, 1(2), pp. 279-293.
- Kim, W., Bennett, E. J., *et al.* (2011) 'Systematic and quantitative assessment of the ubiquitin modified proteome', *Molecular Cell*, 44(2), pp. 325-340.
- Komander, D. (2009) 'The emerging complexity of protein ubiquitination', *Biochem Soc Trans.* 2009/09/17, 37(5), pp. 937-953.
- Komander, D. and Rape, M. (2012) 'The Ubiquitin Code', *Annual Review of Biochemistry*, 81(1), pp. 203-229.
- Kraut, D. A. and Matouschek, A. (2011) 'Proteasomal degradation from internal sites favors partial proteolysis via remote domain stabilization', *ACS Chem Biol.* 2011/08/06, 6(10), pp. 1087-1095.
- Lee, D. H. and Goldberg, A. L. (1998a) 'Proteasome inhibitors: valuable new tools for cell biologists', *Trends Cell Biol.* 1998/10/28, 8(10), pp. 397-403.
- Lee, D. H. and Goldberg, A. L. (1998b) 'Proteasome inhibitors cause induction of heat shock proteins and trehalose, which together confer thermotolerance in *Saccharomyces cerevisiae*', *Mol Cell Biol.* 1998/01/07, 18(1), pp. 30-38.
- Li, J. *et al.* (2017) 'Capzimin is a potent and specific inhibitor of proteasome isopeptidase Rpn11', *Nature Chemical Biology*, 13(5), pp. 486-493.
- Lundgren, J. *et al.* (2003) 'Use of RNA Interference and Complementation To Study the Function of the Drosophila and Human 26S Proteasome Subunit S13', *Mol Cell Biol.* 23(15), pp. 5320-5330.
- Lundgren, J. *et al.* (2005) 'Identification and Characterization of a Drosophila Proteasome Regulatory Network', *Mol Cell Biol.*
- Mayor, T. *et al.* (2007) 'Quantitative profiling of ubiquitylated proteins reveals proteasome substrates and the substrate repertoire influenced by the Rpn10 receptor pathway', *Mol Cell Proteomics.* 2007/07/24, 6(11), pp. 1885-1895.
- Meierhofer, D. *et al.* (2008) 'Quantitative analysis of global ubiquitination in HeLa cells by mass spectrometry', *J Proteome Res.* 2008/09/11, 7(10), pp. 4566-4576.
- Mohrmann, L. *et al.* (2004) 'Differential Targeting of Two Distinct SWI / SNF-Related Drosophila Chromatin-Remodeling Complexes Differential Targeting of Two Distinct SWI / SNF-Related Drosophila Chromatin-Remodeling Complexes', 24(8), pp. 3077-3088.
- Molden, R. C. *et al.* (2015) 'Multi-faceted quantitative proteomics analysis of histone H2B isoforms and their modifications', *Epigenetics & Chromatin.* 8(1), p. 15.
- Moshkin, Y. M. *et al.* (2007) 'Functional differentiation of SWI/SNF remodelers in transcription and cell cycle control.', *Molecular and cellular biology*, 27, pp. 651-661.
- Nezis, I. P. *et al.* (2008) 'Ref(2)P, the Drosophila melanogaster homologue of mammalian p62, is required for the formation of protein aggregates in adult brain', *J Cell Biol.* 2008/03/19, 180(6), pp. 1065-1071.
- Ordureau, A., M?nch, C. and Harper, J. W. (2015) 'Quantifying Ubiquitin Signaling', *Molecular Cell*, 58(4), pp. 660-676.
- Parcellier, A. *et al.* (2003) 'HSP27 is a ubiquitin-binding protein involved in I-kappaBalpha proteasomal degradation.', *Molecular and cellular biology*, 23(16), pp. 5790-5802.

- Ramos, P. C. *et al.* (1998) 'Ump1p is required for proper maturation of the 20S proteasome and becomes its substrate upon completion of the assembly', *Cell*. 1998/03/10, 92(4), pp. 489–499.
- Reddy, B. A. *et al.* (2014) 'Nucleotide Biosynthetic Enzyme GMP Synthase Is a TRIM21-Controlled Relay of p53 Stabilization', *Molecular Cell*, 53, pp. 458–470.
- San Miguel, J. F. *et al.* (2008) 'Bortezomib plus melphalan and prednisone for initial treatment of multiple myeloma', *N Engl J Med*. 2008/08/30, 359(9), pp. 906–917.
- Sap, K. A. *et al.* (2015) 'Global quantitative proteomics reveals novel factors in the ecdysone signaling pathway in *Drosophila melanogaster*', *Proteomics*, 15(4), pp. 725–738.
- Sarraf, S. a. *et al.* (2013) 'Landscape of the PARKIN-dependent ubiquitylome in response to mitochondrial depolarization', *Nature*. Nature Publishing Group, pp. 1–7.
- Schubert, U. *et al.* (2000) 'Rapid degradation of a large fraction of newly synthesized proteins by proteasomes', *Nature*. 2000/04/28, 404(6779), pp. 770–774.
- Szlanka, T. *et al.* (2003) 'Deletion of proteasomal subunit S5a/Rpn10/p54 causes lethality, multiple mitotic defects and overexpression of proteasomal genes in *Drosophila melanogaster*', *Journal of Cell Science*, 116(6), pp. 1023–1033.
- Thompson, J. W. *et al.* (2014) 'Quantitative Lys- ϵ -Gly-Gly (diGly) proteomics coupled with inducible RNAi reveals ubiquitin-mediated proteolysis of DNA damage-inducible transcript 4 (DDIT4) by the E3 Ligase HUWE1', *Journal of Biological Chemistry*, 289(42), pp. 28942–28955.
- Tyanova, S. *et al.* (2016) 'The Perseus computational platform for comprehensive analysis of (pro)teomics data.', *Nature methods*, 13(9), pp. 731–40.
- Tyanova, S., Temu, T. and Cox, J. (2016) 'The MaxQuant computational platform for mass spectrometry – based shotgun proteomics', *Nature Protocols*. Nature Publishing Group, 11(12), pp. 2301–2319.
- Udeshi, N. D. *et al.* (2013) 'Large-scale identification of ubiquitination sites by mass spectrometry.', *Nature protocols*. Nature Publishing Group, 8(10), pp. 1950–60.
- Wagner, S. a *et al.* (2011) 'A Proteome-wide, Quantitative Survey of In Vivo Ubiquitylation Sites Reveals Widespread Regulatory Roles.', *Molecular & cellular proteomics: MCP*, 10(10), p. M111.013284.
- Walter, P. and Ron, D. (2011) 'The unfolded protein response: from stress pathway to homeostatic regulation', *Science*. 2011/11/26, 334(6059), pp. 1081–1086.
- Walther, D. M. *et al.* (2015) 'Widespread Proteome Remodeling and Aggregation in Aging *C. elegans*', *Cell*. 2015/05/11, 161(4), pp. 919–932.
- Wilson 3rd, D. M., Deutsch, W. A. and Kelley, M. R. (1993) 'Cloning of the *Drosophila* ribosomal protein S3: another multifunctional ribosomal protein with AP endonuclease DNA repair activity', *Nucleic Acids Res*. 1993/05/25, 21(10), p. 2516.
- Wójcik, C. and DeMartino, G. N. (2002) 'Analysis of *Drosophila* 26 S proteasome using RNA interference.', *The Journal of biological chemistry*, 277(8), pp. 6188–97.
- Worby, C. A., Simonson-Leff, N. and Dixon, J. E. (2001) 'RNA interference of gene expression (RNAi) in cultured *Drosophila* cells.', *Science's STKE: signal transduction knowledge environment*. United States, 2001(95), p. p11.
- Xu, P. *et al.* (2009) 'Quantitative Proteomics Reveals the Function of Unconventional Ubiquitin Chains in Proteasomal Degradation', *Cell*, 137(1), pp. 133–145.
- Yeh, C. H., Jansen, M. and Schmidt-Glenewinkel, T. (2011) 'Role of the proteasome in fly models of neurodegeneration', *Methods Mol Biol*. 2011/09/14, 793, pp. 149–165.
- Zhang, Y. (2003) 'Transcriptional regulation by histone ubiquitination and deubiquitination', *Genes Dev*. 2003/11/25, 17(22), pp. 2733–2740.

Chapter 4

Depletion of the proteasome-associated deubiquitinase RPN11, but not UCHL5 and USP14, results in an extensive remodeling of the ubiquitinome.

Karen A. Sap, Karel Bezstarosti, Dick H.W. Dekkers and Jeroen A.A. Demmers

Manuscript in preparation

Abstract

The 26S proteasome is responsible for the degradation of a large complement of polyubiquitin-tagged proteins in the cell. In *Drosophila melanogaster* the proteasome harbors three deubiquitinating enzymes (DUBs), i.e. RPN11, UCHL5 and USP14, which are involved in the removal of ubiquitin from substrates destined for the proteasome. RPN11 is essential for the execution of protein degradation by removing the polyubiquitin tag, whereas the precise role of UCHL5 and USP14 in proteasomal degradation is still under debate. UCHL5 and USP14 have been reported to either decrease or enhance degradation of specific substrates in seemingly conflicting studies. Additionally, these DUBs have been implicated in non-proteolytic processes. All of these studies, however, monitored only one or at most a few selected proteasome substrates, or used chemical DUB inhibitors that might show off-target effects.

Here, we investigate the role of the proteasome-associated DUBs in proteasome dependent protein degradation by combining targeted dsRNA mediated knockdown of individual proteasome-bound DUBs in *Drosophila* S2 cells and large scale SILAC proteomics, ubiquitinome analysis and label free quantitative mass spectrometry. Our data imply that RPN11 is important for the structure and function of the proteasome and plays the major role in the degradation of a large majority of protein targets. In contrast, depletion of UCHL5 or USP14 or both DUBs simultaneously did not affect the structure and/or assembly of the proteasome monitored via glycerol gradient sedimentation, nor did it result in observable changes at the global proteome level. We focused specifically on the dynamics of ubiquitinated proteins upon depletion of RPN11, UCHL5 or USP14 by exploiting a diGly-peptide enrichment proteomics protocol in an attempt to identify potential targets for each of these DUBs. While many targets were identified for RPN11, virtually no specific targets for UCHL5 or USP14 were observed. Next, we tested whether a remodeling of the ubiquitinome goes together with a redistribution of the various ubiquitin pools. Overall ubiquitin levels rose over two-fold when RPN11 was depleted as compared to UCHL5 and USP14. This was in agreement with the results from the SILAC assay, where the total ubiquitin level was upregulated more than two-fold upon RPN11 depletion compared to control cells. In conclusion, even though accumulation of ubiquitin is likely to occur as a result of RPN11 depletion, an increase in the total level of ubiquitin indicates that the pool of free ubiquitin is supplemented and that ubiquitin is newly synthesized. Finally, polyubiquitin linkage type analysis did not give any indications that the three different DUBs have distinct or complementary roles with respect to linkage type cleavage specificity.

Taken together, the global proteome and ubiquitinome dynamics study presented here suggests that RPN11 serves as the major DUB in proteasomal functioning in that proteins are no longer degraded when this DUB is absent. In contrast, the roles of both UCHL5 and USP14 remain enigmatic since no major effects were observed after their depletion at the proteome level, nor at the ubiquitinome level.

Introduction

The 26S proteasome is a cellular protein complex, which plays an essential role in the degradation of proteins in the cell and, thus, in proteostasis. Proteins are typically targeted for 26S proteasome-mediated degradation through the post-translational attachment of a polyubiquitin tag (Finley, 2009). This tag is recognized by ubiquitin receptors at the proteasome 19S regulatory particle (RP), which in turn uses the tag to dock the substrate to the proteasome. Prior to proteolysis, this polyubiquitin tag has to be removed from the substrate, as this facilitates substrate translocation into the narrow pore of the 20S core particle (CP), and, additionally, allows for recycling of ubiquitin. The process of deubiquitination is carried out by specialized deubiquitinating enzymes (DUBs). In *Drosophila melanogaster*, there are three DUBs associated to the 26S proteasome: RPN11 (POH1 or PSMD14 in human), UCHL5 (also known as UCH37 or UCHL3) and USP14 (Ubp6 in *S. cerevisiae*). RPN11 and USP14 are evolutionary well conserved, whereas homologs of UCHL5 have been found in mammals and zebrafish, but not in *S. cerevisiae*. The proteasome associated DUBs RPN11, UCHL5 and USP14 belong to different deubiquitinase families, *i.e.* the JAMM, Uch and USP families, respectively (reviewed in (Komander, Clague and Urbe, 2009)). There are evident differences between these DUBs in terms of both molecular mechanism and cellular function.

RPN11 is the only essential proteasome-associated DUB (Gallery *et al.*, 2007; Finley, 2009), and is required for both the structure of the 26S proteasome and for the promotion of degradation of proteasome substrates (Maytal-Kivity *et al.*, 2002; Verma *et al.*, 2002; Yao and Robert E Cohen, 2002). Purified RPN11 is instable, but addition of RPN8 induces the formation of stable RPN8-RPN11 dimers which are catalytically active *in vitro*, albeit with a low propensity to deubiquitinate folded substrates including ubiquitin (Worden, Padovani and Martin, 2014). RPN11 and RPN8 also form heterodimers within the 26S proteasome complex where they are located at the center of the 19S Regulatory Particle (RP) (Fu *et al.*, 2002; Sanches *et al.*, 2007; Pathare *et al.*, 2014; Worden, Padovani and Martin, 2014). RPN11 is activated >100-fold when incorporated into the proteasome (Mansour *et al.*, 2015). Characteristic for RPN11 is that it removes ubiquitin chains from substrate *en bloc* by hydrolyzing the isopeptide bond between a substrate lysine and the C terminus of the first ubiquitin (Lam *et al.*, 1997; Verma *et al.*, 2002; Yao and Robert E Cohen, 2002). This activity is coupled to ATP-dependent substrate translocation into the 20S core and subsequent protein degradation (Yao and Robert E Cohen, 2002; M. J. Lee *et al.*, 2011). RPN11 acts thus relatively late in the process, that is when the proteasome is committed to degrade the substrate (Verma *et al.*, 2002). Importantly, RPN11 does not show ubiquitin linkage specificity towards di-ubiquitin substrates of different linkage types (Worden, Padovani and Martin, 2014). Taken together, co-translocational deubiquitination by RPN11 promotes substrate degradation by the 26S proteasome (Maytal-Kivity *et al.*, 2002; Verma *et al.*, 2002; Yao and Robert E Cohen, 2002; Worden, Dong and Martin, 2017).

Like RPN11, UCHL5 is a constituent subunit of the 26S proteasome in *Drosophila* (Hölzl *et al.*, 2000), mammals (Lam *et al.*, 1997) and *Schizosaccharomyces pombe* (Li *et al.*, 2000), although it seems not essential for its structure and proteolytic activity. UCHL5 is recruited to the proteasome by RPN13 and it associates with RPN2 in the 19S RP (Yao *et al.*, 2006; Chen *et al.*, 2010). The activity of UCHL5 is enhanced by RPN13 upon proteasome binding (Hamazaki *et al.*, 2006; Qiu *et al.*, 2006; Yao *et al.*, 2006). UCHL5 trims single ubiquitin moieties from the distal end of polyubiquitin chains (Lam *et al.*, 1997). In contrast, USP14 may not be a constituent subunit of the proteasome (Borodovsky *et al.*, 2001; Kuo and Goldberg, 2017), which we confirmed in this work as well (Figure 1). The amount of the USP14 homolog Ubp6 was found to be only ~30% of the canonical RP subunits in yeast as measured by quantitative label free mass spectrometry (Aufderheide *et al.*, 2015). In contrast, in HeLa cells 26S proteasomes contained approximately stoichiometric levels of USP14, but most cellular USP14 was found not to be associated with the proteasome (Elena Koulich, Xiaohua Li, 2008). The presence of ubiquitinated substrate at the proteasome promotes USP14 recruitment to the 26S proteasome (Kuo and Goldberg, 2017). USP14 interacts with proteasome subunit RPN1 via its N-terminal ubiquitin-like domain (UBL) (Elsasser *et al.*, 2002; Rosenzweig *et al.*, 2012) and its DUB activity is increased to a great extent upon binding to the 26S proteasome (Borodovsky *et al.*, 2001; David S. Leggett *et al.*, 2002; Hu *et al.*, 2005). Like for UCHL5, in the canonical model USP14 removes single ubiquitin moieties from the distal end of polyubiquitin chains (Lam *et al.*, 1997; Hanna *et al.*, 2006; M. J. Lee *et al.*, 2011), although this idea was challenged recently by Finley and coworkers, who showed that USP14 removes chains from Cyclin-B *en bloc* and showed that it can act in a very short time span even before the proteasome can initiate degradation (Lee *et al.*, 2016).

To date it is not clear how the activities of UCHL5 and USP14 affect proteasome dependent protein degradation rates or whether these DUBs might have a different substrate specificity from RPN11. Proteasomes can efficiently degrade substrates without USP14 (Hanna *et al.*, 2006; Lee *et al.*, 2010; Kim and Goldberg, 2017). In several proposed models UCHL5 and USP14 can decrease substrate degradation rates through the trimming of polyubiquitin chains from their distal ends, which results in a decreased affinity of the substrate (Lam *et al.*, 1997; Elena Koulich, Xiaohua Li, 2008; Lee *et al.*, 2010). However, UCHL5 and USP14 have also been reported to enhance degradation of substrates by the proteasome (Elena Koulich, Xiaohua Li, 2008; Mazumdar *et al.*, 2010; Mialki *et al.*, 2013). It should be noted here that such functional studies were often based on single or a limited number of substrates and many of these studies involve *in vitro* experiments with purified proteasomes. Although the differences in catalytic function between both DUBs are not clear, they have apparent redundant functions because depletion of both creates a phenotype not exhibited by depletion of either alone (Elena Koulich, Xiaohua Li, 2008). In a recent paper, Ubp6 (USP14) in yeast was shown to be activated especially when the proteasome adopts the substrate-engaged state, which suggests that its catalytic activity would

not prevent substrate degradation, but rather plays a facilitating role in substrate degradation and ubiquitin recycling (Bashore *et al.*, 2015).

Here, we investigate the roles of RPN11, UCHL5 and USP14 in proteasome-dependent protein degradation using a SILAC based proteomics approach, similarly as used in chapter 3 (Sap *et al.*, 2017). Our main objective was to monitor the dynamic behavior of the global cellular proteome and the ubiquitinome upon dsRNA mediated knockdown of the target DUBs in order to find out whether they may have a preference for specific substrates or specific polyubiquitin structures. We observed an extensive remodeling of both the proteome and the ubiquitinome upon RPN11 KD, whereas knockdown of UCHL5 KD, USP14 KD or a combination of both had virtually no effect on either the proteome or the ubiquitinome. Analysis of polyubiquitin dynamics did not reveal any specificity for linkage type for UCHL5 or USP14. Although the cellular pools of free (mono)ubiquitin and substrate conjugated (poly)ubiquitin were upregulated upon depletion of RPN11, no clear preference for any specific linkage type was observed.

We also investigated the nature of the interaction of USP14 to the proteasome in *Drosophila* by label free quantitative (LFQ) mass spectrometry. In contrast to RPN11 and UCHL5, USP14 (Ubp6) has previously been characterized as a non-constitutive interactor of the proteasome in mammals (Elena Koulich, Xiaohua Li, 2008) and yeast (David S. Leggett *et al.*, 2002; Rosenzweig *et al.*, 2012). In yeast, the Ubl domain in USP14 mediates reversible, salt-sensitive binding to the Rpn1/Rpn2 subunits (David S. Leggett *et al.*, 2002). To our knowledge, the interaction of USP14 with the proteasome has not yet been characterized in *Drosophila*. In our assays USP14 experiences salt-sensitive binding to the proteasome and therefore behaves as a weak or transient interactor, which is in agreement with its behavior in other eukaryotes.

In this study we showed that USP14 behaves like a transient interactor of the proteasome in *Drosophila*, which is in agreement with studies performed in yeast (David S. Leggett *et al.*, 2002; Rosenzweig *et al.*, 2012) and human cell lines (Elena Koulich, Xiaohua Li, 2008). Furthermore, we found that Rpn11 plays an important role in the degradation of proteolytic substrates, given its importance for proteasome complex stability, as well as its effect on both proteome and ubiquitinome dynamics upon Rpn11 KD. In contrast, the role of UCHL5 and USP14 remains elusive as we did not observe remodeling of the proteome, nor the ubiquitinome, upon depletion of UCHL5, USP14, or both of them. Furthermore, we observed a ~ 2-fold upregulation of the total pool of ubiquitin upon RPN11 KD, probably contributed via synthesis of ubiquitin, whereas we did not observe upregulation of specific polyubiquitin linkages, suggesting that the DUBs under investigation did not show a preference for specific polyubiquitin linkage types. In conclusion, our data show that RPN11 plays an important role in proteasome-mediated protein degradation, while the role of USP14 and UCHL5 is not yet clear.

Results

USP14 is a weak interactor of the proteasome complex in *Drosophila*

USP14/Ubp6 has been described as a transient or weak interactor of the proteasome in both yeast (David S. Leggett *et al.*, 2002; Rosenzweig *et al.*, 2012) and human (Elena Koulich, Xiaohua Li, 2008). Here we set out to assess the nature of the interaction of USP14 with the proteasome in *Drosophila* by specific co-immunoprecipitation (co-IP) of the complex using antibodies against RPN8 or RPN10 followed by an LFQ proteomic approach. Negative control experiments were performed with non-specific antibodies isolated from rabbit preimmune serum (PPI). After the co-IP, protein complexes were washed using buffers containing either low, medium or high salt concentrations (50 mM, 150 mM and 500 mM KCl, respectively) to challenge the binding of the retained co-purified proteins. Weak interactors are likely to dissociate with increasing salt concentrations. IPs were performed in triplicates and purified proteins were resolved by SDS-PAGE, in-gel trypsinized and analyzed by mass spectrometry. Raw data were then analyzed using the LFQ option in the MaxQuant software suite to discriminate putative interactors from co-purifying contaminants. This strategy is based on comparing the protein abundances identified in the RPN8 or RPN10 co-IPs with those identified in the PPI (control) co-IPs, based on accumulated tryptic peptide spectral intensities. Putative interaction partners are expected to be more abundant in the RPN8 or RPN10 IPs, while, in contrast, non-specific contaminants would have an approximate 1:1 ratio as they are expected to be equally abundant in both co-IPs. Proteins present with significantly increased abundances according to two-sided T-test statistics in either of the IPs are shown in black in Figure 1. Proteasome subunits are shown in red and the three proteasomal DUBs are individually specified in the plot. USP14 was enriched to a similar extent as the other proteasome subunits below (50mM) and at physiological salt concentrations (150 mM), in both the α -RPN8 and α -RPN10 co-IPs, suggesting a stable interaction with the proteasome. In contrast, USP14 was enriched to a severely lesser extent under high salt conditions compared to other proteasome subunits. This may indicate that USP14 is a relatively weak interactor of the proteasome. This observation is in agreement with previous studies in yeast and human and may also suggest that the DUB may have additional functions in the cell as has been hypothesized before (Elena Koulich, Xiaohua Li, 2008).

RPN11 is important for the stability and activity of the 26S proteasome

To investigate the role of each of the proteasome bound DUBs we used a dsRNA mediated knockdown (KD) approach to specifically deplete for RPN11, UCHL5, USP14 or UCHL5/USP14 simultaneously (referred to here as double knockdown or '2xKD'). To test the efficiency of this approach, expression levels of target proteins were assessed by either immunoblotting (RPN11, Figure 2A) or by real time RT-qPCR (UCHL5 and USP14, Figure 2B) as no antibodies were available for the latter two. Control samples were treated with dsRNA directed against GFP, which is absent from the cells used in this study. dsRNA was added to the

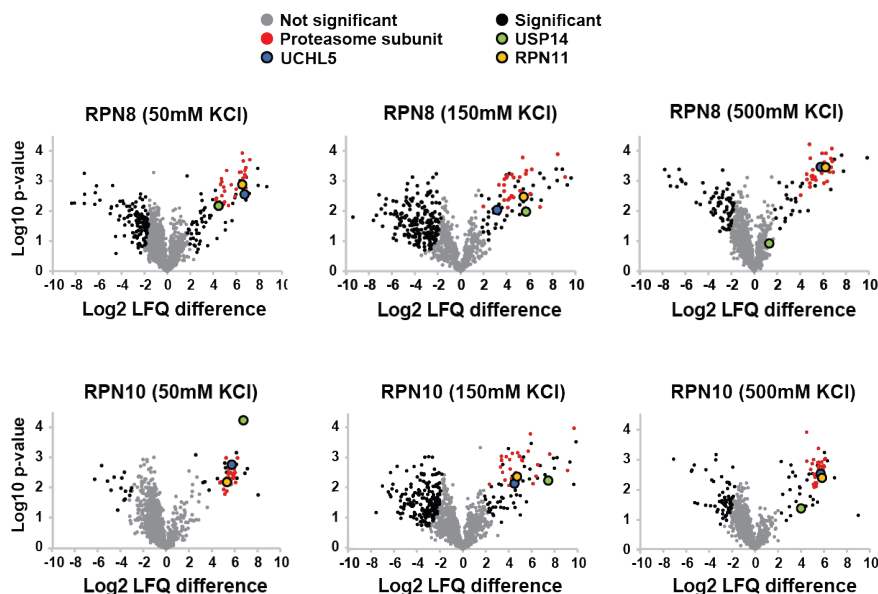


Figure 1. USP14 dissociates from the proteasome under high salt conditions in *Drosophila* S2 cells. Proteins were purified upon immunoprecipitation with antibodies directed against RPN8 or RPN10 or antibodies not specific for any proteasome subunits (Control) from whole cell extracts of S2 cells. Low, medium and high salt concentration (50 mM, 150 mM and 500 mM KCl, respectively) washing buffers were used to challenge the binding capacity of the retained purified proteins. Differential analysis of LFQ mass spectrometry results of the IPs is shown. Welch's t-tests were performed on Log2-transformed LFQ intensity values of controls (left side of volcano plots) and RPN8 or RPN10 IPs (right side). Proteins showing significantly higher abundance values are indicated in black. Proteasome subunits (red data points) were all enriched compared to control IPs, including the DUBs of interest RPN11, UCHL5 and USP14. Clearly, under increasingly stringent IP conditions, USP14 was much less effectively enriched than all other proteasome subunits, indicating a weaker binding efficiency.

cells during 48h, which is in correspondence with previous knockdown assays on different proteasome subunits (Sap *et al.*, 2017). Longer incubation times with dsRNA turned out to negatively affect cell viability. In conclusion, dsRNA mediated knockdown of RPN11, USP14 or UCHL5 results in a substantial reduction of protein expression levels (RPN11) or mRNA expression levels (UCHL5 and USP14) of the target protein products (Figures 2A and 2B), indicating that this knockdown approach is effective. dsRNA mediated interference of gene expression results in a cessation of target protein synthesis and thus also affects the assembly of novel proteasome complexes. First, we investigated the stability of the proteasome upon RPN11, USP14 or UCHL5 knockdown by glycerol gradient fractionation of protein complexes based on their size. Immunoblotting of adjacent glycerol gradient fractions shows the distribution of both

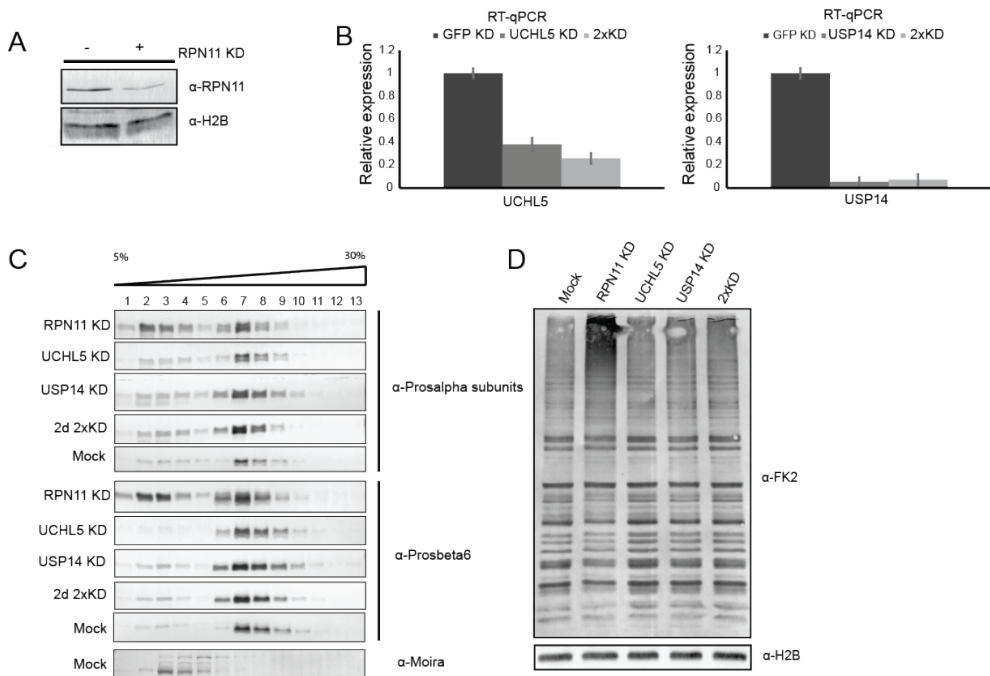


Figure 2. RPN11 is important for stability and activity of the proteasome

A) Immunoblots of RPN11 in control (left) and upon dsRNA mediated knockdown (right) in *Drosophila* S2 cells, indicating the depletion efficiency of the protocol. H2B is used as a loading control. B) UCHL5 and USP14 are downregulated upon dsRNA mediated knockdown. Since no antibodies were available for these proteins, RT-qPCR was used to assess the depletion efficiency. Total RNA was extracted from cell pellets and mRNA expression of UCHL5 and USP14 was measured (mRNA expression is shown relative to GFP dsRNA serving as the negative control here). C) Glycerol gradients were used to investigate proteasome stability upon depletion of RPN11, USP14 or UCHL5. Whole cell lysates were prepared under non-denaturing conditions and proteins and protein assemblies were separated in a 5-30% gradient. Each of the 13 resulting fractions was analyzed by SDS-PAGE and immunoblotted with α-Prosalpha and α-Prosbeta6 antibodies; α-Moira was used as a negative control. RPN11 KD affects the stability and/or assembly of the 20S proteasome core. Clearly, RPN11 knockdown results in a remarkable shift towards lower size fractions, suggesting disintegration of the 26S proteasome. D) Immunoblot with FK2 antibody of cell lysates from RPN11 KD, USP14 KD and UCHL5 KD cells. Mock cells were treated with dsRNA against GFP. RPN11 KD results in the accumulation of ubiquitinated proteins, whereas no obvious effects are observed for UCHL5 and USP14 KD.

Prosbeta6 and Prosalpha CP subunits under standard conditions (Mock, Figure 2C). As expected for intact proteasomes, distribution patterns observed for Prosbeta6 and Prosalpha subunits were comparable. The distribution patterns for Prosbeta6 and Prosalpha upon knockdown of UCHL5, USP14, and both DUBs simultaneously (2xKD) were comparable to the control

sample, whereas a substantial distribution shift to lower glycerol percentage fractions was observed upon knockdown of RPN11 (Figure 2C). This suggests that knockdown of RPN11, but not of UCHL5 and USP14, affects 26S proteasome stability to a great extent. Although the effects on proteasome stability are obvious, intact proteasomes were still observed. This may be the results of incomplete RPN11 depletion, of slow proteasome turnover or of a combination of both.

Taken together, RPN11 appears to be crucial for both proteasome stability and/or assembly, while both USP14 and UCHL5 are not. Also, the USP14/UCHL5 double knockdown did not noticeably affect proteasome stability.

Knockdown of RPN11, in contrast to UCHL5 KD, USP14 KD, or 2xKD, results in remarkable protein abundance dynamics of the global proteome

Of all proteasome associated DUBs, the role of RPN11 in promotion of protein degradation is best established (Maytal-Kivity *et al.*, 2002; Verma *et al.*, 2002; Yao and Robert E Cohen, 2002). In contrast, the roles of both UCHL5 and USP14 have not yet been fully elucidated. Several studies have shown that these DUBs can inhibit protein degradation (Lam *et al.*, 1997; Elena Koulich, Xiaohua Li, 2008; Lee *et al.*, 2010), whereas other studies have shown that they can enhance proteolysis (Elena Koulich, Xiaohua Li, 2008; Mazumdar *et al.*, 2010; Mialki *et al.*, 2013). However, in all of these studies only limited selections of specific proteasome substrates were used. We reasoned that by taking a global quantitative proteome analysis a wider range of potential substrates could be covered in order to reveal potentially specific functions for UCHL5 and USP14.

The SILAC proteomics approach in *Drosophila* S2 cells that was exploited has been described previously (Sap *et al.*, 2017). Cells were grown in culture medium with either light or heavy isotope labeled amino acids and dsRNA mediated interference of target gene expression was exploited to deplete RPN11, USP14, UCHL5 or UCHL5 and USP14 simultaneously. For control samples, dsRNA constructs to deplete for GFP were added to the cells. Label swap analyses were performed to correct for errors because of the labeling procedure. Cells were then harvested and the global proteome was analyzed by LC-MS/MS. From the heavy-to-light (H:L) ratios the relative up- or downregulation of all identified proteins as compared to the control situation could be established. The (log transformed) H:L ratio plots are shown in Figure 3. Proteins that show increased abundances because they are upregulated or accumulated as a result of the experimental condition show up in the left upper quadrant of these scatterplots. The red data points represent the knockdown target proteins in the respective assays, confirming the effectiveness of the depletion at the protein level. Proteins with either increased or decreased abundances (>1.5-fold) were considered up- or downregulated (Sap *et al.*, 2017). Only those proteins that exhibit consistent ratios in forward and reverse duplicate experiments were taken

into account for further analysis and were considered targets that specifically responded to the respective treatments.

Upon RPN11 knockdown, the global proteome is remodeled remarkably, as illustrated by the appearance of a large number of upregulated and/or accumulated proteins in the left upper quadrant. In contrast, no such an effect was observed upon knockdown of USP14, UCHL5, or the combined knockdown of these DUBs (Figure 3A). Table 1 lists the numbers of identified and quantified proteins in the various screens; Supplementary Table 1 lists all identified and quantified proteins including their H:L ratios.

Table 1. Numbers of identified and quantified proteins in global proteome datasets

Samples	Total exp #1 or #2	Total exp #1	Total exp #2	Up exp #1	Up exp #2	Up exp #1 and #2	Down exp #1	Down exp #2	Down exp #1 and #2
2d 3xKD	5381	5234	5257	810	758	535	124	146	38
RPN11 KD	5279	5085	5107	420	361	195	131	141	22
UCHL5 KD	5253	4984	5094	99	108	9	124	94	7
USP14 KD	5227	5026	4992	245	123	3	170	171	20
2d 2xKD	5293	5135	5136	117	93	5	73	117	5
4d 2xKD	4956	4711	4705	161	132	9	116	154	8

Approximately 4% of all identified proteins in the RPN11 knockdown assay were increased, while for the UCHL5 and USP14 knockdown assays only a few proteins were upregulated (Figure 3B). For reference purposes, the results of an assay in which multiple subunits (with both DUB and proteolytic activities) were knocked down simultaneously and that was published previously are included (Sap *et al.*, 2017). In this case the global proteome was remodeled extensively and approximately 10% of all detectable proteins had increased abundances.

Functional annotation analysis of increased proteins upon RPN11 knockdown revealed that many of these play a role in protein catabolic processes, cytoskeleton organization, cell cycle regulation and proteolysis (Figure 4A), which is similar to the increased protein population 3xKD (Sap *et al.*, 2017). Increased abundances of various cell cycle proteins were observed upon RPN11 knockdown (Figure 4B), which most likely are short-lived proteins that cannot be degraded anymore because of loss of proteasome functionality. Interestingly, most proteasome subunits were also increased, which is in agreement with previous reports (Wójcik and DeMartino, 2002; Lundgren *et al.*, 2005; Sap *et al.*, 2017), with the exceptions of RPT3, RPN2,

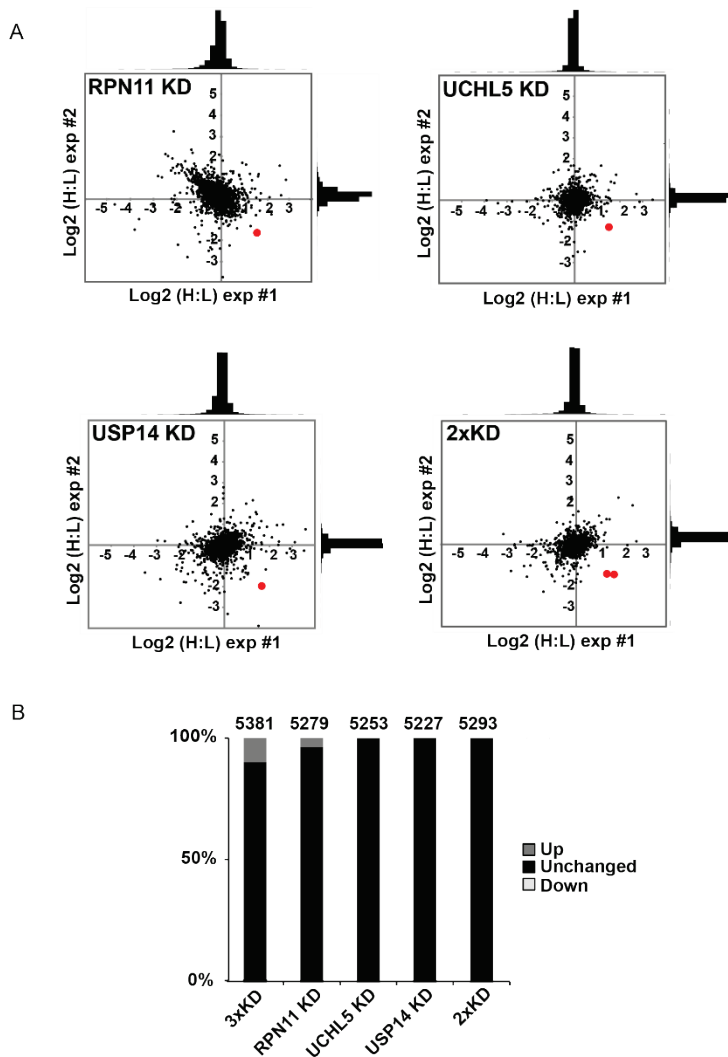


Figure 3. Depletion of RPN11, in contrast to, USP14, UCHL5 or 2xKD, results in increased abundances for a substantial part of the global proteome. A) Scatterplots of normalized forward and reverse SILAC ratios for cells in which DUBs have been knocked down versus control cells. Proteins with increased abundances appear in the left upper quadrant, proteins with decreased abundance in the right lower quadrant. The red data points indicated the proteins targeted for knockdown in the respective assays. B) The percentage of identified proteins whose abundances are affected in the global proteome dynamics assay. Approximately 4% of the global proteome was increased upon RPN11 KD. For comparative purposes, the abundance changes as a result of complete proteasome activity abolishment upon simultaneous dsRNA mediated knockdown of Prosalph5, Prosbeta6 and RPN11 (referred to as ‘3xKD’ and published previously (Sap *et al.*, 2017) is shown (approximately 10% of the global proteome).

RPN6, and RPN10 (Figure 4C). The reason for the aberrant behavior of these four subunits is unclear and needs to be investigated further. Possibly, these specific subunits have different turnover characteristics because of extraproteasomal functions, several of which have been described in the literature (*e.g.* for RPN10 (Matiuhin *et al.*, 2008)) or because of their specific role in the assembly of the 26S proteasome (reviewed in (Hochstrasser, 2013)). In accordance with a model where protein degradation is inhibited as a result of RPN11 lacking proteasomes and proteins are likely to be accumulated, there are only very few proteins quantified with decreased abundances upon RPN11 KD (Table S1). These proteins are most likely expressed to a lesser extent as a result of the stress induced upon the system. In contrast to the RPN11 knockdown, the effects as a result of the UCHL5, USP14 or combined knockdown were much less severe. The levels of only very few proteins were either increased or decreased in these experiments (Table S2, S3).

We have previously observed that several proteins are upregulated at a fast rate as a result of the stress imposed on the cell by inactivating the proteasome, most notably several stress response proteins, such as heat shock proteins (Sap *et al.*, 2017). Although it is not possible to differentiate between protein biosynthesis and accumulation based on these SILAC assays alone, we can assume based on these earlier studies that heat shock proteins in the RPN11 KD that are increased are also synthesized as a response to the knockdown. There is no indication that a similar response takes place in cells lacking USP14 or UCHL5. It is obvious that only in the RPN11 KD the global proteome was remodeled to some extent, while in the other cases protein abundances remained largely unchanged. There is a substantial overlap in increased proteins upon 3xKD (Sap *et al.*, 2017) and RPN11 KD: 75% of the increased proteins in RPN11 KD were also more abundant upon 3xKD (Figure 4D).

Based on these results we argue that knockdown of RPN11 alone has essentially a similar effect on global proteome dynamics as abolishing both DUB activity (by depletion of RPN11) and proteolytic activity (by depletion of Proasalpha5 and Prosbeta6) simultaneously. Altogether, these data confirm that RPN11 is essential for proper functioning of proteasome-mediated protein degradation. In contrast, while RPN11 promotes protein degradation, both UCHL5 and USP14 do not noticeably enhance nor inhibit proteasome-mediated protein degradation, at least as assessed by accumulation of proteins in a proteome-wide SILAC screen.

In conclusion, although for the RPN11 knockdown an increased remodeling of the global proteome was observed, we did not observe a major impact on global proteome dynamics upon depletion of UCHL5, USP14 or both enzymes simultaneously, suggesting that these DUBs do not seem to play a general role in the degradation of a major complement of cellular proteins.

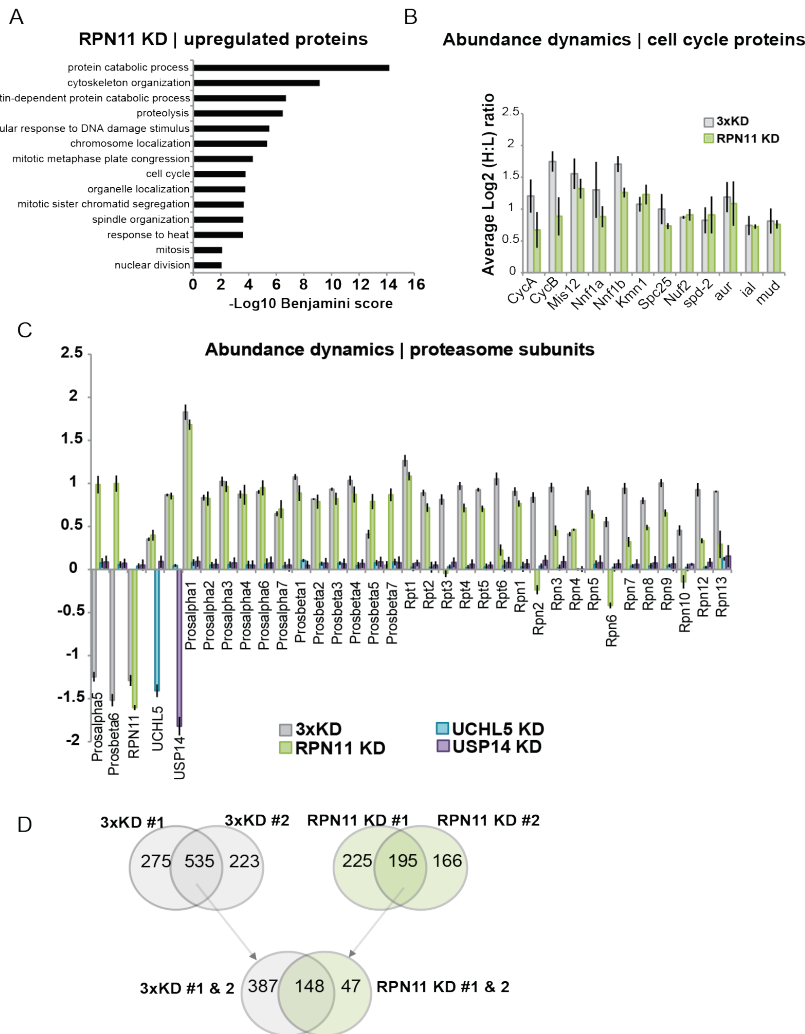


Figure 4. Cell cycle, mitotic spindle and UPS regulators are increased upon RPN11 depletion. A) Gene Ontology (GO) analysis of proteins with increased abundance upon RPN11 depletion. Functional annotation analysis was performed and a representative selection of enriched biological process GO terms is shown (enrichment probability represented by $-\text{Log}_{10}$ Benjamini score). B) Abundance increases of a selection of proteins involved in cell cycle regulation and mitotic spindle organization. C) Average normalized SILAC ratios of all subunits of the proteasome show that all proteasome components, except RPT3, RPN2, RPN6 and RPN10, are upregulated or accumulated upon depletion of RPN11, but not of USP14 or UCHL5. '3xKD' represents the simultaneous knockdown of Prosalpha5, Prosbeta6 and RPN11 (Sap *et al.*, 2017) and functions as a reference dataset in this study. D) Overlap of proteins with increased

abundance upon RPN11 KD and complete proteasome activity abolishment showing that ~75% of all proteins present with increased abundance upon RPN11 KD was also more abundant upon 3xKD.

Knockdown of RPN11, in contrast to UCHL5 and USP14, results in extensive ubiquitinome remodeling

One reason could be that the mode of action and specificity of these DUBs, in contrast to RPN11, cannot be assessed by monitoring the global proteome dynamics alone. We hypothesized that UCHL5 and USP14 may have specific functions which do not *per se* result into changing protein abundances. We therefore decided to further focus on the effects of the target ubiquitination process itself by monitoring both the global ubiquitin levels as well as the dynamic ‘ubiquitinome’. The rationale here is that proteins with increased ubiquitination upon knockdown of a DUB are likely to be substrates for that specific DUB.

Proteins targeted for proteasome dependent degradation are generally tagged with (poly-)ubiquitin chains. Therefore, a quantitative determination of ubiquitinated proteins may serve as a tool to monitor proper proteasome functioning in the cell. First, we assessed global levels of ubiquitin in cells lacking RPN11, USP14 or UCHL5 using western blots and detection by an FK2 antibody, which recognizes only conjugated ubiquitin. A detectable increase in the level of protein ubiquitination could only be observed upon RPN11 KD (Figure 2D). In cells under USP14 or UCHL5 knockdown conditions no changes in ubiquitination levels were observed.

Next, we tested whether a remodeling of the ubiquitinome goes together with a redistribution of the various ubiquitin pools (*i.e.*, free, monomeric and polymeric conjugated, activated) and whether changes in the total amount of free mono-ubiquitin occur. The free ubiquitin pool has been suggested to be a rate limiting factor in the ubiquitination process (Hanna, Leggett and Finley, 2003) and the amount of free monomeric ubiquitin in relation conjugated and polyubiquitin highly depends on the cell type (Kaiser *et al.*, 2011). We used protein separation by SDS-PAGE combined with label free quantitation by mass spectrometry (Figure 5A) and found that the amount of free ubiquitin in the RPN11 KD is twice as high as in the 2xKD (Figure 5B). The level of poly- and/or conjugated (poly)ubiquitin was about three times higher than that of free ubiquitin, both for the RPN11 KD as for the 2xKD samples (figure 5B). This means that overall the ubiquitin levels become approximately twice as high when RPN11 is depleted as compared to the depletion of UCHL5 and USP14. This is in agreement with the results from the SILAC assay, where the total ubiquitin level (*i.e.*, the sum of free, mono-, conjugated and polyubiquitin) was upregulated almost 2-fold (Figure 5C).

In conclusion, even though accumulation of ubiquitin is likely to occur as a result of RPN11 depletion, an increase in the total level of ubiquitin suggests that the pool of free ubiquitin is supplemented and that ubiquitin is newly synthesized

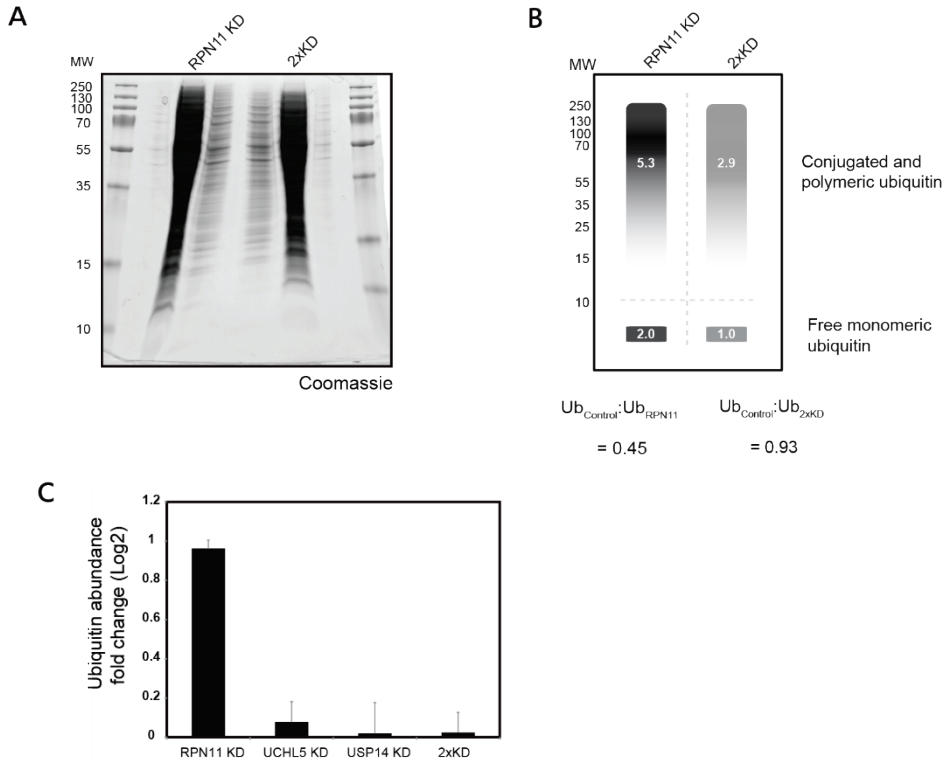


Figure 5. Upregulation of the monomeric free and polymeric and conjugated ubiquitin pools upon RPN11 KD. A) *Drosophila* S2 cells were treated for 2 days with dsRNA against RPN11 or against UCHL5 and USP14. Lysates were resolved by SDS-PAGE and Coomassie stained. Both lanes were subjected to LFQ-based mass spectrometry. B) Quantification of the free monomeric ubiquitin pool (<10kDa) and the conjugated and polymeric ubiquitin pool (>10kDa) upon RPN11KD and 2xKD by LFQ based LC-MS/MS of samples shown in 5A. The amount of free ubiquitin in the RPN11 KD is twice as high as in the 2xKD. C) Quantification of the abundance dynamics of the total pool of ubiquitin in the global proteome datasets. ~ 2-fold upregulation of the total pool of ubiquitin upon RPN11 KD.

Next, we applied a strategy where we used monoclonal antibodies to enrich for peptides derived from ubiquitinated proteins after trypsin digestion ('diGly' peptides) to monitor the dynamics of the ubiquitinome, the complement of all ubiquitinated proteins in a cell (Kim, Eric J. Bennett, *et al.*, 2011; Wagner *et al.*, 2011; Udeshi *et al.*, 2012; Sap *et al.*, 2017). We have previously applied this technology to study the ubiquitinome in cells that completely lack proteasomal activity. Here, we combine SILAC proteomics, dsRNA mediated knockdown of RPN11, UCHL5 and USP14 with the analysis of the ubiquitinome to investigate the functional roles of these DUBs. Upon RPN11 KD, the majority of diGly peptides were upregulated as compared to the control

situation, suggesting an increase in the extent of ubiquitination for many proteins and, therefore, extensive remodeling of the ubiquitinome (Figure 6A). It should be noted here that the new ubiquitination events, in which cases peptides in the control situation would not carry a diGly remnant at all, are not included in this plot by definition. All diGly peptides, including those with no corresponding detection in the control, are listed in Supplementary Table 2 with their H:L ratios.

Table 2 lists the numbers of identified and quantified diGly peptides for each dataset, where 1.5-fold changes were used as threshold values for either up- or downregulation. Only peptides identified and quantified in both forward and reverse SILAC experiments and with consistent ratios were taken into account for further analysis. Upon RPN11 KD, more than 70% of all diGly peptides were upregulated. Functional annotation analysis revealed that the proteins they are associated with play diverse roles in the cell, such as protein catabolic processes, the cell cycle and programmed cell death (Figure 6B). Several proteins with downregulated ubiquitination sites were identified (Table S4), including ribosomal and transport proteins.

Table 2. Numbers of identified and quantified diGly modified peptides

Samples	Total	Total FW	Total REV	Up FW	Up REV	Up FW & REV	Down FW	Down REV	Down FW & REV
2d 3xKD	8211	7780	2956	6716	2173	1756	278	182	82
Rpn11 KD	4210	3427	2752	2355	1873	1089	148	97	36
UCL5 KD	1758	1442	1226	107	54	3	33	55	8
USP14 KD	2860	2098	2406	280	89	2	167	298	11
2d 2xKD	4009	3674	2651	215	119	2	153	156	0
4d 2xKD	3526	2701	3209	172	173	12	98	202	0

In sharp contrast, the abundances of only a very small set of diGly peptides were affected upon knockdown of both UCL5 and USP14 whereas those of the majority remained unchanged (Table 2, Table S5). Of the few cases where the extent of ubiquitination is affected, ribosomal proteins (in the UCL5 knockdown) and ATP synthesis proteins (in the USP14 knockdown) were remarkable. Downregulated diGly peptides upon USP14, UCL5 or 2d 2xKD were all associated with ribosomal proteins (Table S6).

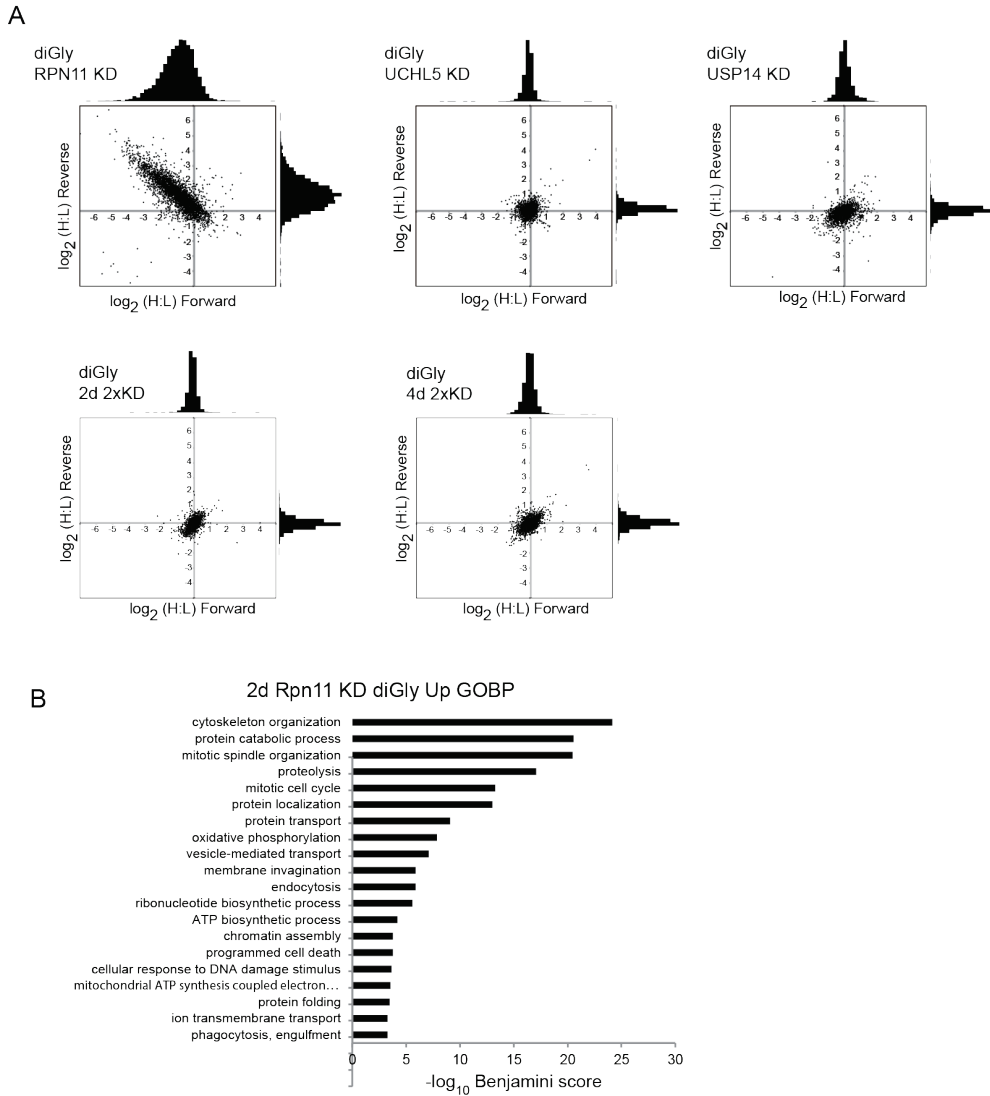


Figure 6 | Remodeling of the global ubiquitinome as a result of proteasome associated DUB interference. A) Abundance increases of diGly peptides derived from proteins in cells upon depletion of the indicated DUB. Data are from duplicate SILAC (forward and reverse) experiments. B) GO analysis of proteins with associated upregulated diGly peptides; a representative selection of enriched biological process terms is shown (enrichment probability represented by $-\log_{10}$ Benjamini score).

Proteasomes contain at least three DUBs that remove ubiquitin chains from substrates. It has been hypothesized that their intrinsic linkage preference might therefore affect the residence time of a substrate at the proteasome lid (Finley, 2009). Thus, it could be that, although UCHL5 and USP14 do not seem to target specific proteins, their suggested polyubiquitin chain editing function could have an effect on the relative amounts of specific linkage types. In order to investigate whether this may be true for the proteasome-associated DUBs under investigation in this study we decided to focus on polyubiquitin derived diGly peptides. In the RPN11 KD assay, all polyubiquitin specific diGly peptides and non-modified peptides were upregulated (Figure 7A). This is in agreement with earlier findings that the relative abundances of ubiquitin increase as an effect of destabilizing this DUB. Although most diGly peptides are upregulated 1.4 – 2.3 fold, the diGly peptide representing the K27 linkage stands out at >5-fold upregulation (Figure 7A). This is unexpected, since the canonical linkage type for proteasome mediated degradation is K48 and would therefore be expected to become accumulated in the absence of proteasome DUB activity.

In contrast, for the USP14 KD, UCHL5 KD and the double knockdown (2xKD), diGly peptides did not show significant up- or downregulation and no preference or specificity for any of the polyubiquitin linkage types was observed. These data do therefore not give conclusive information on the putative editing function of both UCHL5 and USP14 (Figure 7A, 7B).

In conclusion, major changes in diGly peptide abundances were observed upon RPN11 KD, suggesting that an extensive remodeling of the ubiquitinome takes place upon depletion of RPN11. The affected diGly peptide population shows a remarkable overlap with the ubiquitination sites observed after complete abolishment of the proteasome (Sap *et al.*, 2017), indicating that either the catalytic activity and/or the structural role of RPN11 within the proteasome is important for proteasome-dependent protein degradation. In contrast, depletion of UCHL5, USP14 or both enzymes simultaneously did not lead to detectable modulation of the ubiquitinome. This observation suggests that either these DUBs do not target a broad range of protein substrates for deubiquitination or that the sensitivity of the assay is a limiting factor. Also, no specificity for specific polyubiquitin linkage types could be detected for USP14 and UCHL5. For RPN11, K27 linked polyubiquitin seems to be upregulated and/or accumulated to a higher extent than other linkage types. Taken together, our data show that knockdown of RPN11 results in a substantial increase of both protein abundance and protein ubiquitination, suggesting inhibition of proteasome-dependent degradation of a large complement of proteins in *Drosophila* S2 cells. On the other hand, knockdown of two other proteasome-associated DUBs, UCHL5 and USP14, did not result in detectable changes in the proteome, the ubiquitinome nor in the linkage-type specific composition of polyubiquitin.

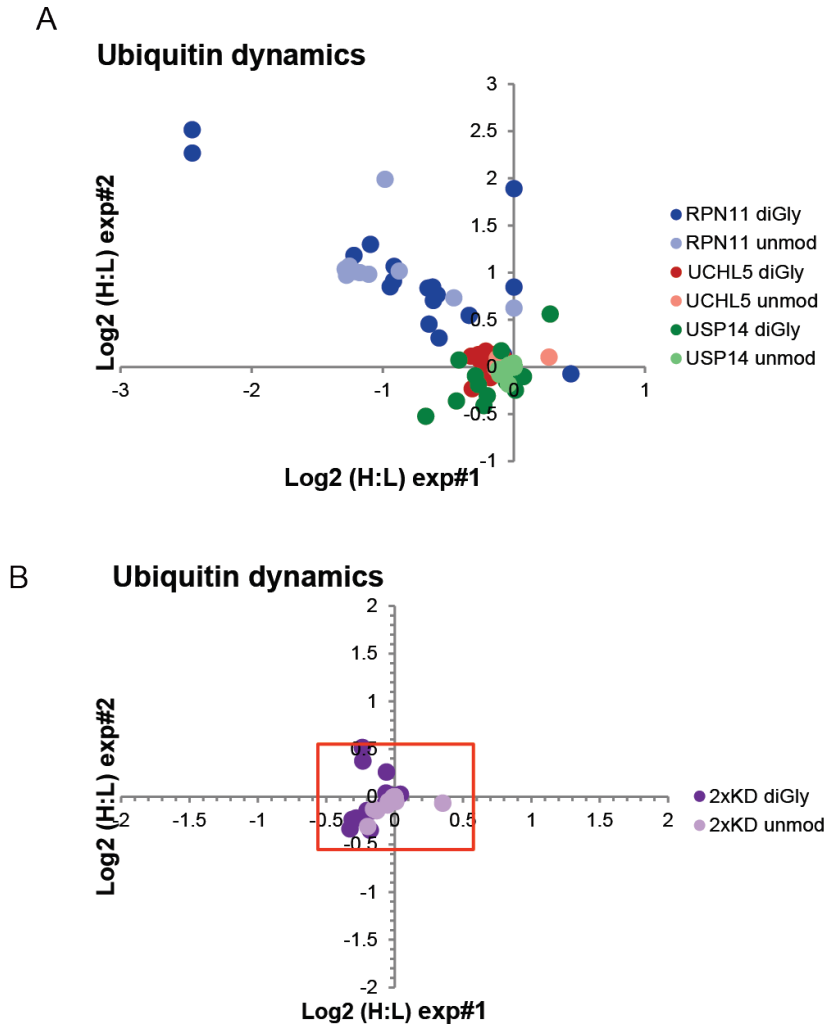


Figure 7. Ubiquitin linkage dynamics upon proteasome-bound DUB knockdown

A) Log2 fold changes of both unmodified and diGly-modified ubiquitin peptides upon single DUB knockdown of RPN11, UCHL5 or USP14. Fold changes of both modified and unmodified ubiquitin peptides were unaffected upon KD of UCHL5 or USP14. Fold changes of both modified and unmodified ubiquitin peptides upon RPN11 KD were increased about 1.4 – 2.3 fold, suggesting that the total pool of ubiquitin was upregulated including the conjugated ubiquitin pool. The top left corner shows two strongly upregulated ubiquitin K27 diGly-modified ubiquitin peptides. B) Fold changes of both modified and unmodified ubiquitin peptides were not affected upon simultaneous KD of both UCHL5 and USP14. Red box shows 1.5-fold upregulation cutoff.

Discussion

In this study, we set out by assessing the stability of three DUBs that have been extensively reported as being constituent subunits of the proteasome. For this purpose, proteasomes were isolated from *Drosophila* S2 cells by immunoprecipitation of Rpn8 or Rpn10 and washed under increasingly stringent buffer conditions. Label free quantitative mass spectrometry revealed that the strength of interaction of RPN11 and UCHL5 with the proteasome was comparable with other proteasome subunits, whereas the interaction of USP14 with the proteasome was completely lost at high salt concentrations. This result indicates USP14, but not RPN11 and UCHL5, is a relatively weak or transient interactor of the proteasome and suggests that it is not a constitutive subunit.

Next, we have investigated the effect of depletion of three known proteasome-associated DUBs by dsRNA-mediated knockdown on the UPS by monitoring both the global proteome and ubiquitinome dynamics in *Drosophila* S2 cells. While the global proteome and especially the ubiquitinome were extensively remodeled upon depletion of RPN11, the effects at the global proteome and ubiquitinome level were surprisingly small or simply absent upon depletion of USP14 or UCHL5. These findings indicate that RPN11 deubiquitinase activity plays an important role in proteasome-mediated protein degradation whereas the roles of UCHL5 and USP14 in general proteostasis remain unclear. Furthermore, we found that RPN11, but not USP14 or UCHL5, is essential for the assembly and/or stability of the proteasome. Therefore, the possibility that the absence of a stable proteome holocomplex and not the absence of deubiquitinase activity alone is responsible for the observed effects cannot be excluded. Interestingly, USP14, in contrast to RPN11 and UCHL5, was found to interact with the proteasome in a reversible manner. This suggests that it could have an additional cellular role apart from its deubiquitinase activity as part of the proteasome.

Some of our findings confirm previously reported observations in the literature. The importance of RPN11 for both the stability and the activity of the proteasome has been reported in various studies (Maytal-Kivity *et al.*, 2002; Yao and Robert E Cohen, 2002; Gallery *et al.*, 2007; Elena Koulich, Xiaohua Li, 2008; Finley, 2009). As a consequence, it is not straightforward to design assays to characterize the biological function of this subunit. Several studies have attempted to functionally characterize RPN11 by using active site mutants in yeast, *Drosophila* or human cell lines. Although one such study in yeast indeed described a viable RPN11 site-mutant (Guterman and Glickman, 2004), in all other studies these mutants were non-viable (unpublished data from our lab, Verma *et al.*, 2002; Yao and Robert E Cohen, 2002; Lundgren *et al.*, 2003; Gallery *et al.*, 2007). These findings underline its relevance also in a cellular context. Our finding that depletion of UCHL5 does not affect the stability and - seemingly - the activity of the proteasome is in agreement with reported data showing that RNAi of UCHL5 in *Drosophila* S2 cells had little apparent effect on the structure or peptidase activities of the 26S proteasome (Wójcik and

DeMartino, 2002). Additionally, no increase in the level of ubiquitinated proteins was observed. Furthermore, it has been shown that USP14 dissociates from the proteasome upon increased salt concentrations, whereas there was only little effect on UCHL5 or RPN11 under the same conditions, which is in agreement with our data (Elena Koulich, Xiaohua Li, 2008). Recently it was shown that USP14 cycles towards the proteasome upon the presence of ubiquitinated substrates at the proteasome complex and after degradation of the substrate, USP14 subsequently dissociates from the proteasome (Kuo and Goldberg, 2017).

Our results do not confirm the model that describes UCHL5 and USP14 as DUBs that antagonize substrate degradation (Lam *et al.*, 1997; Elena Koulich, Xiaohua Li, 2008; Lee *et al.*, 2010). In this model, UCHL5 and USP14 initiate the removal of ubiquitin from substrates upon docking of the ubiquitinated substrate at the proteasome ubiquitin receptors, whereby they trim polyubiquitin chains from the distal end (Lam *et al.*, 1997; Hu *et al.*, 2005; M. J. Lee *et al.*, 2011). The shortening of polyubiquitin chains may then result in a decreased binding capacity of substrate to the proteasome which in turn could slow down degradation rates or even prevent the degradation of substrate. Cohen and coworkers observed enhanced degradation of especially monoubiquitinated globin peptides and other lower-order conjugates upon isopeptidase inhibition by Ub-aldehyde *in vitro* (Lam *et al.*, 1997). Their results suggest that an ‘editing isopeptidase’ could decrease the degradation rates of substrates which are poorly ubiquitinated. Finley and coworkers have shown that inhibition of USP14 by the small molecule inhibitor IU1 enhances the degradation of Cyclin B and of Sic1 *in vitro* (Lee *et al.*, 2010). They hypothesized that deubiquitination of substrates by USP14 at a faster rate than the proteasome initiates degradation could cause rejection of otherwise competent substrates from the proteasome. In addition, they observed reduced levels of tau, TDP-43 and ataxin-3 upon IU1 treatment in murine embryonic fibroblasts, although others were unable to confirm a robust role for USP14 in tau or TDP-43 degradation (Ortuno, Carlisle and Miller, 2016). DeMartino and coworkers showed reduced levels of ubiquitinated proteins upon RNAi mediated knockdown of USP14 or UCHL5 in HeLa cells, although a double knockdown of UCHL5 and USP14 counteracted this effect (Elena Koulich, Xiaohua Li, 2008). b-AP15, a chemical inhibitor of both UCHL5 and USP14, has been shown to elicit a similar response as the proteasome inhibitor Bortezomib, which results in an accumulation of ubiquitinated proteins (D’Arcy *et al.*, 2011; Brnjic *et al.*, 2013; Feng *et al.*, 2014; Tian *et al.*, 2014; Wang *et al.*, 2014). However, the specificity of this small molecule drug is contested by others and unspecific inhibition of other proteasome subunits may occur, thereby blurring the effects of UCHL5 and USP14 (Huang, Jung and Chen, 2014).

The canonical signal for proteasome-dependent degradation is the presence of K48-linked polyubiquitin chains on substrate. An editing function for USP14 or UCHL5 would result in an upregulation of K48-polyubiquitin linkages upon knockdown of the respective DUBs. An *in vitro* study using di-ubiquitin probes revealed that USP14 had a preference for K11, K33 and K48 linkages (Flierman *et al.*, 2016). We did not observe an upregulation of polyubiquitin linkages,

neither did we observe an upregulation in total ubiquitin levels upon KD of USP14, UCHL5, or both of them. Altogether, we cannot confirm these studies in that we did not observe major protein abundance dynamics upon knockdown of USP14 and/or UCHL5 at a proteome-wide scale. *Drosophila* homologs of tau, TDP-43 and ataxin-3 were not identified in this study. We also did not observe abundance dynamics of ubiquitin and polyubiquitin linkages.

In contrast to the editing model, recent data from Finley and coworkers suggests that USP14 removes ubiquitin chains *en bloc* and very fast, *i.e.* before the proteasome can initiate degradation (Lee *et al.*, 2016). *In vitro* experiments with Cyclin-B, the canonical substrate of USP14, showed that all supernumerary chains were removed until a single ubiquitin chain remained. In our study, we did not observe a change in abundance at the global proteome level upon USP14 knockdown, although this finding is not in disagreement with those *per se*. No diGly peptides were identified for Cyclin-B and, thus, no information is available on the extent of Cyclin-B ubiquitination as an effect of USP14 depletion.

The findings of our study are not in disagreement with a model in which USP14 (Ubp6) is a DUB that can facilitate substrate degradation by non-catalytically delaying the degradation process in order to provide a time window to allow gradual deubiquitination of the substrate. In this model, ubiquitin-bound USP14 interferes with degradation-coupled RPN11-mediated *en bloc* deubiquitination of polyubiquitin chains (Hanna *et al.*, 2006; Peth, Besche and Goldberg, 2009; Aufderheide *et al.*, 2015; Bashore *et al.*, 2015). Furthermore, ubiquitin-bound USP14 causes the proteasome to adopt the substrate-engaged conformational state, which is characterized by the coaxial alignment of the regulatory particle base subunits and the channel of the 20S core particle, and this state positions RPN11 close to the entrance of this channel (Matyskiela, Lander and Martin, 2013; Unverdorben *et al.*, 2014). Proteasomes which adopt the substrate-engaged state cannot process new substrates (Bashore *et al.*, 2015). Both mechanisms, locking the proteasome in the substrate-engaged state and inhibiting the deubiquitinating activity of RPN11, are mechanisms by which USP14 can delay substrate degradation (Aufderheide *et al.*, 2015; Bashore *et al.*, 2015). This would suggest USP14 acting as a timer to coordinate individual substrate processing steps at the proteasome, thereby facilitating, but not regulating, protein degradation. These mechanisms do not require the catalytic activity of USP14, but merely require its ability to bind ubiquitin. The catalytic activity of USP14, on the other hand, plays a role in ubiquitin recycling and is important for the maintenance of the free ubiquitin pool. It should be noted though that this model was proposed based on experiments in *S. cerevisiae*, which lacks (an ortholog of) UCHL5. Therefore, it may not be directly translated to higher eukaryotes that express both UCHL5 and USP14.

The reason that we did not observe major changes at the global proteome level upon depletion of USP14 in our assay may be explained by the property of USP14 to only temporarily delay substrate degradation for correct processing of the ubiquitin-substrate conjugate.

Several studies have shown that ubiquitin undergoes accelerated degradation by the proteasome in the absence of USP14/Ubp6 *in vivo* (David S. Leggett *et al.*, 2002; Chernova *et al.*, 2003; Hanna, Leggett and Finley, 2003; Hanna *et al.*, 2006). We did not observe a depletion of total ubiquitin upon simultaneous depletion of USP14, UCHL5 or both DUBs simultaneously (2xKD). In contrast, ubiquitin was upregulated upon RPN11 depletion. Our assay did not allow comparing differences between free ubiquitin levels in USP14 depleted cells versus control cells. Ubiquitin levels are highly regulated in the cell and an elaborate evaluation of the effects of UCHL5 and USP14 depletion on the total ubiquitin pool, the free ubiquitin pool, but also on the proteasome-bound ubiquitin pool would be an interesting supplement for this study.

Although the 26S proteasome contains approximately stoichiometric levels of UCHL5 and USP14 (Figure 1B) (Elena Koulich, Xiaohua Li, 2008), both DUBs also have a substantial non-proteasomal population, which could serve as a latent protein reservoir or may have other functions related or unrelated to their catalytic activity. *In vitro* studies have shown that RPN11 (Mansour *et al.*, 2015), UCHL5 (Yao *et al.*, 2006) and USP14 (David S. Leggett *et al.*, 2002; Hu *et al.*, 2005; Hanna *et al.*, 2006; Lee *et al.*, 2010; Bashore *et al.*, 2015) have relatively low activity outside the proteasome holocomplex. We cannot rule out the possibility that the approximately three-fold depletion of UCHL5 and USP14 levels by dsRNA mediated knockdown in our assay may be – partially or exclusively - targeted at the free, non-proteasomal protein population. In that case, large effects would not be observed because of the supposed relative low DUB activity of these proteins when not associated to the proteasome. On the other hand, the results of the RPN11 knockdown assay have shown that even a three-to-four-fold depletion is sufficient to detect major differences.

Perspective

One possibility is that the sensitivity of our assay is not sufficiently high to pick up a potentially highly specific, but only small set of target proteins. We are currently improving the coverage and sensitivity of the diGly IP assay (Van Der Wal *et al.*, 2018). Another possibility may be that the knock-down efficiency is too low and that the remaining population of the target DUB may prevent clear effects in the assay. One solution for this is to create knock-out cell lines, although it remains to be seen whether these would be viable. Finally, it cannot be excluded that the activities of UCHL5 and USP14 are indeed affected in the knockdown albeit in such a way that the readout that we have used here is inadequate to measure these effects. For instance, clipping off a single ubiquitin subunit from the distal end of a polyubiquitin chain for editing purposes may not noticeably affect the degradation rate of the target, nor may it affect the redistribution of ubiquitin pools if the removed ubiquitin residue would somehow not be included in the pool of monomeric free ubiquitin. In both the dynamic global proteome and ubiquitinome assays described here such events would go unnoticed.

Material and Methods

Nomenclature for the 26S proteasome: the core 20S proteasome subunits are designated by the α/β nomenclature and the 19S subunits are designated by the Rpn/Rpt nomenclature (Finley *et al.*, 1998).

Cell culture. *Drosophila melanogaster* Schneider's line 2 cells (S2 cells, R690-07, Invitrogen) were cultured in Schneider's medium (Invitrogen) supplemented with 10% fetal calf serum (Thermo) and 1% Penicillin-Streptomycin.

SILAC labelling. S2 cells were cultured in custom-made Schneider's *Drosophila* medium (Athena Enzyme Systems, Baltimore, MD), based on the Invitrogen recipe mentioned above, with several alterations required for the SILAC approach: yeastolate was dialyzed (3500 kD MWCO) and the medium was deficient for both lysine and arginine. Before use, the medium was supplemented with 10% dialyzed Fetal Bovine Serum (F0392, Sigma-Aldrich), 1% Penicillin-Streptomycin and either 2 mg/ml light ($^{12}\text{C}_6$) lysine (A6969, Sigma-Aldrich) and 0.5 mg/ml light ($^{12}\text{C}_6$, $^{14}\text{N}_4$) arginine (L5751, Sigma-Aldrich), or 2 mg/ml heavy ($^{13}\text{C}_6$) lysine (CLM-2247, Cambridge Isotope laboratories) and 0.5 mg/ml heavy ($^{13}\text{C}_6$, $^{15}\text{N}_4$) arginine (CNLM-539, Cambridge Isotope Laboratories). Cells were cultured at 27 °C for at least 7 cell doublings for complete labelling.

dsRNA mediated knockdown. For dsRNA-mediated targeted knockdown studies, S2 cells were treated with dsRNA constructs directed against RPN11 (Uniprot identifier Q9V3H2), USP14 (Q9VKZ8) or UCHL5 (Q9XZ61), or a combination of the latter two, referred in the text to as '2xKD'. Control samples were treated with dsRNA directed against GFP which is not present in the cells used here. The final concentration of total dsRNA was 6 $\mu\text{g}/\text{ml}$. In general, S2 cells were incubated with dsRNA at 27°C for 48h (2 days), although some 2xKD experiments were performed for 96h (4 days). dsRNA constructs were synthesized using the Ambion Megascript T7 kit according to the manufacturer's protocol. Oligonucleotide sequences used for dsRNA synthesis can be provided upon request. Knockdown experiments were further performed as described previously (Worby, Simonson-Leff and Dixon, 2001). FACS analysis was performed as described in (Moshkin *et al.*, 2007).

RNA isolation and real time RT-qPCR. For gene expression assays, cell pellets were immediately frozen in liquid nitrogen and stored at -80°C until further processing. Total RNA was extracted from 5×10^6 cells using Trizol (15596-026, Invitrogen) and 4 μg RNA was used for random hexamer primed cDNA synthesis using the Superscript II Reverse Transcriptase (Invitrogen). Quantitative PCR (qPCR) was performed on a CFX96 realtime PCR detection system (Bio-Rad). Reactions were performed in a total volume of 25 μl containing 1x reaction buffer, SYBR Green I (Sigma), 200 μM dNTPs, 1.5 mM MgCl_2 , platinum Taq polymerase (Invitrogen), 500 nM of

corresponding primers and 1 μ l of cDNA. Primers were made for both the C-terminus and N-terminus of both UCHL5 and USP14. Data analysis was performed by applying the $2^{-\Delta\Delta CT}$ method (Livak & Schmittgen, 2001). Values obtained from amplification of α -1,2-mannosidase (CG11874) were used to normalize the data as described previously (Moshkin *et al.*, 2007).

Antibodies, SDS-PAGE and immunoblotting: Polyclonal antibodies were generated by immunizing guinea pigs or rabbits with GST fusion proteins expressed in *Escherichia coli* and were affinity purified as described previously (Chalkley and Verrijzer, 2004). The following antigens were used: full length Prosalpha5, full length Prosbeta6, full length RPN11, full length RPN8, full length RPN10, full length RPT4 or C-terminal (aa220–405) RPT6. In-house generated polyclonal antibodies used were α -H2B (PV57/58, raised against purified core histones and mainly recognizing H2B, described in (Chalkley and Verrijzer, 2004)) and α -Moir (described in (Mohrmann *et al.*, 2004)). Commercial antibodies against conjugated ubiquitin (FK2, PW8810, Enzo Life Sciences) and Prosalpha subunits (SC-65755, Santa Cruz Biotechnology) were used. SDS-PAGE and immunoblotting experiments were performed as described previously (Chalkley *et al.*, 2008).

Glycerol density gradients: Glycerol gradients were prepared according to (Mohrmann *et al.*, 2004). Briefly, gradients with 5-30% glycerol were prepared in Beckman polyallomer tubes (331374 Beckman). Whole cell lysates were prepared under non-denaturing conditions (50 mM HEPES-KOH pH 7.6, 100 mM KCl, 0.1% NP40, protease inhibitors) and subsequently loaded on top of the gradient and ultracentrifuged (SW40 rotor, Beckman L-80) at 32 krpm for 17 h at 4°C. Twenty-six 500 μ l fractions were taken starting from the top of the gradient using a P1000 pipet. Fractions were stored in aliquots at -80°C. Two consecutive fractions were combined starting from fraction 3, resulting in a total of 13 fractions. Of each of these fractions, 25 μ l was analyzed by SDS-PAGE and target proteins were visualized by immunoblotting.

Immunopurifications: Immunopurification (IP) procedures were performed essentially as described (Chalkley and Verrijzer, 2004). Briefly, α -RPN8 or α -RPN10 antibodies were crosslinked to Protein A beads by using dimethylpimelimidate. Antibody coupled beads were incubated with whole cell lysate for 2 h. Subsequently, the beads were washed extensively with HEMG based washing buffer containing either 50 mM, 150 mM or 500 mM KCl (25mM HEPES-KOH, pH 7.6, 0.1mM EDTA, 12.5mM MgCl₂, 10% glycerol, 50 mM / 150 mM / 500 mM KCl, 0.1% NP-40, containing a standard cocktail of protease inhibitors). Proteins that were retained on the beads were then eluted with 100 mM sodium citrate buffer (pH 2.5), resolved by SDS-PAGE and visualized by Coomassie staining. Finally, lanes were cut in 1 mm slices and prepared for and analyzed by nanoflow LC-MS/MS (see below).

LFQ mass spectrometry: In-gel protein reduction, alkylation and tryptic digestion was performed as described previously (Sap *et al.*, 2015). Peptides were extracted with 30% acetonitrile 0.5% formic

acid and analyzed on an 1100 series capillary LC system (Agilent Technologies) coupled to an LTQ-Orbitrap hybrid mass spectrometer (Thermo). Peptide mixtures were trapped on a ReproSil C18 reversed phase column (Dr Maisch GmbH; column dimensions 2 cm × 100 µm, packed in-house) at a flow rate of 8 µl/min. Peptide separation was performed on a ReproSil C18 reversed phase column (Dr Maisch GmbH; column dimensions 15 cm × 75 µm, packed in-house) using a linear gradient from 0-50% B (A = 0.1% formic acid; B = 80% (v/v) acetonitrile, 0.1% formic acid) in 120 min at a constant flow rate of 300 nl/min using a splitter. The column eluent was directly electrosprayed into the mass spectrometer. Mass spectra were acquired in continuum mode; fragmentation of the peptides was performed in data dependent acquisition mode by CID using top 8 selection.

LFQ data analysis: RAW files were analyzed using MaxQuant software (version 1.5.3.30 | <http://www.maxquant.org>), which includes the Andromeda search algorithm (Cox *et al.*, 2009, 2011) for searching against the Uniprot database (version January 2016, taxonomy: *Drosophila melanogaster* | <http://www.uniprot.org/>). Follow-up data analysis was performed using the Perseus analysis framework (<http://www.perseus-framework.org/>). Perseus (version 1.5.0.31) was used to analyze protein abundance dynamics in the different samples. ProteinGroups.txt files were uploaded to Perseus and rows containing proteins designated ‘Only identified by site’, ‘Reverse’ and ‘Contaminant’ were removed from the matrix. LFQ intensities were Log2-transformed and the LFQ intensity columns of triplicates of RPN8 and RPN10 IPs were grouped together. To ensure a high data quality standard, rows that did not contain at least two valid values in at least one group were removed from the matrix. To identify proteasome interacting proteins, a Welch two-sided t-test was performed for each α-RPN8 or α-RPN10 IP versus the α-PPI (control) IPs. A permutation-based FDR of 0.05 was used for truncation and the number of randomizations was 250. Tables containing proteins with significant abundance changes for each two-sample t-tests were exported to Excel and annotations were added. The software suite R was used to merge the tables for the α-RPN8 or α-RPN10 comparisons with the α-PPI IPs based on the common ‘Id’ columns. Rows containing significantly changed proteins in the α-RPN8 and α-RPN10 versus control comparisons were merged using R.

Global proteome and diGly-peptide analysis: sample preparation, fractionation & LC-MS/MS: SILAC cell cultures were used for all global proteome and ubiquitinome analyses. After treatment of 2 days (or 4 days) with dsRNA against RPN11, USP14, UCHL5 or GFP (control), cells were harvested and used for 1) immunoblotting or 2) global proteome and ubiquitinome analyses. For immunoblotting, cells were washed 3 times with ice-cold PBS and spun down for 5 min at 1100 rpm at 4°C. Cell pellets were lysed in SDS-PAGE sample buffer (2% SDS, 10% glycerol, 60 mM Tris-HCl pH 6.8, plus protease inhibitors) and lysates were kept on ice and sonicated for 5 min 30 min with an ‘on/off’ cycle. BCA assay (Pierce) was used to estimate protein concentration. Global proteome and ubiquitinome experiments were performed in duplicate, including a light-heavy label swap (‘forward’ (light channel DUB treated cells) and ‘reverse’ (heavy channel DUB

treated cells) experiment). After 2 days (or 4 days) of incubation with dsRNA, cells were harvested, counted (Beckman Coulter Z2) and heavy and light cultures were mixed in a 1:1 ratio (based on cell count). Cells were washed 3 times with ice-cold PBS and lysed in 7 ml lysis buffer (8 M urea, 50 mM Tris-HCl pH 8.0, 50 mM NaCl) for combined global proteome and ubiquitinome analysis. Lysates were incubated on ice for 10 min and sonicated, debris was removed by centrifugation. Protein concentrations were measured in a BCA assay (Pierce). Cell lysates containing 20 mg total protein were collected for combined global proteome and ubiquitinome analyses. Protein lysates were reduced with 10 mM dithiothreitol (DTT) for 1 h at RT followed by alkylation with 55 mM chloroacetamide for 1 h in the dark. The mixture was diluted 1:1 with 50 mM Tris-HCl pH 8.0 and proteins were digested with 1:100 LysC (129-02541 Wako Chemicals) for 1 h at RT. The mixture was diluted with 25 mM Tris HCl (pH 8.2) to a final concentration of 1.6 M urea. CaCl_2 was added (1 mM final concentration) and the sample was digested overnight with 1:100 sequencing grade trypsin (cat # 03708969001, Roche) at RT. Peptide mixtures were acidified with 1% trifluoroacetic acid (TFA) and the precipitate was removed by centrifugation. At this point, digests of combined global proteome and ubiquitinome were splitted: 1 mg for the global proteome and approximately 20 mg for the ubiquitinome analysis (same amount of digest for Forward and Reverse). Global proteome digests were desalted using a Sep-Pak® Vac tC18 column (WAT036820, Waters) and eluted with 1 ml 80% acetonitrile / 0.1% FA and fractionated by HILIC on an Agilent 1100 HPLC system using a 5 μm particle size 4.6 x 250 mm TSKgel amide-80 column (Tosoh Biosciences). 200 μg of the desalted tryptic digest in 80% acetonitrile was loaded onto the column. Peptides were eluted using a nonlinear gradient from 80% B (100% acetonitrile) to 100% A (20 mM ammonium formate in water) with a flow of 1 ml/min. Sixteen 6 ml fractions were collected, lyophilized (ScanVac Coolsafe, Scala Scientific) and pooled into 8 final fractions. Each fraction was then analyzed by nanoflow LC-MS/MS as described below.

DiGly-modified peptides were enriched by immunoprecipitation using PTMScan® ubiquitin remnant motif (K- ϵ -GG) antibody bead conjugate (#5562, Cell Signaling Technology), according to the manufacturer's protocol. Unbound peptides were removed by washing and the captured peptides were eluted with low pH buffer (0.15% TFA). Eluted peptides were analyzed by nanoflow LC-MS/MS.

Nanoflow LC-MS/MS was performed on an EASY-nLC system (Thermo) coupled to a Q Exactive mass spectrometer (Thermo), operating in positive mode and equipped with a nanospray source. Peptide mixtures were trapped on a ReproSil C18 reversed phase column (Dr Maisch GmbH; column dimensions 1.5 cm \times 100 μm , packed in-house) at a flow rate of 8 μl /min. Peptide separation was performed on ReproSil C18 reversed phase column (Dr Maisch GmbH; column dimensions 15 cm \times 50 μm , packed in-house) using a linear gradient from 0-80% B (A = 0.1% formic acid; B = 80% (v/v) acetonitrile / 0.1% formic acid) in 70 min and at a constant flow rate of 200 nl/min. The column eluent was directly sprayed into the orifice of

the mass spectrometer. Mass spectra were obtained in continuum mode; fragmentation of the peptides was performed in data-dependent mode by HCD using top 15 selection.

SILAC LC-MS/MS data analysis: Mass spectrometric raw data were analyzed using the MaxQuant software (versions 1.5.3.30) for identification and relative quantification of protein groups. A false discovery rate (FDR) of 0.01 for proteins and peptides and a minimum peptide length of 7 amino acids were required. The Andromeda search engine was used to search the MS/MS spectra against the *Drosophila melanogaster* Uniprot database (release 2016_01.fasta, taxonomy: *Drosophila melanogaster*, <http://www.uniprot.org/>). For SILAC data the multiplicity was set to two and a maximum of two missed cleavages were allowed. The enzyme specificity was set to trypsin and cysteine carbamidomethylation was set as a fixed modification, whereas variable modifications were methionine oxidation, protein N-term acetylation and lysine ubiquitination (GlyGly (K)). The minimum ratio count was set to 1, although peptide spectra for proteins quantified with ratio count 1 were checked manually for data quality. Only proteins that were identified and quantified in both forward and reverse experiments and with consistent ratios, were taken into account for further analysis. Protein sets were further functionally analyzed using Perseus (version 1.5.0.31), the gene ontology (GO) software DAVID (version 6.7, available from <http://david.abcc.ncifcrf.gov/>) and in-house developed software.

References

- Aufderheide, A. *et al.* (2015) 'Structural characterization of the interaction of Ubp6 with the 26S proteasome.', *Proceedings of the National Academy of Sciences of the United States of America*, 112(28), pp. 8626–31.
- Bashore, C. *et al.* (2015) 'Ubp6 deubiquitinase controls conformational dynamics and substrate degradation of the 26S proteasome', *Nature Structural & Molecular Biology*. Nature Publishing Group, 22(9), pp. 712–719.
- Borodovsky, A. *et al.* (2001) 'A novel active site-directed probe specific for deubiquitylating enzymes reveals proteasome association of USP14', *EMBO Journal*, 20(18), pp. 5187–5196.
- Brnjic, S. *et al.* (2013) 'Induction of Tumor Cell Apoptosis by a Proteasome Deubiquitinase Inhibitor Is Associated with Oxidative Stress.', *Antioxidants & redox signaling*, 21(17), p. 24011031.
- Chalkley, G. E. *et al.* (2008) 'The transcriptional coactivator SAYP is a trithorax group signature subunit of the PBAP chromatin remodeling complex.', *Molecular and cellular biology*, 28(9), pp. 2920–9.
- Chalkley, G. E. and Verrijzer, C. P. (2004) 'Immuno-Depletion and Purification Strategies to Study Chromatin-Remodeling Factors In Vitro', *Methods in Enzymology*, 377(2001), pp. 421–442.
- Chen, X. *et al.* (2010) 'Structure of proteasome ubiquitin receptor hRpn13 and its activation by the scaffolding protein hRpn2.', *Molecular cell*. United States, 38(3), pp. 404–415.
- Chernova, T. A. *et al.* (2003) 'Pleiotropic Effects of Ubp6 Loss on Drug Sensitivities and Yeast Prion Are Due to Depletion of the Free Ubiquitin Pool', *Journal of Biological Chemistry*. in Press, 278(52), pp. 52102–52115.
- Cox, J. *et al.* (2009) 'A practical guide to the MaxQuant computational platform for SILAC-

based quantitative proteomics.’, *Nature protocols*, 4, pp. 698–705.

Cox, J. *et al.* (2011) ‘Andromeda: a peptide search engine integrated into the MaxQuant environment.’, *Journal of proteome research*, 10(4), pp. 1794–805.

D’Arcy, P. *et al.* (2011) ‘Inhibition of proteasome deubiquitinating activity as a new cancer therapy’, *Nature Medicine*, 17(12), pp. 1636–1641.

Elena Koulich, Xiaohua Li, and G. N. D. (2008) ‘Relative Structural and Functional Roles of Multiple Deubiquitylating Proteins Associated with Mammalian 26S Proteasome’, *Molecular biology of the cell*, 19, pp. 1072–1082.

Elsasser, S. *et al.* (2002) ‘Proteasome subunit Rpn1 binds ubiquitin-like protein domains’, *Nature Cell Biology*, 4(9), pp. 725–730.

Feng, X. *et al.* (2014) ‘Proapoptotic effects of the novel proteasome inhibitor b-AP15 on multiple myeloma cells and natural killer cells’, *Experimental Hematology. ISEH - Society for Hematology and Stem Cells*, 42(3), pp. 172–182.

Finley, D. *et al.* (1998) ‘Unified nomenclature for subunits of the *Saccharomyces cerevisiae* proteasome regulatory particle.’, *Trends in biochemical sciences*. ENGLAND, pp. 244–245.

Finley, D. (2009) ‘Recognition and Processing of Ubiquitin-Protein Conjugates by the Proteasome’, *Annual review of biochemistry*, pp. 477–513

Flierman, D. *et al.* (2016) ‘Non-hydrolyzable Diubiquitin Probes Reveal Linkage-Specific Reactivity of Deubiquitylating Enzymes Mediated by S2 Pockets’, *Cell Chemical Biology*, 23(4), pp. 472–482.

Fu, H. *et al.* (2002) ‘Subunit interaction maps for the regulatory particle of the 26S proteasome and the COP9 signalosome’, *EMBO Journal*, 20(24), pp. 7096–7107.

Gallery, M. *et al.* (2007) ‘The JAMM motif of human deubiquitinase Pdh1 is essential for cell viability’, *Molecular Cancer Therapeutics*, 6(1), pp. 262–268.

Guterman, A. and Glickman, M. H. (2004)

‘Complementary Roles for Rpn11 and Ubp6 in Deubiquitination and Proteolysis by the Proteasome’, *Journal of Biological Chemistry*, 279(3), pp. 1729–1738.

Hamazaki, J. *et al.* (2006) ‘A novel proteasome interacting protein recruits the deubiquitinating enzyme UCH37 to 26S proteasomes’, *The EMBO Journal*, 25(19), pp. 4524–4536.

Hanna, J. *et al.* (2006) ‘Deubiquitinating Enzyme Ubp6 Functions Noncatalytically to Delay Proteasomal Degradation’, *Cell*, 127(1), pp. 99–111.

Hanna, J., Leggett, D. S. and Finley, D. (2003) ‘Ubiquitin depletion as a key mediator of toxicity by translational inhibitors’, *Molecular and Cellular Biology*, 23(24), pp. 9251–9261.

Hochstrasser, R. J. T. J. and M. (2013) ‘Molecular Architecture and Assembly of the Eukaryotic proteasome’, (3).

Hölzl, H. *et al.* (2000) ‘The regulatory complex of *Drosophila melanogaster* 26S proteasomes. Subunit composition and localization of a deubiquitylating enzyme.’, *The Journal of cell biology*, 150(1), pp. 119–30.

Hu, M. *et al.* (2005) ‘Structure and mechanisms of the proteasome-associated deubiquitinating enzyme USP14’, *The EMBO Journal*, 24(21), pp. 3747–3756.

Huang, L., Jung, K. and Chen, C. H. o (2014) ‘Inhibitory effect of b-AP15 on the 20S proteasome’, *Biomolecules*, 4(4), pp. 931–939.

Kaiser, S. E. *et al.* (2011) ‘Protein standard absolute quantification (PSAQ) method for the measurement of cellular ubiquitin pools.’, *Nature methods*, 8(8), pp. 691–6.

Kim, H. T. and Goldberg, A. L. (2017) ‘The Deubiquitinating Enzyme Usp14 Allosterically Inhibits Multiple Proteasomal Activities and Ubiquitin-Independent Proteolysis.’, *The Journal of biological chemistry*, (3), p. jbc.M116.763128.

Komander, D., Clague, M. J. and Urbe, S. (2009) ‘Breaking the chains: structure and function of the deubiquitinases’, *Nat Rev Mol Cell Biol*. Nature Publishing Group, 10(8), pp. 550–563.

- Kuo, C.-L. and Goldberg, A. L. (2017) 'Ubiquitinated proteins promote the association of proteasomes with the deubiquitinating enzyme Usp14 and the ubiquitin ligase Ube3c', *Proceedings of the National Academy of Sciences*, 114(17), pp. E3404–E3413.
- Lam, Y. A. *et al.* (1997) 'Editing of ubiquitin conjugates by an isopeptidase in the 26S proteasome.', *Nature*, pp. 737–740.
- Lee, B.-H. *et al.* (2010) 'Enhancement of proteasome activity by a small-molecule inhibitor of USP14', *Nature*. Nature Publishing Group, 467(7312), pp. 179–184.
- Lee, B.-H. *et al.* (2016) 'USP14 deubiquitinates proteasome-bound substrates that are ubiquitinated at multiple sites', *Nature*. Nature Publishing Group, pp. 1–16.
- Lee, M. J. *et al.* (2011) 'Trimming of ubiquitin chains by proteasome-associated deubiquitinating enzymes.', *Molecular & cellular proteomics: MCP*, 10(5), p. R110.003871.
- Leggett, D. S. *et al.* (2002) 'Multiple associated proteins regulate proteasome structure and function', *Molecular Cell*, 10(3), pp. 495–507.
- Li, T. T. *et al.* (2000) 'Identification of a 26S proteasome-associated UCH in fission yeast.', *Biochemical and biophysical research communications*, 272(1), pp. 270–275.
- Livak, K. J., & Schmittgen, T. D. (2001). Analysis of relative gene expression data using real-time quantitative PCR and the 2⁻(Delta Delta C(T)) Method. *Methods* (San Diego, Calif.), 25(4), 402–408.
- Lundgren, J. *et al.* (2003) 'Use of RNA Interference and Complementation To Study the Function of the Drosophila and Human 26S Proteasome Subunit S13', *Mol Cell Biol*, 23(15), pp. 5320–5330.
- Mansour, W. *et al.* (2015) 'Disassembly of Lys<inf>11</inf> and mixed linkage polyubiquitin conjugates provides insights into function of proteasomal deubiquitinases Rpn11 and Ubp6', *Journal of Biological Chemistry*, 290(8), pp. 4688–4704.
- Matihuhin, Y. *et al.* (2008) 'Extraproteasomal Rpn10 Restricts Access of the Polyubiquitin-Binding Protein Dsk2 to Proteasome', *Molecular Cell*. Elsevier Inc., 32(3), pp. 415–425.
- Matyskiela, M. E., Lander, G. C. and Martin, A. (2013a) 'Conformational switching of the 26S proteasome enables substrate degradation.', *Nature structural & molecular biology*. 20(7), pp. 781–8.
- Maytal-Kivity, V. *et al.* (2002) 'MPN+, a putative catalytic motif found in a subset of MPN domain proteins from eukaryotes and prokaryotes, is critical for Rpn11 function.', *BMC biochemistry*, 3, p. 28.
- Mazumdar, T. *et al.* (2010) 'Regulation of NF-kappaB activity and inducible nitric oxide synthase by regulatory particle non-ATPase subunit 13 (Rpn13).', *Proceedings of the National Academy of Sciences of the United States of America*, 107(31), pp. 13854–13859.
- Mialki, R. K. *et al.* (2013) 'Overexpression of USP14 protease reduces I-??B protein levels and increases cytokine release in lung epithelial cells', *Journal of Biological Chemistry*, 288(22), pp. 15437–15441.
- Mohrmann, L. *et al.* (2004) 'Differential Targeting of Two Distinct SWI / SNF-Related Drosophila Chromatin-Remodeling Complexes Differential Targeting of Two Distinct SWI / SNF-Related Drosophila Chromatin-Remodeling Complexes', 24(8), pp. 3077–3088.
- Moshkin, Y. M. *et al.* (2007) 'Functional differentiation of SWI/SNF remodelers in transcription and cell cycle control.', *Molecular and cellular biology*, 27, pp. 651–661.
- Ortuno, D., Carlisle, H. J. and Miller, S. (2016) 'Does inactivation of USP14 enhance degradation of proteasomal substrates that are associated with neurodegenerative diseases ? *F1000Research* 5(137)
- Pathare, G. R. *et al.* (2014) 'Crystal structure of the proteasomal deubiquitylation module Rpn8-Rpn11', *Proceedings of the National Academy of Sciences*, 111(8), pp. 2984–2989.
- Peth, A., Besche, H. C. and Goldberg, A. L. (2009) 'Ubiquitinated Proteins Activate the Proteasome

- by Binding to Usp14/Ubp6, which Causes 20S Gate Opening', *Molecular Cell*, 36(5), pp. 794–804.
- Qiu, X. *et al.* (2006) 'hRpn13/ADRM1/GP110 is a novel proteasome subunit that binds the deubiquitinating enzyme, UCH37', *The EMBO Journal*, 25(24), pp. 5742–5753.
- Rosenzweig, R. *et al.* (2012) 'Rpn1 and Rpn2 coordinate ubiquitin processing factors at proteasome', *Journal of Biological Chemistry*, 287(18), pp. 14659–14671.
- Sanches, M. *et al.* (2007) 'The Crystal Structure of the Human Mov34 MPN Domain Reveals a Metal-free Dimer', *Journal of Molecular Biology*, 370(5), pp. 846–855.
- Sap, K. A. *et al.* (2015) 'Global quantitative proteomics reveals novel factors in the ecdysone signaling pathway in *Drosophila melanogaster*', *Proteomics*, 15(4), pp. 725–738.
- Sap, K. A. *et al.* (2017) 'Quantitative Proteomics Reveals Extensive Changes in the Ubiquitinome after Perturbation of the Proteasome by Targeted dsRNA-Mediated Subunit Knockdown in *Drosophila*', *Journal of Proteome Research*, 16(8), pp. 2848–2862.
- Tian, Z. *et al.* (2014) 'A novel small molecule inhibitor of deubiquitylating enzyme USP14 and UCHL5 induces apoptosis in multiple myeloma and overcomes bortezomib resistance', *Blood*, 123(5), pp. 706–716.
- Udeshi, N. D. *et al.* (2012) 'Methods for Quantification of in vivo Changes in Protein Ubiquitination following Proteasome and Deubiquitinase Inhibition', *Molecular & Cellular Proteomics*, 11, pp. 148–159.
- Unverdorben, P. *et al.* (2014) 'Deep classification of a large cryo-EM dataset defines the conformational landscape of the 26S proteasome', *Proceedings of the National Academy of Sciences of the United States of America*, 111(15), pp. 5544–9.
- Verma, R. *et al.* (2002) 'Role of Rpn11 Metalloprotease in Deubiquitination and Degradation by the 26S Proteasome', *Science*, 298(5593), pp. 611–615.
- Wagner, S. a *et al.* (2011) 'A Proteome-wide, Quantitative Survey of In Vivo Ubiquitylation Sites Reveals Widespread Regulatory Roles.', *Molecular & cellular proteomics: MCP*, 10(10), p. M111.013284.
- Van Der Wal, L. *et al.* (2018) 'Improvement of ubiquitylation site detection by Orbitrap mass spectrometry', *Journal of Proteomics*, 172, pp. 49–56.
- Wang, X. *et al.* (2014) 'The 19S Deubiquitinase inhibitor b-AP15 is enriched in cells and elicits rapid commitment to cell death.', *Molecular pharmacology*, 85(6), pp. 932–45.
- Wójcik, C. and DeMartino, G. N. (2002) 'Analysis of *Drosophila* 26 S proteasome using RNA interference.', *The Journal of biological chemistry*, 277(8), pp. 6188–97.
- Worby, C. A., Simonson-Leff, N. and Dixon, J. E. (2001) 'RNA interference of gene expression (RNAi) in cultured *Drosophila* cells.', *Science's STKE: signal transduction knowledge environment*. United States, 2001(95), p. pl1.
- Worden, E. J., Dong, K. C. and Martin, A. (2017) 'An AAA Motor-Driven Mechanical Switch in Rpn11 Controls Deubiquitination at the 26S Proteasome', *Molecular Cell*. Elsevier Inc., pp. 1–13.
- Worden, E. J., Padovani, C. and Martin, A. (2014a) 'Structure of the Rpn11-Rpn8 dimer reveals mechanisms of substrate deubiquitination during proteasomal degradation.', *Nature structural & molecular biology*. Nature Publishing Group, 21(3), pp. 220–7.
- Yao, T. *et al.* (2006) 'Proteasome recruitment and activation of the Uch37 deubiquitinating enzyme by Adrm1', *Nature Cell Biology*, 8(9), pp. 994–1002.
- Yao, T. and Cohen, R. E. (2002) 'A cryptic protease couples deubiquitination and degradation by the proteasome.', *Nature*, 419(6905), pp. 403–407.

Supporting information available online

Table 1 | Numbers of identified and quantified proteins in the global proteome datasets

Table 2 | Numbers of identified and quantified diGly modified peptides

(The 3xKD dataset published previously (Sap *et al.*, 2017) serve as a reference.)

Supporting information available in this thesis

Supplementary Table S1 | List of proteins with decreased abundances upon RPN11 KD

Supplementary Table S2 | List of proteins with increased abundances upon USP14 KD, UCHL5 and 2xKD

Supplementary Table S3 | List of proteins with decreased abundance upon USP14 KD, UCHL5 and 2xKD

Supplementary Table S4 | List of diGly modified peptides with decreased abundances upon RPN11 KD

Supplementary Table S5 | List of diGly modified peptides with increased abundances upon USP14 KD, UCHL5 or 2xKD

Supplementary Table S6 | List of diGly modified peptides with decreased abundances upon USP14 KD, UCHL5 or 2xKD

Table S1. List of proteins with decreased abundance upon Rpn11 KD

Protein names	Gene names	Down Rpn11 KD	Down 2d 3xKD	Description
Organic cation transporter-like protein	Orc2	+	+	Positive regulation of cell growth, organic cation transport
Intrinsic protein 259	Ip259	+	+	Phagocytosis, neurogenesis
CG4829	CG4829	+	+	Glutathione metabolic process, neuron projection morphogenesis
26S proteasome non-ATPase regulatory subunit 14	Rpn11	+	+	Proteasome DUB
CG8034	CG8034	+	+	Transmembrane transport
Parathion hydrolase-related protein	CG18473	+	+	Hydrolase, catabolic process
Glutathione S transferase T4	GstT4	+	+	Glutathione transferase activity
CG13367	CG13367	+		Unknown
CG32850	CG32850	+		Ubiquitin ligase, structurally related to RNF11
Coenzyme Q-binding protein COQ10, mitochondrial	Coq10	+		Mitochondrial membrane protein, required for the function of coenzyme Q in the respiratory chain
Transmembrane protein windpipe	wdp	+		Trachea development, synaptic target recognition
Vking	vkg	+		Extracellular matrix structural constituent
Division abnormally delayed	daily	+		Cell surface proteoglycan that bears heparan sulfate
CG6860	Lrch	+		Cell cortex, Ras protein signal transduction
Fat-spondin	fat-spondin	+		Extracellular region, serine-type endopeptidase inhibitor activity
CG10184	CG10184	+		Cellular amino acid metabolic process
Tiggrin	Tig	+		Cell adhesion, phagocytosis, axon guidance
CG15820	CG15820	+		Unknown
Phosphoenolpyruvate carboxykinase	Pepck ZDF4	+		Carbohydrate biosynthesis
CG18088	CG18088	+		Metabolic process
CG13366	CG13366	+		Developmental protein
CG33462	CG33462	+		Proteolysis, serine-type endopeptidase activity

Table S2. Proteins with increased abundance upon UCHL5 KD, USP14 KD or 2xKD

Protein names	Gene names	Up Uchl5 KD	Up USP14 KD	Up 2d 2xKD	Up 4d 2xKD	Up 2d 3xKD	Up Rpn11 KD	Description
CG7222	CG7222	+				+	+	Unknown
Puckered	puc	+				+		JUN kinase phosphatase
Atacin-D	AtiD	+				+		Defense response to Gram-positive bacteria
CG7130	CG7130	+				+		Unknown
Glutathione S transferase S1	GstS1	+						Glutathione peroxidase activity
Glutathione S-transferase D2	GstD2	+						Glutathione peroxidase activity
CG6674	CG6674	+						Unknown
Drosha	drosha	+						Primary mRNA processing
Vacuolar H ⁺ ATPase M9.7 subunit c	VhaM9.7-c	+						ATP hydrolysis coupled proton transport
Real-time	reim		+					phosphatidylinositol transporter activity
CG32039	CG32039		+					Unknown
CG7200	CG7200		+					Unknown
CG31886	CG31886			+				Unknown
TMS1	TMS1			+				Unknown
cAMP-dependent protein kinase type II regulatory subunit	Pka-R2			+				cAMP-binding, axon guidance
CG6650	CG6650			+				Carbohydrate metabolic process
CG9691	CG9691			+				Unknown
Tubulin gamma chain	gamma1 ub37C				+			Major constituent of microtubules
Histone H3-like centromeric protein cid	cid				+			Histone H3-like variant required for recruitment and assembly of kinetochore proteins, mitotic progression and chromosome segregation
CG33096	CG33096				+			Hydrolase
Fu2	fu2				+			Nucleic acid binding
CG4901	CG4901				+			ATP-dependent RNA helicase activity
tamas	tam				+			Replication of mitochondrial DNA
CG16771	CG16771				+			Alkaline phosphatase activity
Methyltransferase-like protein 14 homolog	CG7818				+			mRNA methylation
Mutator 2	mu2				+			Double-strand break repair

Table S3. List of proteins with decreased abundance upon UCHL5 KD, USP14 KD or 2xKD

Protein names	Gene names	Down Uchl5 KD	Down USP14 KD	Down 2d 2xKD	Down 4d 2xKD	Down Rpn11 KD	Down 2d 3xKD	Description
Ubiquitin carboxyl-terminal hydrolase	UCHL5	+		+	+			Proteasome DUB
Protein cueball		+					+	Wnt-activated receptor activity
KLHL18	KLHL18	+						Actin-binding
Kokopelli	koko	+						Regulation of cyclin-dependent protein serine/threonine kinase activity
CG42307	mus312	+						Unknown
Anaphase-promoting complex subunit 10	APC10	+						Component of the Anaphase-promoting complex, cell cycle regulation
Probable cytochrome P450 12a5, mitochondrial	Cyp12a5	+						Oxidoreductase
Ubiquitin carboxyl-terminal hydrolase	USP14		+	+	+			Proteasome DUB
CG9691	CG9691		+					Unknown
Kinetochore protein Spc25	Spc25		+					Component of Ndc80 complex, chromosome segregation, spindle checkpoint, kinetochore integrity, organization of stable microtubule binding sites
Expanded	ex		+					Endocytic recycling, negative regulation of proliferation and growth
DREV1	Rev1 drev1		+					Regulation of double-strand break repair via homologous recombination
Protein gustavus	gus		+					Developmental protein, primordial germ cell formation
Beta-glucuronidase	CG15117		+					Lysosome, degradation of dermatan and keratan sulfates
Nuclear export factor 3	Nxf3		+					mRNA export from nucleus
CG8170	CG8170		+					Proteolysis, serine-type endopeptidase activity
Saxophone	sax		+					Kinase, developmental protein, actin filament organization
Mel-P26	mel-P26		+					Ubiquitin ligase, meiotic nuclear division
CG30116	CG30116		+					Peptidase activator activity involved in apoptotic process
CG10188	CG10188		+					Positive regulation of Rho protein signal transduction
CG30387	CG30387		+					Unknown
Ankyrin 2	Ank2		+					Cytoskeleton protein binding, signal transduction
CG9780	CG9780		+					Proteolysis, metalloendopeptidase activity
CG3563	jvl		+					Developmental protein, actin filament bundle assembly
Glycerol kinase	Gk		+					Carbohydrate metabolic process
Insulin-like receptor	InR dimr Dir-a Inr-a		+					Ligand-stimulated tyrosine-protein kinase activity, Regulates body size and organ size, involved in development of embryonic nervous system.
LpR2	LpR2		+					Neuron projection morphogenesis
CG13001	CG13001			+				Unknown
CG2698	CG2698			+				Unknown
Serine protease 7 3.4.21.	Sp7			+				Proteolysis, carboxypeptidase activity
Cyclin A	CycA				+			Regulation of cyclin-dependent protein serine/threonine kinase activity
Cappuccino	capu				+			Actin nucleation
CG30359	Mal-A5				+			Carbohydrate metabolic process
CG41434	CG41434				+			Unknown
RabX4	RabX4				+			Protein transport, recycling endosome
CG10903	CG10903				+			Neurogenesis, methyltransferase activity

Table S4. Selection of proteins with increased abundance upon both 3xKD & Rpn11 KD

Entry	Protein names	Gene names	protein catabolic process	proteolysis	Cytoskeleton organization	Description
P40301	Proteasome subunit alpha type-2	Prosalpha2	protein catabolic process	proteolysis	cytoskeleton organization	20S Proteasome subunit alpha
P18053	Proteasome subunit alpha type-4	Prosalpha3	protein catabolic process	proteolysis	cytoskeleton organization	20S Proteasome subunit alpha
P22769	Proteasome subunit alpha type-7-1	Prosalpha4	protein catabolic process	proteolysis	cytoskeleton organization	20S Proteasome subunit alpha
AQAQ10	Proteasome subunit beta type	Prosbeta1	protein catabolic process	proteolysis	cytoskeleton organization	20S Proteasome catalytic subunit
Q9VJU1	Proteasome subunit beta type	Prosbeta2	protein catabolic process	proteolysis	cytoskeleton organization	20S Proteasome catalytic subunit
Q9XYN7	Proteasome subunit beta type-3	Prosbeta3	protein catabolic process	proteolysis	cytoskeleton organization	20S Proteasome subunit beta
Q9VJU0	Proteasome subunit beta type	Prosbeta4	protein catabolic process	proteolysis	cytoskeleton organization	20S Proteasome subunit beta
Q7KMQ0	Rpt1	Rpt1	protein catabolic process	proteolysis	cytoskeleton organization	20S Regulatory particle triple A
P48601	26S protease regulatory subunit 4	Rpt2	protein catabolic process	proteolysis	cytoskeleton organization	20S Regulatory particle triple A
Q9VU14	Regulatory particle triple-A ATPase 4	Rpt4	protein catabolic process	proteolysis	cytoskeleton organization	20S Regulatory particle triple A
Q9V3V6	26S proteasome regulatory complex subunit p50	Rpt5	protein catabolic process	proteolysis	cytoskeleton organization	20S Regulatory particle triple A
Q9VM54	26S proteasome regulatory complex subunit p97	Rpt1	protein catabolic process	proteolysis	cytoskeleton organization	Proteasome regulatory subunit
Q9VKZ8	USP14	USP14	protein catabolic process	proteolysis	cytoskeleton organization	DUB proteasome
Q9VH79	Rpt3R	Rpt3R	protein catabolic process	proteolysis	cytoskeleton organization	ATP binding
Q9VA54	Rpt6R	Rpt6R	protein catabolic process	proteolysis	cytoskeleton organization	ATP binding
Q9VN58	CG42574	ctrip	protein catabolic process	proteolysis	cytoskeleton organization	Ubiquitin ligase, circadian rhythm
Q7Y296	CG9772	Skp2	protein catabolic process	proteolysis	cytoskeleton organization	SCF ubiquitin ligase complex
A1Z7K9	CG8232	PAN2	protein catabolic process	proteolysis	cytoskeleton organization	poly(A) specific ribonuclease activity
Q24044	Ftzy	Ftzy	protein catabolic process	proteolysis	cytoskeleton organization	Anaphase Promoting Complex
Q7KN62	Transitional endoplasmic reticulum ATPase	TER94	protein catabolic process	proteolysis	cytoskeleton organization	ER and Golgi vesicle transport, UPS, oskar mRNA localization
Q7JQ11	CG8830	DUBA1	protein catabolic process	proteolysis	cytoskeleton organization	Deubiquitinating apoptotic inhibitor
Q9VM45	Nu42	Nu42	protein catabolic process	proteolysis	cytoskeleton organization	Ndc80 complex, kinetochore
Q9VRK9	Kinesin-like protein at 64D	Kip64D	protein catabolic process	proteolysis	cytoskeleton organization	kinesin complex
Q9VKM7	Aurora kinase B	lal	protein catabolic process	proteolysis	cytoskeleton organization	Regulates chromosome segregation
Q8SX98	Verprolin 1	Vrp1	protein catabolic process	proteolysis	cytoskeleton organization	Actin filament organization
Q8SX11	Phosphatidylinositol 5-phosphate 4-kinase	PIP4K	protein catabolic process	proteolysis	cytoskeleton organization	Actin filament organization
P35220	Catenin alpha	alpha-Cat	protein catabolic process	proteolysis	cytoskeleton organization	Interaction with cadherins, cell adhesion
Q9VUJ5	Pomp	Pomp	protein catabolic process	proteolysis	cytoskeleton organization	mitotic spindle elongation, proteasome maturation protein
A4V164	Phosphoinositide-dependent kinase 1	Pdk1	protein catabolic process	proteolysis	cytoskeleton organization	required for actin cytoskeleton stability
P20439	G2/mitotic-specific cyclin-B	CycB	protein catabolic process	proteolysis	cytoskeleton organization	Essential for the control of the cell cycle at the G2/M (mitosis) transition
Q9V9Y9	Spn-F	spn-F	protein catabolic process	proteolysis	cytoskeleton organization	minus-end-directed microtubule motor activity
Q9VGF9	Aurora	aur	protein catabolic process	proteolysis	cytoskeleton organization	Kinase, centrosome separation
Q9VSW5	Kinesin-like protein at 67A	Kip67A	protein catabolic process	proteolysis	cytoskeleton organization	Plus-end-directed microtubule motor activity
Q9VNS0	Protein maelstrom	mael	protein catabolic process	proteolysis	cytoskeleton organization	Position microtubule-organizing center in oocytes
Q9V3V7	Kinetochore protein Spc25	Spc25	protein catabolic process	proteolysis	cytoskeleton organization	Ndc80 complex, kinetochore integrity
Q59DY7	Grapes	grp	protein catabolic process	proteolysis	cytoskeleton organization	Centrosome separation, mitotic cell cycle checkpoint
Q6NN29	Nuclear fallout	nuf	protein catabolic process	proteolysis	cytoskeleton organization	Actin cytoskeleton reorganization

Table S5. List of diGly peptides with decreased abundance upon Rpn11 KD

Gene names	Protein names	Description	Sequence	Down Rpn11 KD	Down 2d 3xKD
RpS2 sop	40S ribosomal protein S2 (Protein strings of pearls)	Protein synthesis, developmental protein	EMPLGSTPYQAYSDFLSKPTPR EMPLGSTPYQAYSDFLSKPTPR EDSKEWPTVK	+	+
RpS3	40S ribosomal protein S3	Cytoplasmic translation, DNA repair	KPLPDNVSVPEKKEK	+	+
RpL11	60S ribosomal protein L11	Structural constituent of ribosome, rRNA binding, mitotic spindle organization, centrosome duplication	VLEQLTQQQPVFSKAR	+	+
RpL22	60S ribosomal protein L22	Structural constituent of ribosome, mitotic spindle elongation, translation	VNGKYNLGNNVTFER VVAEKDSVELR	+	+
path	Pathetic	Amino acid transmembrane transporter activity, growth	VMYKIQPR	+	+
CG8177	CG8177	Membrane protein, inorganic anion exchanger	HAQDEMEQFLPGEKVMYK	+	+
Ord2	Organic cation transporter-like protein	Organic cation transmembrane transporter activity, positive regulation of cell growth	YNSYISLONLSIGTDDKK APEAQPLKSGSETNGSTIANGHK GSGETNGSTIANGHK	+	+
Vha55	V-type proton ATPase subunit B	ATP hydrolysis coupled proton transport, vacuolar acidification	FPKFAEVQLR	+	+
Gp150	Gp150 protein	Transmembrane receptor protein tyrosine phosphatase signaling pathway	LSEDNVKTPTSKEQK LSEDNVKTPTS NSFYVYQKLSEDNVKTPTS MALLASKNSFYVQK	+	+
CG8468	CG8468	Transmembrane transport	GLVSKQPENIK SODELASKGLVSK	+	+
CIC-b	CG8594	Ion transport, sensory perception of touch	EAGPTSKAVQDFGLHQR	+	+
CG5021	Uncharacterized Golgi apparatus membrane protein-like protein CG5021	Multipass membrane protein	DLNSAATDFVKTQFFK	+	+
Sdc Syd	Syndecan	Cell surface proteoglycan, energy homeostasis, axon guidance	RSPANINSYAKNANNR	+	+
wgn	TNFR superfamily protein (Wengen)	Tumor necrosis factor-activated receptor activity, apoptotic process, cell surface receptor signaling pathway	RLDQDVEELSTKLMAK	+	+
egh zw4	Protein egghead	Axon guidance, cell fate commitment, developmental protein	FYVQKQDVR	+	+
CG3164	CG3164	Hydrolase, ATPase activity	LGTAGAGQLKAQIVPAQPK TKNDNANLLNDNR ARNDLVKVQNLK NDLVKVQNLK	+	+
CG16771	CG16771	Alkaline phosphatase activity, metabolic process	AOIVPAQPKTLQHLPK	+	+
rost	Protein rolling stone	Developmental protein, muscle protein, myoblast fusion	RSGETPINSQKFR MQLFDDFCCKSFNK MQLFDDFCCKSFNK	+	+
CG4668	CG42389	Unknown	GPETHFTIDNLAAGTCYQFR IVCKVTSLSNR	+	+

Table S6. List of diGly peptides with increased abundance upon UCHL5 KD, USP14 KD or 2xKD

Gene Names	Protein Names	Description	Sequence	Uchl5 KD	USP14 KD	2d 2xKD	4d2xKD	2d 3xKD	Rpn11 KD
ref(2)P	Protein ref(2)P	Clearance protein aggregates	CELAHKHPEHMLR	+					+
CaBP1	Calcium-binding protein 1	Protein disulfide isomerase activity, protein folding, cell redox homeostasis	GFTPIKFGANK	+					
pirk	Poor lmd response upon knock-in	Negative regulation of immune response	NAKPTPTDAGGK	+					
LanB2	Laminin subunit gamma-1	cell adhesion	ALADKLESEAQFDLK		+				
Mct1	Monocarboxylate transporter 1	transmembrane transport	VLPKDOYLQLPQRDTAVSGGALCR		+				+
key	NF-kappa-B essential modulator	Positive regulation immune response	QEVKGLQIQNDIYR			+			+
Rps11	40S ribosomal protein S11	rRNA binding, translation, mitotic spindle	AFCKDFGVNLNRK			+			
CG5555	CG5555	Zinc ion binding	LFONKSDGKLVASQTEK				+		+
			SDGKLVASQTEKDEREEK				+		+
Rpl3, Rpl3R	26S proteasome regulatory complex subunit p48A	Proteasome subunit	WGSEFVKYLGEGPR				+		+
CG9372	CG9372	serine-type endopeptidase activity	MPELKNDVWR				+		+
blanks	blanks	RNA interference, regulation of chromatin silencing	MEAKQLLAESCAG				+		
CG5555	CG5555	Zinc ion binding	SDGKLVASQTEKDER				+		+
Rpl 15	60S ribosomal protein L15	Structural constituent of the ribosome, translation	AKQGFVYR				+		+
Argk	Arginine kinase	phosphorylation	AVQQQLIDHFLFKEGDRFLQANACR				+		
eca.p24-2	Transmembrane emp24 domain-containing protein eca	Developmental protein, Wnt signaling, ER to Golgi-vesicle mediated transport	QLLDQVEQITKEQNYQR				+		
CG2765	CG2765	myosin binding	SGYTDLTKELETSR				+		
CG18343-RA	CG18343	Unknown	MEKSCSIGNGR				+		
Rpl 13	60S ribosomal protein L13	Structural constituent of the ribosome, translation, mitotic spindle	GPVLPIKNEQPAVVEFR				+		

Chapter 5

The *Drosophila* 26S proteasome interactome is modulated under stress conditions as revealed by LFQ mass spectrometry.

Karen A. Sap, Dick H.W. Dekkers and Jeroen A.A. Demmers

Manuscript in preparation

Abstract

Selective proteasome-dependent degradation of proteins is important to maintain cellular homeostasis and viability under both stress and non-stress conditions. Despite extensive research, the molecular mechanism by which ubiquitin-dependent proteasomal degradation is adapted to different intracellular environments is poorly understood. Here we set out to identify differential interactor dynamics of the 19S proteasome to investigate the adaptive recruitment of specific interactors under both stress and non-stress conditions in the ubiquitin-dependent protein degradation pathway. Proteasomes were immunopurified using antibodies directed against both Rpn8 and Rpn10 from *Drosophila melanogaster* S2 cell lysates. Using a label free quantification mass spectrometry approach, we identified specific interacting proteins of the 19S/26S proteasome under various stress conditions, *i.e.* proteasome inhibition (MG132/Lactacystin), endoplasmatic reticulum stress (Tunicamycin) and oxidative stress (hydrogen peroxide). We observed an increased association of 20S core particles and 19S caps upon MG132/Lact treatment, and additionally an enhanced recruitment of several interactors including hsp23 and hsp68, REG (PA28) and ref(2)p, and a putative novel UBL-domain containing ubiquitin shuttle protein, CG7546 (Human Bat3). On the other hand, ubiquitin shuttle protein Rad23 was only found in association with the 19S cap in non-stress conditions. One other interesting finding of our study is that deubiquitinating enzyme UCHL5 was more abundant at proteasomes under all applied stress conditions, while it was clearly less recruited under non-stress conditions. Together, these data give more insight in the dynamic adaptation of ubiquitin-dependent proteasomal protein degradation under different intracellular environments. This information is relevant to understand proteasome regulation in disease states and may lead to novel therapeutic targets for the treatment of diseases in which cellular stress and homeostasis misbalance play a role.

Introduction

The 26S proteasome complex

The 26S proteasome is a 2.5-MDa enzyme complex which is responsible for the regulated degradation of a large complement of proteins in the cell (Voges, Zwickl and Baumeister, 1999; Pickart and Cohen, 2004; Finley, 2009). The 26S proteasome comprises a barrel-shaped 20S core particle (CP) and a 19S regulatory particle (RP, also known as PA700) on one or both sides (Murata et al. 2009; Ho Min Kim, Yadong Yu 2008). The 20S core subunit contains two inner heteroheptameric rings composed of Prosbeta1-7 subunits. Prosbeta1, 2 and 5 are responsible for the catalytic cleavage of proteasome substrate and exhibit respectively caspase-like, trypsin-like and chymotrypsin-like activity (Marques et al. 2009; Loidl et al. 1999). The barrel furthermore contains two outer heteroheptameric alpha rings which consist of Prosalpha1-7 subunits. These

rings function as a gate to regulate substrate entry towards the proteolytic chamber. These rings also function as docking stations for substrates, proteasome interacting proteins as well as proteasome activators, such as the 19S RP (Pickart & Cohen 2004; Groll et al. 1997).

The 19S RP regulates the proteasome-dependent degradation of polyubiquitinated substrates. This involves binding, deubiquitination and unfolding of substrate followed by opening of the 20S CP and translocation of the unfolded substrate into the catalytic core (Pickart & Cohen 2004; Verma et al. 2004; Elsasser & Finley 2005; Verma et al. 2002). The 19S RP is composed of two subcomplexes: the base and the lid (Glickman et al. 1998; Schmidt et al. 2005). The 19S RP binds with its base to the 20S CP alpha ring. The 19S base consists of a heterohexameric ring of AAA-ATPase subunits Rpt1-6 which use ATP to unfold proteasome substrate and possibly induce conformational changes of the proteasome complex upon substrate engagement. Other subunits of the base include Rpn1 and Rpn2 which function as protein interaction platforms, and ubiquitin receptors RPN10 and Rpn13. The 19S lid complex comprises eight non-ATPase subunits (RPN3, Rpn5-9, RPN11 and RPN12). Rpn11 is a deubiquitinating enzyme and the other components are probably (also) functionally supportive for the structure. The activities of the 19S RP and its assembly with the 20CP are strictly ATP-dependent.

Despite its physiological importance, many aspects of the proteasome's structural organization and regulatory mechanisms are not yet well defined. In addition to the constitutive proteasome subunits, there is increasing evidence that proteasomal function is affected by a wide variety of proteasome interacting proteins (PIPs). A broad class of PIPs has been identified, including ubiquitin ligases, ubiquitin receptors, deubiquitinases, proteasome activators and inhibitors, chaperones, and other types of modulators (Hanna et al. 2007; Finley 2009; Schmidt et al. 2005; Wang & Huang 2008; Kaake et al. 2011; Verma et al. 2000; Leggett et al. 2002; Wang et al. 2007; Guerrero 2005; Scanlon et al. 2009). These proteins interact with the proteasome in a dynamic manner in response to environmental changes and affect the function and structure of the proteasome complex.

Here, we present a systematic interactome profiling methodology to study the effects of different environmental conditions on the 19S proteasome interactome. We analyzed the adaptive recruitment of 19S interactors upon proteasome inhibition (MG132/Lact), ER stress (Tunicamycin), oxidative stress (30 min H₂O₂) and recovery after oxidative stress (24h H₂O₂) by immuno precipitations and label free quantification (LFQ)-based proteomics. Below, an overview of the stress conditions is given including the current knowledge of proteasome involvement herein.

Oxidative stress

Oxidative stress is caused by either the excessive production of reactive oxygen species (ROS) or their insufficient elimination by antioxidants (Schieber and Chandel, 2014; Tong et al. 2015) and has been implicated in aging and several diseases, such as cancer and neurodegenerative disorders. ROS are mainly produced in mitochondria (~80%), but also in peroxisomes and the endoplasmic reticulum (ER) (Holmström & Finkel 2014; Brand 2010; Fransen et al. 2012). ROS can oxidize proteins which in turn may alter their function. Furthermore, chronic oxidative stress can result in protein misfolding. This buildup of oxidized proteins can be cytotoxic, hence the rescue of oxidized proteins by protein repair pathways or their destruction via cellular degradation pathways is of utmost importance for cell viability and the maintenance of homeostasis. The immunoproteasome could degrade oxidized proteins (Pickering & Davies 2012), but the major degradation machinery is the 20S proteasome core complex which recognizes exposed hydrophobic patches on oxidatively damaged proteins (extensively reviewed: (Goldberg 2003; Breusing & Grune 2008; Jung & Grune 2008; Raynes et al. 2016)). In contrast, the 26S proteasome is considered more vulnerable for oxidative stress (Reinheckel et al. 1998; Reinheckel et al. 2000) as the 19S and 20S particles dissociate shortly after intensive or prolonged H_2O_2 -induced oxidative stress (Wang et al. 2011; Reinheckel et al. 1998). In the recovery phase the UPS was shown to be activated again (Grune et al. 2011). We set out to identify the adaptive interactome of the 19S proteasome during mild H_2O_2 -induced stress and during the recovery phase.

ER stress

The ER is the site of biosynthesis of transmembrane and secreted proteins. When proteins enter the ER co-translationally, they are subsequently folded and undergo glycosylation or lipidation. The correct folding and transport of these proteins is dependent on chaperones inside the ER and on an oxidizing environment to generate disulfide bond formation between protein chains. Protein folding, modification, and transport inside the ER are strictly regulated by the protein quality control system (Wang & Kaufman 2012). ER stress emerges upon accumulation of misfolded or unfolded proteins within the ER lumen. This may be the result of various intracellular and extracellular stimuli, such as nutrient deprivation, depletion of ER calcium stores, changes in the cellular redox state, the impairment of glycosylation, impairment of vesicular transport, increased ER protein synthesis, impairment of ER-associated degradation (ERAD), or the expression of mutated ER proteins. In ER stress, unfolded proteins accumulate within the ER and this buildup affects cellular activities. Cells can respond to ER stress in two different ways, *i.e.* through survival or apoptosis. Cells can then activate the unfolded protein response (UPR) in order to survive. This response involves three different stages: 1) increasing the ER volume and decreasing protein synthesis rates (Harding et al. 1999), 2) induction of transcription of genes encoding for proteins with a role in ER protein folding and degradation (MJ Gething & Sambrook 1992), 3) induction of ERAD in order to retrotranslocate misfolded proteins from the ER to the cytoplasm for proteasome-dependent degradation (Mori 2000). By

these mechanisms, the folding capacity of the ER can be restored. We characterized the adaptive interactome of the 19S proteasome upon Tunicamycin-induced ER stress.

Proteasome inhibition mediated stress

Misregulation of the ubiquitin-proteasome system (UPS) has been associated with a number of diseases, including cancer and neurodegenerative disorders. Inhibition of the proteasome by drugs has been shown to be effective in the treatment of several types of cancers, such as the inhibitor Bortezomib for the treatment of multiple myeloma (MM). Treatment of MM cells with proteasome inhibitors (PIs) result in the accumulation of misfolded immunoglobulin in the ER (Obeng et al. 2006) and hence induces the UPR (Obeng et al. 2006; Lee et al. 2003). Usually, the UPR allows the cell to survive temporary stress conditions. However, during prolonged stress conditions caused by PIs, UPR induction may lead to a cell cycle arrest (Brewer et al. 1999) and eventually the activation of apoptosis (Ri, 2016). Induction of the UPR and apoptosis by PIs is especially observed in cells with high Ig production (Meister et al. 2007). Thus, partial inhibition of proteasomes *in vivo*, which is not toxic to normal cells, may be sufficient to eliminate MM plasma cells (Meister et al. 2007). We identified the dynamic 19S interactome upon prolonged MG132/Lactacystin-induced proteasome inhibition.

Identification of proteasome interacting factors under specific stress conditions could reveal how the 26S proteasome is regulated in response to perturbations of the intracellular environment. In this study we used a label free quantitative mass spectrometry-based approach to identify the interactome of the 19S regulatory particle under different stress conditions, *i.e.* proteasome inhibition, ER-stress and oxidative stress. It is important to note that we directly target 19S subunits (Rpn8 and Rpn10) and not 20S subunits. We therefore only focus on 19S interactors as well as 26S proteasome interactors which are involved in ubiquitin-dependent protein degradation, and we do not analyze changes in alternative proteasomes. First of all we identified all constitutive 26S proteasome subunits as specific interactors in all immunoprecipitations (IP's), which validates our approach. Furthermore, we found that ubiquitin shuttle protein Rad23 was only associated with the proteasome in non-stress conditions. Additionally, we found an enhanced recruitment of deubiquitinating enzyme UCHL5 under stress conditions, to levels almost similar as general 19S subunits. A relatively unknown UBL-domain containing protein, CG7546, was identified as interaction partner of the proteasome only with proteasome inhibition. Lastly, we used relatively mild conditions for oxidative stress and we did not observe enhanced dissociation of 26S proteasomes directly after H₂O₂ treatment but on the other hand we did observe enhanced stability of the 26S proteasome upon chemical proteasome inhibition, two phenomena often described in literature (Wang et al. 2011; Reinheckel et al. 1998; Kleijnen et al. 2007). Taken together, our data gives more insight in the responses of the ubiquitin-proteasome system on stress conditions.

Results

H₂O₂ and TM induce different stress responsive genes in *Drosophila* S2 cells

We are interested in the effect of cellular stress on the composition and stability of the 26S proteasome interactome. In order to induce different types of intracellular stress, the proteasome inhibitors MG132/Lact, ER stress inducer Tunicamycin (TM) and oxidative stress inducer H₂O₂ were used for cellular perturbations. It has been shown that the 26S proteasome complex is relatively sensitive for H₂O₂ treatment (Reinheckel et al. 1998; Reinheckel et al. 2000), and that the 26S proteasome plays an important role in the recovery after oxidative stress (Grune et al. 2011). Thus, in order to maintain proper 26S proteasome homeostasis during our study we applied relatively mild oxidative stress conditions (1mM H₂O₂). First, we set out to verify the effect of H₂O₂ in *Drosophila* S2 cells by monitoring RNA expression levels of known responsive genes by Real-Time Quantitative Reverse Transcription PCR at different time points after the induction of oxidative stress (Chow et al. 2013). Cells were treated with 1 mM H₂O₂, which was quenched by the addition with catalase after 30 min. Total RNA was isolated from either untreated cells (0 min) or treated cells after 30 min, 1h, 4h, 8h, 16h or 24h following H₂O₂ treatment. H₂O₂ responsive genes GstD5, Hsp70 and Hsp68 were strongly upregulated already 30 min after induction and expression levels started to decline 8h after the treatment and then became relatively stable (Figure 1A). One early (30 min) and one late (24h) time point after H₂O₂ treatment were chosen for further analysis, *i.e.* the investigation of the effect of stress inducers on proteasome stability and the identification of proteasome interaction partners. Furthermore, cells were treated with 1 μ M tunicamycin and total RNA was isolated at the same time points as were used for H₂O₂ treatment (Figure 1B). Tunicamycin responsive genes were selected based on results of a published quantitative mass spectrometry-based global proteome study on tunicamycin-treated human neuroblastoma cells (Bull & Thiede 2012). Induction of TM responsive genes was observed 4h after the treatment and this upregulation remained relatively stable upon prolonged exposure (Figure 1B). We used 24h treatments of 1 μ M Tunicamycin in further analyses. Lastly, cells were treated with a combination of proteasome inhibitors MG132 and Lactacystin for 16h. In Chapter 3 of this thesis we have shown that 16h MG132/Lactacystin treatment causes a remarkable accumulation of ubiquitinated proteins, without severely affecting cell viability (Sap et al. 2017).

Investigation of 20S proteasome stability upon H₂O₂, TM or MG132/Lact treatment

The integrity of the proteasome complex upon MG132/Lact, TM and H₂O₂ treatment was assessed by glycerol gradient analysis (Figure 2). The largest effects were observed upon treatment with MG132/Lact. Immunoblotting glycerol gradient fractions against Prosalpha subunits revealed that MG132/Lact resulted in both an increase in lower molecular weight (sub)complexes (fractions #1-4) and higher molecular weight complexes (fractions #9-11).

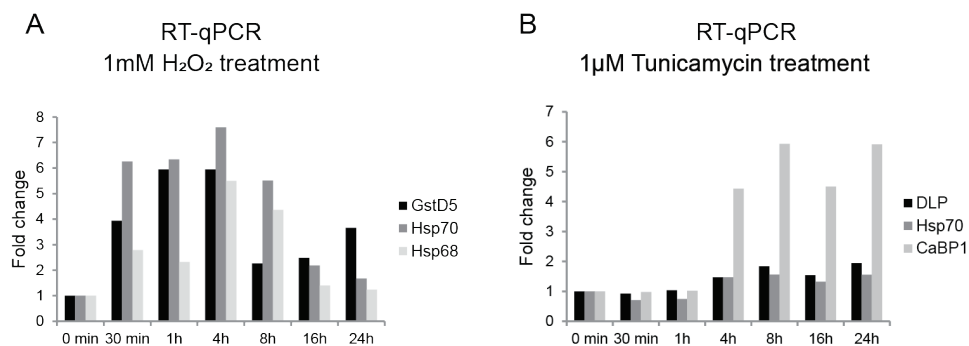


Figure 1. Upregulation of H₂O₂ and TM responsive genes. Total RNA was isolated followed by cDNA synthesis and real time RT-qPCR. Values obtained from amplification of alpha-mannosidase-lb (CG11874) were used to normalize the data as described previously (Sap et al. 2015). Fold change compared to untreated cells (0 min) is shown on the y-axis. A) Fold change upregulation of a selection of H₂O₂ responsive genes. Based on these data, treatment of 30 min and 24h were chosen as short incubation resp. long incubation time for further investigation. B) Fold change upregulation of a selection of TM responsive genes. Based on these data, treatment of 24h was chosen for further investigation.

Lower molecular weight complexes may either indicate that the proteasome became unstable or that proteasome assembly was affected, whereas the higher molecular weight complexes may suggest either the recruitment of additional proteins or protein complexes, or the formation of protein aggregates. No apparent distortion of the proteasome core complex integrity was observed upon treatment with H₂O₂ (30 min) or TM, although upon longer exposure to H₂O₂ (24 h) the appearance of higher molecular weight complexes was observed (Figure 2).

Label Free Quantification of co-immunopurified proteins of the 19S/26S proteasome

We set out to identify proteins that were recruited by the 19S/26S proteasome upon exposure to a variety of cellular stress factors. Cellular stress was induced by treatment with the following compounds: MG132 (50 μM, 16 h) and Lactacystin (5 μM, 16h) ('MG132/Lact'), TM (1 μM, 24 h) or H₂O₂ (1mM, 30 min or 24 h) in *Drosophila* S2 cells. Antibodies directed against the proteasome subunits Rpn8 or Rpn10 were used for immune purification (IP) of the proteasome in lysates of cells treated with the above-mentioned stress inducers and compared against untreated cells. Additional controls involve IPs with nonspecific antibodies, *i.e.* antibodies derived from rabbit preimmune serum (here referred to as 'PPI') performed in untreated cell lysates. Purified proteins were resolved by SDS-PAGE (Figure 3A, 3B, 3C) and analyzed by mass spectrometry, while quantitative analysis was performed using label free quantification (LFQ) to discriminate putative interactors from co-purifying contaminants. All IPs were performed in triplicate for solid back-end statistical analysis. Control coimmunopurifications with α-Rpn8 or α-Rpn10 antibodies showed that the proteasome subunits could efficiently be enriched for by both antibodies (Figure 3D).

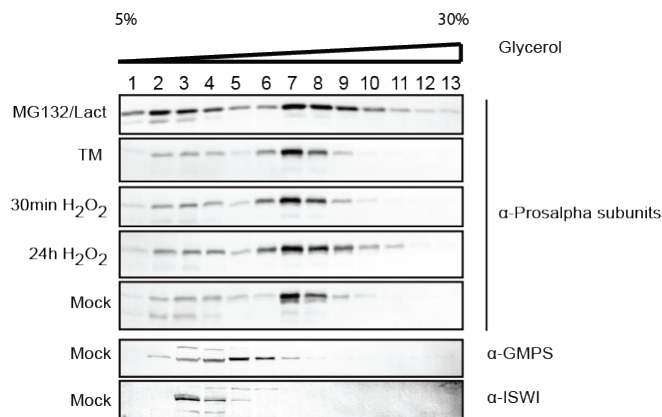


Figure 2. TM and H₂O₂ have no major effect on proteasome stability under the tested conditions. Cells were treated either for 16h with 50 μ M MG132 and 5 μ M Lactacystin, for 24h with 1 μ M TM, or for 30 min or 24h with 1mM H₂O₂. Mock cells were treated with DMSO only (also described as ‘untreated’). Whole cell lysates were prepared under non-denaturing conditions and proteins were separated on a 5 - 30% glycerol gradient by ultracentrifugation. Proteins in the 13 different fractions were resolved by SDS-PAGE and proteasome Prosalpha subunits were visualized by immunoblotting. GMPs and ISWI were used as controls for the glycerol gradient.

To identify putative 26S proteasome interacting proteins (PIPs), proteins that were identified in the negative control (PPI) were subtracted from the data set of identified proteins in the α -Rpn8 or α -Rpn10 IPs. We used relatively stringent criteria for the selection of putative interactors, *i.e.* interactors of Rpn8 or Rpn10 should be identified in at least two replicates and statistical t-testing was used for the identification of significantly enriched proteins (Welch two-sided student T-tests, permutation-based FDR of 0.05. Number of randomizations was 250). Interactors of the 19S/26S proteasome must have been identified as specific interactors of both Rpn8 and Rpn10. In the second part of this work, where we analyze the dynamic interactome, we only take into account the proteasome interactors already identified in the first interactome study (PPI IP vs proteasome IP under both non-stress and stress conditions). With these criteria we filtered out a lot of background binders.

Figure 4 shows an overview of the proteasome interactome analysis. Proteins which were significantly enriched in either of the IPs are shown in black and known proteasome subunits are shown in red. The numbers of significantly enriched proteins in each of the IPs are listed in Table 1. We identified between 87 and 96 putative interactors of Rpn8 and between 82 and 151 putative interactors of Rpn10. The Venn diagram in Figure 5 shows the overlap of these interactors as a response to the different perturbations. Between 50 and 67 proteins were enriched in both α -Rpn8 and α -Rpn10 purifications, suggesting that these proteins are *bona fide* interactors of the 19S/26S proteasome complex.

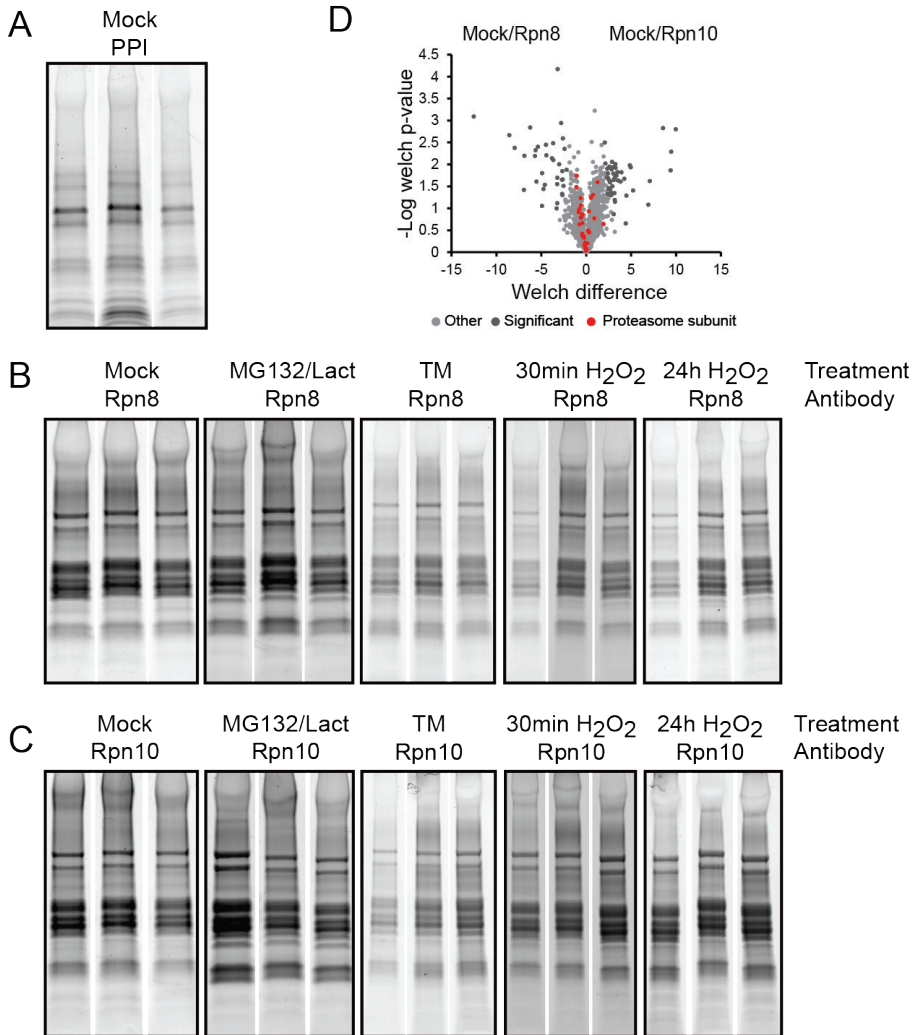


Figure 3. Immunopurification of Rpn8 and Rpn10. For each condition Immunopurification assays (IPs) were performed in triplicate from lysates of either untreated S2 cells (mock) or stress-treated cells (MG132/Lact, TM or H₂O₂). Purified proteins were resolved by SDS-PAGE and stained with Coomassie. A) IP with antibodies derived from pre-immune serum (PPI) that are not specific for proteasome subunits serve as a control for the identification of proteasome subunits and proteasome interactors. B) IPs with antibodies directed against Rpn8 under the indicated conditions. C) IPs with antibodies directed against Rpn10 under the indicated conditions. D) Welch's t-test shows that the α -Rpn8 and α -Rpn10 IPs in untreated lysates were comparable in terms of proteasome subunit (red) enrichment.

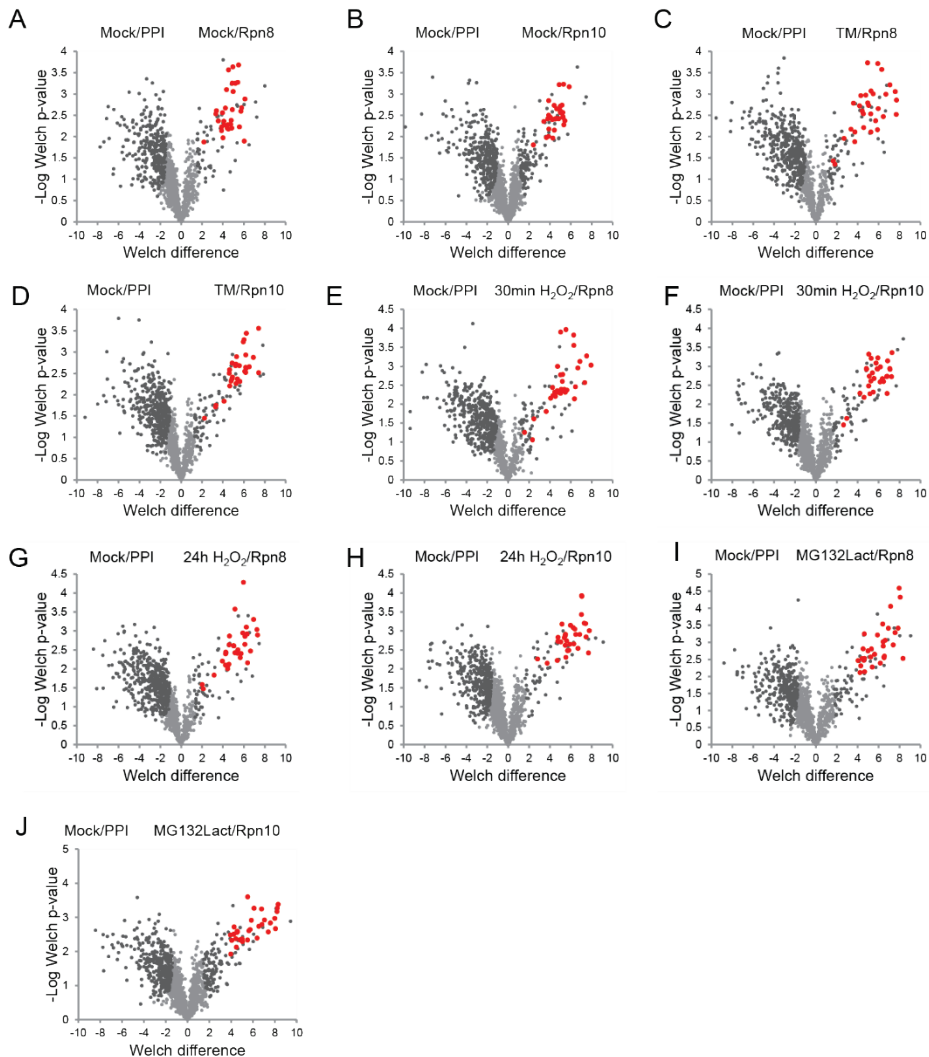


Figure 4. Identification of specific proteasome interacting proteins. Volcano plots based on Welch's t-tests performed on log₂-transformed LFQ intensity values of mock treated and PPI purified samples versus A) mock-treated and Rpn8 purified samples, B) mock-treated and Rpn10 purified samples, C) TM-treated and Rpn8 purified samples, D) TM-treated and Rpn10 purified samples, E) 30min H₂O₂-treated and Rpn8 purified samples, F) 30min H₂O₂-treated and Rpn10 purified samples, G) 24h H₂O₂-treated and Rpn8 purified samples, H) 24h H₂O₂-treated and Rpn10 purified samples, I) MG132/Lact-treated and Rpn8 purified samples, J) MG132/Lact-treated and Rpn10 purified samples. Proteins enriched in the Rpn8 or Rpn10 IPs are found at the right side in each volcano plot. Proteins which were significantly enriched are shown in black; proteasome subunits are shown in red. The multi-angle comparison of Rpn8

versus mock and PPI-mock provides an extra layer of stringency, resulting in higher confidence interactor analysis.

Table 1. Numbers of significantly enriched proteins compared to PPI IP.

Immuno purification	Mock	MG132 Lact	TM	30min H ₂ O ₂	24h H ₂ O ₂
Rpn8 IP	87	96	87	91	89
Rpn10 IP	136	151	105	92	82
Rpn8 & Rpn10 IP	55	67	52	54	50

In general, the interactors identified with both antibodies were very similar per condition, however there were also some interesting differences. Rpn4 (CG9588/PSMD9), a chaperone involved in proteasome assembly, was enriched in all datasets, except for the α -Rpn10 IP in MG132/Lact treated cells. In addition, two E2 ubiquitin conjugating enzymes were specifically enriched in α -Rpn10 IPs in MG132/Lact treated cells: Ben/UBE2N and Effete/UBE2D2. When proteins were only enriched with the use of the Rpn10 antibody, the interaction might take place with free Rpn10 outside the proteasome. For a complete list of identified proteins for each of the purifications see Supplementary Table 1 one at the end of this chapter or online. To be sure to analyze interactors of the proteasome complex and not those for free Rpn10 we only took into account proteins that were enriched in both α -Rpn8 and α -Rpn10 IPs in all further analyses (Suppl. Table 1).

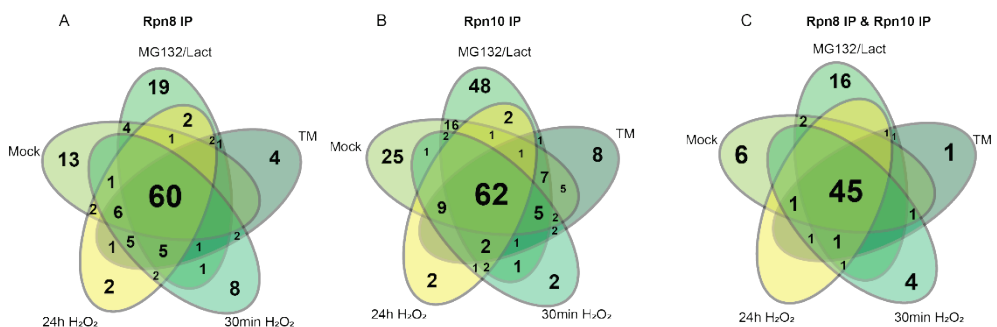


Figure 5. Overlap of significantly enriched proteins in the different IPs.

Overlap of significantly enriched proteins in A) Rpn8 purifications and B) Rpn10 purifications C) in both Rpn8 and Rpn10 purifications.

The 26S proteasome interactome independent of stress conditions

We identified 45 interaction partners of Rpn8 and Rpn10 that were present in all conditions studied here (Figure 5C). These proteins thus interacted with our bait independent of stress. Obviously, the majority of these proteins are constitutive proteasome subunits, such as the seven alpha and beta subunits of the 20S core particle. Additionally, all described 19S RP base complex constitutive subunits were identified, *i.e.* Rpt1-6 and the three non-ATPases Rpn1, Rpn2 and Rpn13, as well as all constitutive subunits of the 19S RP lid complex, Rpn3, Rpn5-9, Rpn11 and Rpn12. In conclusion, all constitutive 26S proteasome subunits were copurified through the enrichment of Rpn8 and Rpn10 in S2 cell lysates (Figure 4; Suppl. Table 1), suggesting that intact 26S proteasomes were present in all lysates. This result also validates our approach for the robust and reproducible isolation of 26S proteasomes from cell lysates.

In addition to all constitutive proteasome subunits, this data set comprises twelve additional common interactors of the 26S proteasome, some of which are known interactors that have been described in the literature. For instance, the deubiquitinating enzymes UCHL5 and USP14 were significantly enriched in all Rpn8 and Rpn10 IPs (Figure 4; Suppl. Table 1). We also identified Sem1/Rpn15, a known proteasome subunit in mammalian cells. It has been shown that Sem1 enforces incorporation of Rpn3 and Rpn7 into the assembling 26S proteasome lid complexes (Tomko & Hochstrasser 2014). However, it also functions as a stoichiometric component of the 19S RP of mature proteasomes (Bohn et al. 2013; Funakoshi 2004; Sone et al. 2004), where it has been proposed to be the third identified ubiquitin receptor of the proteasome which, unlike Rpn10 and Rpn13, interacts with ubiquitin via an unstructured ubiquitin binding site (Paraskevopoulos et al. 2014). CG12096, the *Drosophila* homolog of human S5b/PSMD5 and of yeast Hsm3, was also identified as an interaction partner in all Rpn8 and Rpn10 IPs. Hsm3 is a chaperone and supports 19S base assembly (Le Tallec et al. 2009; Barrault et al. 2012) through association with Rpt1, Rpt2 and Rpn1 (Kaneko et al. 2009). Another proteasome chaperone, CG11885, the *Drosophila* homolog of proteasome assembly chaperone 3 (PAC3), was enriched as associating factor of the proteasome in all IPs. Additionally, we identified the proteasome inhibitor Ecm29 homolog as proteasome interactor in all α -Rpn8 and α -Rpn10 IPs. Binding of Ecm29 to the proteasome induces a closed conformation of the 20S substrate entry channel and Ecm29 inhibits proteasomal ATPase activity (De La Mota-Peynado et al. 2013). Ecm29 has been proposed to couple the 26S proteasome to secretory compartments engaged in quality control and to other sites of enhanced proteolysis (endosomes, ER, ERGIC) (Gorbea et al. 2004; Gorbea et al. 2010). Ecm29 also plays a role in 26S proteasome dissociation following oxidative stress (Wang et al. 2011; Haratake et al. 2016). Furthermore, Rpt3R and Rpt6R, AAA-ATPases related to respectively Rpt3 and Rpt6, were identified as proteasome interactors in all IPs. A protein of unknown function, CG13319, was enriched in all IPs. This protein was previously found to colocalize with the proteasome in *Drosophila melanogaster* (Guruharsha et al. 2011). In addition, we identified Thioredoxin-like (TxI), the *Drosophila*

homolog of human TXNL1/TRP32, as putative interactor of Rpn8 and Rpn10. Txnl1 associates with the 19S RP directly via Rpn11 and exhibits thioredoxin activity (Andersen et al. 2009). Thioredoxins are disulfide-containing proteins that regulate the redox status of the cell and play a role in diverse oxidative cellular processes. Txl targets eEF1A1 *in vivo* (Andersen et al. 2009), which transfers misfolded nascent proteins from the ribosome to the 26S proteasome for degradation (Chuang et al. 2005). This suggests that Txl plays a role in proteasome-mediated degradation of misfolded proteins. Furthermore, ttm50 (human TIMM50/ yeast Tim50) was found to be a proteasome interactor under all conditions. Ttm50 is a member of the inner membrane translocase TIM23 complex and was picked up in a yeast two hybrid screen as an interaction partner of Prosalpha 6 (Giot et al. 2003), but a functional link between the proteasome and ttm50 has not been established yet. Finally, we identified tousled-like kinase (TLK) as a putative interaction partner of Rpn8 and Rpn10. Tlk plays a role in cell cycle progression through the regulation of chromatin dynamics (Carrera et al. 2003; Pilyugin et al. 2009). To our knowledge, the interaction of tlk with the proteasome has not been described before.

Concluding, we identified all known constitutive proteasome subunits in all purification conditions, which indicates that intact 26S proteasomes were indeed purified. Additional interactors were also identified in all purifications, some of which are well known proteasome interactors, such as UCHL5, USP14, Sem1, Ecm29 homolog and Thioredoxin-like, while several others had not been described before. These might be interesting targets for further studies.

Identification of Proteasome Interacting Proteins (PIPs) in untreated S2 cells

On top of the 45 common proteasome constituents and interaction partners identified in all IPs, 10 additional proteins were purified with both Rpn8 and Rpn10 under non-stress conditions (Suppl. Table 1). Six of these were copurified exclusively under non-stress conditions. This group comprises the phosphatase PP2A 55 kDa regulatory subunit twins (tws) Twins/tws, CG30185/Gr59f (unknown function), CG40042 (human TIMM23/yeast Tim23) (mitochondrial inner membrane translocase), Rad23, Dpck and CG13887/BCAP31.

Rad23 was copurified with Rpn10 in all conditions, although it only precipitated with both Rpn8 and Rpn10 under non-stress conditions. This suggests that Rad23 interacts with the proteasome complex only under non-stress conditions. Rad23 is known to interact with the proteasome and facilitates substrate degradation by substrate shuttling (Chen and Madura, 2002). Rad23 contains a Ubiquitin-like (UBL) domain, by which it interacts with Rpn10 (Hiyama et al. 1999; Walters et al. 2002), Rpn13 (Husnjak et al. 2008) and Rpn1 (Elsasser et al. 2002). Furthermore, it contains ubiquitin-associated (UBA) motifs that could bind specifically to K48 polyubiquitin chains and hence stimulates the interaction of K48-polyubiquitin linked substrates with the proteasome (Nathan et al. 2013). Interestingly, Rad23 is an essential component of the ERAD pathway (Medicherla et al. 2004) and functions downstream of Cdc48, which translocates misfolded or

otherwise aberrant proteins from the ER to the cytoplasm for proteasome-mediated protein degradation (Jarosch et al. 2002; Richly et al. 2005). CG13887 (human/mouse BCAP31 or BAP31), one of the most abundant ER proteins, was also identified as proteasome interactor under non-stress conditions. BCAP31 functions as a chaperone protein and targets misfolded proteins for ER-associated degradation (ERAD) (Wakana et al. 2008).

In conclusion, we identified several proteasome interactors specifically under normal, non-stress conditions, such as the proteasome substrate shuttle Rad23. Several other interacting proteins with Rpn8 or Rpn10 of diverse functions were identified.

Identification of PIPs upon proteasome inhibition by MG132/Lact

Besides the 45 common interactors described above, 22 additional proteins were copurified with Rpn8 and Rpn10 upon proteasome inhibition by MG132/Lact treatment. 16 of these interacted exclusively with the proteasome upon inhibition, including hsp23 and hsp68, REG (PA28), ref(2)p, cactus, zetaCOP, Syb, CG9306, RpS15Ab, Cisd2, DAD1, CG7375, CG12321/PAC2, CG2046 and finally CG7546 (Suppl. Table 1). Several of these proteins are known to play important roles in the UPS. For instance, CG12321 (human PSMG2/PAC2), a chaperone with a role in 20S proteasome core assembly, binds together with PSMG1 to proteasome subunits PSMA5 (*Drosophila* Prosalpha5) and PSMA7 (*Drosophila* Prosalpha4) and promotes the assembly of the proteasome alpha subunits into the heteroheptameric alpha ring and prevents alpha ring dimerization. The proteasome activator REG (REG γ / PA28 γ , human PSME3) is another interactor and is a member of the 11S/REG/PA28 family of proteins which can activate the catalytic function of the 20S proteasome (Rechsteiner & Hill 2005). The 11S proteasome activator (REG or PA28) is a heptameric structure consisting of REG α and REG β subunits in the cytoplasm and REG γ subunits in the nucleus. These entities markedly activate the peptidase activities of the 20S proteasome but do not promote degradation of intact proteins in general (Chu-Ping, Clive A. Slaughter, et al. 1992), although it has been shown to be able to degrade several intact proteins like the steroid receptor coactivator SRC-3 (Li et al. 2006), the HCV core protein (Moriishi et al. 2007) and the cell cycle regulators p21 (Chen et al. 2007) and p53 (Zhang & Zhang 2008). Furthermore, Refractory to Sigma P (Ref(2)p), the *Drosophila melanogaster* homolog of mammalian p62, was found to associate with the proteasome exclusively upon inhibition. P62 functions as a shuttle for ubiquitinated proteins (Pankiv et al. 2007) with a preference for Lys63 ubiquitination and consequently primarily targets proteins for autophagy. However, it also interacts with Lys48 polyubiquitin chains and can thus also shuttle proteins for proteasomal degradation (Seibenhener & Babu 2004). UBL-domain containing protein CG7546 is another factor that associated exclusively with the proteasome upon MG132/Lact treatment. Homologous UBL-domains are found in the *Xenopus leavis* and human Scythe/Bat3 proteins, and Scythe was shown to interact with a specific splice variant of Rpn10 in *Xenopus* proteasomes (Kikukawa et al. 2005).

Interestingly, the heat shock proteins, Hsp23 and Hsp68 also associate with the proteasome upon proteasome inhibition. The heat shock protein family is a highly conserved protein family which accounts for 1–2% of the total protein pool. Although not all functions of HSPs are clear, most of them function as molecular chaperones to assist in folding of newly synthesized, misfolded and damaged proteins and as such are part of a major quality control system. In Chapter 3 of this thesis, we have described a major upregulation of many Hsp's upon proteasome inhibition. These results suggest that at least some of these physically interact with the proteasome either directly or via the substrate.

Other proteins that exclusively interacted with the proteasome upon MG132/Lact treatment in our screen include mitochondrial membrane protein CG1458 (human CISD2) and the 40S ribosomal protein S15Ab, which is a structural constituent of the ribosome. Also, Cactus (human NFkB1A), a protein that acts as a negative regulator of the NF-kappa-B signaling pathway was co-precipitated in Rpn8 and Rpn10 IPs upon proteasome inhibition. Additionally, CG7375 (human Ube2M/NEDD8-conjugating enzyme Ubc12), a NEDD8 conjugating enzyme which is, together with E3 ubiquitin ligase RBX1, involved in cell proliferation via neddylation of cullins, were enriched with Rpn8 and Rpn10 upon MG132/Lact treatment. Further research is required in order to address the role of many of these interactions with the proteasome.

Proteasome activator PI31 interacts specifically with the 19S/26 proteasome upon stress induction.

The proteasome activator PI31 associated with the proteasome in all applied stress conditions and in non-stress conditions it co-precipitated only with Rpn10. PI31 is the *Drosophila* homolog of human PSMF1 and was originally identified and characterized as an *in vitro* inhibitor of the 20S proteasome activity (Chu-Ping, Clive A Slaughter, et al. 1992; Bader et al. 2011; Mccutchen-Maloney et al. 2000). Additionally, via interaction with the 20S core particle, PI31 can inhibit the assembly of both 26S proteasomes and PA28 proteasomes by blocking interaction with 19S subunits and, respectively, 11S subunits *in vitro* (Zaiss et al. 1999; Mccutchen-Maloney et al. 2000). Interestingly, in contrast to the inhibitory effect on the 20S proteasome, PI31 has also been found to enhance the activity of 26S proteasomes both *in vitro* and *in vivo* (Bader et al. 2011). PI31 can act as a selective modulator of the proteasome-dependent steps in MHC class I antigen processing and can interfere with the maturation of immunoproteasome precursor complexes (Zaiss et al. 2002). More research is required in order to determine the role of PI31 at the 26S proteasome in more detail, especially in relation with cellular stress conditions.

Identification of PIPs upon ER-stress or oxidative stress

Only a subset of proteasome interacting proteins copurified specifically upon ER stress or oxidative stress, e.g. Tspo, a translocator protein located in the outer mitochondrial membrane. Superoxide dismutase (Sod2), an antioxidant protein which can protect the cell against excessive reactive oxygen species, was only identified under TM-induced ER stress conditions. On the

other hand, four proteins interacted specifically with Rpn8 and Rpn10 upon short oxidative stress exposure, *i.e.* AP-1sigma, ATPsynG, CG9662 and CG30159. AP-1sigma is involved in vesicle mediated transport. ATPsynG is involved in ATP synthesis coupled proton transport. CG9662 plays a role in translocating proteins across the rough ER membrane, while CG30159 is a protein with yet unknown function. Further research is required in order to address the role of these interactions with the proteasome.

Identification of dynamic proteasome interacting proteins by label free quantification

Next, we applied label free quantitative (LFQ) mass spectrometry to investigate the dynamics of the proteasome interactome by characterizing differential recruitment of interactors between mock-treated samples and stress-treated samples. Figure 6 shows an overview of the results; the numbers of proteins that were specifically enriched for are listed in Table 2, while a more detailed table can be found online (Suppl. Table 2). Here, we focused solely on proteins which were differentially recruited as a result of the perturbation, while the proteasome IP's under non-stress conditions were treated as controls. Only proteins that were already identified as specific proteasome interactors in the previously described analysis were accepted (grey rows in Table 2).

The abundance of several proteasome subunits was clearly affected upon stress (Figure 6, Table 3). Upon MG132/Lact treatment larger amounts of 20S core proteasome subunits were copurified, which might be the result of the inhibition of 26S proteasome dissociation by the binding of the chemical proteasome inhibitors (Kleijnen et al. 2007). Several studies report dissociation of 19S and 20S subunits following oxidative stress (Wang et al. 2011; Reinheckel et al. 1998; Haratake et al. 2016). We therefore used relatively mild conditions (1mM H₂O₂) which did not lead to dissociation and is in agreement with other studies (Wang et al. 2011; Reinheckel et al. 1998). We like to mention again that Figure 1 shows that we obtained a proper stress response upon H₂O₂ treatment.

UCHL5 was identified as a specific interactor in all purifications, but by assessing the dynamic interactome we clearly see an enhanced recruitment of this enzyme under all applied stress conditions as compared to non-stress conditions. In contrast, another deubiquitinase, USP14, was associated with the proteasome to a lesser extent as a result of H₂O₂ and TM treatment. Furthermore, the 19S subunits Rpn8, Rpn9, Rpn11, Rpn12 and Rpn13 were enriched in one or two of the applied stress conditions. However, it should be noted that the variation between the different samples is relatively small. Upon MG132/Lact treatment, several more interacting proteins were increasingly enriched compared to non-stress conditions, such as proteasome assembly chaperone CG12321/PAC2, proteasome inhibitor ECM29 homolog, proteasome activator REG, Hsp70, Hsp23 and Hsp68, ref(2)P, zetaCOP (involved in endosomal trafficking) and the ER-membrane protein DAD1. Finally, several proteins became less enriched upon the imposed cellular stress, such as Apoptosis Inducing Factor (AIF), Cisd2 and tws.

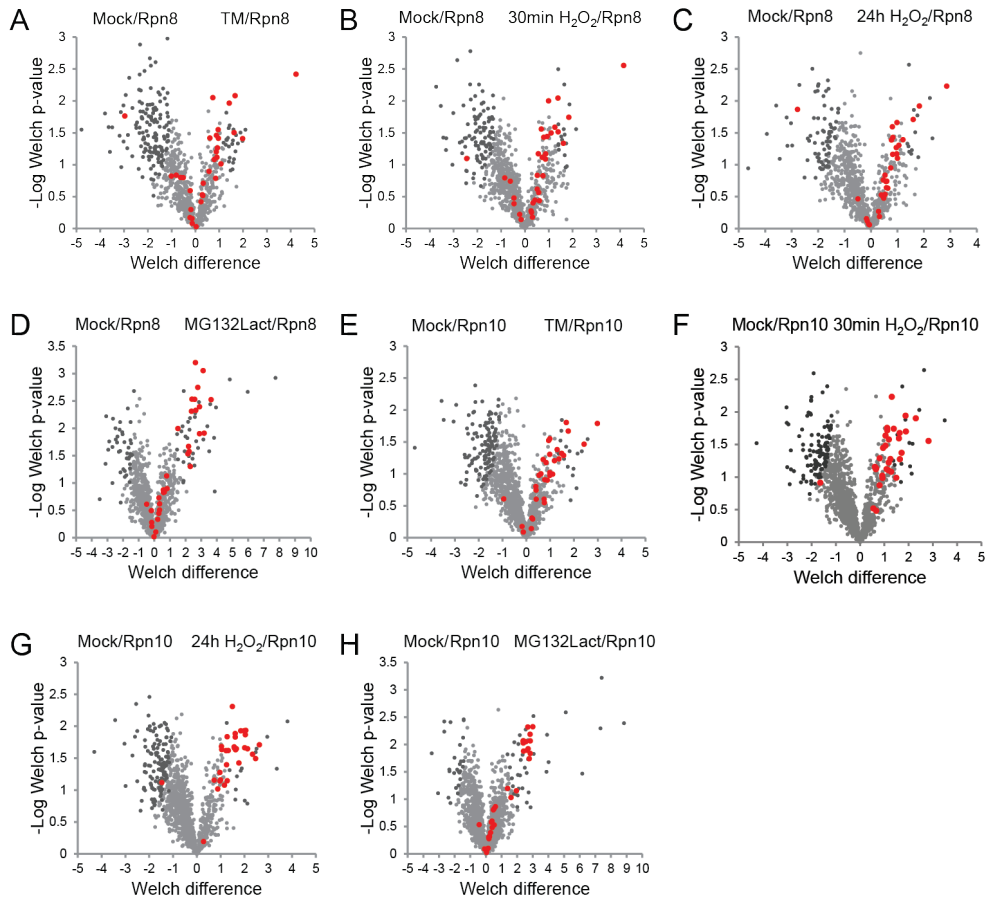


Figure 6. Identification of differential and specific interactors for each stress condition. Volcano plots based on Welch's t-tests performed on log₂-transformed LFQ intensity values of proteins identified and quantified in mock-treated cells versus stress-treated cells. Rpn8 was used as the bait in panels A-D; the treatments were A) TM, B) 30 min H₂O₂, C) 24 h H₂O₂ and D) MG132/Lact. Rpn10 was used as the bait in panels E-H the treatments were E) TM, F) 30 min H₂O₂, G) 24 h H₂O₂ and H) Mg132/Lact. Proteins which were significantly more enriched are shown in black. Proteasome subunits are shown in red.

Table 2. Numbers of recruited interactors in stress conditions. Numbers of significantly enriched proteins in stress-treated lysates are shown in the table. Numbers of proteins which were significantly enriched in both Rpn8 and Rpn10 IPs and additionally were identified as specific proteasome interactors in the previously described analysis (Suppl. Table 1) are shown in the grey colored rows. These proteins were selected for further investigation.

Immuno purification	Side volcano plot	MG132/Lact	TM	30min H ₂ O ₂	24h H ₂ O ₂
Rpn8 IP	Left	41	139	101	76
Rpn10 IP	Left	27	121	111	133
Rpn8 & Rpn10 IP	Left	4	39	32	24
Rpn8 IP & Rpn10 IP – PPI & Mock	Left	0	2	1	1
Rpn8 IP	Right	52	30	22	15
Rpn10 IP	Right	51	25	24	35
Rpn8 IP & Rpn10 IP	Right	28	7	5	4
Rpn8 IP & Rpn10 IP – PPI & Mock	Right	28	3	4	4

UCHL5 was identified as a specific interactor in all purifications, but by assessing the dynamic interactome we clearly see an enhanced recruitment of this enzyme under all applied stress conditions as compared to non-stress conditions. In contrast, another deubiquitinase, USP14, was associated with the proteasome to a lesser extent as a result of H₂O₂ and TM treatment. Furthermore, the 19S subunits Rpn8, Rpn9, Rpn11, Rpn12 and Rpn13 were enriched in one or two of the applied stress conditions. However, it should be noted that the variation between the different samples is relatively small. Upon MG132/Lact treatment, several more interacting proteins were increasingly enriched compared to non-stress conditions, such as proteasome assembly chaperone CG12321/PAC2, proteasome inhibitor ECM29 homolog, proteasome activator REG, Hsp70, Hsp23 and Hsp68, ref(2)P, zetaCOP (involved in endosomal trafficking) and the ER-membrane protein DAD1. Finally, several proteins became less enriched upon the imposed cellular stress, such as Apoptosis Inducing Factor (AIF), Cisd2 and tws.

Table 3. Log2 transformed LFQ intensities and significantly enriched proteins (+) in α -Rpn8 and α -Rpn10 IPs under cellular stress conditions

												More abundant on proteasome w. stress				More abundant on proteasome w/o stress			
ProtiD	Protein names											MG132/Lact	TM	30min H2O2	24h H2O2	MG132/Lact	TM	30min H2O2	24h H2O2
		Mock_Rpn8	MG132_Rpn8	TM_rpn8	H2O2 30 min_rpn8	H2O2 24h_rpn8	Mock Rpn10	MG132 Rpn10	TM Rpn10	H2O2 30 min Rpn10	H2O2 24h Rpn10								
E1JG29	Prosalpha1	30	32	29	29	30	31	33	31	31	32	+							
P40301	Prosalpha2	30	32	29	29	29	30	33	31	31	32	+							
P18053	Prosalpha3	29	32	29	28	29	30	33	30	31	32	+							
P22769	Prosalpha4	29	32	29	29	30	30	33	30	32	32	+							
Q95083	Prosalpha5	29	31	28	29	28	30	32	30	31	31	+							
P12881	Prosalpha6	28	32	28	29	29	30	33	31	31	32	+							
Q9V5C6	Prosalpha7	29	31	29	28	29	30	33	31	31	32	+							
A0AQH0	Prosbeta1	29	31	29	29	29	29	32	30	31	32	+							
Q9VUJ1	Prosbeta2	29	31	29	29	29	30	32	30	31	32	+							
Q9XYN7	Prosbeta3	28	31	28	29	29	29	32	30	30	31	+							
Q9VJJ0	Prosbeta4	29	31	28	29	29	29	32	30	31	32	+							
Q7K148	Prosbeta5	29	31	28	28	28	29	32	30	30	31	+							
P40304	Prosbeta6	29	31	28	29	29	30	33	30	31	31	+							
Q9VNA5	Prosbeta7	28	31	28	28	28	29	32	30	30	31	+							
Q7KMQ0	Rpt1	33	34	34	34	34	34	34	35	35	35								
P48601	Rpt2	33	34	34	34	34	34	34	34	35	34								
Q9V405	Rpt3	34	34	35	35	34	34	35	35	35	35								
Q9W414	Rpt4	33	34	34	34	34	34	34	35	35	35								
Q9V3V6	Rpt5	33	33	34	34	34	33	34	34	34	34								
O18413	Rpt6	34	34	34	34	34	34	34	34	35	35								
Q9VW54	Rpn1	35	35	35	36	36	35	35	36	36	36								
Q9V3P6-2	Rpn2	35	36	36	36	36	35	35	36	36	37								
M9PG62	Rpn3	34	34	35	35	35	34	34	35	35	35					+			
Q9V3Z4	Rpn5	34	34	35	35	35	34	34	35	35	35					+			
Q7KLV9	Rpn6	34	34	35	35	35	34	34	35	35	35								
Q9V3G7	Rpn7	34	34	35	35	35	33	34	35	35	35								
P26270	Rpn8	33	34	35	34	35	33	34	34	35	35					+			
Q7KMP8	Rpn9	33	34	35	35	35	33	34	34	35	35					+			
M9PIG8	Rpn10	32	33	33	33	33	33	33	35	35	35								
Q9V3H2	Rpn11	33	33	35	35	34	33	33	35	34	34		+	+					
Q9V436	Rpn12	33	33	35	34	35	33	33	34	34	35			+	+				
Q7K2G1-2	Rpn13	33	34	34	34	34	33	34	34	34	35		+	+					
Q9XZ61	UCHL5	29	32	33	33	31	30	32	33	33	33	+	+	+	+				
Q9VKZ8	USP14	27	26	24	24	24	28	28	27	26	26								+
Q9V677	ECM29 homolog, CG8858	30	32	29	29	29	30	32	30	30	31	+							
P02825	Hsp70Aa	27	30	29	29	29	29	31	29	30	29	+							
M9NE68	Hsp23	24	27	22	23	23	22	28	21	22	22	+							
O97125	Hsp68	22	27	23	24	24	24	27	24	25	25	+							
Q9V3P3	REG	27	30	27	27	27	26	31	26	26	25	+							
P14199	Protein ref(2)P	22	26	20	22	21	24	28	23	24	23	+							
Q8IQP2	zetaCOP	22	24	21	22	21	24	26	23	23	23	+							
Q9VLM5	DAD1	22	26	23	23	21	25	28	25	25	24	+							
Q9VEC2	CG12321	20	27	20	20	20	22	29	22	22	24	+							
Q9VQ79	AIF	23	23	21	22	21	24	24	22	23	23						+		
Q9VAM6	Cisd2	25	26	23	24	24	26	27	25	25	26						+		
P36872	twc	26	24	22	22	23	26	25	25	24	26							+	

In conclusion, using LFQ proteomics we observed the dynamic interaction of proteasome subunits and proteasome-interacting proteins that was dependent on cellular stress. We purified more 26S proteasomes upon proteasome inhibition. Interestingly, co-purification of UCHL5 was enhanced upon stress induction, while USP14 was less efficiently enriched, suggesting distinct roles for these DUBs. Other proteins that became increasingly enriched upon MG132/Lact treatment include the proteasome inhibitor ECM29, heat shock proteins, the proteasome activator REG and Ref(2)p. Recruitment of these factors to the proteasome under stress conditions may indicate that the UPS interfaces with diverse cellular processes.

Discussion

19S/26S interactome (in)dependent of stress conditions

Using both α -Rpn8 and α -Rpn10 antibodies we have immunopurified 19S particles and intact 26S proteasomes from cell lysates to study both the interactome as well as the dynamic interactome of the 19S particle under both stress and non-stress conditions. All constitutive proteasome subunits were identified independent of the used conditions. Besides these constitutive subunits, a variety of additional interactors were identified in all purifications, including several chaperones with a role in proteasome (dis)assembly, activators and inhibitors and UCHL5, USP14, Sem1, ECM29 homolog and Thioredoxin-like. Identification of these 26S proteasome constitutive subunits and well-known interactors in all purifications validates our approach to specifically enrich 19S as well as 26S proteasomes from S2 cell lysates.

Our data give novel insights into proteasome composition dynamics upon non-stress and stress conditions. For instance, Ub shuttle protein Rad23 was identified as a proteasome interactor under non-stress conditions. But under stress conditions only the interaction with Rpn10 was maintained, while interaction with Rpn8 was lost, suggesting that Rad23 interacts with free Rpn10 outside the proteasome complex under stress conditions. This observation raises several questions. For instance, it is unclear why Rad23 is only enriched for the 26S proteasome under non-stress conditions and what the function of a Rpn10-Rad23 complex outside the 26S proteasome would be. It was shown before that free Rpn10 inhibits the interaction of Ub shuttle protein Dsk2 and the proteasome in budding yeast (Matiuhin et al. 2008). In this way free Rpn10 could be used to regulate the delivery of ubiquitinated substrates to the proteasome via shuttle protein Dsk2 (Matiuhin et al. 2008). Our data might point in a similar direction: free Rpn10 may also inhibit the interaction of Rad23 with the proteasome, but then only under stress conditions. Obviously, additional experiments are required to elucidate the mechanism behind the interplay of ubiquitin receptor Rpn10 and the shuttle factor Rad23 in both stress and non-stress conditions.

Refractory to Sigma P (Ref(2)p)/human p62 was identified as an interactor of the proteasome upon MG132/Lact mediated inhibition. We have shown before that the pharmacological inhibition of the proteasome increased Ref(2)p expression levels (Sap et al. 2017) and it is also known that Ref(2)p interacts with Rpt1 (Seibenhener & Babu 2004; Geetha et al. 2008) and that it serves as a substrate shuttling factor for proteasomal degradation (Geetha et al. 2008). Our data suggest that the interaction of Ref(2)p with the 26S proteasome is dependent on the inhibition status of the proteasome. However it should be excluded whether we identified more Ref(2)p as a result of MG132/Lact-induced increased 26S proteasome stability.

In addition, we observed specific physical interactions of stress responsive proteins (Hsp's) upon proteasome inhibition and oxidative stress. Hsp's function as chaperones that mediate proper folding of substrate proteins with non-native conformations, thereby protecting substrates from aggregation. Chaperones are also involved in proteasome-dependent degradation of misfolded proteins. Hsp70s are among the most prominent chaperone families that assist in chaperone-mediated proteasomal degradation of misfolded proteins (Kettern et al. 2010; Arndt et al. 2007). They can improve recognition of the substrate by ubiquitin ligases and shuttle them to the proteasome once they are ubiquitinated. Additionally, HSP70 is also involved in dissociation of 26S proteasome complexes into free 20S particles and bound 19S regulators and in reconstitution of 26S proteasomes shortly after mild oxidative stress (Grune et al. 2011). We immunopurified 19S particles and our data clearly shows that we enriched for 26S proteasomes but also 19S alone. It might be possible that Hsp70 which we identified in our screen is the interacting chaperone of free 19S particles. Finally, chaperones are also able to affect proteasome activity. It has been shown that Hsp27 interacts directly with the 26S proteasome and with polyubiquitin, and that overexpression of Hsp27 increases the activity of the proteasome upon stress induction by inflammatory cytokines and cytotoxic drugs (Parcellier et al. 2003). Our data suggest that chaperones also play a role in proteasome-dependent degradation upon treatment with chemical proteasome inhibitors, however here as well it should be excluded whether we precipitated more heat shock proteins as a result of increased proteasome levels due to proteasome inhibition.

CG7546, a protein of yet unknown function, was found to interact with the proteasome exclusively upon cytotoxic stress induction. Its homolog in *Xenopus*, Scythe, interacts with a splice variant of Rpn10 (Kikukawa et al. 2005). CG7546 bears furthermore structural similarity to Bag6, who's N-terminal UBL domain suggests involvement in protein degradation (Minami et al. 2010). Bag6 is known to interact with pro-apoptotic proteins and targets them to Rpn10 for subsequent proteasome-dependent degradation (Kikukawa et al. 2005). Thus, CG7546 might be a novel shuttle factor involved in targeting substrates to the proteasome.

Proteasome activator PI31 was specifically interacting with the proteasome in all tested stress conditions, in non-stress conditions it only interacted with Rpn10. The molecular mechanism by which PI31 affects proteasome activity remains unknown. A previous study showed that PI31

can increase the activity of the 26S proteasome *in vivo* under conditions where maximal proteolytic activity is required, for instance for the removal of cellular proteins during the terminal differentiation of sperm (Bader et al. 2011). Similarly, PI31 activity might also be beneficial for boosting the degradation of rapidly and highly elevated proteasome substrate loads during cellular stresses in our experiments.

Dynamic 19S/26S interactome during stress and non-stress conditions

The abundance of several purified proteasome subunits was clearly affected upon stress (Figure 6, Table 3). More intact 26S proteasomes were enriched upon proteasome inhibition, which might be the result of decreased proteasome disassembly through the use of proteasome inhibitors (Kleijnen et al. 2007). We furthermore used relatively mild oxidative stress conditions since the 26S proteasome is relatively sensitive for this type of stress (Reinheckel et al. 1998; Reinheckel et al. 2000). Therefore, we did not observe enhanced dissociation of 19S and 20S particles following H_2O_2 treatment, which is in agreement with other studies (Reinheckel et al. 1998; Wang et al. 2011).

Interestingly, we observed an enhanced interaction of deubiquitinating enzyme UCHL5 with the proteasome under stress conditions. In general, the role of UCHL5 at the proteasome has not been clearly defined yet and could be multifaceted and for now we could only speculate about the role of UCHL5 at the proteasome during stress. It has for instance been proposed that UCHL5 performs an editing function by removing distal ubiquitin moieties from polyubiquitin chains and that this might be a method by which inadequately targeted proteins can be released from the proteasome and spared from degradation (Lam et al. 1997). Since UCHL5 is recruited and activated by Rpn13, the editing function of UCHL5 might be specific for Rpn13 targeted substrates, which might be important during stress conditions. Alternatively, UCHL5 could play a role in the deubiquitination of proteasome subunits. At least four proteasome subunits are targets for regulatory ubiquitination: Rpn10, Rpn13, UCHL5 and Rpt5 (Jacobson et al. 2014). Ubiquitination of these proteasome subunits impairs substrate binding, deubiquitination and degradation. The ubiquitination of these proteasome subunits is also influenced by certain cellular stress (Jacobson et al. 2014). For instance, the ubiquitination of all four proteasome subunits was found to be decreased upon H_2O_2 and MG132 treatment (Jacobson et al. 2014). Our results may indicate that decreased proteasome ubiquitination under stress conditions could be the result of increased UCHL5 recruitment and, thus, an increased deubiquitinating activity. Another possibility is that UCHL5 breaks down unanchored polyubiquitin chains that bind to proteasome-associated ubiquitin receptors and thereby block substrate access (Zhang et al. 2011). This process could be useful under stress conditions, when the proteasome substrate load is increased. It should be noted that UCHL5 is also present outside the proteasome, albeit in a non-active form as part of the chromatin remodeling INO80 complex (Yao et al. 2008), but we did not pick up any of the INO80 complex subunits as interactors in our screen.

Upon MG132/Lact treatment, several interacting proteins were increasingly enriched compared to non-stress conditions, such as proteasome assembly chaperone CG12321/PAC2, proteasome inhibitor ECM29 homolog, proteasome activator REG, Hsp70, Hsp23 and Hsp68, ref(2)P, zetaCOP (involved in endosomal trafficking) and the ER-membrane protein DAD1. We however also found an enrichment of intact 26S proteasomes upon MG132/Lact treatment. Therefore, it should be determined whether enhanced enrichment of interacting partners was due to enhanced recruitment or due to enhanced 26S proteasome levels.

Concluding remarks

Although we did several interesting findings as described above, in general we did not observe many specific effects for each individual stress that we applied. This might be explained in several ways. First, there is a lot of cross talk between the induced regulatory pathways and cellular responses inflicted by the different stress conditions. For instance, proteasome inhibition (Obeng et al. 2006; Lee et al. 2003), ER stress (Oslowski & Urano 2013) and oxidative stress (Kupsco & Schlenk 2015) may all induce the unfolded protein response (UPR). Furthermore, proteasome inhibition may lead to ER stress due a diminished removal of damaged and misfolded proteins (Bush et al. 1997). Additionally, proteasome inhibition may induce oxidative stress (Fribley et al. 2004), but an opposite effect is also observed in some cell types (Yamamoto et al. 2007). Cross-talk between the different stress conditions makes it difficult to distinguish specific responses for each individual condition. Second, in this study we used LFQ-based quantitative proteomics in combination with immune purifications (IPs) to study the differential recruitment of proteasome interactors. IPs are primarily suitable to identify stable interactors. Techniques which might be applied in order to pick up more transient interactors are BioID (Varnaite & MacNeill 2016) and APEX (Kim & Roux 2016), this might however give more background/false positive hits. Thirdly, in this study we focused on enrichment of 19S caps, however, changes might also be found in other proteasome caps, such as PA28 $\alpha\beta$, PA28 γ , PA200, PI31, or in solely the standard 20S proteasome or the immunoproteasome. These different proteasome complexes could be separated from each other by fractionation on glycerol gradients followed by LC-MS/MS and protein correlation profiling (Fabre et al. 2015). Fourth, proteasome activity may also be regulated at the level of post translational modifications (PTMs). For instance, it has been demonstrated that ubiquitination of Rpn10, Rpn13, UCHL5 and Rpt5 impairs substrate binding, deubiquitination and degradation (Jacobson et al. 2014). In fact, more than 345 sites at the proteasome can be modified and 11 different modifications were identified, reviewed in (Hirano et al. 2015). Thus, differential modification of proteasome subunits with and without stress might also contribute to altered proteasome regulation.

Finally, our data show that the combination of classical immune purifications with LFQ-based quantitative proteomics is a powerful approach to specifically detect (sub)stoichiometric interaction partners, as well as dynamic interactors, of a large and important cellular machinery. We identified several proteasome interactors, which responded differently upon stress

conditions, such as UCHL5, Rad23, CG7546 and Ref(2)p. Further research is required to elucidate their function in proteasome-dependent degradation in conditions with and without stress. Differential proteasome interactors upon specific stressors may act as therapeutic targets for the treatment of diseases in which cellular stress and homeostasis misbalance play a role.

Material and Methods

Cell culture. *Drosophila melanogaster* Schneider's line 2 cells (S2 cells) (R690-07, Invitrogen) were cultured in Schneider's medium (Invitrogen) supplemented with 10% fetal calf serum (Thermo) and 1% Penicillin-Streptomycin. Cells were treated for 16h with 50 μ M MG132 and 5 μ M Lactacystin (MG132/Lact), or for 24h with 1 μ M TM (Sigma), or for 30 min or 24h with 1mM H₂O₂ (Invitrogen). For H₂O₂ treatments, cells were incubated in serum free medium and directly exposed to H₂O₂. After 30 min H₂O₂ was quenched with catalase and two volumes of complete medium was added. Cells were harvested directly (30 min) or after 24h.

Antibodies. Polyclonal antibodies were generated by immunizing rabbits with GST fusion proteins expressed in *Escherichia coli* and were affinity purified as described previously (Chalkley & Verrijzer 2004). The full length Rpn8 and full length Rpn10 were used as antigens. Pre-immune serum (PPI) of Rpn10 immunized rabbit was used. SDS-PAGE and Immunoblotting experiments were performed as described previously (Chalkley et al. 2008).

RNA isolation and real time RT-qPCR. For gene expression assays, cell pellets were immediately frozen in liquid nitrogen and -80°C until further processing. Total RNA was extracted from 5x10⁶ cells using Trizol (15596-026, Invitrogen) and 4 μ g RNA was used for random hexamer primed cDNA synthesis using the Superscript II Reverse Transcriptase (Invitrogen). Quantitative real-time RT-PCR was performed on a CFX96 realtime PCR detection system (Bio-Rad). Reactions were performed in a total volume of 25 μ l containing 1x reaction buffer, SYBR Green I (Sigma), 200 μ M dNTPs, 1.5 mM MgCl₂, platinum Taq polymerase (Invitrogen), 500 nM of corresponding primers and 1 μ l of cDNA. The primer sequences used were GsdD5: 5'-TATGCCAACGCCAAGAAGGT-3', 5'-CGGCACCTTTCCAGTTCTCT-3'; Hsp70: 5'-AAGAACCTCAAGGGTGAGCG-3', 5'-CGTCGATGGTCAGGATGGAG-3'; Hsp68: 5'-AGCAACAGAAATAGCCAAGATGC-3', 5'-GTGTGGTACGGTTACCCTGG-3'; DLP: 5'-CTAGCAGCTCGGGATCACTG-3', 5'-TCGCTCTCGGCTTTTGTGAA-3'; CaBP1: 5'-TGTTGCTGGCATTGTGTCGTG-3', 5'-ATCGCTGGGCGAATAGAAGG-3'. Data analysis was performed by applying the 2- $\Delta\Delta$ CT method (Livak & Schmittgen 2001). Values obtained from amplification of α -Mannosidase class I b (CG11874) were used to normalize the data as described previously (Moshkin et al. 2007).

Glycerol gradient. Preparation of glycerol gradients is previously described (Mohrmann et al. 2004). Briefly, gradients with 5% - 30% glycerol were made in Beckman polyallomer tubes (331374 Beckman). Whole cell lysates were made under non-denaturing conditions (50 mM HEPES-KOH pH 7.6, 100 mM KCl, 0.1% NP40, protease inhibitors), loaded on top of the gradient and ultracentrifuged (SW40 rotor, Beckman L-80) with 32 krpm for 17h by 4°C. Approximately 26 x 500 µl fractions were taken starting from the top of the gradient with a P1000 pipet. Fractions were stored in aliquots in -80°C. Two consecutive fractions were combined starting from fraction 3, which resulted in a total of 13 fractions. Of each fraction, 25 µl was resolved by SDS-PAGE and visualized by immunoblotting.

Immuno purifications. Immunopurification (IP) procedures were performed essentially as described (Chalkley & Verrijzer 2004). Briefly, α -Rpn8 or α -Rpn10 antibody was crosslinked to ProtA beads (GE Healthcare) by using dimethylpimelimidate. As a control, antibodies from pre-immune serum were coupled to ProtA beads. After 2 h incubation of the antibody coupled beads with whole cell lysate (125×10^6 cells), the beads were washed extensively with HEMG-based washing buffer (25mM HEPES-KOH, pH 7.6, 0.1mM EDTA, 12.5mM MgCl₂, 10% glycerol, 200mM KCl, 0.1% NP-40, containing a cocktail of protease inhibitors). Proteins retained on the beads were eluted with 100mM sodium citrate buffer (pH 2.5), TCA precipitated, resolved by SDS-PAGE and visualized by Coomassie staining. Lanes were cut in 1 mm slices and combined to in total 13 fractions per lane and analyzed by LC-MS/MS.

Mass spectrometry. In-gel protein reduction, alkylation and tryptic digestion was done as described previously (van den Berg et al. 2010). Peptides were extracted with 30% acetonitrile 0.5% formic acid and analyzed on an 1100 series capillary LC system (Agilent Technologies) coupled to an LTQ-Orbitrap hybrid mass spectrometer (Thermo). Peptide mixtures were trapped on a ReproSil C18 reversed phase column (Dr Maisch GmbH; column dimensions 2 cm × 100 µm, packed in-house) at a flow rate of 8 µl/min. Peptide separation was performed on a ReproSil C18 reversed phase column (Dr Maisch GmbH; column dimensions 15 cm × 75 µm, packed in-house) using a linear gradient from 0 to 50% B (A = 0.1% formic acid; B = 80% (v/v) acetonitrile, 0.1% formic acid) in 120 min at a constant flow rate of 300 nl/min (using a splitter for the 1100 system). The column eluent was directly electrosprayed into the mass spectrometer. Mass spectra were acquired in continuum mode; fragmentation of the peptides was performed in data dependent acquisition mode by CID using top 8 selection.

LFQ data analysis. RAW files were analyzed using MaxQuant software (v1.5.1.2 | <http://www.maxquant.org>), which includes the Andromeda search algorithm (Jurgen Cox et al. 2011) for searching against the Uniprot database (version November 2014, taxonomy: *Drosophila melanogaster* | <http://www.uniprot.org/>). Follow-up data analysis was performed using the Perseus analysis framework (<http://www.perseus-framework.org/>).

Perseus (version 1.4.1.3) was used to analyze protein abundance dynamics in the different samples. ProteinGroups file was uploaded to Perseus. Rows containing proteins designated ‘Only identified by site’, ‘Reverse’ and ‘Contaminant’ were removed from the matrix. LFQ intensities were log-transformed (log2). LFQ Intensity columns of triplicates of Rpn8 and Rpn10 IPs were grouped. Rows which did not contain at least two valid values in at least one group were removed from the matrix. Next, columns were grouped similarly as just mentioned however now also the PPI triplicate was grouped.

To identify proteasome interacting proteins, Welch two-sided t-tests were performed for each α -Rpn8 or α -Rpn10 IP versus the α -PPI IPs. First groups (right) were the LFQ intensities of Rpn8 or Rpn10 IPs, second groups (left) were the LFQ intensities of PPI IPs. Permutation-based FDR of 0.05 was used for truncation. Number of randomizations was 250. $-\log_{10}$ scale. Annotations were added to the tables. Tables containing the significant proteins for each two-sample t-tests were exported to excel. R was used to merge the tables for the α -Rpn8 or α -Rpn10 comparisons with α -PPI IPs based on the common ‘id’ columns. Rows containing significant proteins in α -Rpn8 and α -Rpn10 comparisons were merged using R and table was used to describe proteasome interacting proteins.

To identify dynamic proteasome interacting proteins, Welch two-sided t-tests were performed for each α -Rpn8 + stress or α -Rpn10+stress IP versus the Mock α -Rpn8 or α -Rpn10 IPs (thus excluding the PPI samples). First groups (right) were the LFQ intensities of either α -Rpn8+stress or α -Rpn10+stress IPs, second groups (left) were either the LFQ intensities of α -Rpn8 Mock IPs or α -Rpn10 mock IPs. Permutation-based FDR of 0.05 was used for truncation. Number of randomizations was 250. $-\log_{10}$ scale. Annotations were added to the tables. Tables containing the significant proteins for each two-sample t-test were exported to excel. R was used to merge the tables for the α -Rpn8+stress or α -Rpn10+stress comparisons with mock IPs based on the common ‘id’ columns. Rows containing significant proteins in α -Rpn8 and α -Rpn10 comparisons were merged using R and table was used to describe dynamic proteasome interacting proteins.

References

- Andersen, K.M. et al., 2009. Thioredoxin Txn1/TRP32 Is a Redox-active Cofactor of the 26 S Proteasome. *Journal of Biological Chemistry*, 284(22), 15246–15254.
- Arndt, V., Rogon, C. & Höhfeld, J., 2007. To be, or not to be - Molecular chaperones in protein degradation. *Cellular and Molecular Life Sciences*, 64(19–20), pp.2525–2541.
- Bader, M. et al., 2011. A conserved F box regulatory complex controls proteasome activity in Drosophila. *Cell*, 145(3), pp.371–382.
- Barrault, M.-B. et al., 2012. Dual functions of the Hsm3 protein in chaperoning and scaffolding

- regulatory particle subunits during the proteasome assembly. *Proceedings of the National Academy of Sciences of the United States of America*, 109(17), pp.E1001-10.
- van den Berg, D.L.C. et al., 2010. An Oct4-Centered Protein Interaction Network in Embryonic Stem Cells. *Cell Stem Cell*, 6(4), pp.369–381.
- Bohn, S. et al., 2013. Localization of the regulatory particle subunit Sem1 in the 26S proteasome. *Biochemical and Biophysical Research Communications*, 435(2), pp.250–254.
- Brand, M.D., 2010. The sites and topology of mitochondrial superoxide production. *Exp Gerontol.*, 45(7-8): 466–472.
- Breusing, N. & Grune, T., 2008. Regulation of proteasome-mediated protein degradation during oxidative stress and aging Introduction: protein degradation and the proteasome. *Biol. Chem.*, 389, pp.203–209.
- Brewer, J.W. et al., 1999. Mammalian unfolded protein response inhibits cyclin D1 translation and cell-cycle progression. *Proceedings of the National Academy of Sciences of the United States of America*, 96(15), pp.8505–10.
- Bull, V.H. & Thiede, B., 2012. Proteome analysis of tunicamycin-induced ER stress. *Electrophoresis*, 33(12), pp.1814–23.
- Bush, K.T., Goldberg, A.L. & Nigam, S.K., 1997. Proteasome Inhibition Leads to a Heat-shock Response, Induction of Endoplasmic Reticulum Chaperones, and Thermotolerance. *The Journal of biological chemistry*, 272(14), pp.9086–9092.
- Carrera, P. et al., 2003. Tousled-like kinase functions with the chromatin assembly pathway regulating nuclear divisions. *Genes and Development*, 17(20), pp.2578–2590.
- Chalkley, G.E. et al., 2008. The Transcriptional Coactivator SAMP Is a Trithorax Group Signature Subunit of the PBAP Chromatin Remodeling Complex. *Molecular and Cellular Biology*, 28(9), pp.2920–2929.
- Chalkley, G. E. and Verrijzer, C. P. (2004) 'Immuno-Depletion and Purification Strategies to Study Chromatin-Remodeling Factors In Vitro', *Methods in Enzymology*, 377(2001), pp. 421–442.
- Chen, L. and Madura, K. (2002) 'Rad23 Promotes the Targeting of Proteolytic Substrates to the Proteasome', *molecular and cellular biology*, 22(13), pp. 4902–4913
- Chen, X. et al., 2007. Ubiquitin-Independent Degradation of Cell-Cycle Inhibitors by the REG γ Proteasome. *Molecular Cell*, 26(6), pp.843–852.
- Chow, C.Y., Wolfner, M.F. & Clark, A.G., 2013. Using natural variation in *Drosophila* to discover previously unknown endoplasmic reticulum stress genes. *Proceedings of the National Academy of Sciences of the United States of America*, 110(22), pp.9013–8.
- Chu-Ping, M., Slaughter, C.A. & DeMartino, G.N., 1992. Identification, purification, and characterization of a protein activator (PA28) of the 20 S proteasome (macropain). *Journal of Biological Chemistry*, 267(15), pp.10515–10523.
- Chuang, S.-M. et al., 2005. Proteasome-mediated degradation of cotranslationally damaged proteins involves translation elongation factor 1A. *Molecular and cellular biology*, 25(1), pp.403–13.
- Elsasser, S. et al., 2002. Proteasome subunit Rpn1 binds ubiquitin-like protein domains. *Nature Cell Biology*, 4(9), pp.725–730.
- Elsasser, S. & Finley, D., 2005. Delivery of ubiquitinated substrates to protein-unfolding machines. *nature cell biology*, 7(8). Pp. 742-749
- Fabre, B. et al., 2015. Deciphering preferential interactions within supramolecular protein complexes: the proteasome case. *Molecular systems biology*, 11, p.771.
- Finley, D., 2009. Recognition and Processing of Ubiquitin-Protein Conjugates by the Proteasome. *Annual review of biochemistry*, pp. 477–513
- Fransen, M. et al., 2012. Role of peroxisomes in ROS/RNS-metabolism: Implications for human disease. *Biochimica et Biophysica Acta - Molecular Basis of Disease*, 1822(9), pp.1363–1373.
- Fribley, A., Zeng, Q. & Wang, C., 2004. Proteasome Inhibitor PS-341 Induces Apoptosis

through Induction of Endoplasmic Reticulum Stress-Reactive Oxygen Species in Head and Neck Squamous Cell Carcinoma Cells. *Society*, 24(22), pp.9695–9704.

Funakoshi, M., 2004. Sem1, the yeast ortholog of a human BRCA2-binding protein, is a component of the proteasome regulatory particle that enhances proteasome stability. *Journal of Cell Science*, 117(26), 6447–6454.

Geetha, T. et al., 2008. p62 serves as a shuttling factor for TrkA interaction with the proteasome. *Biochemical and Biophysical Research Communications*, 374(1), pp.33–37.

Giot, L. et al., 2003. A protein interaction map of *Drosophila melanogaster*. *Science* (New York, N.Y.), 302(5651), pp.1727–36.

Glickman, M.H. et al., 1998. The regulatory particle of the *Saccharomyces cerevisiae* proteasome. *Molecular and cellular biology*, 18(6), pp.3149–3162.

Goldberg, A.L., 2003. Protein degradation and protection against misfolded or damaged proteins. *Nature*, 426, pp.895–899.

Gorbea, C. et al., 2010. A Protein Interaction Network for Ecm29 Links the 26 S Proteasome to Molecular Motors and Endosomal Components. *Journal of Biological Chemistry*, 285(41), 31616–31633

Gorbea, C. et al., 2004. Characterization of mammalian Ecm29, a 26 S proteasome-associated protein that localizes to the nucleus and membrane vesicles. *Journal of Biological Chemistry*, 279(52), pp.54849–54861.

Groll, M. et al., 1997. Structure of 20S proteasome from yeast at 2.4 Å resolution. *Nature*, 386(6624), pp.463–471.

Grune, T. et al., 2011. HSP70 mediates dissociation and reassociation of the 26S proteasome during adaptation to oxidative stress. *Free Radical Biology and Medicine*, 51(7), pp.1355–1364.

Guerrero, C., 2005. An Integrated Mass Spectrometry-based Proteomic Approach: Quantitative Analysis of Tandem Affinity-purified

in vivo Cross-linked Protein Complexes (qtax) to Decipher the 26 s Proteasome-interacting Network. *Molecular & Cellular Proteomics*, 5(2), pp.366–378.

Guruharsha, K.G. et al., 2011. A Protein Complex Network of *Drosophila melanogaster*. *CELL*, 147, pp.690–703.

Hanna, J. et al., 2007. A Ubiquitin Stress Response Induces Altered Proteasome Composition. *Cell*, 129(4), pp.747–759.

Haratake, K. et al., 2016. KIAA0368 -deficiency affects disassembly of 26S proteasome under oxidative stress condition. *Journal of Biochemistry*, 159(6), pp.609–618.

Harding, H.P., Zhang, Y. & Ron, D., 1999. Protein translation and folding are coupled by an endoplasmic-reticulum-resident kinase. *Nature*, 397(6716), pp.271–274.

Hirano, H., Kimura, Y. & Kimura, A., 2015. Biological significance of co- and post-translational modifications of the yeast 26S proteasome. *Journal of Proteomics*, 134, pp.37–46.

Hiyama, H. et al., 1999. Interaction of hHR23 with S5a. The Ubiquitin-Like Domain Of Hhr23 Mediates Interaction With S5a Subunit Of 26 S Proteasome*. *The Journal of biological chemistry*, 274(39), pp.28019–28025.

Ho Min Kim, Yadong Yu, and Y.C., 2008. Structure characterization of the 26S proteasome. *Biochim Biophys Acta*, 141(4), pp.520–529.

Holmström, K.M. & Finkel, T., 2014. Cellular mechanisms and physiological consequences of redox-dependent signalling. *Nature reviews. Molecular cell biology*, 15(6), pp.411–21.

Husnjak, K. et al., 2008. Proteasome subunit Rpn13 is a novel ubiquitin receptor. *Nature*, 453(7194), pp.481–488.

Jacobson, A.D. et al., 2014. Autoregulation of the 26S proteasome by in situ ubiquitination. *Molecular biology of the cell*, 25(12), pp.1824–35

Jarosch, E. et al., 2002. Protein dislocation from the ER requires polyubiquitination and the AAA-ATPase Cdc48. *Nature Cell Biology*, 4.

- Jung, T. & Grune, T., 2008. The proteasome and its role in the degradation of oxidized proteins. *IUBMB Life*, 60(11), pp.743–752.
- Kaake, R.M. et al., 2011. Characterization of Cell Cycle Specific Protein Interaction Networks of the Yeast 26S Proteasome Complex by the QTAX Strategy. *J Proteome Res.* 72(2), pp.181–204.
- Kaneko, T. et al., 2009. Assembly Pathway of the Mammalian Proteasome Base Subcomplex Is Mediated by Multiple Specific Chaperones. *Cell*, 137(5), pp.914–925.
- Kettern, N. et al., 2010. Chaperone-assisted degradation: Multiple paths to destruction. *Biological Chemistry*, 391(5), pp.481–489.
- Kikukawa, Y. et al., 2005. Unique proteasome subunit Xrpn 10c is a specific receptor for the antiapoptotic ubiquitin-like protein Scythe. *FEBS Journal*, 272(24), pp.6373–6386.
- Kim, D.I. & Roux, K.J., 2016. Filling the Void: Proximity-Based Labeling of Proteins in Living Cells. *Trends in Cell Biology*, 26(11), pp.804–817.
- Kleijnen, M.F. et al., 2007. Stability of the proteasome can be regulated allosterically through engagement of its proteolytic active sites. *Nature structural & molecular biology*, 14(12), pp.1180–8.
- Kupsco, A. & Schlenk, D., 2015. Oxidative Stress, Unfolded Protein Response, and Apoptosis in Developmental Toxicity. *International Review of Cell and Molecular Biology*, 317, pp.1–66.
- De La Mota-Peynado, A. et al., 2013. The proteasome-associated protein Ecm29 inhibits proteasomal ATPase activity and in vivo protein degradation by the proteasome. *Journal of Biological Chemistry*, 288(41), pp.29467–29481.
- Lam, Y.A. et al., 1997. Editing of ubiquitin conjugates by an isopeptidase in the 26S proteasome. *Nature*, 385, pp.737–740.
- Lee, A.-H. et al., 2003. Proteasome inhibitors disrupt the unfolded protein response in myeloma cells. *Proceedings of the National Academy of Sciences of the United States of America*, 100(17), pp.9946–51.
- Leggett, D.S. et al., 2002. Multiple Associated Proteins Regulate Proteasome Structure and Function. *Molecular Cell*, 10(3), pp. 495–507
- Li, X. et al., 2006. The SRC-3/AIB1 coactivator is degraded in a ubiquitin- and ATP-independent manner by the REG?? proteasome. *Cell*, 124(2), pp.381–392.
- Livak, K.J. & Schmittgen, T.D., 2001. Analysis of relative gene expression data using real-time quantitative PCR and the 2(-Delta Delta C(T)) Method. *Methods (San Diego, Calif.)*, 25(4), pp.402–8.
- Loidl, G. et al., 1999. Bifunctional inhibitors of the trypsin-like activity of eukaryotic proteasomes. *Chemistry and Biology*, 6(4), pp.197–204.
- Marques, A.J. et al., 2009. Catalytic mechanism and assembly of the proteasome. *Chemical Reviews*, 109(4), pp.1509–1536.
- Matiuhin, Y. et al., 2008. Extraproteasomal Rpn10 Restricts Access of the Polyubiquitin-Binding Protein Dsk2 to Proteasome. *Molecular Cell*, 32(3), pp.415–425.
- Mccutchen-Maloney, S.L. et al., 2000. cDNA Cloning, Expression, and Functional Characterization of PI31, a Proline-rich Inhibitor of the Proteasome*. *Journal of Biological Chemistry*, 275(24), 18557–18565
- Medicherla, B. et al., 2004. A genomic screen identifies Dsk2p and Rad23p as essential components of ER-associated degradation. *EMBO reports*, 5(7), pp.692–697.
- Meister, S. et al., 2007. Extensive Immunoglobulin Production Sensitizes Myeloma Cells for Proteasome Inhibition. *Cancer Res*, 67(4), pp.1783–92.
- Minami, R. et al., 2010. BAG-6 is essential for selective elimination of defective proteasomal substrates. *Journal of Cell Biology*, 190(4), pp.637–650.
- MJ Gething, J. & Sambrook, 1992. Protein folding in the cell. *Nature*, 355, pp.242–244.
- Mohrmann, L. et al., 2004. Differential targeting of two distinct SWI/SNF-related Drosophila

chromatin-remodeling complexes. *Molecular and cellular biology*, 24(8), pp.3077–88.

Mori, K., 2000. Tripartite Management Minireview of Unfolded Proteins in the Endoplasmic Reticulum. *Cell*, 101, pp.451–454.

Moriishi, K. et al., 2007. Critical role of {PA28gamma} in hepatitis C virus-associated steatogenesis and hepatocarcinogenesis. *Proceedings of the National Academy of Sciences of the United States of America*, 104(5), pp.1661–1666.

Moshkin, Y.M. et al., 2007. Functional Differentiation of SWI/SNF Remodelers in Transcription and Cell Cycle Control. *Molecular and Cellular Biology*, 27(2), pp.651–661.

Murata, S., Yashiroda, H. & Tanaka, K., 2009. Molecular mechanisms of proteasome assembly. *Nature reviews. Molecular cell biology*, 10(2), pp.104–115.

Nathan, J.A. et al., 2013. Why do cellular proteins linked to K63-polyubiquitin chains not associate with proteasomes? *The EMBO journal*, 32(4), pp.552–65.

Obeng, E.A. et al., 2006. Proteasome inhibitors induce a terminal unfolded protein response in multiple myeloma cells. *Blood*, 107(12), pp.4907–4916.

Osowski, C.M. & Urano, F., 2013. Measuring ER stress and the unfolded protein response using mammalian tissue culture system. *Methods in Enzymology*, 490(508), pp.71–92.

Pankiv, S. et al., 2007. p62/SQSTM1 binds directly to Atg8/LC3 to facilitate degradation of ubiquitinated protein aggregates by autophagy*[S]. *Journal of Biological Chemistry*, 282(33), pp.24131–24145.

Paraskevopoulos, K. et al., 2014. Dss1 is a 26S proteasome ubiquitin receptor. *Molecular Cell*, 56(3), pp.453–461.

Parcellier, A. et al., 2003. HSP27 is a ubiquitin-binding protein involved in I-kappaBalpha proteasomal degradation. *Molecular and cellular biology*, 23(16), pp.5790–5802.

Pickart, C.M. & Cohen, R.E., 2004. Proteasomes and their kin: proteases in the machine age. *Nature reviews. Molecular cell biology*, 5(3), pp.177–187.

Pickering, A.M. & Davies, K.J.A., 2012. Differential roles of proteasome and immunoproteasome regulators Pa28αβ, Pa28γ and Pa200 in the degradation of oxidized proteins. *Archives of Biochemistry and Biophysics*, 523(2), pp.181–190.

Pilyugin, M. et al., 2009. Phosphorylation-mediated control of histone chaperone ASF1 levels by tousel-like kinases. *PLoS ONE*, 4(12), pp.1–6.

Raynes, R., Pomatto, L.C.D. & Davies, K.J.A., 2016. Degradation of oxidized proteins by the proteasome: Distinguishing between the 20S, 26S, and immunoproteasome proteolytic pathways. *Molecular Aspects of Medicine*, pp.1–15.

Rechsteiner, M. & Hill, C.P., 2005. Mobilizing the proteolytic machine: Cell biological roles of proteasome activators and inhibitors. *Trends in Cell Biology*, 15(1), pp.27–33.

Reinheckel, T. et al., 1998. Comparative resistance of the 20S and 26S proteasome to oxidative stress. *The Biochemical journal*, 335, pp.637–42.

Reinheckel, T. et al., 2000. Differential impairment of 20S and 26S proteasome activities in human hematopoietic K562 cells during oxidative stress. *Archives of biochemistry and biophysics*, 377(1), pp.65–8.

Ri, M. (2016). Endoplasmic-reticulum stress pathway-associated mechanisms of action of proteasome inhibitors in multiple myeloma. *International Journal of Hematology*, 104, 273

Richly, H. et al., 2005. A series of ubiquitin binding factors connects CDC48/p97 to substrate multiubiquitylation and proteasomal targeting. *Cell*, 120(1), pp.73–84.

Sap, K.A. et al., 2015. Global quantitative proteomics reveals novel factors in the ecdysone signaling pathway in *Drosophila melanogaster*. *Proteomics*, 15(4), pp.725–738.

Sap, K.A. et al., 2017. Quantitative Proteomics Reveals Extensive Changes in the Ubiquitinome

- after Perturbation of the Proteasome by Targeted dsRNA-Mediated Subunit Knockdown in *Drosophila*. *Journal of Proteome Research*, 16(8), pp.2848–2862.
- Scanlon, T.C. et al., 2009. Isolation of human proteasomes and putative proteasome-interacting proteins using a novel affinity chromatography method. *Experimental Cell Research*, 315(2), pp.176–189.
- Schieber, M and Chandel, N.S., 2014. ROS Function in Redox Signaling and Oxidative Stress. *Curr Biol.*, 24(10), 453–462.
- Schmidt, M. et al., 2005. Proteasome-associated proteins: Regulation of a proteolytic machine. *Biological Chemistry*, 386(8), pp.725–737.
- Seibenhener, M. & Babu, J., 2004. Sequestosome 1 / p62 Is a Polyubiquitin Chain Binding Protein Involved in Ubiquitin Proteasome Degradation. *Molecular and Cellular Biology*, 24(18), pp.8055–8068.
- Sone, T. et al., 2004. Sem1p Is a Novel Subunit of the 26 S Proteasome from *Saccharomyces cerevisiae*. *Journal of Biological Chemistry*, 279(27), 28807–28816.
- Le Tallec, B. et al., 2009. Hsm3/S5b Participates in the Assembly Pathway of the 19S Regulatory Particle of the Proteasome. *Molecular Cell*, 33(3), pp.389–399.
- Tomko, R.J. & Hochstrasser, M., 2014. The Intrinsically Disordered Sem1 Protein Functions as a Molecular Tether during Proteasome Lid Biogenesis. *Molecular Cell*, 53(3), pp.433–443.
- Tong, L. et al., 2015. Reactive oxygen species in redox cancer therapy. *Cancer Letters*, 367, pp.18–25.
- Jurgen Cox, J. et al., 2011. Andromeda: A Peptide Search Engine Integrated into the MaxQuant Environment. *J. Proteome Res*, 10, pp.1794–1805.
- Varnaite, R. & MacNeill, S.A., 2016. Meet the neighbors: Mapping local protein interactomes by proximity-dependent labeling with BioID. *Proteomics*, 16(19), pp.2503–2518.
- Verma, R. et al., 2004. Multiubiquitin chain receptors define a layer of substrate selectivity in the ubiquitin-proteasome system. *Cell*, 118(1), pp.99–110.
- Verma, R. et al., 2000. Proteasomal proteomics: identification of nucleotide-sensitive proteasome-interacting proteins by mass spectrometric analysis of affinity-purified proteasomes. *Molecular biology of the cell*, 11(10), pp.3425–3439.
- Verma, R. et al., 2002. Role of Rpn11 Metalloprotease in Deubiquitination and Degradation by the 26S Proteasome. *Science*, 298(5593), pp.611–615.
- Voges, D., Zwickl, P. & Baumeister, W., 1999. The 26S proteasome: a molecular machine designed for controlled proteolysis. *Annual review of biochemistry*, 68(1), pp.1015–68.
- Wakana, Y. et al., 2008. Bap31 Is an Itinerant Protein That Moves between the Peripheral Endoplasmic Reticulum (ER) and a Juxtanuclear Compartment Related to ER-associated Degradation. *Molecular biology of the cell*, 19, pp.1825–1836.
- Walters, K.J. et al., 2002. Structural studies of the interaction between ubiquitin family proteins and proteasome subunit S5a. *Biochemistry*, 41(6), pp.1767–1777.
- Wang, S. & Kaufman, R.J., 2012. The impact of the unfolded protein response on human disease. *Journal of Cell Biology*, 197(7), pp.857–867.
- Wang, X. et al., 2007. Mass spectrometric characterization of the affinity-purified human 26S proteasome complex. *Biochemistry*, 46(11), pp.3553–3565.
- Wang, X. & Huang, L., 2008. Identifying dynamic interactors of protein complexes by quantitative mass spectrometry. *Molecular & cellular proteomics. MCP*, 7(1), pp.46–57.
- Wang, X.Y.J., Kaiser, P. & Huang, L., 2011. Regulation of the 26S proteasome complex during oxidative stress. *Sci Signal*, 3(151), pp.1–17.
- Yamamoto, N. et al., 2007. Proteasome inhibition induces glutathione synthesis and protects cells from oxidative stress: Relevance to Parkinson disease. *Journal of Biological Chemistry*, 282(7), pp.4364–4372.

Yao, T. et al., 2008. Distinct Modes of Regulation of the Uch37 Deubiquitinating Enzyme in the Proteasome and in the Ino80 Chromatin-Remodeling Complex. *Molecular Cell*, 31(6), pp.909–917.

Zaiss, D.M.W. et al., 2002. PI31 is a modulator of proteasome formation and antigen processing. *Proceedings of the National Academy of Sciences of the United States of America*, 99(22), pp.14344–9.

Zaiss, D.M.W. et al., 1999. The proteasome inhibitor PI31 competes with PA28 for binding to

20S proteasomes. *FEBS Letters*, 457(3), pp.333–338.

Zhang, N.Y. et al., 2011. Ubiquitin chain trimming recycles the substrate binding sites of the 26 S proteasome and promotes degradation of lysine 48-linked polyubiquitin conjugates. *Journal of Biological Chemistry*, 286(29), pp.25540–25546.

Zhang, Z. & Zhang, R., 2008. Proteasome activator PA28c regulates p53 by enhancing its MDM2-mediated degradation. *The EMBO Journal*, 27(25), pp.852–864.

Supporting information available in this thesis

Supplementary Table S1. Proteasome co-precipitating factors

Supplementary Table S2. Dynamic proteasome co-precipitating factors

Suppl. Table1. Average LFQ intensities and significant abundant proteins in α -Rpn8 and α -Rpn10 IPs

Protein IDs	Mock_PPI	Mock_Rpn8	MG132_Rpn8	TM_24h_Rpn8	H2O2_30m_Rpn8	H2O2_24h_Rpn8	Mock_PPI	Mock_Rpn10	MG132_Rpn10	TM_24h_Rpn10	H2O2_30m_Rpn10	H2O2_24h_Rpn10	Gene names	Protein names	Description	Mock	MG132/Lact	TM	30min H2O2	24h H2O2
Q9XZJ4	28	30	32	29	29	30	28	31	33	31	31	31	32	Prosalpha1	Proteasome subunit	+	+	+	+	+
P40301	25	30	32	29	29	29	26	30	33	31	31	31	32	Prosalpha2	Proteasome subunit	+	+	+	+	+
P18053	26	29	32	29	28	29	27	30	33	30	31	32	Pros25	Prosalpha3	Proteasome subunit	+	+	+	+	+
P22769	25	29	32	29	29	30	26	30	33	30	32	32	Pros28.1	Prosalpha4	Proteasome subunit	+	+	+	+	+
Q95083	24	29	31	28	29	28	25	30	32	30	31	31	Prosalpha5	Prosalpha5	Proteasome subunit	+	+	+	+	+
P12881	24	28	32	28	29	29	25	30	33	31	31	32	Pros35	Prosalpha6	Proteasome subunit	+	+	+	+	+
Q9V5C6	23	29	31	29	28	29	24	30	33	31	31	32	Prosalpha7	Prosalpha7	Proteasome subunit	+	+	+	+	+
A0AQH0	23	29	31	29	29	24	29	32	30	31	32	Prosbeta1	Prosbeta1	Proteasome subunit	+	+	+	+	+	
Q9VUJ1	23	29	31	29	29	24	30	32	30	31	32	Prosbeta2	Prosbeta2	Proteasome subunit	+	+	+	+	+	
Q9XVY7	24	28	31	28	29	29	24	29	32	30	30	31	Prosbeta3	Prosbeta3	Proteasome subunit	+	+	+	+	+
Q9VLJ0	22	29	31	28	29	29	22	29	32	30	31	32	Prosbeta4	Prosbeta4	Proteasome subunit	+	+	+	+	+
Q7K148	24	29	31	28	28	28	25	29	32	30	30	31	Prosbeta5	Prosbeta5	Proteasome subunit	+	+	+	+	+
P40304	25	29	31	28	29	26	30	33	30	31	31	32	Prosbeta6	Prosbeta6	Proteasome subunit	+	+	+	+	+
Q9VNA5	23	28	31	28	28	24	29	32	30	30	31	32	Prosbeta7	Prosbeta7	Proteasome subunit	+	+	+	+	+
Q7KMQ0	29	33	34	34	34	30	34	34	35	35	35	35	Rpt1	Rpt1	Proteasome subunit	+	+	+	+	+
P48601	29	33	34	34	34	30	34	34	35	35	34	35	Pros26.4	Rpt2	Proteasome subunit	+	+	+	+	+
Q9V405	30	34	35	35	34	30	34	35	35	35	35	35	Rpt3	Rpt3	Proteasome subunit	+	+	+	+	+
Q9W414	29	33	34	34	34	29	34	34	35	35	35	35	Rpt4	Rpt4	Proteasome subunit	+	+	+	+	+
Q9V3V6	29	33	33	34	34	30	34	33	34	34	34	34	Tbp-1	Rpt5	Proteasome subunit	+	+	+	+	+
O18413	30	34	34	34	34	30	34	34	35	35	35	35	Pros45	Rpt6	Proteasome subunit	+	+	+	+	+
Q9VW54	31	35	35	35	36	36	31	35	35	36	36	36	Rpn1	Rpn1	Proteasome subunit	+	+	+	+	+
Q9V3P6	31	35	36	36	36	31	35	35	36	36	37	Rpn2	Rpn2	Proteasome subunit	+	+	+	+	+	
P25161	29	34	34	35	35	35	29	34	34	35	35	35	Rpn3	Rpn3	Proteasome subunit	+	+	+	+	+
Q9V3Z4	28	34	34	35	35	35	29	34	34	35	35	35	Rpn5	Rpn5	Proteasome subunit	+	+	+	+	+
Q9V32A	28	34	34	35	35	35	29	34	34	35	35	35	Rpn6	Rpn6	Proteasome subunit	+	+	+	+	+
Q7KLV9	28	34	34	35	35	35	29	34	34	35	35	35	Rpn7	Rpn7	Proteasome subunit	+	+	+	+	+
Q9V3G7	29	34	34	35	35	35	29	33	34	35	35	35	Rpn8	Rpn8	Proteasome subunit	+	+	+	+	+
P26270	28	33	34	35	35	35	29	33	34	34	35	35	Mov34	Rpn9	Proteasome subunit	+	+	+	+	+
Q7KMP8	27	33	34	35	35	35	28	33	34	35	35	35	Rpn9	Rpn9	Proteasome subunit	+	+	+	+	+
P55035	27	32	33	33	33	33	28	33	33	35	35	35	Pros54	Rpn10	Proteasome subunit	+	+	+	+	+
Q9V3H2	27	33	33	35	35	34	28	33	33	35	34	34	Rpn11	Rpn11	Proteasome subunit	+	+	+	+	+
Q9V436	28	33	33	35	34	35	28	33	33	34	35	35	Rpn12	Rpn12	Proteasome subunit	+	+	+	+	+
Q7K2G1-2	28	33	34	34	34	28	33	34	34	34	35	35	Rpn13	Rpn13	Proteasome subunit	+	+	+	+	+
Q9XZ61	25	29	32	33	33	31	26	30	32	33	33	33	UCHL5	UCHL5	Proteasome subunit	+	+	+	+	+

Suppl. Table1. Average LFQ intensities and significant abundant proteins in α -Rpn8 and α -Rpn10 IPs (continued)

Uniprot ID	Mock_Rpn8	MG132_Rpn8	TM_24h_Rpn8	H2O2_24h_Rpn8	Mock_PPI	Mock_Rpn10	MG132_Rpn10	TM_24h_Rpn10	H2O2_30m_Rpn10	H2O2_24h_Rpn10	Gene name	Protein name	Description	Mock	MG132/Lact	TM	30m H2O2	24h H2O2
Q9VKZ8	22	27	26	24	24	23	28	28	27	26	USP14	USP14	Proteasome subunit	+	+	+	+	+
Q9VH79	24	28	29	28	28	25	29	29	29	30	Rpt3R	Rpt3R	ATPase	+	+	+	+	+
Q9VA54	22	27	27	26	26	22	27	27	27	27	Rpt6R	Rpt6R	ATPase	+	+	+	+	+
Q9VM46	21	26	25	25	26	21	24	25	25	26	CG13779	sem1	Proteasome assembly chaperone, Proteasome 19S subunit	+	+	+	+	+
Q9V677	26	30	32	29	29	26	30	32	30	31	ECM29 homolog	ECM29 homolog, CG8858	Proteasome inhibition, coupling of proteasomes to ER	+	+	+	+	+
Q9VYG1	25	30	31	30	31	25	29	29	30	30	CG12096	CG12096	Proteasome assembly chaperone, probable proteasome inhibitor	+	+	+	+	+
Q9VPP7	22	26	26	24	25	23	27	28	27	28	CG11885	CG11885	Probable proteasome assembly chaperone	+	+	+	+	+
Q7JWR4	21	28	28	25	26	27	23	28	29	28	CG13319	CG13319	Colocalizes with proteasome	+	+	+	+	+
Q9VRP3	24	32	31	30	30	25	32	32	33	33	Txi	Thioredoxin-like	Protein disulfide oxidoreductase activity	+	+	+	+	+
Q9W4V8	23	26	26	26	26	24	27	26	27	27	tm50	Tiny tim 50	Component of TIM23 complex, mediates translocation of transit peptide-containing proteins across mitochondrial inner membrane	+	+	+	+	+
B7ZI20	21	23	23	23	23	23	26	27	27	26	tlk	Tousled-like kinase	Kinase, histone phosphorylation, cell cycle regulation	+	+	+	+	+
Q9VQ79-1	20	23	23	21	22	21	24	24	22	23	AIf	Isoform A of Putative apoptosis-inducing factor 1	Mitochondrial ATP synthesis coupled electron transport, Oxidoreductase, cell redox homeostasis, apoptotic process	+	+			
Q9VX82	21	23	23	##	##	23	24	26	23	23	Apc3B	Actin-related protein 2/3 complex, subunit 3B	Structural constituent of the cytoskeleton	+	+			
Q9VFS8	26	30	29	31	31	27	30	29	31	30	CG8588	26S proteasome non-ATPase regulatory subunit 9/ Rpn4	Proteasome (base) assembly chaperone, Transcriptional activator	+	+	+	+	+
Q9VZ99	23	25	24	24	25	24	23	25	26	25	CG9977	Adenosylhomocysteinase	Adenosylhomocysteinase activity	+	+	+	+	+
P36872-2	23	26	24	22	22	23	24	26	25	24	tw5	Twins	PP2A regulator activity, phosphatase, cell cycle, centrosome organization, Wnt signaling pathway	+				
Q8MKK1	24	26	25	23	24	24	25	27	26	26	CG30185; G59f	CG30185	Unknown	+				
Q8MRW1	23	25	24	22	23	24	23	25	25	24	CG40042	CG40042	Mitochondrial inner membrane translocase subunit	+				
Q9V3W9	22	24	23	23	23	23	26	26	26	26	Rad23	DNA repair protein Rad23	Tmn17/Tmn22/Tmn23/peoxisomal protein PIMP24	+				
Q9V67	21	22	20	21	22	21	22	24	22	23	Dpck	DNA repair, shuttles polyubiquitinated proteins to proteasome, interacts with Rpn10, Rpn13 and Rpn1	interacts with Rpn10, Rpn13 and Rpn1	+				
Q9W0M4	21	24	22	22	22	22	22	24	23	23	CG13887	CG13887	Coenzyme A biosynthetic process, kinase activity	+				
													Export of secreted proteins, export of transmembrane proteins, chaperone, targeting to ERAD	+				
Q9V637	22	23	24	24	24	23	22	25	26	27	CG8979	Proteasome inhibitor P81 subunit	Inhibits the hydrolysis of protein and peptide substrates by the 20S proteasome. Enhances 26S proteasome function by promoting its assembly through the interaction with PSM29 and PMSD5.		+	+	+	+

Suppl. Table1. Average LFQ intensities and significant abundant proteins in α -Rpn8 and α -Rpn10 IPs (continued)

Uniprot ID	Mock_PPI	Mock_Rpn8	MG132_Rpn8	TM_24h_Rpn8	H2O2_30m_Rpn8	H2O2_24h_Rpn8	Mock_PPI	Mock_Rpn10	MG132_Rpn10	TM_24h_Rpn10	H2O2_30m_Rpn10	H2O2_24h_Rpn10	Gene name	Protein name	Description	Mock	MG132/Lact	TM	30m H2O2	24h H2O2
P16371-2	23	24	25	24	23	24	24	25	26	25	26	26	gro	Isoform A of Protein Groucho	Negative regulation of transcription from RNA pol II promoter, chromatin interacting protein	+	+	+	+	
Q9Y114	20	###	22	21	21	21	21	23	24	23	22	22	CG8042	CG8042	Endomembrane protein, ERAD, maintenance lipid droplet homeostasis, apoptosis	+	+			
P82910	27	27	30	29	29	29	28	29	31	29	30	29	Hsp70Aa	Major heat shock 70 kDa protein Aa	Heat shock protein, stress response	+	+	+	+	
P02516	23	24	27	22	23	23	24	22	28	21	22	22	Hsp23	Heat shock protein 23	Heat shock protein, stress response	+	+			
Q97125	24	22	27	23	24	24	25	24	27	24	25	25	Hsp68	Heat shock protein 68	Heat shock protein, stress response	+	+			
Q9V3P3	24	27	30	27	27	27	25	26	31	26	26	25	REG	LD45860p	Proteasome activator PA28, mRNA splicing via spliceosome, regulation of G1/S transition of mitotic cell cycle, DNA damage response	+	+			
P14199	23	22	26	20	22	21	25	24	28	23	24	23	ref(2)P	Protein ref(2)P	Clearance of protein aggregates, mitochondrion organization, transcription, regulation of secretion, autophagic vacuole	+	+			
M9PD65	22	23	25	23	23	23	24	25	26	24	25	24	RanGap	Ran GTPase activating protein	Regulator of Ran-dependent transport between cytoplasm and nucleus, GTPase activator for the nuclear Ras-related regulatory protein Ran	+	+			
Q03017-2	21	22	24	23	23	23	18	20	21	18	19	19	cact	Isoform C of NF-kappa B inhibitor cactus	Transcription factor binding, phagocytosis, negative regulation of protein import into nucleus, developmental protein, signal transduction	+	+			
Q9VJ69	21	22	24	21	22	21	22	24	26	23	23	23	zetaCOP	Nonclathrin coat protein zeta-COP	Oxidoreductase, phagocytosis, vesicle-mediated protein transport	+	+			
P18489-4	23	23	25	24	23	23	24	26	26	25	25	25	Syb	Isoform D of Synaptobrevin	Golgi to ER	+	+			
Q9VJZ4	22	24	25	###	23	22	24	25	26	23	24	23	CG8306	ND-B22	synaptic vesicle transport, vesicle-mediated transport	+	+			
Q7KR04	23	24	25	###	24	23	24	25	26	24	24	24	RpS15Ab	40S ribosomal protein S15Ab	NADH dehydrogenase	+	+			
Q9VAM6	24	25	26	23	24	24	25	26	27	25	25	26	Cisd2	CDGSH iron-sulfur domain-containing protein 2 homolog	Structural constituent of the ribosome, translation, mitotic spindle elongation	+	+			
Q9VLN5							24	25	28	25	25	24	DAD1	Dolichyl-phosphooligosaccharide-protein glycosyltransferase subunit DAD1	Mitochondria membrane protein, calcium transport, autophagy	+	+			
Q9VSF3	20	###	23	###	###	###	20	21	24	21	21	21	CG7375	Nedd8-conjugating enzyme subunit DAD1	Translocation of proteins into or across the rough ER membrane	+	+			
Q9VEC2	19	20	27	20	20	20	21	22	29	22	22	24	CG12321	Ubc12	Protein neddylation	+	+			
Q9VNI4	19	20	26	###	###	###	20	20	28	20	21	22	CG2046	Assembly 20S proteasome	Unknown	+	+			
Q9V583	23	23	25	24	24	23	24	25	26	26	26	26	CG7546	CG7546	UBL-domain containing protein	+	+			

Suppl. Table1. Average LFQ intensities and significant abundant proteins in α -Rpn8 and α -Rpn10 IPs (continued)

Uniprot ID	Mock_PPI	Mock_Rpn8	MG132_Rpn8	TM_24h_Rpn8	H2O2_30m_Rpn8	H2O2_24h_Rpn8	Mock_PPI	Mock_Rpn10	MG132_Rpn10	TM_24h_Rpn10	H2O2_30m_Rpn10	H2O2_24h_Rpn10	Gene name	Protein name	Description	Mock	MG132/Lact	TM	30m H2O2	24h H2O2
Q9VPR1	21	22	22	22	23	22	22	24	25	24	24	24	Tspo	Translocator protein, CG2789	Regulation of oxidative phosphorylation, positive regulation of apoptotic process, mitochondrial outer membrane protein			+	+	+
Q00637	22	21	22	23	23	23	24	25	24	26	25	25	Sod2	Superoxide dismutase [Mn], mitochondrial	Oxidation-reduction process, antioxidant activity			+		
Q9VCF4	23	23	24	23	25	23	23	24	25	25	25	23	AP-1sigma	AP-1sigma	Intracellular protein transport, vesicle-mediated transport, synaptic vesicle				+	
Q9VKM3	23	23	24	24	25	24	24	25	26	26	26	26	ATPsynG	ATP synthase, Lethal (2) 06225	ATP synthesis coupled proton transport				+	
Q9VQP9	21	22	22	##	22	22	22	24	24	23	24	22	CG8662	Putative oligosaccharyltransferase complex subunit	Translocation of proteins into or across the rough ER membrane				+	
Q7K332	22	22	22	23	23	23	23	24	24	24	25	24	CG30159	CG30159	Unknown				+	

Chapter 6

Global quantitative proteomics reveals novel factors in the ecdysone signaling pathway in *Drosophila melanogaster*

Karen A. Sap, Karel Bezstarosti, Dick H.W. Dekkers, Mirjam van den Hout, Wilfred van Ijcken, Erikjan Rijkers and Jeroen A.A. Demmers

Published in Proteomics (2015)

Abstract

The ecdysone signaling pathway plays a major role in various developmental transitions in insects. Recent advances in the understanding of ecdysone action have relied to a large extent on the application of molecular genetic tools in *Drosophila*. Here, we used a comprehensive quantitative SILAC mass spectrometry-based approach to study the global, dynamic proteome of a *Drosophila* cell line to investigate how hormonal signals are transduced into specific cellular responses. Global proteome data after ecdysone treatment after various time points were then integrated with transcriptome data. We observed a substantial overlap in terms of affected targets between the dynamic proteome and transcriptome, although there were some clear differences in timing effects. Also, downregulation of several specific mRNAs did not always correlate with downregulation of their corresponding protein counterparts and in some cases there was no correlation between transcriptome and proteome dynamics whatsoever. In addition, we performed a comprehensive interactome analysis of EcR, the major target of ecdysone. Proteins co-purified with EcR include factors involved in transcription, chromatin remodeling, ecdysone signaling, ecdysone biosynthesis and other signaling pathways. Novel ecdysone-responsive proteins identified in this study might link previously unknown proteins to the ecdysone signaling pathway and might be novel targets for developmental studies. To our knowledge, this is the first time that ecdysone signaling is studied by global quantitative proteomics.

Introduction

Drosophila melanogaster belongs to the phylum Arthropoda of the animal kingdom, which includes insects, crustaceans, mites, arachnids, scorpions and myriapods. The rigid exoskeleton of these invertebrate animals inhibits growth, so arthropods replace it periodically by molting. Insect molting hormones or ecdysteroids, such as ecdysone, are key regulators of major post-embryonic events, including the larval-to-larval molts and the larval-to-pupal metamorphic transformation (Riddiford 1993). Ecdysone is a prohormone of the major insect molting hormone 20-hydroxyecdysone (20E; hereafter simply referred to as ‘ecdysone’), which is secreted from the prothoracic glands where it is produced by the enzymatic conversion of cholesterol. The glands are stimulated to undergo steroidogenesis in discrete and periodic surges and this is reflected in peaks of the active ecdysone observed in larvae and pupae, all precisely generated by either increased rates of steroidogenesis or alternative metabolic processing (Warren et al. 2006). In the larvae, the circulating prohormone secreted by the prothoracic gland is only converted to the active hormone in target tissues (Talbot, Swyryd, and Hogness 1993).

Ecdysone is a substrate for the ecdysone receptor, which is a non-covalent heterodimer of two proteins, Ecdysone Receptor (EcR) and ultraspiracle (USP). These nuclear hormone receptor proteins are the *Drosophila* orthologs of the mammalian farnesoid receptor (FXR) and retinoid X receptor (RXR) proteins, respectively. EcR interacts with USP to bind to various ecdysone response elements (EcREs) to transactivate several target genes (Yao et al. 1993) (Figure 1). EcR and USP are the best known dimerization partners which activate ecdysone-responsive genes; however, there is more variation. The *EcR* gene itself already encodes 3 different isoforms; EcR-A, EcR-B1 and EcR-B2 (Koelle et al. 1991), which share common DNA and ligand binding domains, but differ in their N-terminal sequences, which are involved in transcriptional activation. Besides the existence of multiple isoforms of EcR, different EcR binding partners have been described. Recently, it was found that EcR can dimerize with DHR38 (Zoglowek et al. 2012). In addition, there is genetic evidence that USP is not required for the ecdysone-dependent activation of the larval glue genes (Costantino et al. 2008). The ability of nuclear receptors to form multiple, different heterodimers suggests that their role in regulatory events may be more complex than previously anticipated. Additional ecdysone-sensitive nuclear receptor proteins have yet to be elucidated though.

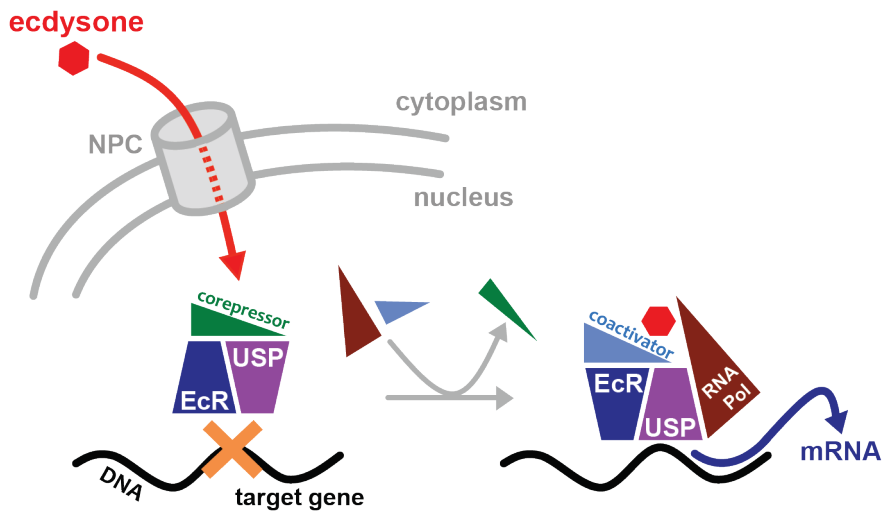


Figure 1. Simplified representation of the mode of action of ecdysone in *Drosophila*. When ecdysone enters the nucleus it binds to the heterodimer EcR/USP, which subsequently recruits coactivators and RNA Pol II to transcribe target genes.

The role of ecdysone in gene regulation was elucidated based on the identification of rapid and delayed puff induction upon hormone treatment of cultured salivary glands (Clever and Karlson 1960). Puff induction can be interpreted as local transcriptional activity and, based on the timing, early and late puffs can be identified. Later, it was experimentally shown that early puffs were directly induced by ecdysone (by Clever in *Chironomus* (Clever and Karlson 1960) and by Ashburner in *Drosophila* (Ashburner 1974) and are direct targets of the ecdysone-bound receptor, while the formation of late puffs was an indirect effect because only the latter were affected by the use of protein synthesis inhibitors. This concept is referred to as the ‘Ashburner model’ (Ashburner 1974, Ashburner 1972). Several ecdysone responsive genes have been identified; examples include *E74*, *E75* and *Broad-Complex* (*BR-C*), which encode transcription factors that, in turn, drive the expression of late genes, while downregulating the expression of early genes (Andres and Thummel 1992). The early genes have been shown, like the early puffs, to be directly and transiently induced by ecdysone (Felix D. Karim and Thummel 1991; F D Karim and Thummel 1992) and mutant analysis has demonstrated that *E74* and *BR-C* functions are essential for proper entry into metamorphosis (Fletcher et al. 1995; Kiss et al. 1988; Restifo and White 1992). Early gene *E63-1* encodes a calcium-binding protein which is closely related to calmodulin (Thummel 2002). Besides early and late genes, a class of ‘early-late’ genes was discovered (Stone and Thummel 1993). These genes require the ecdysone-bound EcR/USP heterodimer, but besides that, do also require an early gene product for optimal transcription induction. Examples of early-late genes are the nuclear receptor proteins DHR3 and DHR4, which repress the early genes *BR-C*, *E74* and *E75*. Both DHR3 and DHR4 are required for *FTZ transcription factor 1* (*ftz-ft1*) expression in mid-prepupae (King-Jones et al. 2005; Lam, Jiang, and Thummel 1997), which strongly suggests that these two factors act in concert to regulate the early genes and *ftz-ft1*. Mutant and knock-down studies have revealed additional proteins involved in ecdysone signaling, for instance WOC (without children) (Wismar et al. 2000), MLD (molding defective) (Neubueser et al. 2005) and DRE4 (Sliter and Gilbert 1992). Several genome-wide (microarray) analyses of ecdysone signaling have been published, for instance on specific *Drosophila* organs (Beckstead, Lam, and Thummel 2005). Another study revealed large differences between cultured Kc cells and salivary glands with regard to their genome-wide transcriptional response to the hormone (Gonsalves et al. 2011). Experiments with conditional mutants have suggested that separable transcriptional responses among ecdysone, the pre-hormone receptor and the post-hormone receptor occur (Davis and Li 2013). However, many aspects of especially early-late and late phases downstream of the ecdysone signaling cascade are still unknown and the roles of many previously identified ecdysone responsive factors, as well as yet unknown factors remain to be elucidated.

We are studying the regulation of *Drosophila* metamorphosis by the steroid hormone ecdysone as a model system for understanding how hormonal signals are transduced into

specific cellular responses, in particular those at the proteome level, and try to link these to developmental pathways. In this study, we used a comprehensive quantitative (SILAC) mass spectrometry-based approach to study the dynamic proteome in an attempt to identify novel proteins that respond to ecdysone stimulation in *Drosophila*. Since gene expression involves the transcription, translation and turnover of mRNAs and proteins, we have monitored how ecdysone treatment affects protein and mRNA abundances in time. This strategy provided a detailed, integrative analysis of proteome and transcriptome composition changes in response to cellular perturbations, and of the dynamic interplay of mRNA and proteins. To our knowledge, this is the first time that ecdysone signaling is studied by quantitative proteomic methods. Previous studies in *Drosophila* and several other species where mRNA and protein levels were compared to provide a quantitative description of gene expression concluded that the correlation is weak (*e.g.*, (Ghazalpour et al. 2011; Laurent et al. 2010; Maier et al. 2011; Schwanhüsser et al. 2011)). One reason for this could be that mRNA and protein levels result from complex coupled processes of synthesis and degradation. In addition, since variation of ecdysone receptor dimerization appears to be important for proper and specific regulation of ecdysone-responsive gene products during different stages of development, we used a comprehensive experimental approach for the identification of novel interactors of endogenous EcR. Novel ecdysone-responsive proteins identified in this study might link previously unknown proteins to the ecdysone signaling pathway and might be targets for further developmental studies.

Results and discussion

Proteome and transcriptome expression analysis

We set out by verifying the effect of ecdysone treatment on two different *Drosophila* cell lines, Kc and S2, by monitoring RNA expression levels of two known ecdysone responders by quantitative real-time RT-PCR. The effect on Kc cells appeared to be larger and as it was suspected that this would therefore result in larger changes at the proteome level we decided to continue all experiments with Kc cells (Suppl Figure 1; data for S2 cells not shown). Since no commercial SILAC medium is available for insect cell lines, medium depleted for arginine and lysine was prepared based on both the composition of commercially available Schneider's insect medium and protocols in the literature (Bonaldi et al. 2008). Details of the SILAC medium formula that was used in this study are given in Suppl Table 1. Cells grown in this medium formula did not show any deviations in size, shape, or growth rate, as compared to cells grown in conventional medium. In order to avoid differences in characteristics of cells grown in light and heavy medium, all experiments were performed in a forward and reverse fashion and only those

identification hits that show consistent H:L ratios in the duplicate experiments were taken into account for further downstream analysis.

We first questioned whether ecdysone treatment of cells results in measurable changes at the level of the final effectors in the cell, *i.e.* its global proteome. Next, we questioned whether ecdysone signaling has similar effects on protein expression as it has on RNA expression in terms of the amount of up- and downregulation and timing. In the SILAC global proteome screen, we identified and quantified in total 5,748 proteins over 6 different time points in the range of 0 – 96 h after hormone induction of Kc cells (Suppl Table 2). These time points were chosen based on transcriptomics studies in the literature, which indicate that early responses already take place within several hours after ecdysone supplement to the cell. Extended time points were chosen to include effects of the putative delay between expression at the proteome level expression versus the transcriptome level. Quantitative proteomics analysis revealed that the abundances of the far majority of proteins remain unchanged (Figure 2): the scatter plots of H:L ratios of forward and reverse experiments after treatment of Kc cells with ecdysone for the indicated incubation times show a narrow distribution of data points around zero. However, although the far majority of protein abundances remain unchanged, there is a small subset of proteins that are up- or downregulated already at early time points. Among this small set of proteins are ecdysone induced protein 71 (Eip71CD or Eip28/29), eater, CG18765, mus309, Regeneration (rgn), glycine N-methyltransferase (CG6188) and BR-C (indicated in red in Figure 2 in the early time point plots). Eip71CD is a repair enzyme for proteins that have been inactivated by oxidation (Abhilash Kumar et al. 2002) and is a known ecdysone early responder, while eater is a major phagocytic receptor for a broad range of bacterial pathogens in *Drosophila* (Kocks et al. 2005). CG18765 is a protein of unknown function with no apparent ortholog in Mammalia, mus309 (Bloom syndrome protein homolog, Blm) is involved in DNA replication and repair (Adams, McVey, and Sekelsky 2003; Andersen et al. 2011) and Rgn controls the timing, the site and the size of blastema formation (McClure, Sustar, and Schubiger 2008). BR-C has also previously been described as an early ecdysone responsive gene. It is required for puffing and transcription of salivary gland late genes during metamorphosis (Crossgrove et al. 1996) and has been associated to a broad range of other cellular events such as oogenesis and organ development. It positively regulates transcription from the RNA polymerase II (RNA Pol II) promoter.

At early time points, BR-C is upregulated at the protein level, but after longer time points the increase levels off (Figure 3A). A similar effect is observed at the mRNA level (see Figure 5D). At later time points, the set of affected proteins grows, but is still small fraction of the total (measurable) proteome. The consistent H:L ratios in the forward and reverse SILAC experiments respectively (Figure 3B), are in agreement with the behavior of BR-C behavior of BR-C on immunoblots after ecdysone stimulus as compared to mock samples (Figure 3D). BR-C was identified by only one tryptic peptide

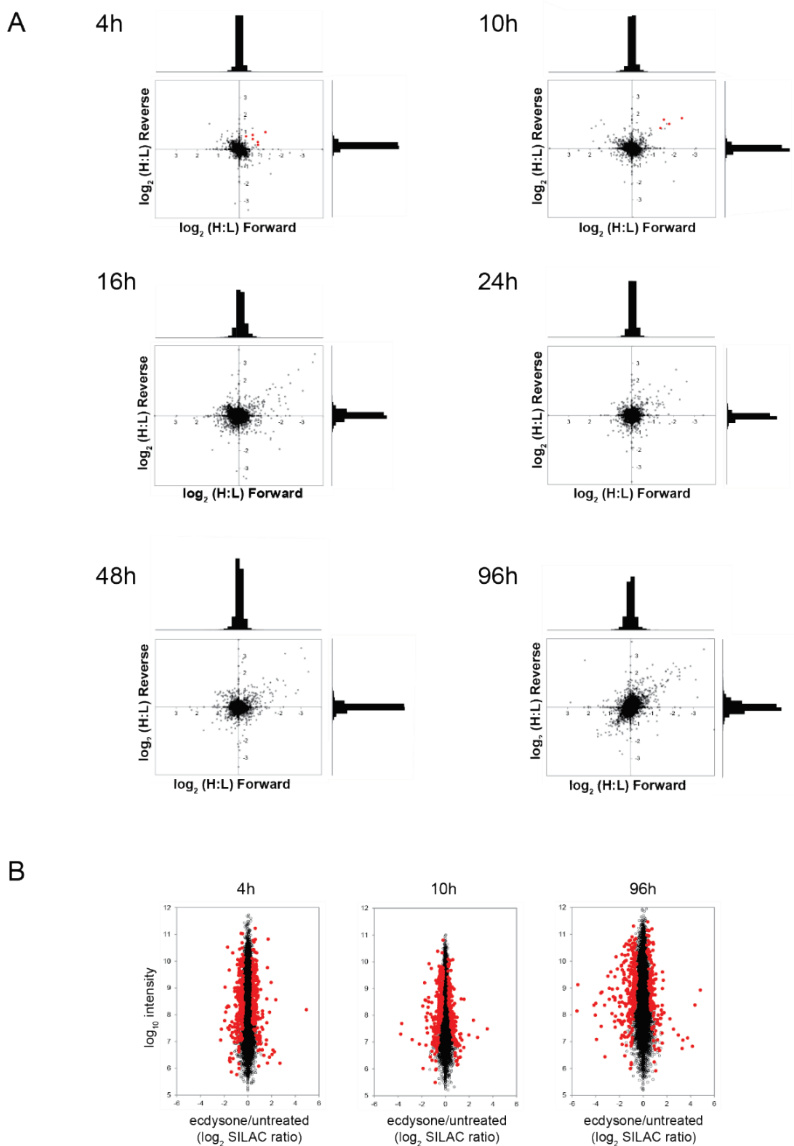


Figure 2. A) Scatter plots of H:L ratios of forward and reverse experiments obtained from SILAC MS assays after ecdysone treatment for the indicated incubation times. Although the far majority of protein abundances remain unchanged after this cellular perturbation, there is a small subset of proteins that show ratios deviating from 1 (0 at a \log_2 scale), *i.e.* proteins which are up- or downregulated, especially at later time points. **B)** Significant outliers (p -value < 0.05) in the SILAC data sets as determined by the Significance B protocol in Perseus for separately treated forward and reverse experiments. Significant outlier analysis was done prior to filtering for consistency of forward and reverse ratios as the additional selection criterion.

in our assay, but manual inspection of the fragmentation spectrum of this peptide firmly confirms its identity (Figure 3C). The quantitative analysis of BR-C shows the proof of concept of the SILAC mass spectrometry setup used in this study.

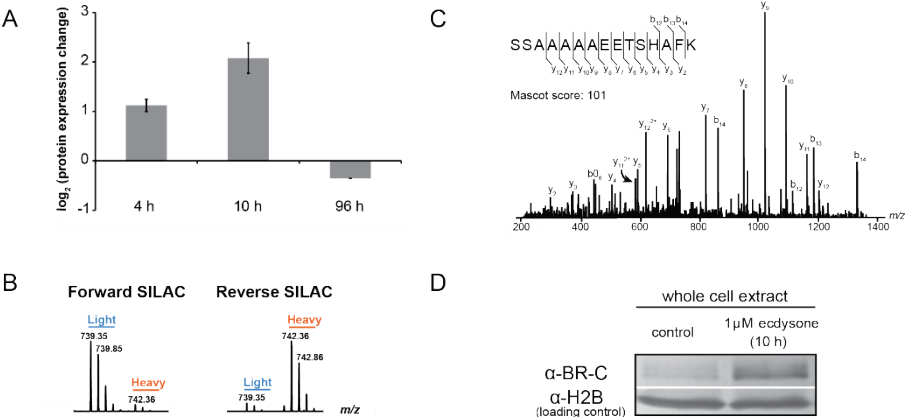


Figure 3. Detailed SILAC data for BR-C. A) Relative protein abundance changes after ecdysone treatment for the indicated time periods. After relative short incubation times, BR-C is upregulated, while after much longer incubation times the abundance returns to pre-treatment values or even lower. Error bars are the SD of two replicates. B) Zoom spectra from forward and reverse SILAC experiments representing a BR-C tryptic peptide in its light (blue) and heavy (orange) form. The H:L ratios in the forward and reverse (after label swap) are consistent and indicate an upregulation of BR-C after 10 h. C) Fragmentation spectrum of the BR-C tryptic peptide (m/z of $[M+2H]^{2+}$: 739.34) confirms its identity; b- and y-ions are indicated. D) Immunoblot using specific antibodies against BR-C on mock cells and cells that were treated with ecdysone for 16 h. The upregulation of BR-C after treatment is in agreement with the relative protein abundance data from the SILAC screen. H2B was used as the input control.

All downstream data analysis hereafter was performed using a subset of the SILAC time points described above, *i.e.* fast, intermediate and long treatment (4, 10 and 96 h, respectively), for technical reasons. The protein numbers in terms of identification and relative quantitation for the data set derived from the Q Exactive based workflow were considerably higher and resulted therefore in the highest-quality data set. In total, 4,503 hits of the SILAC proteome data set and the RNA sequencing (RNAseq) data set were overlapping. From the SILAC experiment, 620 protein hits could not be matched back to the transcriptome data set. Since the majority of these unmatched protein hits were detected with BAQ values comparable to those of proteins that could be matched to mRNA counterparts (Figure 4, green box plot), it is rather unlikely that corresponding mRNAs of these hits have too low intensities so that they would be missed by RNAseq. One alternative explanation is that the conversion of Uniprot entries to Flybase FBgn entries was not optimal and that therefore some mRNA-protein pairs were lost in the

conversion process. Also, the few data points with \log_2 FPKM < 0 may have arisen from falsely matched pairs. At the same time 9,379 hits in the RNAseq data set could not be matched to proteins hits in the SILAC data set. The RNAseq hits that could not be matched (Figure 4, red box plot) are mostly hits with relatively low expression levels that would most likely give rise to undetectable protein levels in the screen used here. In an attempt to compare protein with mRNA abundances, protein intensities as that were directly based on the iBAQ values calculated by the MaxQuant software were directly compared to FPKM values determined by RNAseq and plotted (Figure 4). Although the trend is far from linear ($R^2=0.366$), it is similar to values previously reported in the literature (Schwanh usser et al. 2011). Also, the plot reveals that, in general, higher FPKM values are associated with higher protein intensities. The small cluster in the upper right corner with extremely high mRNA levels represents ribosomal proteins.

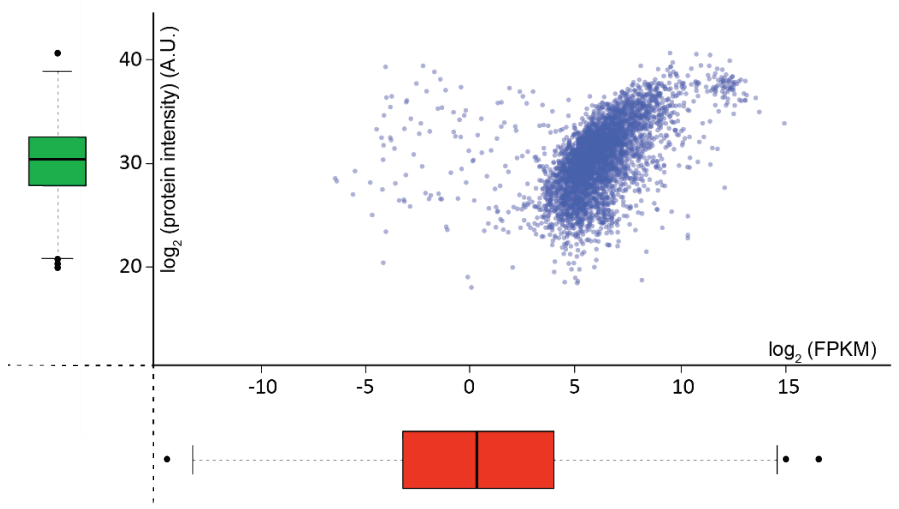


Figure 4. A scatter plot of absolute protein intensities (based on iBAQ values) versus absolute mRNA intensities (based on FPKM values) in untreated, steady state cells shows a relatively weak correlation ($R^2=0.366$). The intensity distribution of proteins for which no corresponding hit in the transcriptome analysis was found is represented by the green box plot. This distribution is very similar to the distribution of overlapping hits (blue data points). However, the distribution of mRNA hits for which no corresponding protein hit was identified (red box plot) shows that their average intensities are much lower than for overlapping hits. For these mRNA hits no corresponding protein hits were identified, most likely because protein concentrations were below the detection limit of the SILAC MS screen. The cluster of hits in the upper right corner with very high FPKM values represents mainly ribosomal proteins.

Clustering analysis revealed that the subset of proteins that are affected by ecdysone triggering could be clustered into 22 groups with similar trends in up- or downregulatory behavior (see Suppl Figure 2A). Several clusters show clear up- and downregulatory

effects and other clusters show interesting timing effects (*e.g.*, clusters 2 and 12). Most of the targets at the proteome level show large abundance changes only after longer incubation times and may therefore be the proteome analogs of late puff effects. Also, mRNA data were subjected to clustering analysis, indicating that many of the clusters are affected already after short incubation times. Some of the clusters show clear timing effects, for instance cluster 6, representing mRNAs that are downregulated at an early stage and then later stabilized.

However, gene ontology (GO) analysis on these clusters did not result in clear patterns of functional protein groups, so we decided to combine multiple clusters into higher-level clusters of up- and downregulated proteins (for complete data set see Suppl Table 3). Proteins that are downregulated upon ecdysone treatment include targets involved in nucleotide and carboxylic acid binding, as well as proteins involved in drug and RNA metabolism. Importantly, this group is enriched for proteins involved in post-embryonic development, for instance transcriptional regulators. The cluster of upregulated proteins is enriched for factors involved in stress response, aging and determination of adult life span. In addition, this set also includes proteins involved in post-embryonic development and morphogenesis, *e.g.* of neurons, and proteins involved in metabolism, catabolic processes and glutathione transferase activity. Examples of proteins involved in oxidation-reduction reactions, besides the known ecdysone response factor methionine sulfoxide reductase (Eip71CD, the *Drosophila* homolog of MsrA), are Cytochrome P450-4e2, Cytochrome P450-6a8 and Cytochrome P450-9f2. Because of their catalytic activity, these proteins are believed to be involved in the metabolism of insect hormones and in the breakdown of synthetic insecticides (Chen and Li 2007). Eip71CD, a repair enzyme for inactivated proteins by oxidation, is a downstream effector of FOXO signaling, which enhances resistance to oxidative stress and as such is believed to increase survival under stress conditions and extend lifespan (Chung et al. 2010) and is involved in neuron projection morphogenesis. Eip71CD is strongly upregulated, but protein levels decrease after very long incubation times. Other proteins that are involved in the response to oxidative stress include CG5346, which belongs to the iron/ascorbate-dependent oxidoreductase family, and CG6770. Interestingly, CG6770, a target gene of the putative FoxA protein Fork head (FKH) transcription factor and known to be induced by rapamycin, was found to be upregulated in the SILAC screen as a result of ecdysone triggering. FKH, besides its established role in embryonic development, controls cell and organismal size and is necessary for the expression of rapamycin and starvation responsive genes as well as for rapamycin induced inhibition of growth (Bülow et al. 2010). Knockdown of CG6770 (and of cabut) leads to increased cell size (Björklund et al. 2006), raising the possibility that it also acts as a negative regulator of growth downstream of FKH. It has been hypothesized that under conditions of dietary protein abundance, the Target Of Rapamycin (TOR) signaling module is active and exerts a negative regulation on FKH, which is

consequently sequestered in the cytoplasm and unable to modulate transcription of CG6770, cabut and Thor. However, when TOR complex 1 activity is inhibited by rapamycin or protein deprivation the repression of FKH activity is diminished, resulting in a significant fraction of the cellular FKH pool accumulating in the nucleus and then activates expression of the growth-inhibiting genes CG6770, cabut and Thor (Bülow et al. 2010). Although Thor was not identified in the SILAC screen, it was found to be upregulated in the RNAseq screen after 24 h ecdysone treatment, while, remarkably, cabut was slightly downregulated. LKR, a cofactor involved in the lysine ketoglutarate reductase / saccharopine dehydrogenase (SDH) process and involved in ecdysone-mediated transcription, was slightly upregulated.

When protein and mRNA abundance changes are directly compared, the delay effect that was observed at the proteome level is immediately clear at the 4 h time point (Figure 5A). Many of the RNAseq hits that are affected at an early stage do not show changes for their corresponding protein counterpart yet. After longer ecdysone treatments though, protein counterparts do show increased up- and downregulation (Figure 5B). In general, mRNA hits that are affected show changes in the same direction as their corresponding protein products (Figure 5B (red data points), Figure 5C), although in most cases the extent of mRNA up- or downregulation is one or two orders of magnitude higher. However, at longer time points several hits are down- or upregulated at the mRNA level that do not show a similar behavior at the proteome level (blue data points). For example, FTZ-F1, a nuclear hormone receptor that represses its own transcription and is repressed by ecdysone, was strongly downregulated at the transcriptome level, but remarkably did show no abundance changes at the proteome level after long ecdysone induction. This protein plays a central role in the prepupal genetic response to ecdysone and provides a molecular mechanism for stage-specific responses to steroid hormones (Woodard, Baehrecke, and Thummel 1994). Also, there are several hits that show an effect at the proteome level, but not at the transcriptome level (orange data points). The heatmap in Figure 5C illustrates that although upregulation of mRNA usually goes together with protein upregulation, mRNA downregulation not always results in lower protein levels, not even at the longer timescale. Finally, a small subset of hits reveals a mild antagonistic effect between mRNA and protein abundance changes, *i.e.* while protein expression goes up, mRNA expression goes down and *vice versa* (green data points). GO analysis reveals that group of proteins is enriched in functional categories such as post-embryonic development and nucleotide binding (see Suppl Table 3). Abundance fold changes for a selection of these proteins, as well as of proteins with clear timing effects, are plotted in Figure 5D. This set of proteins is, among others, enriched for post-embryonic development regulators and DNA binding proteins. Ken is a transcription factor required for terminalia development and is a negative regulator of the JAK/STAT pathway (Arbouzova, Bach, and Zeidler 2006; Lukacovich et al. 2003). In our screen, Ken is downregulated at the mRNA level

and protein levels are decreased at intermediate time points, but the protein seems to stabilize at later stages. Regeneration (Rgn) is a developmental protein and is expressed in blastema cells during the regeneration of imaginal disks and is important for transdetermination, the switching of specific stem-cell like cells to a different fate (McClure, Sustar, and Schubiger 2008). Here, Rgn shows strong upregulation both at the mRNA and protein levels after short incubation times, but is then downregulated at later time points. Mus309 is downregulated at the mRNA levels and, although its protein product abundance is increased at early time points, it seems to be degraded at a later stage. MET (CG30344) is a multidrug efflux transporter and involved in excretion of toxins via renal tubules. It has been shown that exposure to methotrexate in the diet results in an increased expression of MET (Chahine and O'Donnell 2010; Chahine, Seabrooke, and O'Donnell 2012). It is first downregulated and subsequently upregulated; the protein levels show a similar trend as the mRNA levels, albeit with a delayed effect. Interestingly, the peptidases CG30046 and CG33713 are upregulated at an early stage, but later downregulated, whereas the peptidase CG17337 shows an opposite regulative trend. Proteins of uncharacterized function include CG15820 and CG15390. CG15820 is upregulated then downregulated and the protein abundance follows this trend. CG15390 is downregulated at the mRNA level, but at short and intermediate time points it is slightly upregulated at the protein level. Trol is downregulated at early time points, but strongly upregulated at longer time points. The protein Eve (Even skipped), which functions in the trol pathway, has been described to be rescued by the hormone ecdysone (Y. Park et al. 2001). In contrast, the oxidoreductase protein CG5346 is first upregulated and downregulated at later time points.

We speculate that in cases where abundance fold changes between the transcriptome and proteome levels do not correspond, there could be a more complex interplay between these different cellular acting levels. For instance, very different turnover rates of proteins and mRNAs may play a role, as well as posttranslational modifications (PTMs) on proteins that can affect their activity dramatically, but do not *per se* result in abundance changes at the global proteome level. Both turnover rate analysis and the characterization of PTMs were not taken into account in this study and are subject for further analysis. Overall, we observed a substantial overlap in terms of affected targets between the dynamic proteome and transcriptome after ecdysteroid induction. However, there are clear differences in timing effects between the transcriptome and proteome levels; effects in the proteome are usually delayed with respect to the changes in mRNA levels. Also, downregulation of mRNAs in many cases does not correlate to downregulation at the proteome level and in some cases there seems to be no correlation between transcriptome and proteome dynamics at all. Finally, we have found several proteome targets and players in the ecdysone signaling pathway that have not been described before.

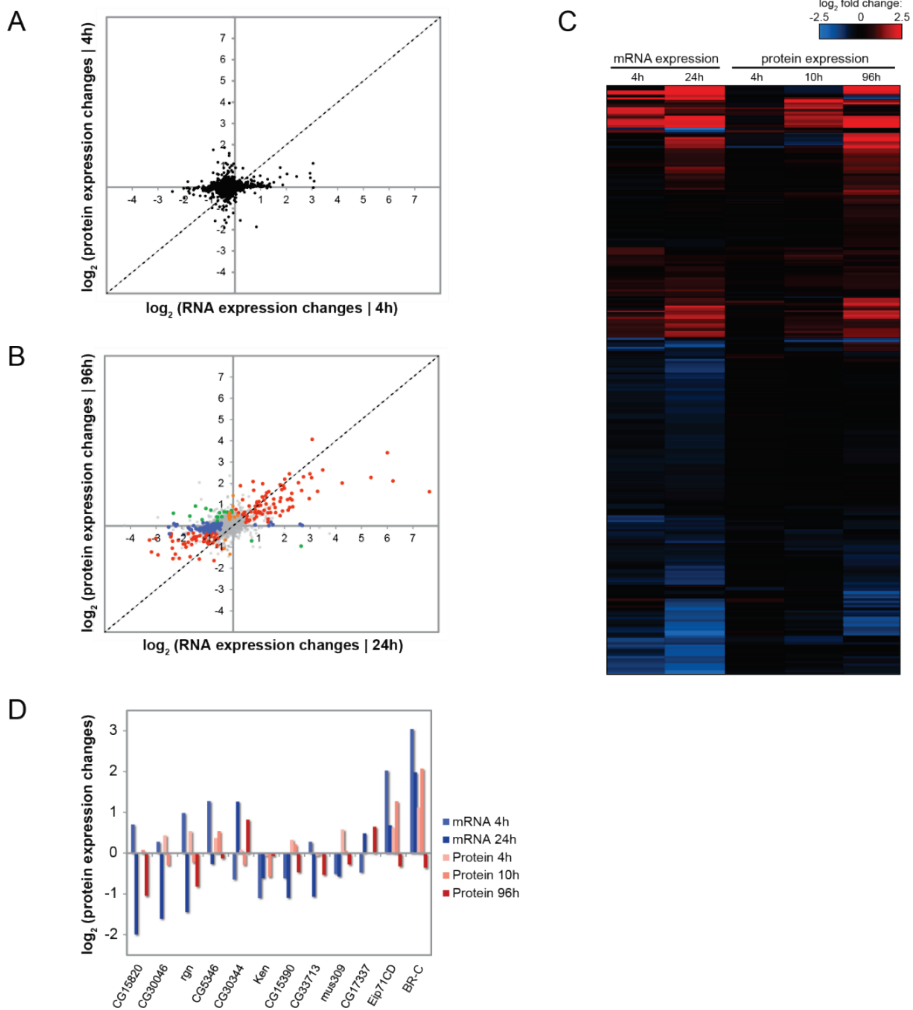


Figure 5. Relationship between mRNA and protein expression values for corresponding hits. **A)** Responses after short time points indicate that the early cellular products are mainly mRNAs, while the corresponding protein products are not (yet) up- or downregulated. **B)** Responses after longer incubation times reveal that hits can be grouped into clusters of specific dynamic behavior (see main text for details). **C)** Dynamics of a selection of overlapping targets from both transcriptome and proteome expression analyses. The majority of hits show a correlation between transcription and protein expression. However, especially for hits that are downregulated at the mRNA levels, in many cases the corresponding protein levels do not show a downregulation, not even after notably longer incubation times. **D)** Several hits show no correlation between mRNA and protein expression, or a remarkable timing effect.

Identification of EcR interaction partners

The ecdysone receptor is a type II nuclear receptor and is most commonly comprised of an EcR protein dimerized with USP. Upon ecdysteroid binding, the receptor activates ecdysone-responsive genes. Different isoforms of the EcR protein exist (Koelle et al. 1991) and various dimerization partners have been described (Bitra and Palli 2009), which supposedly allows the receptor to bind to different EcREs. Different genes can thus be activated and, as a result, the response to ecdysone can be specifically modulated. Here we set out to identify novel interaction partners for the EcR protein. Endogenous EcR was purified from *Drosophila* embryo nuclear extracts using two different commercial antibodies as the bait, Ag10.2 and DDA2.7 (DSHB), which both recognize a common epitope present in all three EcR isoforms (Ag10.2: amino acid residues 649-878, including the Gln/Pro-rich domain; DDA2.7: amino acid residues 335-393). Figure 6 highlights proteins identified in at least one of the IPs that were highly enriched compared to mock IP samples with a pre-immune-derived antibody mixture (for the complete data set see Suppl Table 5). Relative protein abundance values were based on peptide counts and the label free quantitation (LFQ) algorithm available in MaxQuant (Cox et al. 2014). Proteins were defined as being enriched when the LFQ intensity ratio between case and control samples was >3 and the MS/MS count ratio >4 . Also, individual proteins were only included when the MS/MS count was at least 10, to obtain sufficiently reliable quantitation values. It should be noted though that the majority of hits have much higher LFQ intensity and MS/MS count ratios.

EcR was identified in both IPs, as well as its heterodimerization partner USP. Since EcR is a DNA binding nuclear receptor that can activate ecdysone-responsive genes in an RNA Pol II dependent manner, it is no surprise that several of the co-purified proteins and potential interaction partners play diverse roles in transcription. TFIIFalpha and TFIIFbeta, highly enriched in the Ag10.2 IP, are subunits of TFIIF, one of the general transcription factors that make up the RNA Pol II preinitiation complex. In addition, almost the complete Mediator complex, a coactivator of RNA Pol II dependent genes, was identified in the Ag10.2 screen. Other transcription related proteins include Mip120 (Lin-54 homolog), which negatively regulates transcription from the RNA Pol II promoter (Beall et al. 2007), the RNA Pol associated protein RTF1, CG3815 (Pfl), which is part of the Lid complex (Lee et al. 2009) and acts as a positive transcription regulator, and PCAF, part of the SAGA complex and involved in transcriptional regulation. Proteins involved in transcription that have been in one way or another linked to ecdysone signaling include transcription factor HNF-4 homolog (HNF4), a nuclear receptor with basal transcriptional activity that is a key regulator of lipid mobilization and β -oxidation in response to nutrient deprivation (Palanker et al. 2009). Another putative EcR interactor involved in transcriptional regulation is Domino, a SWI/SNF-like ATP-dependent chromatin remodeling enzyme that has been implicated in Notch signaling, as well as Nipped A (Gause et al. 2006).

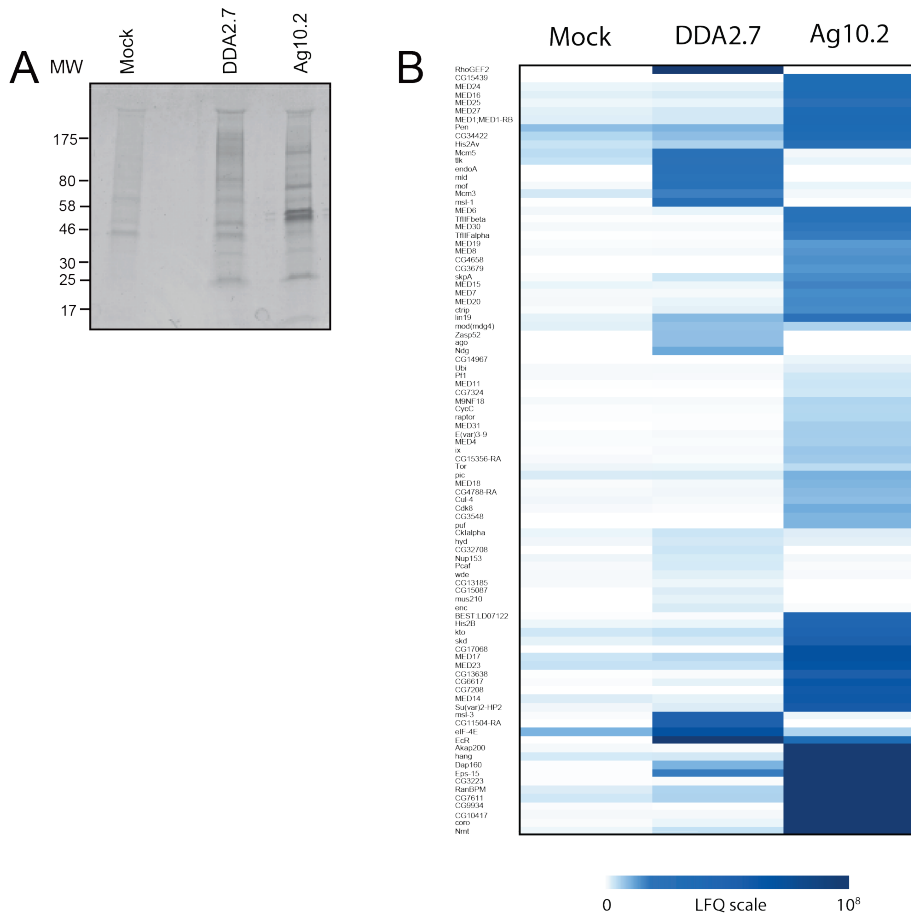


Figure 6 | For EcR IPs, DDA2.7 or Ag10.2 antibodies were first coupled to ProtG beads. Subsequently, IPs were performed in 1 ml *Drosophila* nuclear extract. The mock IP was performed using non-specific pre-immune serum coupled to ProtG beads. Beads were washed under relatively mild conditions and proteins were eluted and separated by SDS-PAGE. The gel was stained with Coomassie (A) and lanes were cut into slices and subjected to in-gel tryptic digestion. Peptides were identified by LC-MS/MS and analyzed by MaxQuant using the label free quantitation (LFQ) module. Relevant hits are shown in the heatmap (B) where the color scale represents the range of LFQ values. Requirements of specific interactors for inclusion in the heatmap were: LFQ intensity case: control >3; MS/MS count ratio case: control >4; MS/MS count for individual proteins >10 and LFQ intensity >500,000. It should be noted though that the majority of hits have much higher LFQ intensity and MS/MS count ratios.

The histone methyltransferase Hmt4-20 that specifically trimethylates H4 K20 and therefore represents a specific tag for epigenetic transcriptional repression was enriched in the EcR IPs. Interestingly, trithorax-related (TRR), which did not show enriched LFQ values in this screen, specifically trimethylates H3 K4 and was previously identified as a coactivator for the ecdysone receptor (Sedkov et al. 2003). It is recruited by EcR in an ecdysone dependent manner and modulates chromatin at ecdysone inducible promoters. Another chromatin modifier that was identified is the histone acetyl transferase MOF, a component of the multisubunit histone acetyltransferase complex (MSL), which is - at least - composed of MOF, MSL1, MSL2 and MSL3. It is also part of a second histone acetyltransferase complex, the NSL complex, at least composed of MOF, NSL1/wah, NSL2/dgt1, NSL3/Rcd1, MCRS2/Rcd5, MBD-R2 and wds. MOF positively regulates sequence specific DNA binding transcription factor activity and is involved in dosage compensation (Gorman, Franke, and Baker 1995). MOF's interactors MSL1 and MSL3, but not MSL2, came down with EcR in our screen. Also, the chromatin modifying enzymes E(var)3-9, which has been implicated in an essential process during embryogenesis (Weiler 2007), Su(var)2-HP2 and the chromatin insulator Mod(mdg)4, a regulatory element that establishes independent domains of transcriptional activity within eukaryotic genomes, were specific for the EcR IP. Several subunits of the SCF (SKP1-CUL1-F-Box protein) E3 ubiquitin-protein ligase complex were identified: FBXW7 (ago), which mediates the ubiquitination and subsequent proteasomal degradation of target proteins, the cullin homolog lin19 and SkpA (Dredd) (Bader, Arama, and Steller 2010), as well as another F-box protein, FBX011, which has been described as a SkpA interacting protein (Stanyon et al. 2004). Encore (enc), specific for the DDA2.7 co-IP, has been shown to interact with Cyclin E, Cul1 (lin19), and components of the SCF-proteasome system (Ohlmeyer 2003). Several co-purified proteins play a role in fly development, such as in embryogenesis and oogenesis. The Ran binding protein homolog RanBPM, for instance, is involved in JAK/STAT signaling (Dansereau and Lasko 2008). Gustavus (gus) is a ubiquitin Cullin-RING E3 ligase expressed in nurse cells and is important for the polarity of the developing oocyte (Kugler et al. 2010). G protein G alpha i plays a role in glial cell differentiation during embryogenesis (Grandérath et al. 1999). We also identified protein kinase A (PKA) regulatory and catalytic subunits, Pka-R2 and Pka-C1, respectively, which transduce signals through phosphorylation of different target proteins. Pka-R2 may play an essential role in the regulation of neuronal activity in the brain (S. K. Park et al. 2000). The zinc finger protein MLD is required for ecdysone biosynthesis and has been linked to different cellular processes, such as determination of adult lifespan, long-term memory development, and the regulation of the circadian sleep/wake cycle (Neubueser et al. 2005). Interestingly, two proteins involved in TOR signaling, raptor and target of rapamycin (TOR) (Wullschlegel, Loewith, and Hall 2006) were co-purified with EcR. TOR regulates growth during animal development by coupling growth factor signaling to nutrient availability (Neufeld 2004). It is of notice that CG6770, which also plays a

role in TOR signaling, was previously identified in our SILAC screen as being strongly upregulated as a result of ecdysone induction. Altogether, these results may suggest a direct connection between ecdysone signaling and the TOR signaling pathway that regulates growth and needs further investigation. Two proteins, Hangover (Scholz 2005) and Akap200 (Kong 2010), are expressed ubiquitously in the nervous system, in neurons but not glia, and are required for normal development of ethanol tolerance. Several proteins involved in vesicle transport and phagocytosis were identified. Coronin (coro) is an actin binding protein which also interacts with microtubules and in some cell types is associated with phagocytosis (Bharathi 2004). Zizimin-related (Zir), a Rho guanine nucleotide exchange factor (RhoGEF) and homologous to the mammalian Dock-C/Zizimin-related family, plays a role in phagocytosis and is also important for the immune response in *Drosophila* (Sampson et al. 2012). Eps15 and its major binding partner Dap160 were both co-purified and control synaptic vesicle membrane retrieval and synapse development (Koh et al. 2007), but also have been suggested to negatively regulate Notch signaling (Tang et al. 2005). Furthermore, N-myristoyltransferase (NMT) is part of a family of myristoyl proteins, which are components of cellular signaling pathways and play important roles during embryonic development, making NMT essential for embryogenesis (Ntwasa 1997). Finally, several proteins involved in the ubiquitin-proteasome system and neurogenesis (Ctrip, CG42574) and DNA repair and replication (*e.g.*, hay and MCM3) were identified as putative interactors. Several yet uncharacterized proteins were found to be specific for the EcR IP, such as CG34422, CG7611 (WDR26), CG6617 and CG13638; these require further analysis.

Although several proteins were identified with high scores and - presumably - in relative high abundances as compared to the mock IP, and therefore seem to be *bona fide* interactor candidates, the overlap between two IPs with different antibody is only rather poor. The reason for this is unknown, although it can be speculated that steric inhibition of EcR antibody binding sites may mask different interaction domains, since the antibodies were raised using different antigen epitopes. Alternative strategies to clarify this would be the construction of tagged versions of the receptor for affinity purification or raising antibodies using partially non-overlapping epitopes. Also, it would be of great interest to investigate the dynamics with quantitative proteomic techniques of EcR interactions and of the EcR/USP dimer in the presence of ecdysone, which introduces a conformational change leading to transcriptional activation of genes under the EcRE control.

Conclusive remarks

In conclusion, we have performed a protein-protein interaction analysis of EcR, a target protein of ecdysone, to shed more light on ecdysone signaling at the interactome and proteome level. Proteins co-purified with EcR include factors involved in RNA Pol II dependent transcription and chromatin modifying enzymes. Also, several proteins previously linked to ecdysone signaling and/or biosynthesis were identified. The identification of several proteins linked to both the TOR and Notch signaling pathways could potentially be interesting targets for follow-up studies and might offer new insights in ecdysone induced protein expression. In addition, we have performed a quantitative, proteome-wide screen to monitor the effect of ecdysone administration to *Drosophila* Kc cells. We have compared changes at the proteome level to more upstream effects at the transcriptome level. We observed a substantial overlap in terms of affected targets between the dynamic proteome and transcriptome after ecdysteroid induction. However, there are clear differences in timing effects between the transcriptome and proteome levels; effects in the proteome are usually delayed with respect to the changes in the transcriptome. Also, downregulation of mRNAs in many cases does not correlate to downregulation at the proteome level and in some cases there seems to be no correlation between transcriptome and proteome dynamics whatsoever. Finally, we have found several proteome targets and players in the ecdysone signaling pathway that have not been described before. It would be of great interest to extrapolate these quantitative proteomics studies from cultured cells to the fly, which is technically possible (Sury, Chen, and Selbach 2010, Gouw et al. 2011) and would allow for the investigation of ecdysone action in a developmental stage dependent and/or even in an organ specific manner.

Experimental methods

20-Hydroxyecdysone treatment. *Drosophila melanogaster* Kc cells were treated with 1 μ M 20-hydroxyecdysone (H5142, Sigma) dissolved in DMSO, or mock-treated with an equal volume of DMSO for 4, 10, 16, 24, 48 or 96 h.

Antibodies and immunoblotting. Cells were washed 3x with cold PBS and lysed in 2x Laemmli sample buffer. Samples were sonicated using a Bioruptor (Diagenode) for 5 min, 30 seconds 'on' and 30 seconds 'off' cycles and boiled at 95 °C. Proteins were resolved by SDS-PAGE and blotted to PVDF membranes. Membranes were blocked with 10% dry milk in PBST (PBS with 0.1% Tween), incubated with primary antibodies in PBS/3% BSA. Following multiple PBST washes, membranes were incubated with alkaline phosphatase (AP) secondary antibodies. Membranes were washed with PBST and developed with NBT/BCIP.

Antibodies. Antibodies against Broad-Complex (BR-C) (α -Broad-core, 25E9.D7) and EcR (DDA2.7 and Ag10.2) were from the Developmental Studies Hybridoma Bank (DSHB); antibodies against H2B (α -H2B, 07-371) were from Millipore.

SILAC and sample preparation for global proteome analysis. Kc cells were cultured in custom made Schneider's *Drosophila* medium (Athena Enzyme Systems, Baltimore, MD), based on Invitrogen's formulation (Invitrogen, #21720-001), with following modifications: dialyzed yeastolate (3500 Da MWCO) and deficient for lysine and arginine. Before use, the medium was supplemented with 5% dialyzed fetal bovine serum (F0392, Sigma-Aldrich), 1% penicillin-streptomycin and 2 mg/ml 'light' ($^{12}\text{C}_6$) lysine (A6969, Sigma-Aldrich) and 0.5 mg/ml 'light' ($^{12}\text{C}_6$ and $^{14}\text{N}_4$) arginine (L5751, Sigma-Aldrich), or 'heavy' ($^{13}\text{C}_6$) lysine (CLM-2247, Cambridge Isotope laboratories) and 'heavy' ($^{13}\text{C}_6$ and $^{15}\text{N}_4$) arginine (CNLM-539, Cambridge Isotope Laboratories). Cells were cultured at 27 °C for at least 7 cell doublings to reach complete labeling. Experiments were done in a forward and reverse manner: in forward, light cells were treated with ecdysone and heavy cells were treated with DMSO, and *vice versa* in the reverse experiment. After ecdysone treatment, 30×10^6 heavy labeled and 30×10^6 light labeled cells were mixed. Cells were washed with cold PBS (3x) and lysed in 100 μl 2x Laemmli sample buffer. Samples were sonicated using a Bioruptor (Diagenode) for 5 min, with 30 seconds 'on' and 30 seconds 'off' cycles and boiled at 95 °C. For the LTQ-Orbitrap workflow (see LC-MS/MS section), proteins were resolved on a 12% SDS-PAGE gel and visualized by Coomassie staining. Lanes were cut in 1mm slices and combined to 80 fractions per lane and analyzed by LC-MS/MS. Alternatively, for the Q Exactive workflow, proteins extracts were digested and fractionated by HILIC on an Agilent 1100 HPLC system using a 5 μm particle size 4.6 x 250 mm TSKgel amide-80 column (Tosoh Biosciences). 200 μg of the desalted tryptic digest was loaded onto the column in 80% acetonitrile. Next, peptides were eluted using a nonlinear gradient from 80% B (100 % acetonitrile) to 100% A (20 mM ammonium formate in water) with a flow of 1 ml/min. Sixteen 6 ml fractions were collected, lyophilized and pooled into 8 final fractions. Each fraction was then analyzed by LC-MS/MS.

Immunopurification. Nuclear extracts (NE) from 0-12 h old *Drosophila* embryos were prepared as described (Chalkley and Verrijzer 2004). Immunopurification (IP) procedures were performed essentially as described (Chalkley and Verrijzer 2004). Briefly, DDA2.7 antibody (1.5 ml, 142 $\mu\text{g}/\text{ml}$) was crosslinked to 100 μl ProtG beads (GE Healthcare) and Ag10.2 antibody (0.5 ml, 207 $\mu\text{g}/\text{ml}$) was crosslinked to 50 μl ProtG beads by using dimethylpimelimidate. As a control, antibodies from pre-immune serum were coupled to ProtG beads. After 2 h incubation of the antibody coupled beads with NE, the beads were washed extensively with HEMG buffer (25 mM HEPES-KOH, pH 7.6, 0.1 mM EDTA, 12.5 mM MgCl_2 , 10% glycerol, 200 mM KCl, 0.1% NP-40, containing a cocktail of protease inhibitors). Proteins retained on the beads were eluted with 100 mM sodium citrate buffer (pH 2.5), resolved by SDS-PAGE and

visualized by Coomassie staining. Lanes were cut in 1 mm slices and combined to in total 12 fractions per lane and analyzed by LC-MS/MS.

LC-MS/MS. In-gel protein reduction, alkylation and tryptic digestion was done as described previously (van den Berg et al. 2010). Peptides were extracted with 30% acetonitrile 0.5% formic acid and analyzed on an 1100 series capillary LC system (Agilent Technologies) coupled to a LTQ-Orbitrap hybrid mass spectrometer (Thermo) or on an EASY-nLC system (Thermo) coupled to a Q Exactive mass spectrometer (Thermo). Peptide mixtures were trapped on a ReproSil C18 reversed phase column (Dr Maisch GmbH; column dimensions 2 cm × 100 µm, packed in-house) at a flow rate of 8 µl/min. Peptide separation was performed on ReproSil C18 reversed phase column (Dr Maisch GmbH; column dimensions 15 cm × 75 µm, packed in-house) using a linear gradient from 0 to 50% B (A = 0.1% formic acid; B = 80% (v/v) acetonitrile, 0.1% formic acid) in 120 min (for IP samples) or 180 min (for SILAC global proteome samples) and at a constant flow rate of 300 nl/min (using a splitter for the 1100 system). The column eluent was directly electrosprayed into the mass spectrometer. Mass spectra were acquired in continuum mode; fragmentation of the peptides was performed in data-dependent acquisition mode by CID using top 8 selection (LTQ-Orbitrap) or HCD using top 15 selection (Q Exactive). Additional settings for Q Exactive operation: MS resolution: 70,000; MS AGC target 3E6; MS maximum injection time: 100 ms; MS scan range 375-1400 m/z; MS/MS resolution: 17,500; MS/MS AGC target: 1E5; MS/MS maximum injection time: 200 ms; intensity threshold: 5E3.

Mass spectrometry data analysis. RAW files were analyzed using MaxQuant software (v1.3.0.5 | <http://www.maxquant.org>), which includes the Andromeda search algorithm (Cox et al. 2011) for searching against the Uniprot database (version December 2013, taxonomy: *Drosophila melanogaster* | <http://www.uniprot.org/>). Follow-up data analysis was performed using the Perseus analysis framework (<http://www.perseus-framework.org/>), the GProX proteomics data analysis software package (v1.1.12, <http://gprox.sourceforge.net/>) (Rigbolt, Vanselow, and Blagoev 2011) or in-house developed software. The ‘Significance B’ option in the Perseus software suite (Cox and Mann 2008), which takes into account the intensity of peptides/proteins, was used to determine significant outliers to determine significant outliers (p-value < 0.05). Additionally, only proteins that were up- or downregulated by at least 1.5-fold were selected for follow-up analysis. An extra requirement to maintain a high quality data set was the presence of consistent ratios in forward and reverse experiments, so a protein hit with a SILAC ratio of >1.5 (log₂ ratio >0.585) in forward should also have a SILAC ratio of <0.66 (log₂ ratio <-0.585) in the reverse experiment and *vice versa*. Relative protein intensities within a sample were directly inferred from the iBAQ values in the label free quantitation module in MaxQuant (Schwanhäusser et al. 2011; Cox et al. 2014).

RNA isolation, quantitative real-time RT-PCR, RNA sequencing and data analysis. Total RNA was extracted from 5×10^6 cells using Trizol (15596-026, Invitrogen) and 4 μ g RNA was used for random hexamer primed cDNA synthesis using the Superscript II Reverse Transcriptase (Invitrogen). Quantitative real-time RT-PCR was performed on a CFX96 realtime PCR detection system (Bio-Rad). Reactions were performed in a total volume of 25 μ l containing 1x reaction buffer, SYBR Green I (Sigma), 200 μ M dNTPs, 1.5 mM $MgCl_2$, platinum Taq polymerase (Invitrogen), 500 nM of corresponding primers and 1 μ l of cDNA. The primer sequences used were: CG11874: 5'-AGTGT'TGCTCTGCCTAAGTGG-3', 5'-CGGATGATGGTGCGGATTGG-3'; E75A: 5'-CCTTTCATTGACTAACTGCCACTC-3', 5'-CGAAACGAAACGAACGGAACG-3'; E23: 5'-CATCACGAGTAGCCACCATAAC-3', 5'-GGTTGGAGCGTTGATTGTAATAG-3'. Data analysis was performed by applying the $2^{-\Delta\Delta CT}$ method (Livak and Schmittgen 2001). Values obtained from amplification of alpha-mannosidase-Ib (CG11874) were used to normalize the data as described previously (Moshkin et al. 2007; van der Knaap et al. 2010). Average amplification of three replicates is shown in graphs. Total RNA was purified from 5×10^6 cells per time point according to Trizol protocol (15596-026, Invitrogen). An indexed sequencing library was obtained from total RNA with the Illumina TruSeq RNA (v4) kit. The libraries were pooled together, and sequenced on two lanes of a flow cell on a Illumina Hiseq 2000 and sequenced for 36 bp + 7 bp index using Illumina v3 chemistry. Illumina BaseCall results were demultiplexed using NARWHAL (Brouwer et al. 2012). The reads were aligned using Tophat (version 1.3.1, (Trapnell, Pachter, and Salzberg 2009)) against the UCSC dm3 reference genome, using Ensembl genes.gtf annotation provided by Illumina iGenomes (<http://www.illumina.com/>, downloaded February 2013). FPKM (Fragments Per Kilobase transcript per Million mapped reads) expression levels were calculated by Cufflinks (version 1.0.3, (Trapnell et al. 2010)). Differential gene expression output was generated with Cuffdiff using fragment length of 300 bases. Differential gene expression data was integrated with differential protein expression data using in-house developed software. Briefly, comparisons for the RNAseq datasets 'mock-4h', 'mock-24h' and '4h-24h' each yielded a gene_exp.diff file and these were loaded into PostgreSQL (<http://www.postgresql.org/>) database tables. Each has a column 'gene_id' that contains the gene name. Next, SILAC data in the format of regular MaxQuant output files were also loaded as PostgreSQL database tables. Since the two data sources (SILAC versus RNAseq) did not use the same identifier system (MaxQuant uses Uniprot accession numbers, while RNAseq data contain the gene names from the Illumina file), accession - gene name mapping tables were generated from the full Uniprot proteome text records. As expected, virtually all RNAseq names could be mapped onto Uniprot accessions. Via this mapping the two datasets were joined together to produce a table for direct comparisons.

Online supplementary information available:

Supplementary Figure 1. Quantitative real-time RT-PCR reveals that the mRNA products of the genes E23 and E75A, which have been described previously to be early responsive genes upon ecdysone treatment, are substantially upregulated in *Drosophila* Kc cells after hormone treatment.

Supplementary Figure 2. A) Clustering analysis shows that, although the majority of protein abundances do not change, the proteins that do show an effect can be divided into specific groups according their up- or downregulation behavior (GProX parameters for SILAC data: upper regulation threshold 0.5; lower regulation threshold -0.5; standardized: false; fuzzification value: 2; iterations: 100; expression changes are plotted on a \log_2 scale). **B)** Clustering analysis of mRNA abundance changes. Also here, although the majority of relative abundances of mRNAs do not change, the mRNAs that do change can be divided into specific groups according their up- or downregulation behavior (GProX parameters for RNAseqdata: upper regulation threshold 0.41; lower regulation threshold -0.41; standardized: false; fuzzification value: 2; iterations: 100; expression changes are plotted on a \ln scale). Only RNA data are shown for which there are overlapping hits between SILAC and RNAseq assays.

Supplementary Figure 3. Pie charts summarizing the GO functional annotation analysis for downregulated, upregulated and non-correlated protein-mRNA pairs after stimulation of Kc cells with ecdysone.

Supplementary Table 1. SILAC cell culture growth medium formula for insect cells.

Supplementary Table 2. MaxQuant SILAC data and RNAseq data including the overlap between these two data sets.

Supplementary Table 3. GO enrichment analysis of hits that are upregulated or downregulated (>1.5 fold) at the mRNA and protein levels, and proteins that show non-correlated behavior compared to the corresponding mRNA levels after ecdysone treatment.

Supplementary Table 4. Expression changes at the mRNA and protein levels for the hits shown in heatmap Figure 5C.

Supplementary Table 5. MaxQuant EcR IP data.

References

- Abhilash Kumar, R., Ahmet Koc, Ronald L. Cerny, and Vadim N. Gladyshev. 2002. "Reaction Mechanism, Evolutionary Analysis, and Role of Zinc in *Drosophila* Methionine-R-Sulfoxide Reductase." *Journal of Biological Chemistry* 277 (40): 37527–35.
- Adams, Melissa D., Mitch McVey, and Jeff J. Sekelsky. 2003. "Drosophila BLM in Double-Strand Break Repair by Synthesis-Dependent Strand Annealing." *Science* 299 (1997): 265–67.
- Andersen, Sabrina L., H. Kenny Kuo, Daniel Savukoski, Michael H. Brodsky, and Jeff Sekelsky. 2011. "Three Structure-Selective Endonucleases Are Essential in the Absence of BLM Helicase in *Drosophila*." *PLoS Genetics* 7 (10).
- Andres, Andrew J., and Carl S. Thummel. 1992. "Hormones, Puffs and Flies: The Molecular Control of Metamorphosis by Ecdysone." *Trends in Genetics* 8 (4): 132–38.
- Arbouzova, Natalia I., Erika A. Bach, and Martin P. Zeidler. 2006. "Ken & Barbie Selectively Regulates the Expression of a Subset of JAK/STAT Pathway Target Genes." *Current Biology* 16 (1): 80–88.
- Ashburner, M., Puffing patterns in *Drosophila melanogaster* and related species. *Results and problems in cell differentiation* 1972, 4, 101-151
- Ashburner, M., Sequential gene activation by ecdysone in polytene chromosomes of *Drosophila melanogaster*. II. The effects of inhibitors of protein synthesis. *Developmental biology* 1974, 39, 141-157
- Bader, M., E. Arama, and H. Steller. 2010. "A Novel F-Box Protein Is Required for Caspase Activation during Cellular Remodeling in *Drosophila*." *Development* 137 (10): 1679–88.
- Beall, Eileen L., Peter W Lewis, Maren Bell, Michael Rocha, D Leanne Jones, and Michael R Botchan. 2007. "Discovery of TMAC: A *Drosophila* Testis-Specific Meiotic Arrest Complex Paralogous to Myb-Muv B." *Genes and Development* 21 (8): 904–19.
- Beckstead, Robert B, Geanette Lam, and Carl S Thummel. 2005. "The Genomic Response to 20-Hydroxyecdysone at the Onset of *Drosophila* Metamorphosis." *Genome Biology* 6 (12): R99–R99.
- Berg, Debbie L.C. van den, Tim Snoek, Nick P Mullin, Adam Yates, Karel Bezstarosti, Jeroen Demmers, Ian Chambers, and Raymond A Poot. 2010. "An Oct4-Centered Protein Interaction Network in Embryonic Stem Cells." *Cell Stem Cell* 6 (4): 369–81.
- Bharathi, V., Pallavi, S. K., Bajpai, R., Emerald, B. S., Shashidhara, L. S., Genetic characterization of the *Drosophila* homologue of coronin. *Journal of cell science* 2004, 117, 1911-1922
- Bitra, Kavita, and Subba Reddy Palli. 2009. "Interaction of Proteins Involved in Ecdysone and Juvenile Hormone Signal Transduction." *Archives of Insect Biochemistry and Physiology* 70 (2): 90–105.
- Björklund, Mikael, Minna Taipale, Markku Varjosalo, Juha Saharinen, Juhani Lahdenperä, and Jussi Taipale. 2006. "Identification of Pathways Regulating Cell Size and Cell-Cycle Progression by RNAi." *Nature* 439 (7079): 1009–13.
- Bonaldi, Tiziana, Tobias Straub, Jürgen Cox, Chanchal Kumar, Peter B. Becker, and Matthias Mann. 2008. "Combined Use of RNAi and Quantitative Proteomics to Study Gene Function in *Drosophila*." *Molecular Cell* 31 (5): 762–72.
- Brouwer, R. W W, M. C G N van den hout, F. G. Grosveld, and W. F J van ijcken. 2012. "NARWHAL, a Primary Analysis Pipeline for NGS Data." *Bioinformatics* 28 (2): 284–85.
- Bülöw, Margret H., Ruedi Aebersold, Michael J. Pankratz, and Martin A. Jünger. 2010. "The *Drosophila* FoxA Ortholog Fork Head Regulates Growth and Gene Expression Downstream of Target of Rapamycin." *PLoS ONE* 5 (12).
- Chahine, Sarah, and Michael J. O'Donnell. 2010. "Effects of Acute or Chronic Exposure

- to Dietary Organic Anions on Secretion of Methotrexate and Salicylate by Malpighian Tubules of *Drosophila Melanogaster* Larvae.” *Archives of Insect Biochemistry and Physiology* 73 (3): 128–47.
- Chahine, Sarah, Sara Seabrooke, and Michael J. O'Donnell. 2012. “Effects of Genetic Knock-down of Organic Anion Transporter Genes on Secretion of Fluorescent Organic Ions by Malpighian Tubules of *Drosophila Melanogaster*.” *Archives of Insect Biochemistry and Physiology* 81 (4): 228–40.
- Chalkley, Gillian E, and C Peter Vertijzer. 2004. “Immuno-Depletion and Purification Strategies to Study Chromatin-Remodeling Factors In Vitro.” *Methods in Enzymology* 377 (148): 421–42.
- Chen, Song, and Xianchun Li. 2007. “Transposable Elements Are Enriched within or in Close Proximity to Xenobiotic-Metabolizing Cytochrome P450 Genes.” *BMC Evolutionary Biology* 7: 1–13.
- Chung, Hyewon, Ae kyeong Kim, Sun Ah Jung, Si Wouk Kim, Kweon Yu, and Joon H. Lee. 2010. “The *Drosophila* Homolog of Methionine Sulfoxide Reductase A Extends Lifespan and Increases Nuclear Localization of FOXO.” *FEBS Letters* 584 (16): 3609–14.
- Clever, U., Karlson, P., [Induction of puff changes in the salivary gland chromosomes of *Chironomus tentans* by ecdysone]. *Exp Cell Res* 1960, 20, 623–626.
- Costantino, Benjamin F.B., Daniel K. Bricker, Kelly Alexandre, Kate Shen, John R. Merriam, Christophe Antoniewski, Jenna L. Callender, Vincent C. Henrich, Asaf Presente, and Andrew J. Andres. 2008. “A Novel Ecdysone Receptor Mediates Steroid-Regulated Developmental Events during the Mid-Third Instar of *Drosophila*.” *PLoS Genetics* 4 (6).
- Cox, J, Nadin Neuhauser, Annette Michalski, Richard A Scheltema, Jesper V Olsen, and Matthias Mann. 2011. “Andromeda: A Peptide Search Engine Integrated into the MaxQuant Environment.” *J. Proteome Res* 10: 1794–1805. .
- Cox, Jürgen, Marco Y. Hein, Christian A. Luber, Igor Paron, Nagarjuna Nagaraj, and Matthias Mann. 2014. “Accurate Proteome-Wide Label-Free Quantification by Delayed Normalization and Maximal Peptide Ratio Extraction, Termed MaxLFQ.” *Molecular & Cellular Proteomics* 13 (9): 2513–26.
- Cox, Jürgen, and Matthias Mann. 2008. “MaxQuant Enables High Peptide Identification Rates, Individualized p.p.b.-Range Mass Accuracies and Proteome-Wide Protein Quantification.” *Nature Biotechnology* 26 (12): 1367–72.
- Crossgrove, Kirsten, Cynthia A. Bayer, James W. Fristrom, and Gregory M. Guild. 1996. “The *Drosophila* Broad-Complex Early Gene Directly Regulates Late Gene Transcription during the Ecdysone-Induced Puffing Cascade.” *Developmental Biology* 180 (2): 745–58.
- Dansereau, David A., and Paul Lasko. 2008. “RanBPM Regulates Cell Shape, Arrangement, and Capacity of the Female Germline Stem Cell Niche in *Drosophila Melanogaster*.” *Journal of Cell Biology* 182 (5): 963–77.
- Davis, Melissa B., and Tongruei Li. 2013. “Genomic Analysis of the Ecdysone Steroid Signal at Metamorphosis Onset Using Ecdysoneless and EcRnull *Drosophila Melanogaster* Mutants.” *Genes and Genomics* 35 (1): 21–46.
- Fletcher, J C, K C Burtis, D S Hogness, and C S Thummel. 1995. “The *Drosophila* E74 Gene Is Required for Metamorphosis and Plays a Role in the Polytene Chromosome Puffing Response to Ecdysone.” *Development* (Cambridge, England) 121 (5): 1455–65.
- Gause, Maria, Joel C Eissenberg, Amy F Macrae, Maia Dorsett, Ziva Misulovin, and Dale Dorsett. 2006. “Nipped-A, the Tra1/TRRAP Subunit of the *Drosophila* SAGA and Tip60 Complexes, Has Multiple Roles in Notch Signaling during Wing Development.” *Molecular And Cellular Biology* 26 (6): 2347–59.
- Ghazalpour, Anatole, Brian Bennett, Vladislav A. Petyuk, Luz Orozco, Raffi

- Hagopian, Imran N. Mungrue, Charles R. Farber, et al. 2011. "Comparative Analysis of Proteome and Transcriptome Variation in Mouse." *PLoS Genetics* 7 (6).
- Gonsalves, Sarah E., Scott J. Neal, Amy S. Kehoe, and J. T. Westwood. 2011. "Genome-Wide Examination of the Transcriptional Response to Ecdysteroids 20-Hydroxyecdysone and Ponasterone A in *Drosophila Melanogaster*." *BMC Genomics* 12.
- Gorman, M, A Franke, and B S Baker. 1995. "Molecular Characterization of the Male-Specific Lethal-3 Gene and Investigations of the Regulation of Dosage Compensation in *Drosophila*." *Development* (Cambridge, England) 121 (2): 463–75.
- Gouw, J. W., Tops, B. B., Krijgsveld, J., Metabolic labeling of model organisms using heavy nitrogen (15N). *Methods Mol Biol* 2011, 753, 29-42
- Granderath, S, a Stollewerk, S Greig, C S Goodman, C J O'Kane, and C Klämbt. 1999. "Loco Encodes an RGS Protein Required for *Drosophila* Glial Differentiation." *Development* (Cambridge, England) 126 (8): 1781–91.
- Karim, F D, and C S Thummel. 1992. "Temporal Coordination of Regulatory Gene Expression by the Steroid Hormone Ecdysone." *The EMBO Journal* 11 (11): 4083–93.
- Karim, Felix D., and Carl S. Thummel. 1991. "Ecdysone Coordinates the Timing and Amounts of E74A and E74B Transcription in *Drosophila*." *Genes and Development* 5 (6): 1067–79.
- King-Jones, Kirst, Jean Philippe Charles, Geanette Lam, and Carl S. Thummel. 2005. "The Ecdysone-Induced DHR4 Orphan Nuclear Receptor Coordinates Growth and Maturation in *Drosophila*." *Cell* 121 (5): 773–84.
- Kiss, Istvan, Amy H Beaton, Jil Tardiff, Dianne Fristrom, and James W Fristrom. 1988. "Interactions and Developmental Effects." New York 259: 247–59.
- Knaap, Jan a van der, Elena Kozhevnikova, Karin Langenberg, Yuri M Moshkin, and C Peter Verrijzer. 2010. "Biosynthetic Enzyme GMP Synthetase Cooperates with Ubiquitin-Specific Protease 7 in Transcriptional Regulation of Ecdysteroid Target Genes." *Molecular and Cellular Biology* 30: 736–44.
- Kocks, Christine, Ju Hyun Cho, Nadine Nehme, Johanna Ulvila, Alan M. Pearson, Marie Meister, Charles Strom, et al. 2005. "Eater, a Transmembrane Protein Mediating Phagocytosis of Bacterial Pathogens in *Drosophila*." *Cell* 123 (2): 335–46.
- Koelle, Michael R., William S. Talbot, William A. Segraves, Michael T. Bender, Peter Cherbas, and David S. Hogness. 1991. "The *Drosophila* EcR Gene Encodes an Ecdysone Receptor, a New Member of the Steroid Receptor Superfamily." *Cell* 67 (1): 59–77.
- Koh, Tong Wey, Viktor I. Korolchuk, Yogesh P. Wairkar, Wei Jiao, Emma Evergren, Hongling Pan, Yi Zhou, et al. 2007. "Eps15 and Dap160 Control Synaptic Vesicle Membrane Retrieval and Synapse Development." *Journal of Cell Biology* 178 (2): 309–22.
- Kong, E. C., Allouche, L., Chapot, P. A., Vranizan, K., et al., Ethanol-regulated genes that contribute to ethanol sensitivity and rapid tolerance in *Drosophila*. *Alcoholism, clinical and experimental research* 2010, 34, 302-316
- Kugler, Jan-Michael, Jae-Sung Woo, Byung-Ha Oh, and Paul Lasko. 2010. "Regulation of *Drosophila* Vasa In Vivo through Paralogous Cullin-RING E3 Ligase Specificity Receptors." *Molecular And Cellular Biology* 30 (7): 1769–82.
- Lam, G T, C Jiang, and C S Thummel. 1997. "Coordination of Larval and Prepupal Gene Expression by the DHR3 Orphan Receptor during *Drosophila* Metamorphosis." *Development* (Cambridge, England) 124: 1757–69.
- Laurent, Jon M., Christine Vogel, Taejoon Kwon, Stephanie A. Craig, Daniel R. Boutz, Holly K. Huse, Kazunari Nozue, et al. 2010. "Protein Abundances Are More Conserved than mRNA Abundances across Diverse Taxa." *Proteomics* 10 (23): 4209–12.

- Lee, Nara, Hediye Erdjument-Bromage, Paul Tempst, Richard S Jones, and Yi Zhang. 2009. "The H3K4 Demethylase Lid Associates with and Inhibits Histone Deacetylase Rpd3." *Molecular And Cellular Biology* 29 (6): 1401–10.
- Livak, Kenneth J., and Thomas D. Schmittgen. 2001. "Analysis of Relative Gene Expression Data Using Real-Time Quantitative PCR and the 2- $\Delta\Delta$ CT Method." *Methods* 25 (4): 402–8.
- Lukacsovich, Tamas, Kazuya Yuge, Wakae Awano, Zoltan Asztalos, Shunzo Kondo, Naoto Juni, and Daisuke Yamamoto. 2003. "The Ken and Barbie Gene Encoding a Putative Transcription Factor with a BTB Domain and Three Zinc Finger Motifs Functions in Terminalia Development of *Drosophila*." *Archives of Insect Biochemistry and Physiology* 54 (2): 77–94.
- Maier, Tobias, Alexander Schmidt, Marc Güell, Sebastian Kühner, Anne Claude Gavin, Ruedi Aebersold, and Luis Serrano. 2011. "Quantification of mRNA and Protein and Integration with Protein Turnover in a Bacterium." *Molecular Systems Biology* 7 (511): 1–12.
- McClure, Kimberly D., Anne Sustar, and Gerold Schubiger. 2008. "Three Genes Control the Timing, the Site and the Size of Blastema Formation in *Drosophila*." *Developmental Biology* 319 (1): 68–77.
- Moshkin, Yuri M, Lisette Mohrmann, Wilfred F J van Ijcken, and C Peter Verrijzer. 2007. "Functional Differentiation of SWI/SNF Remodelers in Transcription and Cell Cycle Control." *Molecular and Cellular Biology* 27: 651–61.
- Neubueser, Dagmar, James T. Warren, Lawrence I. Gilbert, and Stephen M. Cohen. 2005. "Molting Defective Is Required for Ecdysone Biosynthesis." *Developmental Biology* 280 (2): 362–72.
- Neufeld, T. P., Genetic analysis of TOR signaling in *Drosophila*. *Current topics in microbiology and immunology* 2004, 279, 139-152
- Ntwasa, M., Egerton, M., Gay, N. J., Sequence and expression of *Drosophila* myristoyl-CoA: protein N-myristoyl transferase: evidence for proteolytic processing and membrane localisation. *Journal of cell science* 1997, 110 (Pt 2), 149-156
- Ohlmeyer, J. T. 2003. "Encore Facilitates SCF-Ubiquitin-Proteasome-Dependent Proteolysis during *Drosophila* Oogenesis." *Development* 130 (25): 6339–49.
- Palanker, Laura, Jason M Tennessen, Geanette Lam, and Carl S Thummel. 2009. "*Drosophila* HNF4 Regulates Lipid Mobilization and β -Oxidation." *Cell Metabolism* 9 (3): 228–39.
- Park, Sang Ki, Stacey A. Sedore, Claire Cronmiller, and Jay Hirsh. 2000. "Type II CAMP-Dependent Protein Kinase-Deficient *Drosophila* Are Viable but Show Developmental, Circadian, and Drug Response Phenotypes." *Journal of Biological Chemistry* 275 (27): 20588–96.
- Park, Youngji, Miki Fujioka, Masatomo Kobayashi, James B Jaynes, and Sumana Datta. 2001. "Even Skipped Is Required To Produce a Trans-Acting Signal for Larval Neuroblast Proliferation That Can Be Mimicked By Ecdysone." *Development* (Cambridge, England) 128 (10): 1899–1909.
- Restifo, Linda L., and Kalpana White. 1992. "Mutations in a Steroid Hormone-Regulated Gene Disrupt the Metamorphosis of Internal Tissues in *Drosophila*: Salivary Glands, Muscle, and Gut." Roux's *Archives of Developmental Biology* 201 (4): 221–34.
- Riddiford, L. M., Hormone receptors and the regulation of insect metamorphosis. *Receptor* 1993, 3, 203-209
- Rigbolt, Kristoffer T. G., Jens T. Vanselow, and Blagoy Blagoev. 2011. "GProX, a User-Friendly Platform for Bioinformatics Analysis and Visualization of Quantitative Proteomics Data." *Molecular & Cellular Proteomics* 10 (8): O110.007450.
- Sampson, Christopher J., Susanna Valanne, Marie Odile Fauvarque, Dan Hultmark, Mika Rämet, and Michael J. Williams. 2012. "The RhoGEF Zizimin-Related Acts in the *Drosophila* Cellular Immune Response via the Rho GTPases Rac2 and Cdc42."

- Developmental and Comparative Immunology* 38 (1): 160–68.
- Scholz, H., Franz, M., Heberlein, U., The hangover gene defines a stress pathway required for ethanol tolerance development. *Nature* 2005, 436, 845–847
- Schwanhüusser, Björn, Dorothea Busse, Na Li, Gunnar Dittmar, Johannes Schuchhardt, Jana Wolf, Wei Chen, and Matthias Selbach. 2011. “Global Quantification of Mammalian Gene Expression Control.” *Nature* 473 (7347): 337–42.
- Sedkov, Yuri, Elizabeth Cho, Svetlana Petruk, Lucy Cherbas, Sheryl T Smith, Richard S Jones, Peter Cherbas, Eli Canaani, James B Jaynes, and Alexander Mazo. 2003. “Methylation at Lysine 4 of Histone H3 in Ecdysone-Dependent Development of *Drosophila*.” *Nature* 426 (6962): 78–83.
- Sliter, T. J., and L. I. Gilbert. 1992. “Developmental Arrest and Ecdysteroid Deficiency Resulting from Mutations at the *Dre4* Locus of *Drosophila*.” *Genetics* 130 (3): 555–68.
- Stanyon, Clement A, Guozhen Liu, Bernardo A Mangiola, Nishi Patel, Loic Giot, Bing Kuang, Huamei Zhang, Jinhui Zhong, and Russell L Finley. 2004. “A *Drosophila* Protein-Interaction Map Centered on Cell-Cycle Regulators.” *Genome Biology* 5 (12).
- Stone, Bryan L., and Carl S. Thummel. 1993. “The *Drosophila* 78C Early Late Puff Contains E78, an Ecdysone-Inducible Gene That Encodes a Novel Member of the Nuclear Hormone Receptor Superfamily.” *Cell* 75 (2): 307–20.
- Sury, Matthias D, Jia-Xuan Chen, and Matthias Selbach. 2010. “The SILAC Fly Allows for Accurate Protein Quantification in Vivo.” *Molecular & Cellular Proteomics* 9 (10): 2173–83.
- Talbot, William S., Elizabeth A. Swyryd, and David S. Hogness. 1993. “*Drosophila* Tissues with Different Metamorphic Responses to Ecdysone Express Different Ecdysone Receptor Isoforms.” *Cell* 73 (7): 1323–37.
- Tang, H., S. B. Rompani, J. B. Atkins, Y. Zhou, T. Osterwalder, and W. Zhong. 2005. “Numb Proteins Specify Asymmetric Cell Fates via an Endocytosis- and Proteasome-Independent Pathway.” *Molecular and Cellular Biology* 25 (8): 2899–2909.
- Thummel, C. S. 2002. “Ecdysone-Regulated Puff Genes 2000.” *Insect Biochemistry and Molecular Biology* 32 (2): 113–20.
- Trapnell, Cole, Lior Pachter, and Steven L. Salzberg. 2009. “TopHat: Discovering Splice Junctions with RNA-Seq.” *Bioinformatics* 25 (9): 1105–11.
- Trapnell, Cole, Brian A. Williams, Geo Pertea, Ali Mortazavi, Gordon Kwan, Marijke J. Van Baren, Steven L. Salzberg, Barbara J. Wold, and Lior Pachter. 2010. “Transcript Assembly and Quantification by RNA-Seq Reveals Unannotated Transcripts and Isoform Switching during Cell Differentiation.” *Nature Biotechnology* 28 (5): 511–15.
- Warren, James T., Yoram Yerushalmi, Mary Jane Shimell, Michael B. O’Connor, Linda L. Restifo, and Lawrence I. Gilbert. 2006. “Discrete Pulses of Molting Hormone, 20-Hydroxyecdysone, during Late Larval Development of *Drosophila Melanogaster*: Correlations with Changes in Gene Activity.” *Developmental Dynamics* 235 (2): 315–26.
- Weiler, Karen S. 2007. “E(Var)3-9 of *Drosophila Melanogaster* Encodes a Zinc Finger Protein.” *Genetics* 177 (1): 167–78.
- Wismar, Jasmine, Negusse Habtemichael, James T. Warren, Ji Da Dai, Lawrence I. Gilbert, and Elisabeth Gateff. 2000. “The Mutation without Children(Rg1) Causes Ecdysteroid Deficiency in Third-Instar Larvae of *Drosophila Melanogaster*.” *Developmental Biology* 226 (1): 1–17.
- Woodard, Craig T., Eric H. Baehrecke, and Carl S. Thummel. 1994. “A Molecular Mechanism for the Stage Specificity of the *Drosophila* Prepupal Genetic Response to Ecdysone.” *Cell* 79 (4): 607–15.
- Wullschleger, Stephan, Robbie Loewith, and Michael N. Hall. 2006. “TOR Signaling in Growth and Metabolism.” *Cell* 124 (3): 471–84.

Chapter 6

Yao, Tso-Pang, Barry Marck Forman, Zeyu Jiang, Lucy Cherbas, J.-Don Chen, Michael McKeown, Peter Cherbas, and Ronald M. Evans. 1993. "Functional Ecdysone Receptor Is the Product of EcR and Ultraspiracle Genes." *Nature* 366: 476–79.

Zogłówek, Anna, Marek Orlowski, Szymon Pakula, Joanna Dutko-Gwóźdź, Dorota Pajdzik, Tomasz Gwóźdź, Grzegorz Rymarczyk, et al. 2012. "The Composite Nature of the Interaction between Nuclear Receptors EcR and DHR38." *Biological Chemistry* 393 (6): 457–71.

Chapter 7

General Discussion

Discussion

The 26S proteasome plays a central role in the cell through degradation of the majority of unneeded, damaged and misfolded proteins. Consequently, malfunctioning of this complex is associated with various diseases, such as cancer and neurodegenerative disorders. In this work we aimed to get a better understanding of 26S proteasome functioning and regulation under both normal conditions and stress conditions. We focused on identification of 19S/20S interaction partners, as well as monitoring global proteome and ubiquitinome dynamics under different cellular states. We also studied the function of three proteasome-bound deubiquitinating enzymes RPN11, UCHL5 and USP14. A minor part of this work focusses on the transcriptional and translational regulation of the ecdysone hormone which is important for insect development. A common feature in all chapters of this thesis is a solid detailed quantitative mass spectrometry-based analysis.

Chapter 6 describes how we used a comprehensive quantitative SILAC MS-based approach to study how the *Drosophila* proteome is affected upon treatment with a hormone, ecdysone, which is involved in many different regulatory processes. Cellular responses were monitored at three levels: global proteome dynamics, global transcriptome dynamics and finally interaction partners of the ecdysone receptors were identified. We found that the abundances of the far majority of proteins remained unchanged. There was a small subset of proteins that was up- or downregulated already at early time points, including two known early ecdysone responsive genes, *i.e.*, ecdysone-induced protein 71 (Eip71CD or Eip28/29) and BR-C. Increased abundance of BR-C was confirmed with WB. Other early responsive genes include eater, CG18765, mus309, regeneration (rgn) and glycine N-methyltransferase (CG6188). At later time points, the set of affected proteins expanded, but was still a relatively small fraction of the total (measurable) proteome. It remains to be confirmed whether these effects are direct or indirect.

Furthermore, we have compared changes upstream of the proteome *i.e.*, at the transcriptome level. We observed a substantial overlap in terms of affected targets between the dynamic proteome and transcriptome after ecdysteroid induction. However, effects in the proteome are usually delayed with respect to the changes in the transcriptome. Also, downregulation of mRNAs in many cases did not correlate to downregulation at the proteome level and in some cases there seemed to be no correlation between transcriptome and proteome dynamics whatsoever.

In order get a better understanding about ecdysone signaling induction we purified the ecdysone receptor from *Drosophila* embryo nuclear extracts. Proteins co-purified with EcR include factors involved in RNA Pol II dependent transcription and chromatin modifying enzymes. Also, several proteins previously linked to ecdysone signaling and/or biosynthesis were identified. However, the overlap between two different antibodies used for the purification of EcR was

poor. This might be partly explained by steric hindrance of EcR interactors which mask specific antibody epitopes. Using antibodies against the same epitope or against a tagged form of EcR might increase overlap of results.

Next, we turned towards a biochemical system that is supposed to have a large effect on the proteome and includes protein degradation: the 26S proteasome. Manipulation of this system directly affects the proteome, and therefore proteomic techniques, including mass spectrometry, are the methods of choice for readout.

In **Chapter 3** we analyzed the effect of chemical proteasome inhibition and 26S proteasome subunit knockdown (RPN11, Prosalph5 and Prosbeta6) on both the *Drosophila* S2 cell proteome and ubiquitinome. We showed that the global proteome and, to an even greater extent, the ubiquitinome were severely remodeled upon both treatments. We observed that increased protein fold changes were in concert with increased ubiquitination for the majority of the proteins, which suggests that these proteins accumulated as a result of proteasome inhibition or knockdown. However, new protein synthesis also led to increased protein fold changes in some cases, as observed by a 5h cycloheximide treatment. Pulsed SILAC would allow to discriminate between protein accumulation and protein synthesis also during longer incubation times (Schwanhäusser *et al.*, 2009). Protein fold changes were generally lower than diGly peptide fold changes, indicating that in general the increase in protein accumulation was much lower than the extent of ubiquitination. The difference between the responses of both (sub)proteomes may first of all be explained by the relatively low stoichiometry of ubiquitinated proteins, hence major changes in the ubiquitinome may not alter total protein levels. Second, ubiquitination is also involved in a variety of regulatory pathways other than protein degradation and may thus not (directly) affect protein levels (Kaiser *et al.*, 2011; Kim, Eric J Bennett, *et al.*, 2011; Komander and Rape, 2012). In several cases we observed differential ubiquitination dynamics at different lysine residues on the same protein, which may indicate that these are regulatory ubiquitination signals rather than signals for protein degradation.

It remains unclear which part of the ubiquitinome was covered in our screen, and in general it is not known what the size an entire ubiquitinome could be. We identified diGly peptides of 3077 proteins, on a total pool of 5899 identified proteins, suggesting that at least 52% of all unique proteins carry a ubiquitin modification (not including the stoichiometry of ubiquitinated proteins). Recently it was shown that about 75% of the proteins in HeLa lysates could be phosphorylated (Sharma *et al.*, 2014). This percentage of identified phosphoproteins has increased over the years in concert with improved sample preparation protocols and developments in high resolution quantitative mass spectrometry. In line with this it has been proposed that basically every protein could potentially be phosphorylated. We suggest that it would also not be unlikely that every protein should be able to become ubiquitinated. It is mainly for technical reasons that we don't have this proof yet to date. To our knowledge, we presented

here the first global ubiquitinome study upon proteasome malfunctioning in a fly cell line, and therefore our datasets might serve as a valuable repository of protein ubiquitination sites in *Drosophila*.

Taken together we showed that proteasome subunit knockdown could be used in combination with quantitative proteomics to study proteome and ubiquitinome dynamics upon proteasome malfunctioning. This approach would make it possible to functionally characterize specific proteasome subunits, such as the three deubiquitinating enzymes of the 26S proteasome. Understanding the functional mechanism of the proteasome in more detail will be helpful for the development of next generation proteasome inhibitors which could be used in the clinic. Already, proteome and ubiquitinome analyses have been applied to study the specific mode of action of the novel proteasome inhibitor Capzimin (Li *et al.*, 2017).

Finally, diGly peptide screens in combination with global proteome screens give a wealth of information about protein and ubiquitination dynamics in different experimental settings. Often, additional experiments are required to fully understand the nature of these changes.

In **Chapter 4** we studied the effect of proteasome-bound DUB knockdown on global proteome and ubiquitinome dynamics in order to identify DUB specificity in targeted 26S proteasome-dependent protein degradation. First, we showed by the use of Label Free Quantification-based interaction proteomics that USP14, in contrast to RPN11 and UCHL5, is a weak interactor of the proteasome in *Drosophila* S2 cells, which is in correlation with studies in mammalian cells (Elena Koulich, Xiaohua Li, 2008; Kuo and Goldberg, 2017). Next, we found that depletion of RPN11 destabilized the proteasome holocomplex and resulted in extensive remodeling of both the global proteome and ubiquitinome. Our finding that RPN11 is important for proteasome activity and stability is in agreement with published studies (Maytal-Kivity *et al.*, 2002; Verma *et al.*, 2002; Yao and Robert E. Cohen, 2002; Gallery *et al.*, 2007; Elena Koulich, Xiaohua Li, 2008; Finley, 2009). In contrast we found that depletion of UCHL5, USP14, or simultaneous depletion of both UCHL5 and USP14 did not show any effect whatsoever. These findings suggest that RPN11 plays an important role in proteasome-mediated protein degradation whereas the roles of UCHL5 and USP14 in general proteostasis remain unclear. It remains to be determined whether the effects found upon RPN11 depletion were the result of decreased RPN11 activity or of decreased protein levels, for instance by using RPN11 catalytic mutants. Additionally, proteasome-bound DUB knockdown did not affect levels of any polyubiquitin linkage type.

Despite extensive research, the role of USP14 and UCHL5 in proteasome dependent degradation is not yet clear. Proteasomes can efficiently degrade substrates without USP14 (Hanna *et al.*, 2006; Lee *et al.*, 2010; Kim and Goldberg, 2017). In one model, USP14 and UCHL5 could antagonize substrate degradation via their polyubiquitin trimming activity leading to dissociation of substrate from the proteasome prior to degradation (Lam *et al.*, 1997; Lee *et al.*, 2010; M. J. Lee *et al.*, 2011). This model is mainly based on *in vitro* degradation rates, for instance

of monoubiquitinated globin peptides and other lower-order conjugates upon isopeptidase inhibition by ubiquitin aldehyde (Lam *et al.*, 1997). Additionally, Finley and coworkers observed enhanced degradation of Cyclin B and of Sic1 upon chemical inhibition of USP14 with IU1 *in vitro*, and additionally, they observed reduced levels of tau, TDP-43 and ataxin-3 in murine embryonic fibroblasts upon IU1 treatment (Lee *et al.*, 2010). These results could however not be reproduced by Ortuno *et al.* (Ortuno, Carlisle and Miller, 2016). In contrast to the trimming hypothesis, it was recently found that USP14 rather cleaves chains en bloc, and specifically left one intact chain on proteasome substrates (Lee *et al.*, 2016). Altogether, our data is not in agreement with the model that describes USP14 and UCHL5 as proteins that regulate substrate degradation, for instance via Ub trimming, as we did not observe major protein abundance dynamics upon knockdown of UCHL5 and/or USP14.

The findings of our study are not in disagreement with the model that describes USP14/Ubp6 as a protein that can facilitate substrate degradation via non-catalytic induction of 19S structural changes. In this model ubiquitin-bound Ubp6/USP14 inhibits degradation-coupled RPN11-mediated *en bloc* deubiquitination of polyubiquitin chains (Hanna *et al.*, 2006; Peth, Besche and Goldberg, 2009; Aufderheide *et al.*, 2015; Bashore *et al.*, 2015). Furthermore, ubiquitin-bound Ubp6/USP14 causes the proteasome to adopt the substrate-engaged conformational state, which is characterized by the coaxial alignment of the RPT base subunits and the channel of the 20S CP, and moreover this state positions RPN11 close to the entrance of this channel (Matyskiela, Lander and Martin, 2013; Unverdorben *et al.*, 2014). Proteasomes which adopt the substrate-engaged state cannot process new substrates (Bashore *et al.*, 2015). Both mechanisms, locking the proteasome in the substrate-engaged state and inhibiting the deubiquitinating activity of RPN11, are mechanisms by which Ubp6/USP14 can delay substrate degradation (Aufderheide *et al.*, 2015; Bashore *et al.*, 2015). These mechanisms do not require the catalytic activity of Ubp6/USP14 but do require its ability to bind ubiquitin. The catalytic activity of Ubp6/USP14, on the other hand, plays a role ubiquitin recycling. Thus, these results suggest that Ubp6/USP14 acts as a timer to coordinate individual substrate processing steps at the proteasome. This suggests that Ubp6/USP14 facilitates, but not regulates, protein degradation and is important for ubiquitin recycling and maintenance of the free ubiquitin pool (Aufderheide *et al.*, 2015; Bashore *et al.*, 2015). The characteristic of Ubp6/USP14 to just temporarily delay substrate degradation, with just the purpose to correctly process the substrate *e.g.*, deubiquitination of polyubiquitin chains, might explain why we did not observe major global proteome dynamics upon knockdown of this enzyme. However, several studies have shown that either free ubiquitin (David S Leggett *et al.*, 2002; Chernova *et al.*, 2003; Hanna, Leggett and Finley, 2003) or ubiquitinated proteins such as cyclin B (Hanna *et al.*, 2006) undergo accelerated degradation by the proteasome in the absence of Ubp6. We did not focus onto Ub synthesis and degradation in our study, but we observed a stable pool of free ubiquitin monomers as well as a stable pool of total ubiquitin upon simultaneous KD of UCHL5 and USP14 (2xKD), suggesting

that ubiquitin regulation is not affected. It is important to note that the findings of this model with Ubp6 acting as a timer to delay the degradation of subsequent substrates by locking the proteasome in the substrate-engaged state and to inhibit RPN11 activity has been demonstrated in *S. cerevisiae*. This organism does not express an ortholog of UCHL5, and therefore this model might not be directly translatable to higher eukaryotes which express orthologs of both UCHL5 and USP14. Recently in mammalian cells it was shown that proteasome-bound USP14 inhibits ATP hydrolysis, substrate entry into the 20S particle and deubiquitination by RPN11 when no ubiquitinated substrates were bound, thus supporting the mechanism as described above for yeast (Kim and Goldberg, 2017).

Current experiments in our lab, which are however not part of this thesis, focus on more efficient depletion of UCHL5 and USP14 *i.e.*, gene knockouts, since it might be possible that the remainder fraction of these proteins after knockdown could still do the job. Furthermore, if only a small fraction of these DUBs is potentially active, then overexpression studies rather than knockdowns might reveal differences in protein or diGly peptide abundances. Another possibility is that the coverage of ubiquitination sites is still insufficient, although all ubiquitination sites of ubiquitin itself were reliably quantified. We are currently improving the coverage and sensitivity of the diGly IP assay in order to identify more diGly peptides and potential UCHL5 and USP14 KD responsive proteins (Van Der Wal *et al.*, 2018).

Chapter 5 describes the characterization of the (dynamic) interactome of 19S/26S proteasome complexes under both stress and non-stress conditions. Using both α -RPN8 and α -RPN10 antibodies we immunopurified 19S particles and interacting protein complexes including intact 26S proteasomes from *Drosophila* S2 cell lysates under non-stress conditions (DMSO/H₂O), ER stress (24h 1 μ M Tunicamycin), oxidative stress (30 min 1 μ M H₂O₂ or 24h 1 μ M H₂O₂), or upon proteasome inhibition (16h 50 μ M MG132/ 5 μ M Lact). Label Free Quantification (LFQ) based mass spectrometry was used to identify *bona fide* dynamic interaction partners. Identification of all constitutive 26S proteasome subunits, as well as a variety of known proteasome interactors, such as USP14, SEM1, ECM29 homolog and Thioredoxin-like, showed that we efficiently enriched for both 19S and 26S proteasomes in all purifications, thus independent of the imposed stress conditions. Our data gave novel insights into proteasome and interactome composition dynamics upon non-stress and stress conditions. For instance, Ub shuttle protein RAD23 was identified as a proteasome interactor only under non-stress conditions, while CG7546, a UBL domain containing protein of yet unknown function, interacted with the proteasome exclusively upon proteasome inhibition. CG7546 is structurally related to BAG6, a protein which targets pro-apoptotic proteins to RPN10 for subsequent proteasome-dependent degradation (Kikukawa *et al.*, 2005). Thus, CG7546 might be a shuttle factor involved in targeting substrates to the proteasome. In chapter 3 of this thesis we found that Ref(2)p was newly synthesized and upregulated in response to proteasome inhibition (Sap *et al.*, 2017). In chapter 5 we additionally demonstrate that the substrate shuttle Ref(2)p interacts

with the proteasome only upon treatment with proteasome inhibitors. This suggests that Ref(2)p functions as a substrate shuttle under cytotoxic stress condition when proteasome substrate loads are high. Moreover, proteasome activator PI31 interacted with the proteasome exclusively upon all tested stress conditions, while in non-stress conditions it only co-precipitated in α -RPN10 IP's. It was shown that PI31 can increase the activity of the proteasome when elevated levels of proteasome substrates are present (Bader *et al.*, 2011). Finally, heat shock proteins (HSP's) also interacted specifically upon stress conditions. HSP's function as chaperones that mediate proper folding of substrate proteins and could, for instance, facilitate proteasome-dependent degradation of misfolded proteins (Arndt, Rogon and Höhfeld, 2007; Kettern *et al.*, 2010). Additionally, HSP70 is also involved in both association and dissociation of 26S proteasome complexes, for example shortly after mild oxidative stress (Grune *et al.*, 2011). Finally, chaperones are also able to affect proteasome activity, for instance overexpression of HSP27 increases the activity of the proteasome upon stress induction by inflammatory cytokines and cytotoxic drugs (Parcellier *et al.*, 2003). Additionally, in chapter 3 of this thesis we observed new heat shock protein synthesis upon MG132/lact treatment in S2 cells (Sap *et al.*, 2017). Taken together, our data suggests that chaperones also play a role at the proteasome upon treatment with chemical proteasome inhibitors. Additional experiments are however required to proof this.

Besides the characterization of stress and non-stress specific 19S interactomes, we also analyzed the dynamics of these interactomes upon stress. Some of the treatments used could affect proteasome stability. We used relatively mild oxidative stress conditions in order to prevent destabilization of the 26S proteasome (Reinheckel *et al.*, 1998; Wang, Kaiser and Huang, 2011). We however purified more intact 26S proteasomes upon proteasome inhibition, which might be the result of improved proteasome stability through the use of proteasome inhibitors (Kleijnen *et al.*, 2007). We like to note that consequently enhanced enrichment of interacting partners upon proteasome inhibition could be the result of either enhanced recruitment or enhanced 26S proteasome levels.

Interestingly, more UCHL5 was recruited to the proteasome under stress conditions. In general, the role of UCHL5 at the proteasome has not been clearly defined yet but it is proposed to edit proteasome substrate-bound polyubiquitin chains (Lam *et al.*, 1997), deubiquitinate proteasome subunits (Jacobson *et al.*, 2014), or remove unanchored polyubiquitin chains *en bloc* (Zhang *et al.*, 2011). For more information see Chapter 4 of this thesis. These are different ways in which UHL5 might influence proteasome-mediated degradation and our data suggests that stress conditions could enhance these activities by recruiting more UCHL5 enzymes to proteasomes.

In this study we analyzed the response of the 19S/26S proteasome interactome after several different stressors. The majority of the interactors associated with the proteasome during all conditions, several were interacting upon all stress conditions, while we found only few interactors which were specifically interacting upon specific stress conditions. There may be

several explanations for the latter case. First, cross-talk between the different stress conditions makes it difficult to distinguish specific responses for each individual condition (Bush, Goldberg and Nigam, 1997; Lee *et al.*, 2003; Fribley, Zeng and Wang, 2004; Obeng *et al.*, 2006; Osowski and Urano, 2013). Second, proteins which respond to specific stress conditions may be transient interaction partners which were not captured using IP and LFQ-based proteomics but could be picked up with techniques such as BioID (Varnaite and MacNeill, 2016) and APEX (Kim and Roux, 2016). Thirdly, specific responders might interact with other proteasome caps than 19S caps that were the focus of this study, such as PA28 $\alpha\beta$, PA28 γ , PA200, PI31, or with solely the standard 20S proteasome or the immunoproteasome.

Finally, our data show that classical immune purifications in combination with LFQ-based quantitative proteomics is a powerful approach to specifically detect (sub)stoichiometric interaction partners, as well as dynamic interactors, of a large and important cellular machinery such as the proteasome. We identified several proteasome interactors, which showed a different interaction behavior upon different stress conditions, such as UCHL5, RAD23, CG7546 and Ref(2)p. Differential proteasome interactors upon specific stressors may be potential therapeutic targets for the treatment of diseases in which cellular stress and homeostasis misbalance play a role. Further research is required to elucidate their function in proteasome-dependent degradation in conditions with and without stress.

Concluding remarks

A large part of this work includes global proteome and ubiquitinome analyses following proteasome inhibition or proteasome subunit/DUB knockdown. These types of analyses could be the basis for further research, for instance in the field of drug development. In principle, a global ubiquitinome screen of cells treated with and without protein knockdown of a specific DUB may reveal the target proteins for this enzyme, *i.e.*, more diGly peptides derived from the target proteins would be found upon DUB knockdown as compared to samples which were not treated this way. Additionally, knockdown of a ubiquitin ligase would result in a decreased amount of diGly peptides derived from its substrate proteins. Unfortunately, we were unable to identify targets for UCHL5 and USP14 with this method, however, a combination with protein knockout (instead of knockdown) appears to be more promising (unpublished data of our lab). Several examples for DUB or Ub ligase target discovery by means of protein knockdown/knockout/overexpression and quantitative proteomics could be found in the literature (K. A. Lee *et al.*, 2011; Thompson *et al.*, 2014; Potu *et al.*, 2017). Vectors used for protein knockdown or protein knockout are relatively easy to design, since these are based on the DNA sequence which is available for all standard model organisms. Design of very specific small molecules and compounds faces extra challenges due to the diverse nature of proteins in terms of splice variants, PTM's, conformational changes and complex compositions. Hence, with the use of protein knockdown or knockout we could in principle target all single proteasome subunits and analyze the effect of loss of individual subunits on protein degradation. Also, global

proteome and ubiquitinome screens (or other PTM's) of samples treated for protein knockdown or knockout could be compared to similar screens obtained from samples treated with new compounds or small molecules targeting the same protein of interest. In this way the specificity and off-target effects of the compounds could be investigated. Obviously, in the field of drug development small molecules and compounds are preferred over methods to target the DNA or RNA level due to the possibility of oral administration.

Over the past two decades, we saw rapid developments in mass spectrometry instrumentation and analysis strategies. Several years back it was an achievement to identify ~5000 proteins in a single experiment, while specialized labs with the use of state-of-the-art equipment (and extensive sample preparation) could now identify > 12.000 proteins in a single run (Hosp *et al.*, 2017). It is estimated that the depth of proteome coverage by mass spectrometry could reach the comprehensiveness of transcriptome coverage as analyzed by next generation sequencing (Richards, Merrill and Coon, 2015). Increased proteome coverage will open up new possibilities for mass spectrometry-based research, such as the study of proteoforms *i.e.*, the different molecular forms of proteins such as alternative splice variants, single nucleotide polymorphisms, or post-translational modifications (PTMs) (Nedelkov, 2017). Also, the proteogenomics niche, *i.e.*, the integration of genomics, transcriptomics and proteomics will benefit from enhanced proteome coverage. The proteogenomics field studies the relationship between DNA sequence and the global proteome, for instance the effect of DNA mutations, genetic variation and genetic diseases on the global proteome (Barbieri *et al.*, 2016; Menschaert and Fenyő, 2017). Proteomics research would also be a valuable application in the clinic, for instance for the purpose of precision medicine, in which treatment strategies will be based on patient-specific characteristics derived from different 'omics' platforms instead of a 'one disease – one treatment' strategy. Comparative proteomics of the proteome of the patient versus a database average, or in the future, of a patient's recorded healthy proteome and its current proteome during disease has the potential to greatly increase diagnostic accuracy. Hurdles that have to be overcome in realizing the goal of precision medicine include improving high throughput mass spectrometry, while maintaining robustness, reproducibility and sensitivity. Speeding up the data analysis is necessary, for instance by using automated analysis pipelines, and effective handling and storing of big data is required. Lastly, funding should become better available for multidisciplinary, multi-institutional and often multinational research groups (Nice, 2016). We expect that proteomic research will take a more prominent position in the clinic within the next decade.

For this project we performed a substantial number of large scale global mass spectrometry-based analyses. More than once the extent of changes measured between different samples appeared to be lower than we expected, for instance in our first study in which cells were treated for different durations with the ecdysone hormone (Chapter 6). We then changed the focus of our research to the process of proteasome-dependent protein degradation, a central pathway in the cell which operates directly at the protein level. Upon inhibition of this important pathway

we could measure extensive dynamics of both the global proteome and ubiquitinome, approving the suitability of the used method. We also showed that we could induce extensive changes in the global proteome and ubiquitinome by the use of protein knockdown, first with simultaneous knockdown of RPN11, Prosalpha5 and Prosbeta6, and later with RPN11 alone. However, these extents of changes appeared to be rather exceptional as other treatments, such as knockdown of USP14, UCHL5 or knockdown of both simultaneously did not seem to have much effect on global proteome or ubiquitinome dynamics. We also did not observe many changes in the 26S proteasome interactome upon different stress conditions. Thus, overall global proteome changes as measured by such mass spectrometry-based analyses were in many cases rather stable. From a biological point of view this may however be advantageous. This should be kept in mind when considering the application of these type of large time-consuming and expensive projects. Also, often interdisciplinary collaborations are required to answer mechanistic oriented biological questions.

References

- Arndt, V., Rogon, C. and Höhfeld, J. (2007) 'To be, or not to be - Molecular chaperones in protein degradation', *Cellular and Molecular Life Sciences*, 64(19–20), pp. 2525–2541.
- Aufderheide, A. *et al.* (2015) 'Structural characterization of the interaction of Ubp6 with the 26S proteasome.', *Proceedings of the National Academy of Sciences of the United States of America*, 112(28), pp. 8626–31.
- Bader, M. *et al.* (2011) 'A conserved F box regulatory complex controls proteasome activity in *Drosophila*', *Cell*. Elsevier, 145(3), pp. 371–382.
- Barbicri, R. *et al.* (2016) 'Proteogenomics', in *Proteogenomics, Advances in Experimental Medicine and Biology*, pp. 21–47.
- Bashore, C. *et al.* (2015) 'Ubp6 deubiquitinase controls conformational dynamics and substrate degradation of the 26S proteasome', *Nature Structural & Molecular Biology*. Nature Publishing Group, 22(9), pp. 712–719.
- Bush, K. T., Goldberg, A. L. and Nigam, S. K. (1997) 'Proteasome Inhibition Leads to a Heat-shock Response , Induction of Endoplasmic Reticulum Chaperones , and Thermotolerance', *The Journal of biological chemistry*, 272(14), pp. 9086–9092.
- Chernova, T. A. *et al.* (2003) 'Pleiotropic Effects of Ubp6 Loss on Drug Sensitivities and Yeast Prion Are Due to Depletion of the Free Ubiquitin Pool', *Journal of Biological Chemistry*. in Press, 278(52), pp. 52102–52115.
- Elena Koulich, Xiaohua Li, and G. N. D. (2008) 'Relative Structural and Functional Roles of Multiple Deubiquitylating Proteins Associated with Mammalian 26S Proteasome', *Molecular biology of the cell*, 19, pp. 1072–1082.
- Finley, D. (2009) 'Recognition and Processing of Ubiquitin-Protein Conjugates by the Proteasome', *Annual review of biochemistry*, pp. 477–513
- Fribley, A., Zeng, Q. and Wang, C. (2004) 'Proteasome Inhibitor PS-341 Induces Apoptosis through Induction of Endoplasmic Reticulum Stress-Reactive Oxygen Species in Head and Neck Squamous Cell Carcinoma Cells', *Society*, 24(22), pp. 9695–9704.
- Gallery, M. *et al.* (2007) 'The JAMM motif of human deubiquitinase Poh1 is essential for cell

- viability', *Molecular Cancer Therapeutics*, 6(1), pp. 262–268.
- Grune, T. *et al.* (2011) 'HSP70 mediates dissociation and reassociation of the 26S proteasome during adaptation to oxidative stress', *Free Radical Biology and Medicine*, 51(7), pp. 1355–1364.
- Hanna, J. *et al.* (2006) 'Deubiquitinating Enzyme Ubp6 Functions Noncatalytically to Delay Proteasomal Degradation', *Cell*, 127(1), pp. 99–111.
- Hanna, J., Leggett, D. S. and Finley, D. (2003) 'Ubiquitin depletion as a key mediator of toxicity by translational inhibitors', *Molecular and Cellular Biology*, 23(24), pp. 9251–9261.
- Hosp, F. *et al.* (2017) 'Spatiotemporal Proteomic Profiling of Huntington's Disease Inclusions Reveals Widespread Loss of Protein Function.', *Cell reports*. Elsevier, 21(8), pp. 2291–2303.
- Jacobson, A. D. *et al.* (2014) 'Autoregulation of the 26S proteasome by in situ ubiquitination.', *Molecular biology of the cell*, 25(12), pp. 1824–35.
- Kaiser, S. E. *et al.* (2011) 'Protein standard absolute quantification (PSAQ) method for the measurement of cellular ubiquitin pools.', *Nature methods*, 8(8), pp. 691–6.
- Kettern, N. *et al.* (2010) 'Chaperone-assisted degradation: Multiple paths to destruction', *Biological Chemistry*, 391(5), pp. 481–489.
- Kikukawa, Y. *et al.* (2005) 'Unique proteasome subunit Xrpn 10c is a specific receptor for the antiapoptotic ubiquitin-like protein Scythe', *FEBS Journal*. Blackwell Science Ltd, 272(24), pp. 6373–6386.
- Kim, D. I. and Roux, K. J. (2016) 'Filling the Void: Proximity-Based Labeling of Proteins in Living Cells', *Trends in Cell Biology*. Elsevier Ltd, 26(11), pp. 804–817.
- Kim, H. T. and Goldberg, A. L. (2017) 'The Deubiquitinating Enzyme Usp14 Allosterically Inhibits Multiple Proteasomal Activities and Ubiquitin-Independent Proteolysis.', *The Journal of biological chemistry*, (3), p. jbc.M116.763128.
- Kim, W., Bennett, E. J., *et al.* (2011) 'Systematic and Quantitative Assessment of the Ubiquitin-Modified Proteome', *Molecular Cell*. Elsevier Inc., 44(2), pp. 325–340.
- Kleijnen, M. F. *et al.* (2007) 'Stability of the proteasome can be regulated allosterically through engagement of its proteolytic active sites.', *Nature structural & molecular biology*, 14(12), pp. 1180–8.
- Komander, D. and Rape, M. (2012) 'The Ubiquitin Code', *Annual Review of Biochemistry*, 81(1), pp. 203–229.
- Kuo, C.-L. and Goldberg, A. L. (2017) 'Ubiquitinated proteins promote the association of proteasomes with the deubiquitinating enzyme Usp14 and the ubiquitin ligase Ubc3c', *Proceedings of the National Academy of Sciences*, 114(17), pp. E3404–E3413.
- Lam, Y. A. *et al.* (1997) 'Editing of ubiquitin conjugates by an isopeptidase in the 26S proteasome.', *Nature*, pp. 737–740.
- Lee, A.-H. *et al.* (2003) 'Proteasome inhibitors disrupt the unfolded protein response in myeloma cells.', *Proceedings of the National Academy of Sciences of the United States of America*. National Academy of Sciences, 100(17), pp. 9946–51.
- Lee, B.-H. *et al.* (2010) 'Enhancement of proteasome activity by a small-molecule inhibitor of USP14', *Nature*. Nature Publishing Group, 467(7312), pp. 179–184.
- Lee, B.-H. *et al.* (2016) 'USP14 deubiquitinates proteasome-bound substrates that are ubiquitinated at multiple sites', *Nature*. Nature Publishing Group, pp. 1–16.
- Lee, K. A. *et al.* (2011) 'Ubiquitin ligase substrate identification through quantitative proteomics at both the protein and peptide levels', *Journal of Biological Chemistry*, 286(48), pp. 41530–41538.
- Lee, M. J. *et al.* (2011) 'Trimming of ubiquitin chains by proteasome-associated deubiquitinating enzymes.', *Molecular & cellular proteomics: MCP*, 10(5), p. R110.003871.
- Leggett, D. S. *et al.* (2002) 'Multiple associated proteins regulate proteasome structure and function', *Molecular Cell*, 10(3), pp. 495–507.

- Li, J. *et al.* (2017) 'Capzimin is a potent and specific inhibitor of proteasome isopeptidase Rpn11', *Nature Chemical Biology*, 13(5), pp. 486–493.
- Matyskiela, M. E., Lander, G. C. and Martin, A. (2013) 'Conformational switching of the 26S proteasome enables substrate degradation.', *Nature structural & molecular biology*. Nature Publishing Group, 20(7), pp. 781–8.
- Maytal-Kivity, V. *et al.* (2002) 'MPN+, a putative catalytic motif found in a subset of MPN domain proteins from eukaryotes and prokaryotes, is critical for Rpn11 function.', *BMC biochemistry*, 3, p. 28.
- Menschaert, G. and Fenyő, D. (2017) 'Proteogenomics from a bioinformatics angle: A growing field', *Mass Spectrometry Reviews*, 36(5), pp. 584–599.
- Nedelkov, D. (2017) 'Human proteoforms as new targets for clinical mass spectrometry protein tests', *Expert Review of Proteomics*. Taylor & Francis, 14(8), pp. 691–699.
- Nice, E. C. (2016) 'From proteomics to personalized medicine: the road ahead', *Expert Review of Proteomics*. Taylor & Francis, 13(4), pp. 341–343.
- Obeng, E. A. *et al.* (2006) 'Proteasome inhibitors induce a terminal unfolded protein response in multiple myeloma cells.', *Blood*, 107(12), pp. 4907–4916.
- Ortuno, D., Carlisle, H. J. and Miller, S. (2016) 'Does inactivation of USP14 enhance degradation of proteasomal substrates that are associated with neurodegenerative diseases? *F1000Research* 5(137).
- Osowski, C. M. and Urano, F. (2013) 'Measuring ER stress and the unfolded protein response using mammalian tissue culture system', *Methods in Enzymology*, 490(508), pp. 71–92.
- Parcellier, A. *et al.* (2003) 'HSP27 is a ubiquitin-binding protein involved in I-kappaBalpha proteasomal degradation.', *Molecular and cellular biology*, 23(16), pp. 5790–5802.
- Peth, A., Besche, H. C. and Goldberg, A. L. (2009) 'Ubiquitinated Proteins Activate the Proteasome by Binding to Usp14/Ubp6, which Causes 20S Gate Opening', *Molecular Cell*, 36(5), pp. 794–804.
- Potu, H. *et al.* (2017) 'Usp9x regulates Ets-1 ubiquitination and stability to control NRAS expression and tumorigenicity in melanoma'. *Nature Communications* vol.8.
- Reinheckel, T. *et al.* (1998) 'Comparative resistance of the 20S and 26S proteasome to oxidative stress.', *The Biochemical journal*, 335 (Pt 3, pp. 637–42.
- Richards, A. L., Merrill, A. E. and Coon, J. J. (2015) 'Proteome sequencing goes deep', *Current Opinion in Chemical Biology*, pp. 11–17.
- Sap, K. A. *et al.* (2017) 'Quantitative Proteomics Reveals Extensive Changes in the Ubiquitinome after Perturbation of the Proteasome by Targeted dsRNA-Mediated Subunit Knockdown in Drosophila', *Journal of Proteome Research*, 16(8), pp. 2848–2862.
- Schwanhäusser, B. *et al.* (2009) 'Global analysis of cellular protein translation by pulsed SILAC', *Proteomics*. WILEY- VCH Verlag, 9(1), pp. 205–209.
- Sharma, K. *et al.* (2014) 'Ultradeep Human Phosphoproteome Reveals a Distinct Regulatory Nature of Tyr and Ser/Thr-Based Signaling', *CellReports*, 8, pp. 1583–1594.
- Thompson, J. W. *et al.* (2014) 'Quantitative Lys-ε-Gly-Gly (diGly) proteomics coupled with inducible RNAi reveals ubiquitin-mediated proteolysis of DNA damage-inducible transcript 4 (DDIT4) by the E3 Ligase HUWE1', *Journal of Biological Chemistry*, 289(42), pp. 28942–28955.
- Unverdorben, P. *et al.* (2014) 'Deep classification of a large cryo-EM dataset defines the conformational landscape of the 26S proteasome.', *Proceedings of the National Academy of Sciences of the United States of America*, 111(15), pp. 5544–9.
- Varnaite, R. and MacNeill, S. A. (2016) 'Meet the neighbors: Mapping local protein interactomes by proximity-dependent labeling with BioID', *Proteomics*, 16(19), pp. 2503–2518.

Verma, R. *et al.* (2002) 'Role of Rpn11 Metalloprotease in Deubiquitination and Degradation by the 26S Proteasome', *Science*, 298(5593), pp. 611–615.

Van Der Wal, L. *et al.* (2018) 'Improvement of ubiquitylation site detection by Orbitrap mass spectrometry', *Journal of Proteomics*, 172, pp. 49–56.

Wang, X. Y. J., Kaiser, P. and Huang, L. (2011) 'Regulation of the 26S proteasome complex during oxidative stress', 3(151), pp. 1–17.

Yao, T. and Cohen, R. E. (2002) 'A cryptic protease couples deubiquitination and degradation by the proteasome.', *Nature*, 419(6905), pp. 403–407.

Zhang, N. Y. *et al.* (2011) 'Ubiquitin chain trimming recycles the substrate binding sites of the 26 S proteasome and promotes degradation of lysine 48-linked polyubiquitin conjugates', *Journal of Biological Chemistry*, 286(29), pp. 25540–25546.

Appendix

Summary

Nederlandse samenvatting

Curriculum Vitae

List of Publications

Portfolio

Dankwoord

Summary

The 26S proteasome complex plays a central role in the cell through its major function in the selective degradation of ubiquitinated proteins. Consequently, malfunctioning of this protein complex could result in the development of diseases such as cancer or neurodegenerative disorders. Inhibition of proteasome activity with chemical inhibitors is used for the treatment of multiple myeloma patients, however the biological mechanism behind this type of treatments are not fully understood. In the research described in **chapter 3** we aimed to get more insight in the cellular response at both the proteome and ubiquitinome level upon inactivation of the proteasome in *Drosophila* S2 cells. Chemical inhibition through MG132 and Lactacystin (MG132/Lact) or proteasome subunit knockdown (KD) of Prosalpha5, Prosbeta6 and RPN11 were used for proteasome inactivation, while the effect on the proteome and ubiquitinome were monitored through the use of a SILAC-based quantitative mass spectrometry approach. Proteome changes ranged between approximately 4% (4hrs MG132/Lact) and 10% (16hrs MG132/Lact, 2 and 4 days KD), which were either the result of protein accumulation or *de novo* protein synthesis of for instance stress responsive proteins. Next, we focused on global ubiquitinome dynamics. Over all SILAC experiments we identified over 14,000 unique diGly peptides (which are derived from ubiquitinated proteins) of which approximately 70% displayed increased abundances upon proteasome inactivation. Data from the different conditions greatly overlapped with increased ubiquitination observed for proteins involved in diverse processes such as cell cycle regulation, (ubiquitin-dependent) protein catabolism, cytoskeleton and mitotic spindle organization, apoptosis, proteolysis and metabolism. Overall, increased protein fold changes were accompanied by increased diGly peptide fold changes, which is also expected when ubiquitinated proteins accumulate due to proteasome inactivation. However, there were also exceptions, of which the basis may be found in other signaling events. In conclusion, we showed that we could mimic chemical proteasome inhibition through the use of dsRNA-mediated knockdown of specific proteasome subunits. Both treatments resulted in a similar extent of proteome and ubiquitinome dynamics, mainly resulting from (ubiquitinated) proteins present with increased fold changes as a result of either protein accumulation or *de novo* protein synthesis. This approach offers possibilities for the investigation of each individual the proteasome complex component in detail.

In **chapter 4** we applied a similar strategy as used in chapter 3, now with the aim to acquire more insight in the role and specificity of the three proteasome-bound deubiquitinating enzymes (DUBs) in proteasome-mediated degradation. We performed dsRNA-mediated knockdown of USP14, UCHL5 and RPN11 followed by large scale SILAC proteomics, ubiquitinome analysis and label free quantitative mass spectrometry. Our data suggest that RPN11 is important for the stability and function of the 26S proteasome complex and is essential for the degradation of the large majority of proteasome substrates. In contrast, knockdown of UCHL5, USP14 or

simultaneous knockdown of both did not alter the stability of the proteasome, nor did it have an observable effect on global protein or diGly peptide abundances. Thus, while we observed many targets for deubiquitination via RPN11, no specific substrates for USP14 or UCHL5 were identified. Also, poly-ubiquitin linkage type analysis did not reveal specificity towards a specific linkage type for any of the DUBs. In conclusion, our data imply that RPN11 is the major DUB for proteasome-mediated protein degradation while the role of UCHL5 and USP14 remains unclear.

In **chapter 5** we investigated how the proteasome adapts to different intracellular environments by characterizing its dynamic interactomes under several stress conditions. Applied stress conditions include oxidative stress (H_2O_2), endoplasmic reticulum (ER) stress (Tunicamycin) and cytotoxic stress (proteasome inhibitors MG132/Lact). Proteasomes were purified from *Drosophila* S2 cell lysates using antibodies for Rpn8 and Rpn10 and Label Free quantitative mass spectrometry of triplicate samples was used to characterize interaction partners of the 19S/26S proteasome. Enhanced association of 20S core particles and several proteins, including Hsp23, Hsp68, REG (PA28) and Ref(2)p, as well as a putative novel UBL-domain containing Ub shuttle protein CG7546 (Human Bat3) with the 19S cap were observed upon MG132/Lact treatment. In contrast, Ub shuttle protein Rad23 associated with the 19S/26S proteasome only under non-stress conditions. Finally, deubiquitinating enzyme UCHL5 was an interaction partner of the proteasome under all tested conditions, however it was clearly recruited less under non-stress conditions. Further research is required to elucidate the role of enhanced recruitment of UCHL5 at proteasomes under stress conditions. Together, these data give more insight in the dynamics of proteasome-mediated protein degradation under different intracellular conditions, which might be relevant for the understanding of proteasome functioning and regulation in disease states.

Ecdysone is a hormone which plays an important role in insect development. This hormone induces ecdysone-responsive gene expression through interaction with its nuclear receptor (EcR). With the research described in **chapter 6** we aimed to gain more in-depth knowledge about different levels of the ecdysone-signaling pathway. Using a RNA sequencing or a SILAC-based global proteomics approach we monitored and compared global transcriptome resp. global proteome dynamics at different time points after ecdysone stimulation. We identified both known and unknown ecdysone-responsive genes and proteins, however there were clear timing differences between the transcriptional and translational response, which made it difficult to correlate mRNA with proteins at the same time points. We also analyzed the EcR interactome after ecdysone stimulation, and identified proteins with a role in ecdysone signaling, ecdysone biosynthesis, transcription, chromatin remodeling, and other proteins as interaction partners. Novel ecdysone responsive genes, proteins and EcR interaction partners identified in this study would be interesting targets for further detailed (biochemical) studies in cell culture or in the fly.

Nederlandse samenvatting

Het 26S proteasoom complex speelt een centrale rol in de cel door zijn belangrijke functie in de selectieve afbraak van geubiquitineerde eiwitten. Als dit belangrijke eiwit complex niet meer goed functioneert, kan dat resulteren in de ontwikkeling van ziektes zoals kanker of neurodegeneratie. Daarentegen kan het blokkeren van de activiteit van dit complex in sommige gevallen juist gebruikt worden voor de behandeling van patiënten, bijvoorbeeld voor patiënten met de ziekte van Kahler (multipel myeloom). Het biologische mechanisme achter dit type van behandeling is nog niet helemaal bekend. Het doel van ons onderzoek wat beschreven is in **hoofdstuk 3** was om meer inzicht te krijgen in de reactie van de cel na blokkering van het proteasoom. We hebben een analyse gedaan in cellen van een fruitvlieg (S2 cellen) op het niveau van het proteoom (verzameling van alle gemeten eiwitten) en het ubiquitinoom (verzameling van alle gemeten geubiquitineerde eiwitten/diGly peptiden). De kanttekening die we hier willen maken is dat we in deze samenvatting wel spreken over het meten van geubiquitineerde eiwitten omdat dat begrijpelijker klinkt, maar in wezen hebben we diGly peptiden gemeten welke afkomstig zijn van geubiquitineerde eiwitten na digestie met het enzym trypsine. We hebben 2 verschillende manieren gebruikt om het proteasoom te blokkeren. Ten eerste hebben we de veelgebruikte chemische blokkers MG132 en Lactacystine (MG132/Lact) gebruikt. Ten tweede hebben we dubbelstrengs RNA gebruikt voor 3 onderdelen van het proteasoom (Prosalph5, Prosbeta6 en RPN11), wat zorgt voor het post-transcriptioneel verminderen van genexpressie voor deze specifieke onderdelen. Het effect van deze behandelingen op het proteoom en ubiquitinoom werd gemonitord door gebruik te maken van een op SILAC-gebaseerde methode van kwantitatieve massaspectrometrie. Hiermee kunnen we zien welke eiwitten, respectievelijk geubiquitineerde eiwitten, relatief meer of minder aanwezig waren na een behandeling. Na een korte behandeling (4 uur MG132/Lact) zagen we relatieve veranderingen in ongeveer 4% van het proteoom en na lange behandelingen (16 uur MG132/Lact, 2 en 4 dagen vermindering van genexpressie) zagen we relatieve veranderingen in ongeveer 10% van het proteoom. Dit was het gevolg van eiwit ophoping of van eiwit synthese, bijvoorbeeld van eiwitten die reageren op stress. Daarna hebben we gekeken naar relatieve veranderingen in het ubiquitinoom. Met alle SILAC experimenten bij elkaar hebben we meer dan 14000 unieke diGly peptiden geïdentificeerd, waarvan ongeveer 70% meer aanwezig was na blokkering van het proteasoom. Eiwitten die meer geubiquitineerd waren speelden een rol in verschillende processen zoals de regulatie van de celcyclus, (ubiquitine-afhankelijke) eiwit katabolisme, de organisatie van het cytoskelet en de spoelfiguur, apoptose, proteolyse en metabolisme. Over het algemeen waren eiwitten die relatief meer aanwezig waren na de behandelingen ook meer geubiquitineerd, wat ook de verwachting was als geubiquitineerde eiwitten ophopen als gevolg van de inactivatie van het proteasoom. Er waren echter ook uitzonderingen, waarvan de basis waarschijnlijk gevonden kan worden in andere signaal transductie paden. We kunnen concluderen dat we de chemische proteasoom blokkering konden nabootsen door gebruik te maken van specifieke vermindering van

genexpressie met behulp van dubbelstrengs RNA voor specifieke onderdelen van het proteasoom. Beide behandelingen resulteerden in vergelijkbare mate van proteoom en ubiquitinoom dynamiek, wat vooral het gevolg was van (geubiquitineerde) eiwitten die meer aanwezig waren als gevolg van eiwit ophoping of synthese. Deze methode biedt mogelijkheden voor het in detail onderzoeken van de individuele onderdelen van het proteasoom.

In **hoofdstuk 4** hebben we dezelfde strategie toegepast als in hoofdstuk 3, nu met het doel om meer inzicht te krijgen in de rol en de specificiteit van de drie proteasoom-gebonden deubiquitinerings enzymen in proteasoom-afhankelijke eiwit afbraak. We hebben dubbelstrengs RNA gebruikt voor vermindering van genexpressie voor USP14, UCHL5 en RPN11. We hebben daarna gekeken naar relatieve veranderingen in het proteoom en ubiquitinoom door gebruik te maken van kwantitatieve massaspectrometrie met behulp van SILAC. Daarnaast hebben we ook biochemische technieken gebruikt. Onze data laat zien dat RPN11 belangrijk is voor de stabiliteit en de functie van het 26S proteasoom complex en dat het essentieel is voor de afbraak van het merendeel van de eiwitten. Daarentegen had vermindering van genexpressie van UCHL5 en/of USP14 geen effect op de stabiliteit van het proteasoom en ook niet op relatieve veranderingen van het proteoom of ubiquitinoom. We hebben dus heel veel eiwitten geïdentificeerd die RPN11 nodig hebben om afgebroken te worden door de proteasoom, terwijl we geen eiwitten hebben gevonden die UCHL5 en/of USP14 nodig hebben. Eiwitten worden vaak door middel van ubiquitine ketens naar het proteasoom gestuurd. We hebben gekeken naar de verbindingen tussen de ubiquitine moleculen in ketens maar we konden geen voorkeur voor specifieke verbindingstypen voor deze DUBs vinden. Samenvattend suggereert onze data dat RPN11 de belangrijkste DUB is voor proteasoom afhankelijke eiwit afbraak terwijl de rol van UCHL5 en USP14 in dit proces nog onduidelijk blijft.

Het milieu binnen cellen is dynamisch en kan bijvoorbeeld veranderen tijdens ziekte of stress. In **hoofdstuk 5** onderzochten we hoe het proteasoom zich aanpast als het milieu binnen de cel veranderd. Eiwitten werken nooit alleen, ze werken altijd samen met andere eiwitten. We hebben hier gekeken of er andere eiwitten aan het proteasoom binden onder verschillende stress condities. De toegepaste stress condities waren oxidatieve stress (H_2O_2), endoplasmatisch reticulum (ER) stress (Tunicamycine) en cytotoxische stress (proteasoom blokkers MG132/Lact). We hebben proteasomen gezuiverd uit *Drosophila* S2 cellysaten door gebruik te maken van antilichamen tegen Rpn8 en Rpn10. Kwantitatieve massaspectrometrie zonder labels is gebruikt voor de karakterisatie van interactie partners van het 19S/26S proteasoom. Deze metingen zijn in drievoud uitgevoerd. Na de behandeling met MG132/Lact vonden we een verbeterde binding van eiwitten behorende tot de 20S kern van het proteasoom en daarnaast zagen we ook een verbeterde interactie met andere eiwitten, waaronder Hsp23, Hsp68, REG (PA28) en Ref(2)p, alsmede een mogelijk nieuw UBL-domein bevattend ubiquitine shuttle eiwit CG7546 (humaan Bat3). Ub shuttle eiwit Rad23 interacteerde daarentegen alleen onder stress condities met het 19S/26S proteasoom. Als laatste benoemen we hier de DUB UCHL5, welke

onder alle condities interacteerde met het 19S/26S proteasoom, hoewel deze duidelijk minder vaak associeerde wanneer geen stress was geïnduceerd. Verder onderzoek is nodig om de rol van de verbeterde associatie van UCHL5 en het proteasoom onder stress condities te achterhalen. Samengenomen geven deze data meer inzicht in de dynamiek van proteasoom-afhankelijke eiwit afbraak onder verschillende cellulaire milieus, wat weer relevant kan zijn voor het begrijpen van het functioneren en de regulatie van het proteasoom tijdens ziektes.

Ecdysone is een hormoon welke een belangrijke rol speelt in de ontwikkeling van insecten. Dit hormoon induceert genen die reageren op ecdysone via interactie met de ecdysone receptor (EcR) in de celkern. Het onderzoek dat beschreven is in **hoofdstuk 6** is gedaan met het doel om meer inzicht te krijgen in verschillende niveaus van het ecdysone signaal netwerk. Door gebruik te maken van een RNA sequentie analyse en een eiwit expressie analyse hebben we globale transcriptoom en globale proteoom dynamieken op verschillende tijdstippen met elkaar vergeleken. We hebben bekende en nog onbekende genen en eiwitten die op ecdysone reageren geïdentificeerd. We zagen wel verschillen in de timing tussen de transcriptionele en translationele reactie, wat het moeilijk maakte om mRNA en eiwitten met elkaar te vergelijken op dezelfde tijdstippen. We hebben ook het EcR interactoom na ecdysone stimulatie geanalyseerd, en we identificeerden eiwitten met een rol in ecdysone signaaltransductie, ecdysone synthese, transcriptie, chromatine remodelering, en nog andere eiwitten als interactie partners van de receptor. De nieuwe genen, eiwitten en interactie partners die reageren op ecdysone en geïdentificeerd zijn in deze studie kunnen interessant zijn voor gedetailleerde (biochemische) vervolgstudies in cel culturen of in de vlieg.

Curriculum Vitae

Personal details

Name: Karen Alexandra Sap
Gender: Female
Date of birth: 11th of March 1983
Nationality: Dutch
email: k.a.sap@amc.uva.nl

Work experience

2015-current	Postdoc Lab of Prof.dr. Eric Reits, Protein aggregation and degradation, department of Medical Biology, Amsterdam University Medical Centra, Amsterdam, NL
2010 -2014 (4.5 years)	PhD student Lab of Dr. Jeroen Demmers (co-promotor), Proteomics Center, department of Biochemistry. Promotor: Prof.dr. C.P. Verrijzer. Erasmus University Medical Center, Rotterdam, NL
2008 -2009 (7 months)	Intern, MSc research project Lab of Prof.dr. C.P. Verrijzer. Supervisor: Dr. Yuri Moshkin, department of Biochemistry, Erasmus University Medical Center, Rotterdam, NL
2008 (6 months)	Intern, MSc research project Lab of Dr. Hans van Dam, department of Cell Biology Leiden University Medical Center, Leiden, NL
2006 – 2007 (9 months)	Technician Lab of Dr. Andre van Marle, Contract Production team (CPU) Biofocus DPI – a Galapagos Company (now Charles River), Leiden, NL
2006 (5 months)	Intern, BSc research project Lab of Prof.dr. Remko Offringa, Leiden University, Leiden, NL
2004 (5 months)	Intern, BSc research project Lab of Prof.dr. Corina Brussaard, NIOZ, Texel, NL

Education

2007 - 2010	Master of Science, Biomolecular Sciences – Cell Biology, Vrije Universiteit Amsterdam
2002 - 2006	Bachelor of Applied Science, Biochemistry, Hogeschool Rotterdam, NL
2000 - 2001	Bachelor of Applied Science, Civil Engineering, propedeuse, Hogeschool Rotterdam, NL

List of publications

van der Wal L, Bezstarosti K, **Sap KA**, Dekkers DHW, Rijkers E, Mientjes E, Elgersma Y, Demmers JAA. Improvement of ubiquitylation site detection by Orbitrap mass spectrometry. *J Proteomics* (2018) Nov 6. pii: S1874-3919(17)30371-8.

Karen A. Sap, Karel Bezstarosti, Dick H. W. Dekkers, Olaf Voets, Jeroen A. A. Demmers. Quantitative proteomics reveals extensive changes in the ubiquitinome after perturbation of the proteasome by targeted dsRNA mediated subunit knockdown in *Drosophila*. *Journal of Proteome Research* (2017), 16, 2848-2862.

Karen A. Sap, Karel Bezstarosti, Dick H.W. Dekkers, Mirjam van den Hout, Wilfred van Ijcken, Erikjan Rijkers and Jeroen A.A. Demmers. Global quantitative proteomics reveals novel factors in the ecdysone signaling pathway in *Drosophila melanogaster*. *Proteomics* (2015), 15, 725-738

Yuri M. Moshkin, Cecile M. Doyen, Tsung-Wai Kan, Gillian E. Chalkley, **Karen Sap**, Karel Bezstarosti, Jeroen A. Demmers, Zeliha Ozgur, Wilfred F. J. van Ijcken, C. Peter Verrijzer. Histone Chaperone NAP1 Mediates Sister Chromatid Resolution by Counteracting Protein Phosphatase 2A. *PLoS Genetics* (2013) 9(9): e1003719. doi:10.1371/journal.pgen.1003719

Karen A. Sap and Jeroen A.A. Demmers. Labeling Methods in Mass Spectrometry Based Quantitative Proteomics. *Integrative Proteomics* (2012), ISBN 978-953-51-0070-6, Dr. Hon-Chiu Leung (Ed.), InTech

Portfolio

Courses

2014	Biomedical English Writing and Communication, Erasmus MC, R'dam, NL
2013	R programming (basics), Erasmus MC, Rotterdam, NL
2011	Project management for PhDs, Erasmus MC, Rotterdam, NL
2011	MaxQuant Summerschool, Max Planck, Martinsried, DE
2010	Safely working in the lab, Leiden UMC, Leiden, NL
2010	Biomolecular Mass Spectrometry, Utrecht University, NL
2010	Cell and Developmental Biology, Erasmus MC, Rotterdam, NL
2010	Biochemistry and Biophysics, Erasmus MC, Rotterdam, NL
2010	Genetics, Erasmus MC, Rotterdam, NL

Conferences, workshops and presentations

2018	Proteostasis in health and disease (poster), COST, Athens, GR
2017	Dutch Huntington Disease Research Network (oral presentation), LUMC, Leiden
2017	Keystone Omics approaches to study the proteome (poster), Breckenridge, USA
2016	EMBO ubiquitin workshop (oral and poster presentation), Alghero, Sardinia, IT
2016	Cost Proteostasis meeting (poster presentation), Clermont-Ferrand, FR
2015 - 2018	Dutch Huntingtin Disease Research Network, (poster), Maastricht/Groningen, NL
2015 – 2018	Master student course – Biological research approaches (oral), AMC, A'dam, NL
2015 – 2017	Bachelor student course – practical advisor, AMC, Amsterdam, NL
2014	Lab retreat (oral presentation), Natural History Museum, Rotterdam, NL
2013	19th MGC PhD student workshop (oral presentation), Dusseldorf, DE
2013 - 2014	Course Biomedical Research Techniques (oral), Erasmus MC, Rotterdam, NL
2012 – 2013	Netherlands Proteomics Center PhD day, University Utrecht, Utrecht, NL
2012	Proteomics Platform Nederland (oral presentation), Vrije Universiteit, A'dam, NL
2012	18th MGC PhD student workshop (poster presentation), Maastricht, NL
2011	17th MGC PhD student workshop, Colonge, DE
2011	MaxQuant Summerschool 2011 (poster), Martinsried, Max Planck Institute, DE
2011	Proteomic Forum 2011 (poster presentation), Berlin, DE
2011 – 2016	Netherlands Proteomics Center progress meeting (poster presentation), Utrecht, NL
2010 – 2014	Work discussion (oral presentation), Erasmus MC, Rotterdam, NL
2009	Winterschool Transcriptional control of developmental processes (oral pres.), AT

Teaching

2013	supervision of master student (Anika Kötemann)
------	------------------------------------------------

Dankwoord

Ik had dit werk niet kunnen doen zonder hulp van velen en ik wil hen hier bedanken voor hun directe, dan wel indirecte betrokkenheid bij dit werk, of juist tijdens ontspanning erbuiten.

Allereerst wil ik mijn collega's van het Proteomics Center bedanken. Jeroen, bedankt dat ik mijn promotieonderzoek in jouw lab mocht doen. Hier heb ik de kans gekregen om mij te kunnen specialiseren in kwantitatieve proteomics, een kans die niet iedereen krijgt. Ik waardeer de energie die je erin steekt om goede kwaliteit mass spec metingen en analyses te leveren en mee te gaan in de snelle ontwikkelingen in het veld. Ik ben dan ook heel blij dat we ook na mijn PhD de samenwerking hebben voortgezet en wat mij betreft blijven we dit nog lang doen! Dick, je was een hele fijne en behulpzame collega. Ik vond bij jou altijd een luisterend oor, in goede tijden en in minder goede tijden. Ik vind het leuk dat we af en toe nog eens bij elkaar checken hoe het gaat. En natuurlijk bedankt dat je mijn paranimf wilt zijn! Karel, ik heb veel van je geleerd in het mass spec lab en je hebt heel veel samples voor mij gemeten. Bedankt voor alles! Erikjan, van jou heb ik ook heel veel geleerd, in ieder geval al hoe je met een bioinformaticus moet praten ☺. Ik heb respect voor je programmeer vaardigheden en ik hoop het ook ooit te leren. Lennart, leuk dat je mijn opvolger bent in Jeroens groep. Ondertussen zit het er voor jou ook al bijna op, ik wens je veel succes met de laatste loodjes en ik hoop voor je dat je het sneller kan afronden dan ik :)

Ook wil ik mijn collega's van het Biochemie lab bedanken, en als eerste natuurlijk mijn promotor, Peter Verrijzer. Peter, allereerst bedankt dat ik mijn afstudeerstage in jouw lab mocht doen, want daar is het allemaal begonnen. Mijn stageproject werd heel veelzijdig, met leuke resultaten waarvan ook een deel gepubliceerd is. Ik mocht van jou ook naar een ski-meeting in Oostenrijk om mijn resultaten te presenteren, dat vond ik heel leuk. Bedankt dat je mij wees op de promotieplek die beschikbaar was bij Jeroen. I performed my research internship under supervision of Yuri Moshkin in the lab of Peter. Yuri, we were a very good team. You were an inspiring supervisor and scientist, the example of someone who can think outside the box. There was also always something to laugh about. I obtained a lot of results during this internship which we have published as well. We are not really in contact anymore but I hope you are doing well. Ik wil ook Tsung-Wai bedanken voor het leren van veel biochemische technieken tijdens deze stage. Olaf, bedankt dat jij ook mijn paranimf wilt zijn. Ik vond het gezellig om met jou op te trekken tijdens mijn PhD en de MGC meetings. Leuk dat we af en toe nog uit eten gaan om bij te praten! Gill, I like your humor and the stories about your cat. Jan, hoewel je altijd begon met 'uuuhhh ik weet niet', kon ik jou altijd inschak(elen) voor wetenschappelijk advies. Ben, je bent een aardige vent. I also like to thank the previous lab members Cecile, Haleh, Marcel, Alice, Adone, Anna, Ashok, Elena, Adrie, Stavros, Prashant, Noorie, and Ulku for their advice, help and/or contribution to the nice atmosphere in the lab. Natasja, met jou heb ik veel gelachen,

bijvoorbeeld om onze 'kneuzenclub'. Ik hoop dat het ok gaat met je. En Aeijesta, ik ken jou alleen van na mijn PhD, maar ik wil je veel succes wensen met je projecten in Peters lab.

Ook wil ik de leden van de leescommissie, Joost Gribnau, Jurgen Marteiijn, en Alfred Vertegaal, bedanken voor het kritisch lezen van dit proefschrift en voor hun suggesties voor verbeteringen.

En ook de collega's van het secretariaat, inkoop en ICT wil ik graag bedanken voor hun behulpzaamheid: Marike, Jasperina, Bep, Leo, Melle, Koos, Enno, Sjozef. Marike, het is fijn dat ik altijd alle administratie zo vlot met jou kan regelen, niet alleen voor de PhD maar ook als ik af en toe voor mijn huidige baan nog even experimenten kom doen bij het Proteomics Center.

Tokameh, thank you for the scientific discussions and your advice during the work discussions (or in front of the coffee machine). Matheus, I like our little chats every time I come to the Erasmus MC to do some mass spec experiments. I wish you all the best with your research.

Maarten Fornerod, Joost Gribnau and Willy, I also like to thank you for the scientific discussions and critical thinking during the work discussions.

Ik wil ook onze burens, het Biomics team, bedanken. Wilfred, en ook Rutger, bedankt voor de discussies en adviezen. Mirjam, Zeliha en Christel, bedankt voor het uitvoeren, analyse en de hulp met de sequencing experimenten in het begin van mijn PhD.

Thanks to all the other colleagues on the 6th, 7th, 9th and 10th floor voor de gezelligheid and nice and serious chats. It was some ago now, so to avoid forgetting people I will just mention few of you. Eri, we met at Leiden University and it was nice to be colleagues again, here in Rotterdam. KC, you are a friendly guy, wish you all the best. Xiao, you were a nice friend. Indriati, I enjoyed the holidays and dinners with you! Loes, het was gezellig om met jou te kolommen, Jurgen het was gezellig als je langs kwam in het kantoor (om te kijken of je data al klaar was). Ozge, I enjoyed your parties with Turkish food and dancing in the living room. Maikel, ik kende jou van het HBO, het was leuk om je hier weer tegen te komen. Romana and Nesrin I enjoyed our lunches at the AMC (after the PhD). And Nesrin, after the defense I have no excuse anymore to skip bouldering ;)

Nadat mijn PhD contract was afgelopen ben ik bij het AMC (tegenwoordig Amsterdam UMC) gaan werken. Ik heb hier onwijs veel leuke collega's die mij ook adviezen hebben gegeven wat betreft mijn PhD. Maar om te voorkomen dat mijn dankwoord 2x zo lang wordt beperk ik mij hier voornamelijk tot mijn directe collega's/team. Eric, bedankt dat ik bij jou in het lab mag werken en hier mijn proteomics werk voort kan zetten in samenwerking met Jeroens groep. Op naar een doorbraak om de ziekte van Huntington te kunnen genezen! Katrin, you are a great scientist, thank you for your guidance when I started here and I wish you all the best with your new job. Keep in touch! Verder ben ik heel dankbaar voor het gezellige meidenteam waarin ik werk: Alicia, Sabine, Anne Jansen, Jolien, Maidina, Aleksandra and Tugce. I also enjoy the diners

(and drinks) that we regularly have in Amsterdam. Przemyslaw, thank you for helping me with Indesign and your advice about printing.

Ook wil ik mijn vriendinnen bedanken, met name Kylie, Judith en Anique voor alle feestjes, vakanties, meidenavonden enz tijdens en na mijn PhD.

Als laatste wil ik mijn familie bedanken voor hun vertrouwen en support. Mam, bedankt voor je hulp met o.a. het klussen, waardoor ik weer meer tijd had voor het afronden van dit proefschrift. Frank, bedankt voor je advies en hulp met de layout.